1-1-2005

Additional Assessments of the Craney Island Eastward Expansion in the Elizabeth River and Hampton Roads - Hydrodynamic Model Study

Mac Sisson
Virginia Institute of Marine Science

Harry V. Wang
Virginia Institute of Marine Science

Ya Ping Wang
Virginia Institute of Marine Science

Additional Assessments of the Craney Island Eastward Expansion in the Elizabeth River and Hampton Roads - Hydrodynamic Model Study

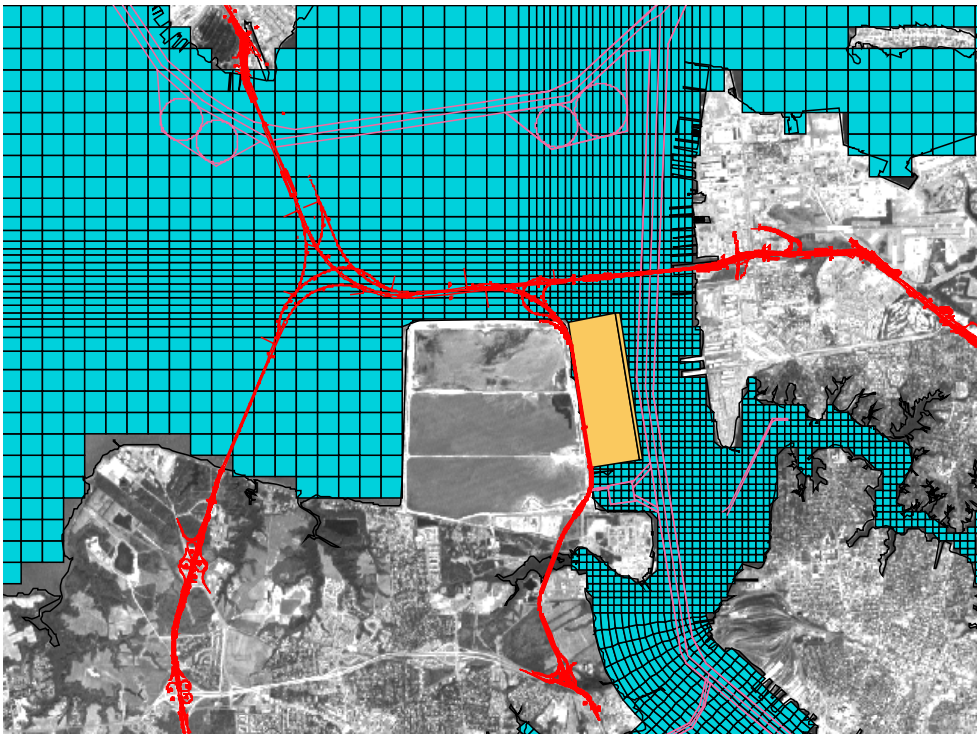

Mac Sisson, Harry Wang, and Ya Ping Wang

Final Report to the
U.S. Army Corps of Engineers, Norfolk District
and the
Virginia Port Authority

Special Report No. 388
In Applied Marine Science and Ocean Engineering

Virginia Institute of Marine Science
Department of Physical Sciences
Gloucester Point, Virginia 23062

January 2005

Additional Assessments of the Craney Island Eastward Expansion in the Elizabeth River and Hampton Roads - Hydrodynamic Model Study

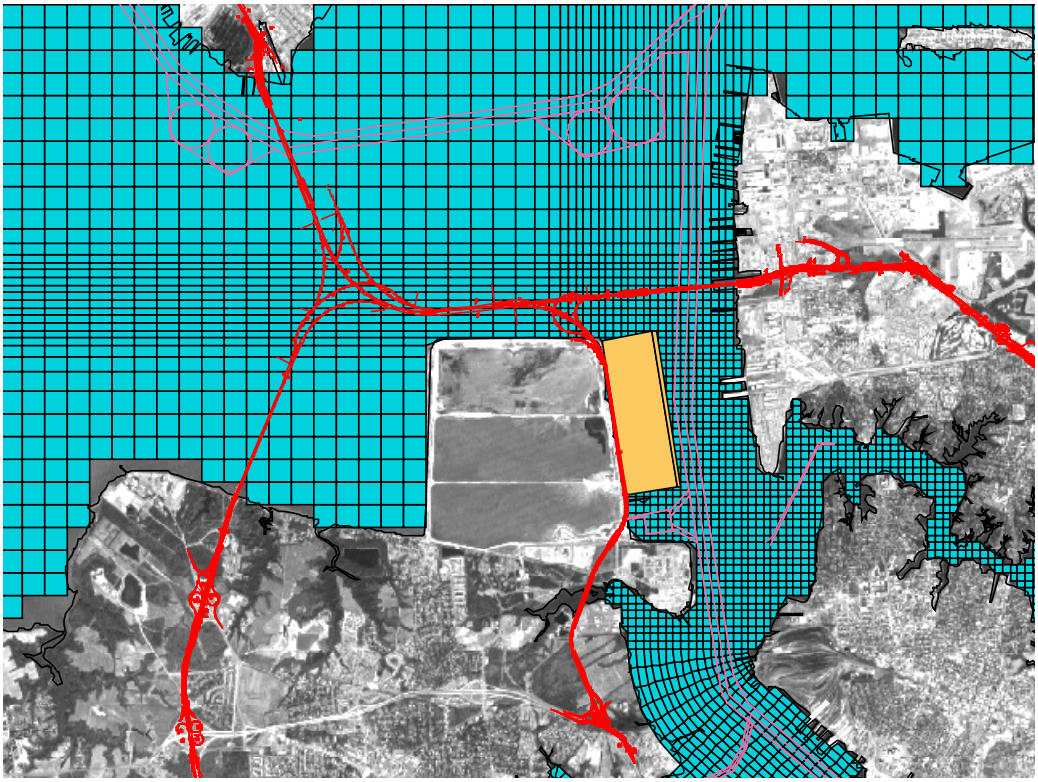

Mac Sisson, Harry Wang, and Ya Ping Wang

Final Report to the
U.S. Army Corps of Engineers, Norfolk District
and the
Virginia Port Authority

Special Report No. 388
In Applied Marine Science and Ocean Engineering

Virginia Institute of Marine Science
Department of Physical Sciences
Gloucester Point, Virginia 23062

January 2005

Additional Assessments of the Craney Island Eastward Expansion in the Elizabeth River and Hampton Roads - Hydrodynamic Model Study

Report Links

EXECUTIVE SUMMARY

"Additional Assessments of the Craney Island Eastward Expansion in the Elizabeth River and Hampton Roads - Hydrodynamic Model Results"

1. For the additional assessments of the CIEE using the VIMS 3D Hydrodynamic Eutrophication Model (HEM-3D), 4 model scenario runs were conducted:
    a. Scenario 1 was for the model testing of the cumulative impact of the CIEE expansion and the deepening of the Maersk Terminal using *single variable runs* (using a single variable, tidal range, for model input).
    b. Scenario 2 was model testing of these combined alterations further combined with ship berthing at both the CIEE and the Maersk Terminal facilities.
    c. Scenario 3 tested a dye release in the Southern Branch using the simulated dye release feature of the model to compare the flushing capability both within the Southern Branch and for the entire Elizabeth River.
    d. Scenario 4 was model testing of this cumulative impact (CIEE land expansion, Maersk Terminal dredging, and ship berthing at both facilities) using a *historical run* (using multiple variables in real time for model input).

2. The approach was to use a global analysis methodology to compare quantitatively the impacts of dredging and ship berthing over the far-field, including the areas of Hampton Roads and the Elizabeth River. This was done by determining percentages of total area associated with class intervals of change from the Base Case as differences in water surface elevation, surface and bottom salinity, surface and bottom current magnitude, surface and bottom residual current magnitude, and sedimentation potential.

3. From single variable runs, it is shown that both the APM terminal dredging and the berthing of ships had minimal impact on either surface elevation or sedimentation potential. The berthing of ships at CIEE, if considered permanent, has a local effect on the salinity distribution, and the velocity distribution, as shown in Table 1.

Table 1. 95th Percentile Values for Impacts of APM Terminal Dredging and Ship Berthing shown against CIEE alone.

Global Change – 95th Percentile (5% of area contains change greater than value listed)				
Single Variable - Cumulative Impact of Dredging and Ship Berthing				
Difference (from Base Case):	**Eastward Expansion Only**	**Eastward + APM Dredging**	**Eastward + APM dredging + triangular ships**	**Eastward + APM dredging + square ships**
Surface Elevation	0.14 cm	0.13 cm	0.13 cm	0.14 cm
Surface Current	2.4 cm/s	2.4 cm/s	2.5 cm/s	**2.6 cm/s**
Bottom Current	1.6 cm/s	1.7 cm/s	2.1 cm/s	**2.5 cm/s**
Surface Salinity	0.00 ppt	0.10 ppt	0.15 ppt	**0.19 ppt**
Bottom Salinity	0.00 ppt	0.06 ppt	0.10 ppt	**0.15 ppt**
Sedimentation Potential	0.08 %	0.08 %	0.09 %	**0.10 %**

4. A second table, Table 2, is created in order to compare the cumulative impacts resulting from both the APM dredging and ship berthing to the previously evaluated land expansion options. Impacts occurred on velocity and salinity distributions, but their magnitudes were less than those of the previously studied land expansion options (In this table, the cumulative impact of the Eastward Expansion, APM dredging, and ship berthing, is shown in the second column and its values are shown in **bold)**.

Table 2. 95th Percentile Values for Cumulative Impacts Shown against Previously Evaluated Land Expansion Options.

Global Change – 95th Percentile (5% of area contains change greater than value listed)					
Single Variable - Comparison to Prior Land Expansion Options					
Difference (from Base Case):	**Eastward Expansion Only**	**Eastward + Dredging + Square Ships**	**Westward Expansion Only**	**Northward Expansion Only**	**North+eastward Expansion Only**
Surface Elevation	0.14 cm	**0.14 cm**	0.34 cm	1.00 cm	1.04 cm
Surface Current	2.4 cm/s	**2.6 cm/s**	5.3 cm/s	12.3 cm/s	11.7 cm/s
Bottom Current	1.6 cm/s	**2.5 cm/s**	3.3 cm/s	7.8 cm/s	6.6 cm/s
Surface Salinity	0.00 ppt	**0.19 ppt**	0.12 ppt	0.71 ppt	0.23 ppt
Bottom Salinity	0.00 ppt	**0.15 ppt**	0.35 ppt	1.00 ppt	0.23 ppt
Sedimentation Potential	0.08 %	**0.10 %**	2.8 %	8.9 %	6.3 %

5. Flushing analysis revealed that neither the flushing of the Southern Branch nor that of the entire Elizabeth showed any detectable adverse response from the combined effects of the APM terminal dredging and ship berthing (see Figures III.3 and III.4).

6. In order to assess the impacts of dredging and ship berthing during extreme conditions, the historical run was conducted testing the cumulative impact of the CIEE land expansion, the dredging of the Maersk Terminal area, and the berthing of ships. In the historical run simulation scenario, the impacts of dredging and ship berthing are tested against extreme conditions comprised of high and low discharge and high wind during a six-month simulation for which the input variables (i.e., discharges, wind, boundary conditions) are taken from historical records. Its impact was compared with those of two expansion options: Option 7 (eastward expansion) and Option 7/5a (combined eastward and westward expansion). The results for this are shown in Table 3. As in the single variable runs, little change was noted in historical run of this cumulative test case while comparing with Option 7. Comparing the results to those of Option 7/5a, the changes were slightly greater in salinity, but less for all other parameters compared.

Table 3. 95th Percentile Values for Cumulative Impacts Shown against Previously Evaluated Land Expansion Options for Periods of Extreme Events as Modeled by the Historical Run Scenario.

Global Change – 95th Percentile (5% of area contains change greater than value listed)			
Historical – High Discharge Event			
Difference (from Base Case):	**Eastward Expansion Only**	**Eastward + Dredging + Square Ships**	**Eastward-Westward Expansion Only**
Surface Elevation	0.20 cm	0.20 cm	**0.33 cm**
Surface Current	5.5 cm/s	5.9 cm/s	**6.7 cm/s**
Bottom Current	2.7 cm/s	3.6 cm/s	**3.7 cm/s**
Surface Salinity	0.00 ppt	**0.08 ppt**	0.02 ppt
Bottom Salinity	0.00 ppt	**0.09 ppt**	0.07 ppt
Sedimentation Potential	1.0 %	1.1 %	**1.9 %**
Historical – Low Discharge Event			
Difference (from Base Case):	**Eastward Expansion Only**	**Eastward + Dredging + Square Ships**	**Eastward-Westward Expansion Only**
Surface Elevation	0.14 cm	0.14 cm	**0.33 cm**
Surface Current	2.7 cm/s	3.0 cm/s	**4.3 cm/s**
Bottom Current	1.9 cm/s	2.7 cm/s	**2.9 cm/s**
Surface Salinity	0.00 ppt	**0.12 ppt**	0.04 ppt
Bottom Salinity	0.01 ppt	**0.16 ppt**	0.09 ppt
Sedimentation Potential	0.9 %	1.0 %	**2.8 %**
Historical – High Wind Event			
Difference (from Base Case):	**Eastward Expansion Only**	**Eastward + Dredging + Square Ships**	**Eastward-Westward Expansion Only**
Surface Elevation	0.21 cm	0.21 cm	**0.46 cm**
Surface Current	2.2 cm/s	2.8 cm/s	**5.0 cm/s**
Bottom Current	1.5 cm/s	2.4 cm/s	**3.0 cm/s**
Surface Salinity	0.00 ppt	**0.09 ppt**	0.00 ppt
Bottom Salinity	0.00 ppt	**0.11 ppt**	0.02 ppt
Sedimentation Potential	0.8 %	0.9 %	**1.7 %**

TABLE OF CONTENTS

LIST OF TABLES

LIST OF FIGURES

LIST OF APPENDICES

Appendix III-A-2 Global Comparisons of Single Variable Runs
Percentile Analysis

Appendix IV-A-1 Global Comparison of Historical Runs
Spatial Distributions

Appendix IV-A-2 Global Comparison of Historical Runs
Percentile Analysis

CHAPTER I. INTRODUCTION

A. BACKGROUND

The Craney Island Dredged Material Management Area (CIDMMA) is a Federally owned and operated facility located in Hampton Roads adjacent to the city of Portsmouth, Virginia (Figure I.1). The proposed expansion of the CIDMMA addresses a Federal interest in increasing the capacity of the CIDMMA and extending its useful life beyond the year 2050. In addition, the expansion would serve a further interest in obtaining logistical and tactical areas for the deployment of national defense forces. It simultaneously addresses the interest of the Commonwealth in future expansion of its deep-water port facilities.

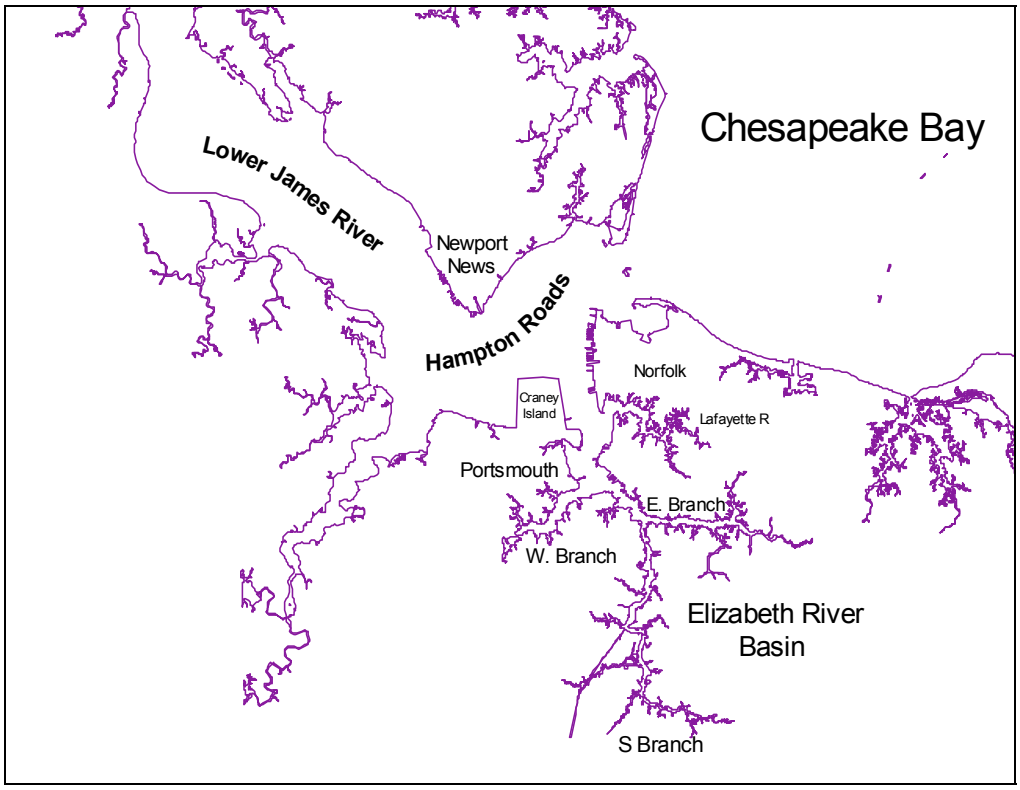

Figure I.1. Hampton Roads and the Elizabeth River Basin.

The representative agencies in charge of the present development efforts are the Norfolk District, U.S. Army Corps of Engineers, and the Virginia Port Authority representing the Commonwealth of Virginia. Following a successful *Reconnaissance Study* that determined the required Federal interest, both parties signed a feasibility cost-sharing agreement and adopted a *Project Study Plan* (PSP) to determine suitable and acceptable means for designing and implementing the expansion. The PSP required, among other items, the development and evaluation of preliminary designs for added material

placement areas and new port facilities, including a marine terminal, to be incorporated in the expansion. More specifically, in order to determine the possible impact that any of these designs might have on the estuarine environment in Hampton Roads and adjacent areas, the PSP provided for a hydrodynamic modeling study to be conducted. The hydrodynamic modeling study, "Three Dimensional Hydrodynamic Modeling Study of Craney Island Eastward Expansion" (Wang et al., 2001) was conducted by the Virginia Institute of Marine Science (VIMS) for the purpose of evaluating the Craney Island land expansion options under consideration until that time. Throughout the present report, the study will be referred to as the *original* hydrodynamic modeling study. Whereas a brief description of this study is provided below, the reader is referred to the website **http://www.vims.edu/craney** for more explanation or to download the report of this study.

1. Original Hydrodynamic Model Study – In the previous study that assessed the impacts of land expansion options for Craney Island, the VIMS three-dimensional Hydrodynamic-Eutrophication Model (HEM-3D) was used to compare expansion options of Craney Island to the east, west, north, northeast, and east/west. Model simulations of one to several months were made for each expansion option, as well as two channel depths being considered at the time. Physical changes to the estuarine environment (i.e., tidal range and phase, strength and direction of tidal and tidally-averaged currents, salinity and its distribution, circulation and flushing ability, and sedimentation potential) were evaluated and ranked according to impact. Additionally, specific features important to the well-being of estuarine processes (e.g., flushing capability, the Newport News Pt. frontal system, tidal prism, etc.) were examined extensively. The conclusions of the study were that the Eastward Expansion of Craney Island had the least impact, the east/west and westward expansions had the next least impact, and the expansions to the north and northeast had the most impact.

2. VIMS HEM-3D Model Description - This intra-tidal finite difference numerical model was first developed by Hamrick (1996). Its purpose is to simulate the hydrodynamic behavior of the estuary by predicting time-varying surface elevation, horizontal and vertical water movement (including both tidal and non-tidal currents), and 3D distributions of conservative water properties such as salinity. It also determines bed shear stress throughout its bottom layer that, in turn, allows for the prediction of sedimentation potential.

3. HEM-3D Model Application for the James and Elizabeth Rivers - The model domain for the James River spans from its mouth to the limit of tide (i.e., Richmond, Virginia). A coarse grid cell of 370 meters was used for the James River to accommodate the length of the river. However, a higher resolution is required in the Elizabeth River, and a cell size there of 123 m was selected. A model grid with a dual scale resolution, as shown in Figure I.2, was developed for use in the original and present studies of the Craney Island expansion.

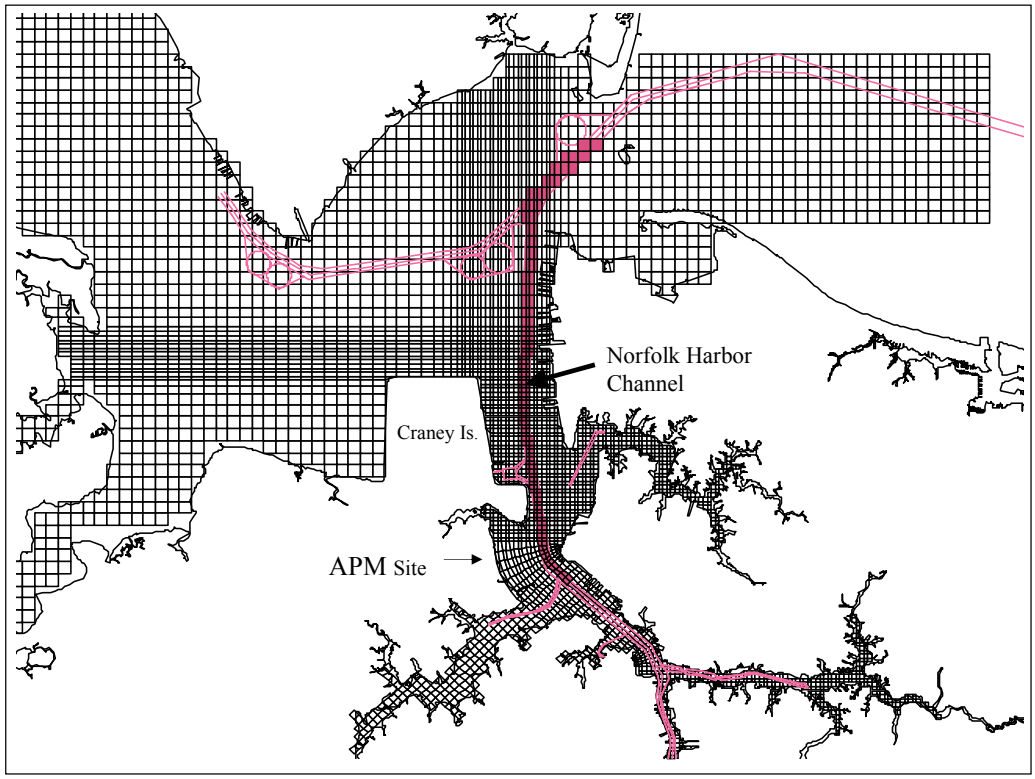

Figure I.2. Dual-scale model grid and Norfolk Harbor Channel.

B. PURPOSE OF THE PRESENT STUDY

The present study, entitled "Additional Assessments of the Craney Island Eastward Expansion in the Elizabeth River and Hampton Roads - Hydrodynamic Model Study", provides additional assessments in reference to the Craney Island Eastward Expansion. The assessments are of the cumulative impacts of:

1) dredging of the Maersk (APM) Terminal area south of Craney Island and
2) the berthing of ships at both the APM and Craney Island Eastward Expansion.

This is in addition to the previous study that provided assessments of the impacts of the eastward, westward, northward, and northward-eastward land expansion options.

C. APPROACH

The approach was to use a global analysis methodology to compare quantitatively the impacts of dredging and ship berthing over the far-field, including the areas of Hampton Roads and the Elizabeth River. This was done by determining percentages of total area

associated with class intervals of change from the Base Case as differences in water surface elevation, surface and bottom salinity, surface and bottom current magnitude, surface and bottom residual current magnitude, and sedimentation potential. Potential changes in one or more of the physical characteristics or features listed in Chapter I, Section A.1 above are investigated in this study through **Simulation Comparisons**. In this approach, the model is used to simulate hydrodynamic behavior at various temporal and spatial scales in the river areas under investigation. Following separate model runs, each driven by the same temporal input data including tidal height, salinity, freshwater discharges, and other boundary variables as specified, results are compared between the **Base Case** and a **Test Case**.

1. Base Case – The Base Case for this study consists of the existing waterway conditions including bridge pilings and tunnel islands associated with a planned Third Crossing of Hampton Roads (Alternative 9) in addition to the I64 and I664 highway crossings (Figure I.3).

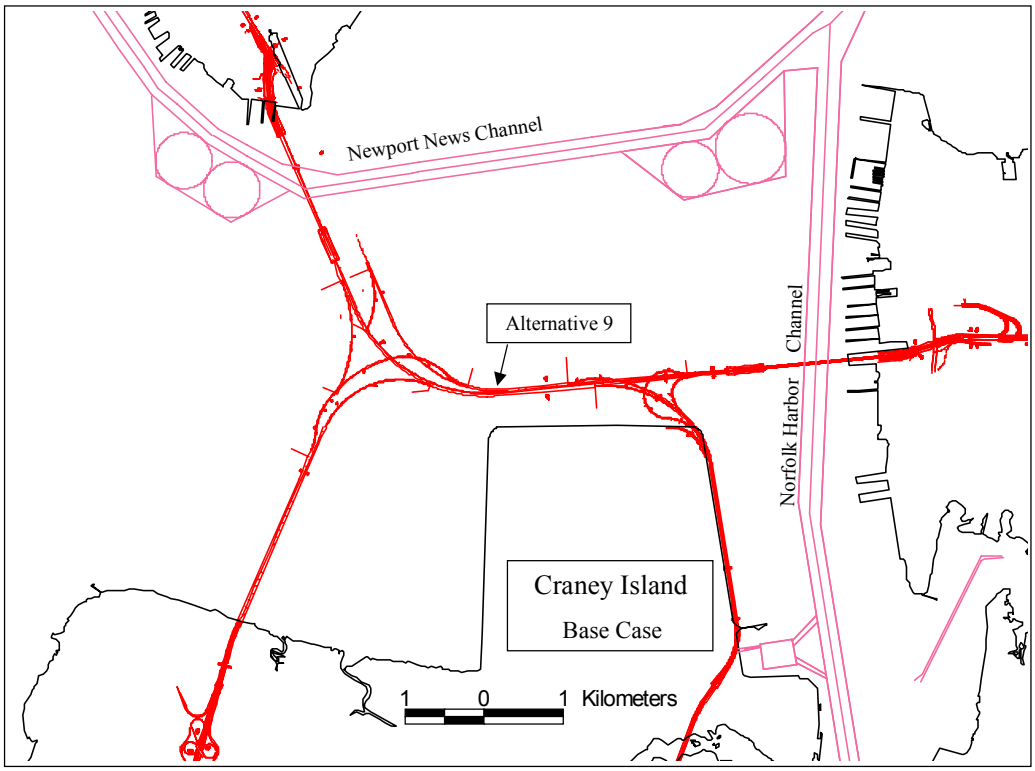

Figure I.3. Base Case, Existing Condition plus Alternative 9 Third Crossing.

2. Test Cases – A Test Case consists of a deviation from the Base Case of the physical domain, which is capable of perturbing one or more features of the hydrodynamic circulation. In the original hydrodynamic modeling study of Craney Island, these were various options of land expansions and depth changes. In the current study, these include the APM Terminal Site deepening (Test Case 1) and the added effects of ships on the wharf (Test Cases 2a and 2b).

Table I.1. Test Cases for the Current Study.

Assessed Impact	Test Case	Scenario *
APM Terminal Dredging	1	1,2,3,4
a. Ship berthing - (triangular cross-section)	2a	3
b. Ship berthing - (square cross-section)	2b	2,3,4

* Test cases included in specified scenario(s)

3. Single Variable Runs – A basic screening approach under controlled conditions, these tests restrict the model input by allowing only a single input variable, tidal range, to vary between astronomical extremes during the course of a run. A three-constituent harmonic model is used including the M_2, S_2, and N_2 tidal constituents with phasing adjusted to produce tides of maximum (perigean-spring), mean, and minimum (apogean-neap) range during a single run of 34 days. The generated time series, used as the boundary condition at the James River mouth in single variable runs, is shown in Figure I.4.

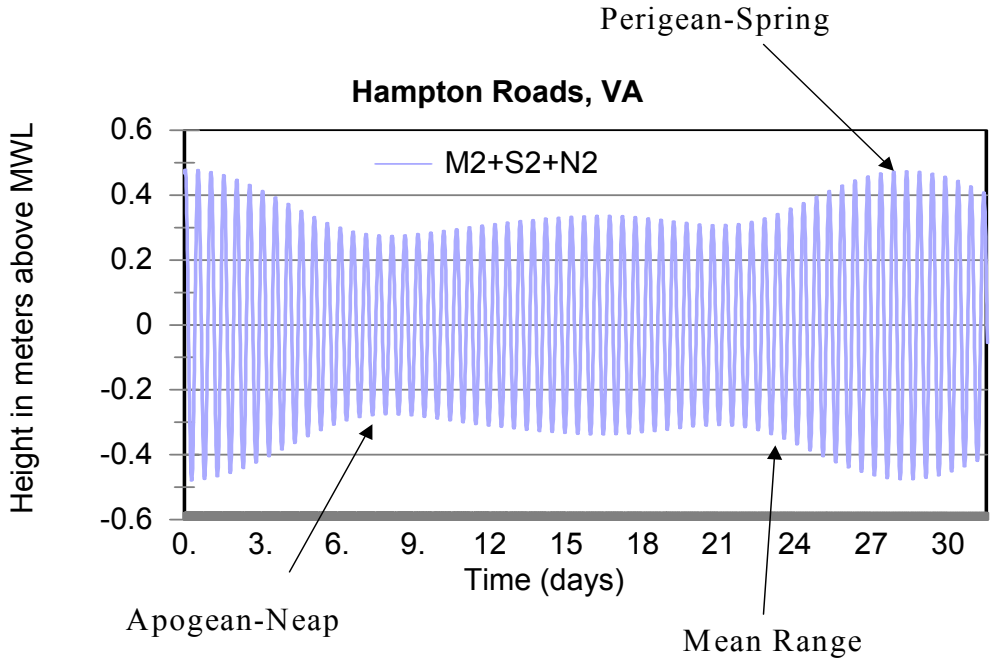

Figure I.4. Tide Curve Generated using M_2, S_2, and N_2 Constituents for Hampton Roads, Virginia.

4. Historical Runs – In these runs, actual values for several input variables are taken from the historical record over a six-month period (mid-March to mid-September, 2000). The variables include real-time measured tidal and non-tidal changes in water level as well as changes in salinity at the open boundary and daily freshwater discharge at points along the closed boundary of the model domain. Local atmospheric winds are included through a surface stress parameter. The six-month simulation for the historical run includes periods of extreme conditions (notably high and low discharge and high wind), and analysis of these provides additional information regarding the impact of the Test Case.

CHAPTER II. DESCRIPTION OF ADDITIONAL ASSESSMENTS FOR THE CRANEY ISLAND EASTWARD EXPANSION

A. THE IMPACT OF THE APM TERMINAL DREDGING

The APM site is located on the Western Shore of the Elizabeth River, a major tributary of the James River, which flows into the Chesapeake Bay. The APM dredging site is shown in Figure II.1 below. Dredging specifications call for a dredge design depth of 52 feet MLLW. The area to be dredged is 189 acres, and the volume of material to be removed is reported as 10.3 million cubic yards.

In the original hydrodynamic modeling study for the CIEE (Wang et al., 2001), the APM Terminal site was not under consideration. A flushing analysis for the APM Terminals was documented in a report by CH2MHILL (2003). However, the study focused on those regions adjacent to the Terminal site. The purpose of this study is to assess the far-field impacts of the dredging in a manner consistent with the assessments of land expansion options performed in the original hydrodynamic study of Craney Island. For this reason, a model simulation of the dredged terminal area was performed and analyzed using the global analysis methodology as described in Chapter III.

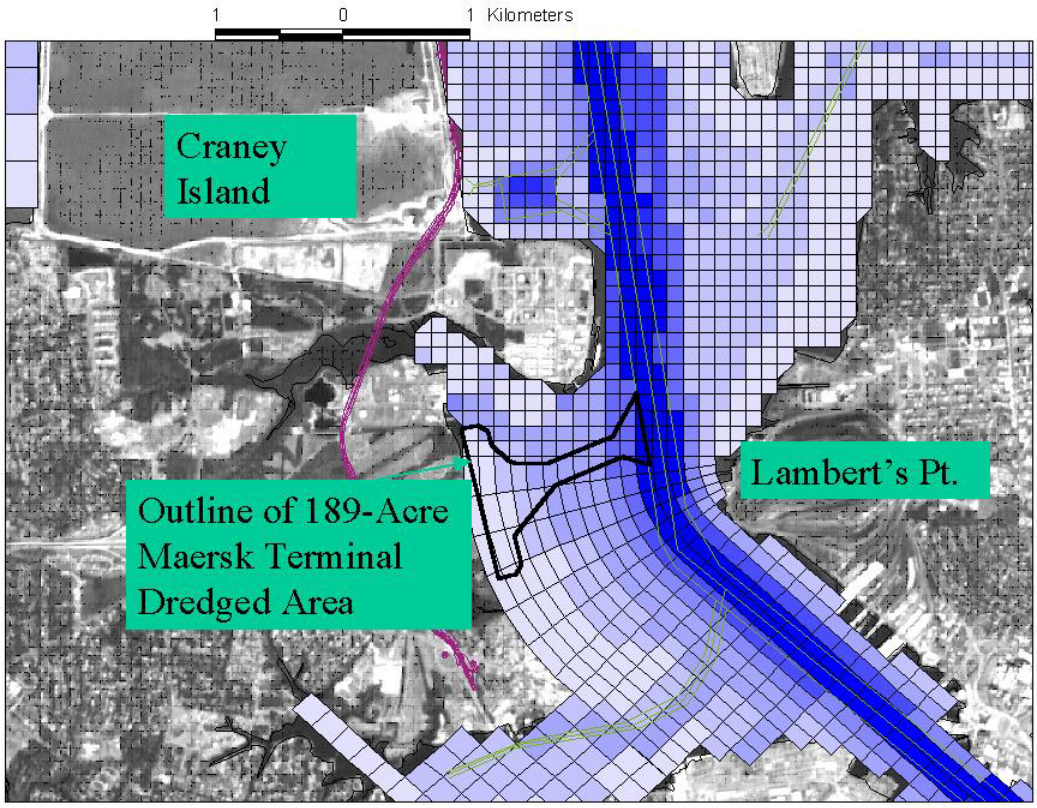

Figure II.1. Location of the APM Dredging Site.

The primary assumption made in the modeling effort was that the Eastward Expansion is to be built along with the APM Terminal facility. For that reason, the model simulation was designed to include both the Eastward Expansion (50-foot channel) and the deepening of the APM Terminal site. For consistency, the model grid was retained from the original hydrodynamic study of Craney Island.

Prior to simulating the deepening of the APM Terminal area, a consistency check of the model representation of APM terminal depths, area, and volume was compared to the design specifications. Model depths were set to 16.2 m (NGVD) for the grid cells corresponding to the dredge area, exactly equivalent to 52 feet MLLW as specified for the dredging. The area of the grid cells was 0.747 km^2, or within 2.4 % of the 189-acre specified area (0.765 km^2) dredge specification. Most importantly, the model dredging volume, 7.837 km^3, was within 0.5 % of the specified dredge volume of 10.3 million cubic yards (7.875 km^3).

The assessment of the impact of the APM Terminal dredging was done using a single variable run which included the eastward expansion along with the dredging, to evaluate the cumulative impact of the eastward expansion along with the dredging. By doing this, the results from the subsequent global analysis of this simulation could be directly compared to those from the eastward expansion alone, as well as the other land expansion options evaluated in the original hydrodynamic study of Craney Island.

B. THE IMPACT OF SHIP BERTHING AT BOTH THE CIEE AND THE APM TERMINAL

The reason that ship berthing becomes an issue is because the present-day container ship is much larger in terms of its beam width, length, and draft. For example, the Maersk Class Container Vessels (i.e., beam widths of 140 feet and draft depths of 47 feet), illustrated below in Figure II.2, provide some of the required modeling specifications.

One purpose of this study is to assess the far-field impacts of the berthing of ships at both the Craney Island Eastward Expansion and the APM Terminal Site in a manner consistent with the assessments of land expansion options performed in the original hydrodynamic study of Craney Island. For this reason, a model simulation of the ship berthing at both sites was performed and analyzed using the global analysis methodology as described in Chapter III.

There were several conservative assumptions that were incorporated into the modeling of ship berthing in this study. The primary assumption made in the modeling effort was that ships would be berthed at both sites at full capacity (i.e., over the entire berthing distances at both the Eastward Expansion and the APM Terminal facility) and at all times.

The cross-sectional profile of the vessel as it is aligned against the flow was not known. For that reason, two tests were conducted. The first test (i.e., Ships - Case 1) assumed a triangular cross-section. The second test (i.e., Ships - Case 2) assumed a square cross-section. Both of these modeled shapes extended from the water surface to the bottom of the river (i.e., 53 feet MLLW), exceeding the 47-foot specified ship draft and providing another conservative estimation of the actual impact of the ship berthing.

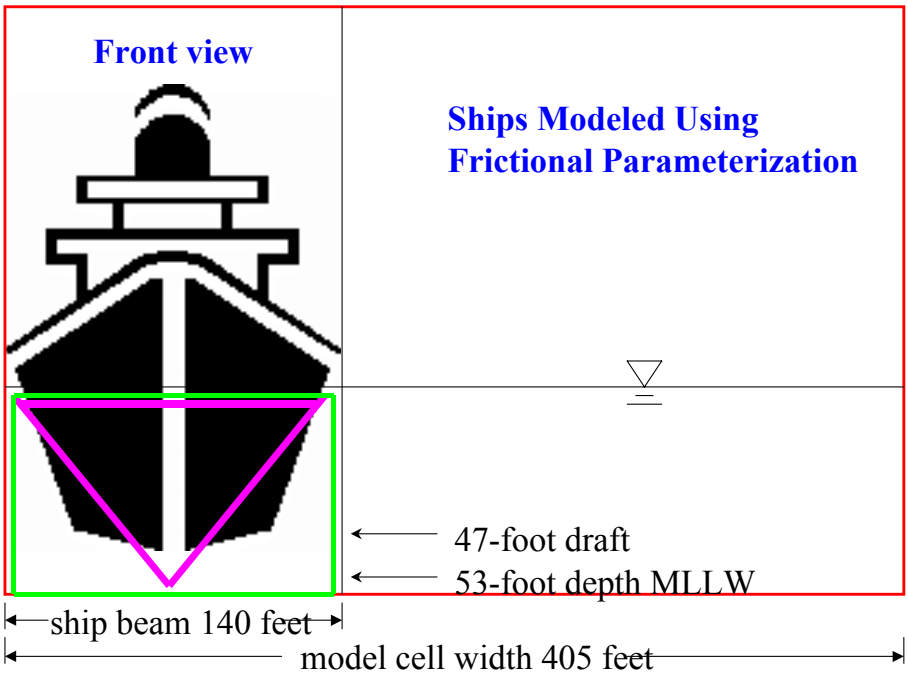

Figure II.2. Schematic of Maersk Class Ship Dimensions shown against Cell Width.

The HEM-3D model can account for forces at the sub-cellular spatial scale that can serve to impede the flow of water. This model feature is known as frictional parameterization (Wang and Kim, 2000) and was used in the original hydrodynamic model study to incorporate the effects of piers, highway causeway pilings, etc. The governing equations of the model include the effects of impedance, constriction, and turbulence production. This feature is described at length in Wang et al. (2001).

Prior to simulating the berthing of ships at both sites, the berthing areas were carefully compared to the model cell and grid dimensions. It was determined that the Eastward Expansion berthing area occupied a distance spanning 16 model cells, whereas the APM Terminal berthing area occupied a distance spanning 3 cells.

The assessment of the impact of ship berthing at both sites was done using a single variable run which also included both the eastward expansion and the APM dredging, to evaluate the cumulative impact of the Eastward Expansion, the dredging, and ship berthing. By doing this, the results from the subsequent global analysis of this simulation could be directly compared to those from the Eastward Expansion alone, or to the Eastward Expansion and the dredging alone, as well as the other land expansion options evaluated in the original hydrodynamic study of Craney Island.

CHAPTER III. THE RESULTS FOR THE SINGLE VARIABLE RUNS

The additional assessments of the current project for the proposed Craney Island expansion plan in the Lower James and Elizabeth River consist of 3 Test Cases: the impact of the APM Terminal area dredging and 2 test cases of ship berthing at both the Eastward Expansion and the APM Terminal sites. These 3 Test Cases comprise all of the scenario simulations for single variable runs. A time series of 74 tidal cycles was designed and used to provide the combination of essential tidal components including spring, neap, perigean-spring and apogean-neap tides. The semi-monthly progression between the extremes in tidal range for the model is shown in Chapter I, Figure I.4. The duration of each single variable scenario run was 134 tidal cycles and the model results were saved every half-hour throughout the entire modeling domain after the model spin-up period of 60 tidal cycles.

In order to assess the impacts exerted on the James/Elizabeth River system, the differences between the Test Case and the Base Case were obtained and analyzed. From the numerical modeling point of view, what these test cases introduce into the system are perturbations from either change in the modeling domain itself (APM Terminal dredging) or frictional effects (ship berthing). In measuring the effect of these perturbations, we first conducted a global analysis using 4 key variables: tidal elevation, current velocity, salinity and the sediment potential. We then shifted the focus onto the most important local effect, namely flushing, to determine whether this had been impacted for either the Southern Branch or the entire Elizabeth River. By combining the global and local analysis, a balanced view of assessment from both large scale as well as local scale can be achieved in a more objective manner.

A. GLOBAL COMPARISONS

Here, the term global is used to refer to the entire spatial domain for Hampton Roads and the Elizabeth River. The global technique described in this section involves the generation of a plotted spatial distribution of a 74 tidal-cycle time average comparison of parameters predicted by the model for the Base Case and the 3 test cases. The comparison is made possible by virtue of the fact that all model output for the 6 layer, 7500-cell domain of the VIMS James/Elizabeth River HEM-3D model version is saved 24 times per tidal cycle (i.e., approximately every half hour). This allows one to compare, for each location in the model domain, time series of the Base Case versus each test case and to quantify the difference as either an RMS (root mean square) difference or a simple average difference:

$$\mathrm{RMS\_DIFFERENCE} = \sqrt{\sum_{i=1}^{n} (MP_{test,i} - MP_{base,i})^2 / n}$$

for tidal elevation, velocity magnitude

$$AVERAGE\_DIFFERENCE = \sum_{i=1}^{n} (MP_{test,i} - MP_{base,i}) / n$$

for salinity, sedimentation potential,
and residual velocity

where: n is number of data points, (1776 for 74 tidal cycles)
MP_{test} is model prediction for the test case
MP_{base} is model prediction for the Base Case

In this fashion, one is able to obtain for each state variable a simple difference between the predicted value of each test case and that of the Base Case for each cell and layer of the model domain.

1. Spatial Distribution – It is not only useful to know the relative size of the differences described above, but also their spatial distributions. Use of ArcView Avenue scripts allows for the mapping of the derived differences into the exact cell areas of this curvilinear, variable cell size grid. Differences were derived for the Hampton Roads portion of the model domain as shown in the spatial plots of Hampton Roads shown in Figures 1-32 of Appendix to Chapter III, Section A.1.

Due to the incorporation of the Eastward Expansion into the 3 test cases, spatial plots of this land expansion alone (as reported by Wang et al., 2001) are also presented for comparison to the cumulative impacts shown subsequently. Therefore Figures 1-8 represent the impact of the Eastward Expansion, Figures 9-16 show the Eastward Expansion and the APM terminal dredging, Figures 17-24 show results from Test Case 2a of the ship berthing, and Figures 25-32 show those from Test Case 2b of the ship berthing.

For each of the 3 test case – Base Case comparisons, the sequence of the 8 spatial plots is as follows:

1) RMS difference of tidal elevation
2-3) average difference of surface and bottom salinity, respectively
4-5) RMS difference of surface and bottom velocity magnitude, respectively
6-7) average difference of surface and bottom residual velocity magnitude, respectively
8) sedimentation potential difference

For purposes of comparing the analyses of the test case comparisons, both the area for display and the legend (class) intervals selected to report the differences were kept constant throughout the comparisons.

The differences are calculated and plotted for each of the test case comparisons. Below is a summary of the findings in each test case.

Eastward Expansion vs. Base Case – Plots for the Eastward Expansion are presented in Figures 1-8 of the Appendix to Chapter III, Section A.1. For surface elevation (Figure 1), all RMS differences fall below 0.25 cm except for a small area adjacent to and north of the proposed expansion area, where differences increase to 0.4 cm. Average differences in surface and bottom salinity (Figures 2-3) fall below 0.2 ppt everywhere except in the immediate area of the expansion. Just to the north and east of the expansion, the salinity differences fall below 1.0 ppt, except for a very small area of bottom salinity in the dredged region east of the expansion. Surface and bottom velocity magnitude RMS differences (Figures 4-5) show a gradual increase to about 20 cm/sec over a very small area just north of the expansion. The small pink coloration north of the James River Bridge represents small differences relative to the currents in this area. Surface and bottom residual velocity magnitude average differences (Figures 6-7) reveal small areas around the structure containing differences up to 5 cm/sec at the surface and up to 3 cm/sec at the bottom. Sedimentation potential is what we define as the percent of time that the bottom shear stress computed by the model remains under 0.1 pascals. The difference between the Eastward Expansion and the Base Case for this parameter is plotted in Figure 8. This plot show a very small area (in red) just north of the expansion with mildly increased sedimentation potential bounded by a similarly small area (in blue) just to its east with mildly decreased sedimentation potential, suggesting a tendency for a small re-allocation of deposition in this area.

Eastward Expansion plus APM Terminal Dredging (Test Case 1) vs. Base Case – Plots for this test case are in Figures 9-16 of the Appendix to Chapter III, Section A.1. For the surface elevation (Figure 9), the RMS difference from the Base Case appears to be identical to that for the Eastward Expansion alone (Figure 1). The average difference in surface salinity due to APM Terminal dredging can be seen by comparing Figure 10 to Figure 2. This shows a small increase in salinity (0.2 to 0.6 ppt) for the area upstream of the dredge site extending into the Western Branch, and a larger increase in salinity (up to 1 ppt) immediately at the dredge site, due to this dredging. The average difference in bottom salinity (Figure 11) can be compared to that for the Eastward Expansion (Figure 3) and it shows a small decrease (0.2 -1.0 ppt) extending upstream along the channel into the Southern Branch. The surface velocity magnitude RMS differences, seen by comparing Figure 12 to Figure 4, shows a small increase (2-4 cm/sec) in the difference adjacent to the APM Terminal site and in small areas just upstream, on both sides of the channel. Bottom velocity magnitude RMS difference, seen by comparing Figure 13 to Figure 5, shows an added change (2-4 cm/sec) moving upstream along the channel towards the mouth of the Southern Branch, and a larger difference (4-8 cm/sec) in a small area immediately at the APM Terminal site. The impact of dredging on surface residual velocity magnitude average differences, seen by comparing Figure 6 to Figure 14, reveals very small areas near and upstream of the APM Terminal with dredging-induced changes of 1-5 cm/sec. The impact of dredging on bottom residual velocity magnitude average

differences, seen by comparing Figure 7 to Figure 15 reveals a very small area near the APM Terminal with dredging-induced changes of 1-5 cm/sec. The impact of dredging on sedimentation potential difference, seen by comparing Figure 8 to Figure 16, shows no effect on this low energy region.

Eastward Expansion plus APM Dredging plus Berthing of Ships (Case 2a) at Both Sites vs. Base Case – Plots for the first test of the impact of ship berthing are shown in Figures 17-24 of the Appendix to Chapter III, Section A.1. For the effect of ship berthing on surface elevation RMS difference (compare Figure 17 to Figure 10), the spatial plot is virtually unchanged. Surface salinity, shown in Figure 18 with ship berthing and in Figure 11 without ship berthing, has more impact at both berthing sites, although it is very localized and confined under 2 ppt. Additionally, the intrusion of a salinity increase into the Western Branch is extended. Bottom salinity, shown in Figure 19 with ship berthing and in Figure 11 without ships, shows a small extension of the area of salinity decrease (0.2 to 1.0 ppt) moving up the channel into the southern Branch. Also, small areas of minimal increase appear in the Western Branch. Surface velocity magnitude RMS differences caused by ship berthing (Figure 20 compared to Figure 12) shows only a very small change in the area impacted. Bottom velocity magnitude RMS differences (shown in Figure 21 with ships and Figure 13 without ships) also shows very small areas (i.e., several model cells) with changes in only the lowest legend class size (2-4 cm/sec). Surface and bottom residual velocity magnitude average differences (Figures 22-23 with ships and Figures 14-15 without ships) show only very subtle changes in the shapes of areas with the lowest differences (1-3 cm/sec for the surface layer and 1-5 cm/sec for the bottom layer). Sedimentation potential difference due to ship berthing, shown by comparing Figure 24 to Figure 16, appears to have almost no impact.

Eastward Expansion plus APM Dredging plus Berthing of Ships (Case 2b) at Both Sites vs. Base Case – Plots for the second test of the impact of ship berthing are shown in Figures 25-32 of the Appendix to Chapter III, Section A.1. For the effect of ship berthing on surface elevation RMS difference (compare Figure 25 to Figure 10), the spatial plot is virtually unchanged. Surface salinity, shown in Figure 26 with ship berthing and in Figure 11 without ship berthing, has more impact at both berthing sites, although it is very localized and confined under 2 ppt. Additionally, the intrusion of a salinity increase into the Western Branch is extended. Bottom salinity, shown in Figure 27 with ship berthing and in Figure 11 without ships, shows a small extension of the area of salinity decrease (0.2 to 1.0 ppt) moving up the channel into the southern Branch. Also, small areas of minimal increase appear in the Western Branch. Surface velocity magnitude RMS differences caused by ship berthing (Figure 28 compared to Figure 12) shows only a very small change in the area impacted. Bottom velocity magnitude RMS differences (shown in Figure 29 with ships and Figure 13 without ships) also shows very small areas (i.e., several model cells) with changes in only the lowest legend class size (2-4 cm/sec). Surface and bottom residual velocity magnitude average differences (Figures 30-31 with ships and Figures 14-15 without ships) show only very subtle changes in the shapes of

areas with the lowest differences (1-3 cm/sec for the surface layer and 1-5 cm/sec for the bottom layer). Sedimentation potential difference due to ship berthing, shown by comparing Figure 32 to Figure 16, appears to have almost no impact.

One caution to this analysis technique should be emphasized. As we compare differences in time series (either RMS or simple differences), we know these differences result from both amplitude and phase change.

The spatial distributions of the case comparison differences discussed in this section can be compared in the qualitative sense. They show regions of maximum change and the important gradients between these regions and those unaffected by expansion. An attempt to quantify these results involves the analysis described in the next section.

2. Percentile Analysis – In order to quantify these differences derived from the case comparisons, a technique using percentile analysis was incorporated. By dividing the aforementioned differences into class intervals and plotting the spatial accumulation as a percentage of the entire model surface area of Hampton Roads, a set of simple histograms can be constructed such as those shown in the Appendix to Chapter III, Section A.2, Figures 1-32.

Figures 1-32 are comprised of 8 figures for each case comparison in numerical order (i.e., Eastward Expansion vs. Base Case are Figures 1-8, Eastward Expansion plus APM dredging (Case 1) vs. Base Case are Figures 9-16, Eastward Expansion plus Dredging plus Berthing of Ship (Case 2a) vs. Base Case are Figures 17-24, Eastward Expansion plus Dredging plus Berthing of Ship (Case 2b) vs. Base Case are Figures 25-32). The 8 figures present the order of state variables in the sequence of the last section.

1) RMS difference of tidal elevation
2-4) average difference of surface and bottom salinity, respectively
4-6) RMS difference of surface and bottom velocity magnitude, respectively
6-8) average difference of surface and bottom residual velocity magnitude, respectively
8) sedimentation potential difference

As with the range of legend intervals of the spatial plots discussed in the last section, the range of class intervals for each variable was selected to be large enough to contain the maximum variability encountered for all the case comparisons. An example of a histogram plot is given below to facilitate discussion. For each of the histograms shown in Figures 1-32, the class interval area is a maroon bin whose percentile value is shown on the left vertical axis. The blue curve plotted shows the cumulative percent of all bins and its value is shown on the right vertical axis.

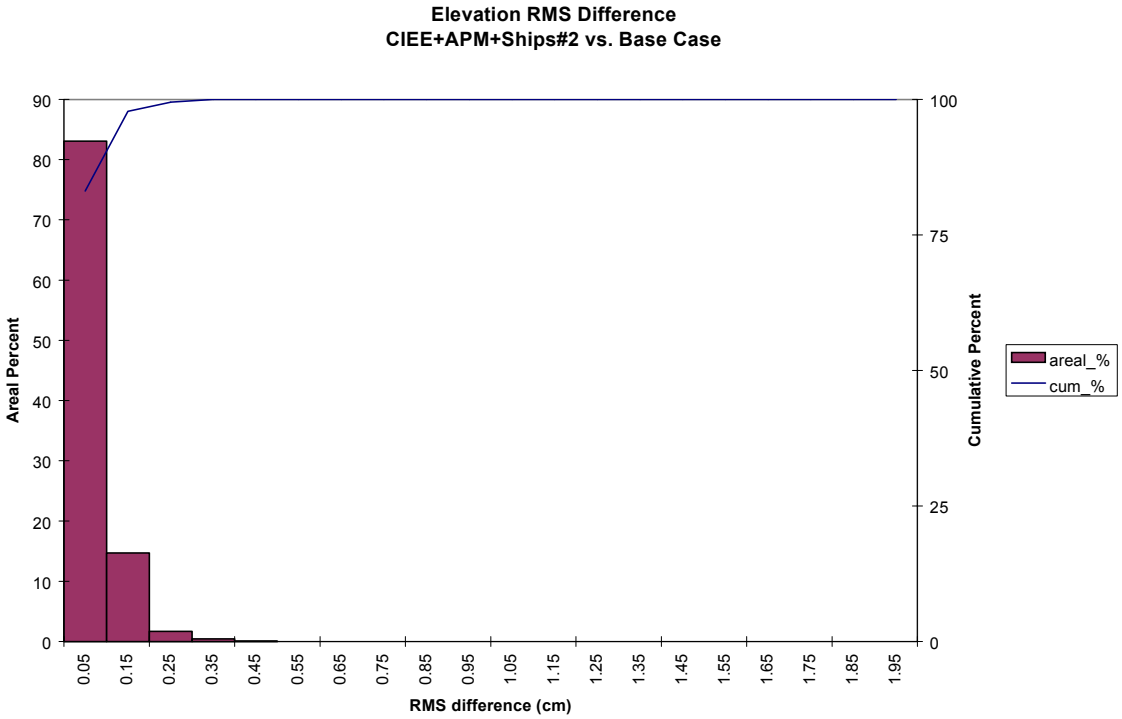

Figure III.1. Example histogram used in percentile analysis.

B. COMPARISON TO VALUES FOR ORIGINAL EXPANSION OPTIONS

To facilitate quantitative comparisons among the results of various scenario runs and the original Craney Island expansion options, a quantity was extracted from each of the histograms presented in the Appendix to Chapter III, Section A.2. The quantity is the 95th percentile value. Taking Figure III.1 for an example, as the cumulative percentage curve crosses the 95th percentile, the corresponding difference value (i.e., 0.14 cm) is the 95th percentile value. By definition, it is exceeded by only 5% of the total area under consideration.

Tables III.1 shows the 95th percentile values for the Eastward Expansion, the Eastward Expansion plus the APM Terminal dredging, and these two combined with both ship berthing tests. Dredging was shown to have a relatively small impact. Both APM terminal dredging and the berthing of ships had minimal impact on either surface elevation or sedimentation potential. The berthing of ships at CIEE has a localized effect on the salinity distribution, and to a lesser extent, the velocity distribution.

Tables III.2 shows the 95th percentile values of this cumulative impact against values from other land expansion options. The cumulative far-field impacts resulting from both dredging and ship berthing occurred on velocity and salinity distributions, but their magnitudes were less than those of the previously studied land expansions.

Table III.1. The 95th percentile values for selected model variables for each Test Case versus the Base Case, Single Variable Runs.

Global Change – 95th Percentile (5% of area contains change greater than value listed)				
Single Variable - Cumulative Impact of Dredging and Ship Berthing				
Difference (from Base Case):	**Eastward Expansion Only**	**Eastward + APM Dredging**	**Eastward + APM dredging + triangular ships**	**Eastward + APM dredging + square ships**
Surface Elevation	0.14 cm	0.13 cm	0.13 cm	0.14 cm
Surface Current	2.4 cm/s	2.4 cm/s	2.5 cm/s	**2.6 cm/s**
Bottom Current	1.6 cm/s	1.7 cm/s	2.1 cm/s	**2.5 cm/s**
Surface Salinity	0.00 ppt	0.10 ppt	0.15 ppt	**0.19 ppt**
Bottom Salinity	0.00 ppt	0.06 ppt	0.10 ppt	**0.15 ppt**
Sedimentation Potential	0.08 %	0.08 %	0.09 %	**0.10 %**

Table III.2. The 95th percentile values for the Cumulative Test Case and Previously Evaluated Land Expansions versus the Base Case.

Global Change – 95th Percentile (5% of area contains change greater than value listed)					
Single Variable - Comparison to Prior Land Expansion Options					
Difference (from Base Case):	**Eastward Expansion Only**	**Eastward + Dredging + Square Ships**	**Westward Expansion Only**	**Northward Expansion Only**	**North+eastward Expansion Only**
Surface Elevation	0.14 cm	0.14 cm	0.34 cm	1.00 cm	**1.04 cm**
Surface Current	2.4 cm/s	2.6 cm/s	5.3 cm/s	**12.3 cm/s**	11.7 cm/s
Bottom Current	1.6 cm/s	2.5 cm/s	3.3 cm/s	**7.8 cm/s**	6.6 cm/s
Surface Salinity	0.00 ppt	0.19 ppt	0.12 ppt	**0.71 ppt**	0.23 ppt
Bottom Salinity	0.00 ppt	0.15 ppt	0.35 ppt	**1.00 ppt**	0.23 ppt
Sedimentation Potential	0.08 %	0.10 %	2.8 %	**8.9 %**	6.3 %

C. FLUSHING CHARACTERISTICS

One of the most important aspects of the hydrodynamic circulation in the Elizabeth River is its overall flushing capability. As was done in the original hydrodynamic modeling study (Wang et al., 2001), the capability of the model to simulate a dye (tracer) release was utilized to evaluate overall flushing rates and residence times for the Test Cases under evaluation.

1. Simulated Dye Release from the Southern Branch - A unit mass of a neutrally buoyant tracer was released in the Southern Branch near the Jordan Bridge (see Figure III.2). The tracer was released instantaneously near the end of flood tide and its concentration was calculated by the mass-balance equation as the model simulation advanced. This was done for the cumulative Test Case (eastward expansion plus APM Terminal dredging plus ships (Case 2b)) and compared with earlier tests for flushing capability for the Base Case and the eastward expansion alone.

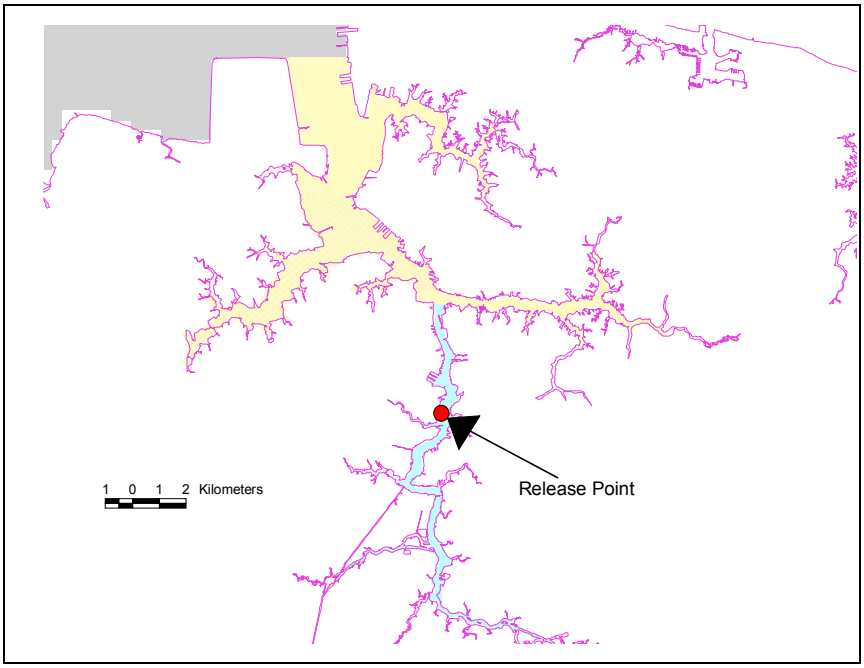

Figure III.2. Location of tracer release in the Southern Branch near the Jordan Bridge.

2. Impact of flushing for the Southern Branch - Figure III.3 shows time series plots of the total mass of dye in the Southern Branch as it decreases after its release. Its half-life period can be seen to be about 6.5 days for all cases shown. Flushing is not reduced as a result of the combined dredging and berthing of ships.

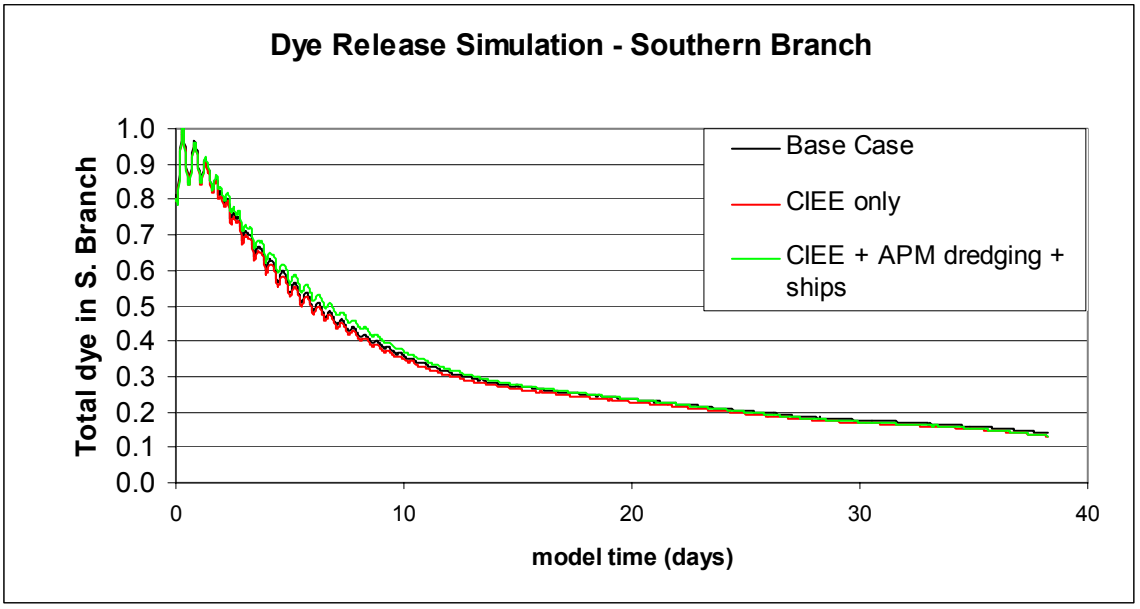

Figure III.3. Time series of dye mass in the Southern Branch for the Base Case (blue), the Eastward Expansion only (red), and the cumulative impact of Eastward Expansion, APM terminal dredging, and ship berthing (green).

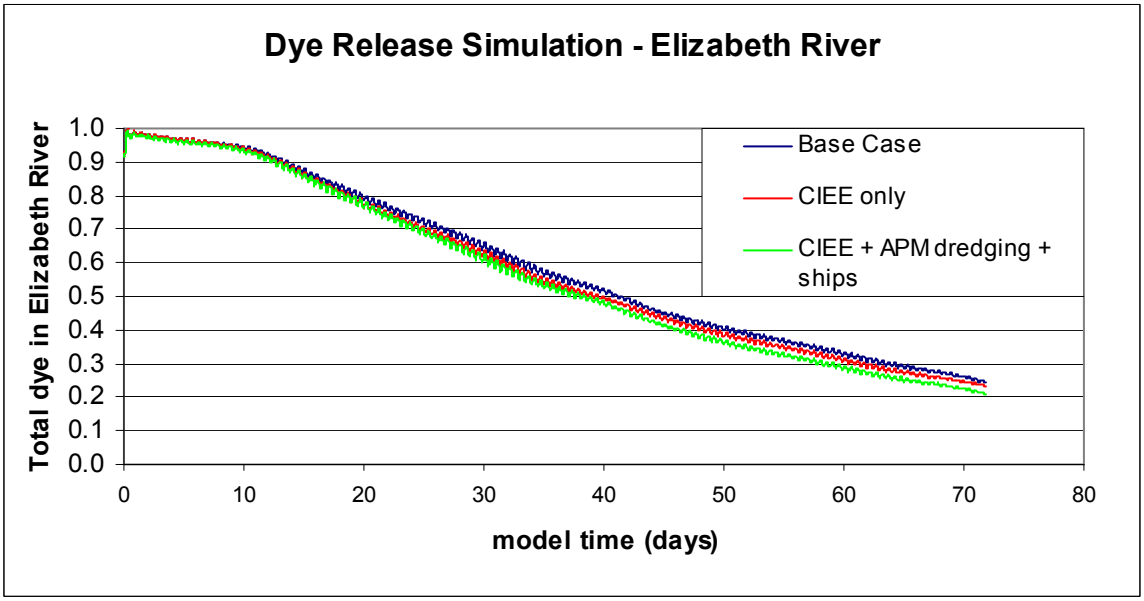

Figure III.4. Time series of dye mass in the Elizabeth River for the Base Case (blue), the Eastward Expansion only (red), and the cumulative impact of Eastward Expansion, APM terminal dredging, and ship berthing (green).

3. Impact of flushing for the entire Elizabeth River - The time series plots of the dye remaining in the Elizabeth River are shown in Figure III.4. Here, the half-life period is about 42.5 days. As with the Southern Branch, there appears to be no adverse effect on flushing capability for the entire Elizabeth River due to the combined effect of dredging and ship berthing.

CHAPTER IV. THE RESULTS FOR THE HISTORICAL RUN

The second of the two types of scenario simulation comparisons performed in this project involved a real-time simulation incorporating all available input conditions (discharge at 8 locations, winds, and open boundary tidal elevation and salinity specifications). This simulation was done for the 180-day period corresponding to Julian days 60-240 of calendar year 2000 (i.e., March 1 to August 27). A single historical run was made, incorporating the cumulative impacts of the Eastward Expansion, the APM Terminal dredging, and the berthing of ships (Case 2b).

From within this simulation period, three 7-day event periods were selected to represent the relatively extreme conditions of 'high discharge event' [Julian days 111-117], 'high wind event' [Julian days 149-155], and 'low discharge event' [Julian days 197-203]. A time series plot of discharge measurements upstream at Richmond is shown in Figure IV.1 and a time series of wind measured at Sewells Pt., VA is shown in Figure IV.2.

Whereas the duration of these events varied, the period of analysis for comparing the Test Case to the Base Case was kept constant at 7 days.

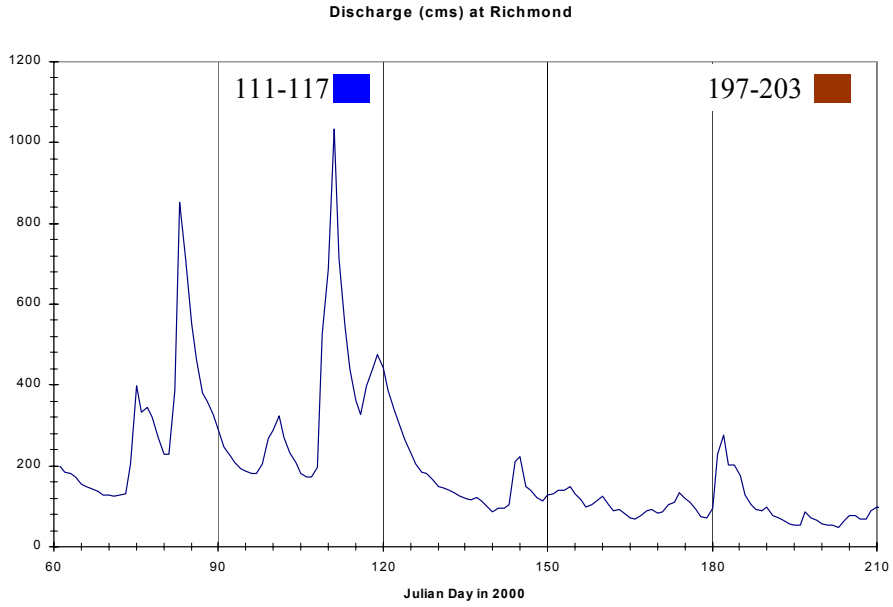

Figure IV.1. Discharge measured at Richmond, VA

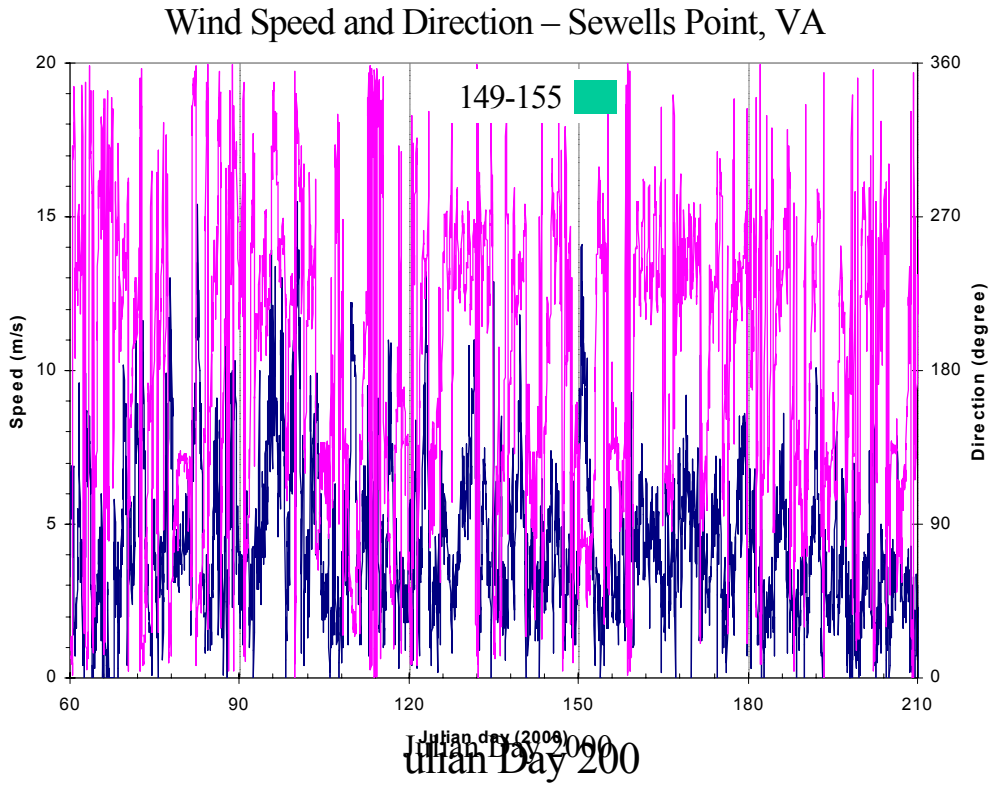

Figure IV.2. Wind measured at Sewells Pt., VA.

A. GLOBAL COMPARISONS

Here, the reader is referred to Chapter III, Section A for a general discussion of global analysis as it was performed for the single variable runs. The difference in its use for this historical simulation is that, for the test case compared to the Base Case, it was applied separately to the 3 event periods in the comparison. Therefore, the number of data points used is 336 (the number of half-hour intervals in a week), rather than 1776 as used for the single variable scenarios.

1. Spatial Distribution – Again, the reader is referred to Chapter III, Section A.1 for a general discussion of spatial plotting of differences of selected state variables between the test case and the Base Case.

Due to the incorporation of the Eastward Expansion into the cumulative test case, spatial plots of the historical simulation results for this land expansion alone (as reported by Wang et al., 2001) are also presented for comparison to the cumulative impacts shown subsequently. Therefore, it is noted here that the total number of spatial plots is 48,

which results from 2 case comparisons each having 3 events with each event involving the following 8 spatial plots:

1) RMS difference of surface elevation
2-3) average difference of surface and bottom salinity, respectively
4-5) RMS difference of surface and bottom velocity magnitude, respectively
6-7) average difference of surface and bottom residual velocity magnitude, respectively
8) sedimentation potential difference between test case and Base Case

These spatial plots are shown in Figures 1-48 of Appendix to Chapter V, Section A.1. The sequence of presentation within this Appendix is as follows:

Eastward Expansion vs. Base Case	high discharge	Figures 1-8
Eastward Expansion vs. Base Case	low discharge	Figures 9-16
Eastward Expansion vs. Base Case	high wind	Figures 17-24
Cumulative (CIEE, Dredging, ships) vs. Base Case	high discharge	Figures 25-32
Cumulative (CIEE, Dredging, ships) vs. Base Case	low discharge	Figures 33-40
Cumulative (CIEE, Dredging, ships) vs. Base Case	high wind	Figures 41-48

The differences were plotted for each of the case/event comparisons. Below is a summary of the findings in each:

Eastward Expansion vs. Base Case (High Discharge Event) – Plots contrasting the Eastward Expansion against the Base Case for the high discharge event are shown in Figures 1-8 of the Appendix to Chapter IV, Section A.1. For surface elevation (Figure 1), all RMS average differences fall below 0.25 cm except for a small area adjacent to the proposed expansion option, where differences above 0.25 cm are shown in pink. Average differences in surface salinity (Figure 2) fall below ±0.2 ppt everywhere except directly adjacent to the expansion option. Bottom salinity average differences (Figure 3) are everywhere under ±0.2 ppt except in small areas around the option and northward in the Norfolk Harbor Channel where differences range to ±1.0 ppt. Surface velocity magnitude differences (Figure 4) and bottom velocity magnitude differences (Figure 5) reach 12 cm/sec and 8 cm/sec, respectively, near the eastward expansion but are limited to 4 cm/sec in the far field. Surface and bottom residual velocity magnitude differences (Figures 6 and 7) show, respectively, limits of ±5 cm/sec and ±3 cm/sec in areas immediately adjacent to the structure. Sedimentation potential difference from the Base Case is plotted in Figure 8, impacting a very small area north of the expansion option0 with a difference of about ±10%.

Eastward Expansion vs. Base Case (Low Discharge Event) – Plots contrasting the Eastward Expansion against the Base Case for the low discharge event are shown in Figures 9-16 of the Appendix to Chapter IV, Section A.1. For surface elevation (Figure 9), all RMS average differences fall below 0.25 cm except for a small area adjacent to the expansion option, where differences above 0.25 cm are shown in pink. Average differences in surface salinity (Figure 10) fall below ±0.2 ppt everywhere except directly adjacent to the expansion option. Bottom salinity average differences (Figure 11) are

everywhere under ±0.2 ppt except in small areas around the option where differences range to ±1.0 ppt. Surface velocity magnitude differences (Figure 12) and bottom velocity magnitude differences (Figure 13) reach 12 cm/sec and 8 cm/sec, respectively, near the eastward expansion but are limited to 4 cm/sec in the far field. Surface and bottom residual velocity magnitude differences (Figures 14 and 15) show, respectively, limits of ±5 cm/sec and ±3 cm/sec in areas immediately adjacent to the structure. Sedimentation potential difference from the Base Case is plotted in Figure 16, impacting a very small area north of the expansion option with a difference of about ±10%.

Eastward Expansion vs. Base Case (High Wind Event) – Plots contrasting Case 2 against the Base Case for the high wind event are shown in Figures 17-25 of the Appendix to Chapter IV, Section A.1. For surface elevation (Figure 17), all RMS average differences fall below 0.25 cm except for small areas northeast of the Eastward Expansion and in the headlands of the Southern and Eastern Branches, where differences above 0.25 cm are shown in pink. Average differences in surface salinity (Figure 18) fall below ±0.6 ppt everywhere except directly adjacent to the expansion. Bottom salinity average differences (Figure 19) are everywhere under ±0.2 ppt except in small areas around the option where differences range to ±1.0 ppt. Surface velocity magnitude differences (Figure 20) and bottom velocity magnitude differences (Figure 21) reach 12 cm/sec and 8 cm/sec, respectively, near the Eastward Expansion but are limited to 4 cm/sec in the far field. Surface and bottom residual velocity magnitude differences (Figures 22 and 23) show, respectively, limits of ±10 cm/sec and ± 3 cm/sec in areas immediately adjacent to the structure. Sedimentation potential difference from the Base Case is plotted in Figure 24, impacting a very small area north of the expansion option with a difference of about ±10%.

Cumulative Test Case (CIEE plus APM Dredging plus Ship Berthing) vs. Base Case (High Discharge Event) – Plots contrasting this cumulative test case against the Base Case for the high discharge event are shown in Figures 25-32 of the Appendix to Chapter IV, Section A.1. For surface elevation (Figure 25), all RMS average differences fall below 0.25 cm except for a small area northeast of the Eastward Expansion, where differences above 0.25 cm are shown in pink. Average differences in surface salinity (Figure 26) fall below ±0.6 ppt everywhere except in areas adjacent to the Eastward Expansion option and the APM Terminal site. Bottom salinity average differences (Figure 27) are everywhere under ±1.0 ppt except in very small areas around both sites. Surface velocity magnitude differences (Figure 28) reaches 20 cm/sec in a very small area north of the Eastward Expansion but is limited to 4 cm/sec in the far field. Bottom velocity magnitude differences (Figure 29) reach about 8 cm/sec near both sites but are limited to 4 cm/sec in the far field. Surface and bottom residual velocity magnitude differences (Figures 30 and 31) show limits of ± 5 cm/sec and ±3 cm/sec, respectively, in areas near both sites and along the Norfolk Harbor Channel. Sedimentation potential difference

from the Base Case is plotted in Figure 32, impacting primarily a very small area north of the expansion option and extending along the Norfolk Harbor Channel with a difference of about ±10%.

Cumulative Test Case (CIEE plus APM Dredging plus Ship Berthing) vs. Base Case (Low Discharge Event) – Plots contrasting this cumulative test case against the Base Case for the low discharge event are shown in Figures 33-40 of the Appendix to Chapter IV, Section A.1. For surface elevation (Figure 33), all RMS average differences fall below 0.25 cm except for a small area mainly east of the expansion option, where differences above 0.25 cm are shown in pink. Average differences in surface salinity (Figure 34) fall below ±0.6 ppt everywhere except directly adjacent to the Eastward Expansion and the dredge area. Bottom salinity average differences (Figure 35) are everywhere under ±1.0 ppt except in small areas around both sites. Surface velocity magnitude differences (Figure 36) and bottom velocity magnitude differences (Figure 37) are limited to 4 cm/sec in the far field. Surface and bottom residual velocity magnitude differences (Figures 38 and 39) show limits of about ±5 cm/sec and ±3 cm/sec, respectively, in areas not immediately adjacent to either site. Sedimentation potential difference from the Base Case is plotted in Figure 40, impacting primarily a very small area north of the Eastward Expansion with a difference of about ±10%.

Cumulative Test Case (CIEE plus APM Dredging plus Ship Berthing) vs. Base Case (High Wind Event) – Plots contrasting this cumulative test case against the Base Case for the high wind event are shown in Figures 41-48 of the Appendix to Chapter IV, Section A.1. For surface elevation (Figure 41), all RMS average differences fall below 0.25 cm for small areas just north of the Eastward Expansion and in the upper headlands of the Southern and Eastern Branches, where differences above 0.25 cm are shown in pink. Average differences in surface salinity (Figure 42) fall below ±0.6 ppt everywhere except directly adjacent to the Eastward Expansion or the dredge site. Bottom salinity average differences (Figure 43) are everywhere under ±1.0 ppt except in very small areas coincident with both sites. Surface velocity magnitude differences (Figure 44) and bottom velocity magnitude differences (Figure 45) reach 16 cm/sec and 12 cm/sec, respectively, near the Eastward Expansion but are limited to 4 cm/sec in the far field. Surface and bottom residual velocity magnitude differences (Figures 46 and 47) show limits of ±10 cm/sec and ± 3 cm/sec, respectively, in areas immediately adjacent to the structure. Sedimentation potential difference from the Base Case is plotted in Figure 48, impacting primarily an area north of the expansion option with a difference of about ±10%.

The spatial distributions of the case comparison differences are useful in delineating areas of maximum impact and yet, they are qualitative in nature. An attempt to quantify this analysis is described in the next section.

2. Percentile Analysis – As was done to compare the single variable test cases against the single variable base case (see Chapter III, Section A.2), the differences of historical test case results from the Base Case results were divided into class intervals. Then each interval's accumulated spatial distribution was plotted as a percentage of the entire model surface area of Hampton Roads. In this fashion, a set of simple histograms showing the distribution of class interval differences of all variables can be constructed, as shown in the Appendix to Chapter IV, Section A.2, Figures 1-48.

For each of the 3 events of the 2 test cases compared to the base case, a histogram was provided for each of the following 8 selected differences in this specified sequence:

1) RMS difference of surface elevation
2-3) average difference of surface and bottom salinity, respectively
4-5) RMS difference of surface and bottom velocity magnitude, respectively
6-7) average difference of surface and bottom residual velocity magnitude, respectively
8) sedimentation potential difference between test case and Base Case

The differences for the high discharge, low discharge, and high wind events comparing the Eastward Expansion to the Base Case are shown, respectively, in Figures 1-8, 9-16, and 17-24. Retaining this sequence of these events, those comparing the cumulative test case to the base case are shown in Figures 25-48. For each of the histograms shown in Figures 1-48, the class interval area is a maroon bin whose percentile value is shown on the left vertical axis, whereas the blue curve plotted shows a cumulative percentage of all bins the value of which is shown on the right vertical axis.

B. COMPARISON TO VALUES FOR ORIGINAL EXPANSION OPTIONS

In order to assess the impacts of dredging and ship berthing during extreme conditions, the historical run was conducted testing the cumulative impact of the CIEE land expansion, the dredging of the Maersk Terminal area, and the berthing of ships. In the historical run simulation scenario, the impacts of dredging and ship berthing are tested against extreme conditions comprised of high and low discharge and high wind during a six-month simulation for which the input variables (i.e., discharges, wind, boundary conditions) are taken from historical records. Its impact was compared with those of two expansion options: Option 7 (eastward expansion) and Option 7/5a (combined eastward and westward expansion). As in the single variable runs, little change was noted in historical run of this cumulative test case while comparing with Option 7. Comparing the results to those of Option 7/5a, the changes were slightly greater in salinity, but less for all other parameters compared.

A final step in comparing the impacts from the different test cases is to construct a table with the 95^{th} percentile values of the aforementioned cumulative curves, as shown in Table IV.1. As was seen in the summary table for single variable runs, there was minimal change in the in the 95^{th} percentile values for surface elevation and sedimentation potential and only small increases for both salinity and velocity for the events of high discharge, low discharge, and high wind.

Table IV.1. The 95th percentile values for selected state variables for the Cumulative Test Case and Previously Evaluated Land Expansions versus the Base Case.

Global Change – 95th Percentile (5% of area contains change greater than value listed)			
Historical – High Discharge Event			
Difference (from Base Case):	**Eastward Expansion Only**	**Eastward + Dredging + Square Ships**	**Eastward-Westward Expansion Only**
Surface Elevation	0.20 cm	0.20 cm	0.33 cm
Surface Current	5.5 cm/s	5.9 cm/s	6.7 cm/s
Bottom Current	2.7 cm/s	3.6 cm/s	3.7 cm/s
Surface Salinity	0.00 ppt	0.08 ppt	0.02 ppt
Bottom Salinity	0.00 ppt	0.09 ppt	0.07 ppt
Sedimentation Potential	1.0 %	1.1 %	1.9 %
Historical – Low Discharge Event			
Difference (from Base Case):	**Eastward Expansion Only**	**Eastward + Dredging + Square Ships**	**Eastward-Westward Expansion Only**
Surface Elevation	0.14 cm	0.14 cm	0.33 cm
Surface Current	2.7 cm/s	3.0 cm/s	4.3 cm/s
Bottom Current	1.9 cm/s	2.7 cm/s	2.9 cm/s
Surface Salinity	0.00 ppt	0.12 ppt	0.04 ppt
Bottom Salinity	0.01 ppt	0.16 ppt	0.09 ppt
Sedimentation Potential	0.9 %	1.0 %	2.8 %
Historical – High Wind Event			
Difference (from Base Case):	**Eastward Expansion Only**	**Eastward + Dredging + Square Ships**	**Eastward-Westward Expansion Only**
Surface Elevation	0.21 cm	0.21 cm	0.46 cm
Surface Current	2.2 cm/s	2.8 cm/s	5.0 cm/s
Bottom Current	1.5 cm/s	2.4 cm/s	3.0 cm/s
Surface Salinity	0.00 ppt	0.09 ppt	0.00 ppt
Bottom Salinity	0.00 ppt	0.11 ppt	0.02 ppt
Sedimentation Potential	0.8 %	0.9 %	1.7 %

CHAPTER V. CONCLUSIONS

For the additional assessments of the CIEE using the VIMS 3D Hydrodynamic Eutrophication Model (HEM-3D), 4 model scenario runs were conducted. Scenario 1 was for the model testing of the cumulative impact of the CIEE expansion and the deepening of the Maersk Terminal using *single variable runs* (using a single variable, tidal range, for model input). Scenario 2 was model testing of these combined alterations further combined with ship berthing at both the CIEE and the Maersk Terminal facilities. Scenario 3 was model testing of this cumulative impact (CIEE land expansion, Maersk Terminal dredging, and ship berthing at both facilities) using a *historical run* (using multiple variables in real time for model input). Scenario 4 tested a dye release in the Southern Branch using the simulated dye release feature of the model to compare the flushing capability both within the Southern Branch and for the entire Elizabeth River.

In order to compare quantitatively the impacts of dredging and ship berthing over the far-field, including the areas of Hampton Roads and the Elizabeth River, the approach was to use a global analysis methodology. This was done by determining percentages of total area associated with class intervals of change from the Base Case as differences in water surface elevation, surface and bottom salinity, surface and bottom current magnitude, surface and bottom residual current magnitude, and sedimentation potential.

From single variable runs (Scenarios 1 and 2) it is shown that both the APM terminal dredging and the berthing of ships had minimal impact on either surface elevation or sedimentation potential. The berthing of ships at CIEE, if considered permanent, has a local effect on the salinity distribution, and to a lesser extent, the velocity distribution. Comparison was made between the cumulative impacts resulting from both the APM dredging and ship berthing and the previously evaluated land expansion options. Impacts occurred on velocity and salinity distributions, but their magnitudes were less than those of the previously studied land expansion options.

For local analysis, flushing tests (Scenario 3) revealed that neither the flushing of the Southern Branch nor that of the entire Elizabeth showed any detectable adverse response from the combined effects of the APM terminal dredging and ship berthing. This is consistent with the findings made in the study of the Elizabeth River Hydrodynamic and Water Quality Modeling Final Report (CH2MHILL, 2002).

In order to assess the impacts of dredging and ship berthing during extreme conditions, the historical run (Scenario 4) was conducted testing the cumulative impact of the CIEE land expansion, the dredging of the Maersk Terminal area, and the berthing of ships. In the historical run simulation scenario, the impacts of dredging and ship berthing are tested against extreme conditions comprised of high and low discharge and high wind during a six-month simulation for which the input variables (i.e., discharges, wind, boundary conditions) are taken from historical records. Its impact was compared with those of two expansion options: Option 7 (eastward expansion) and Option 7/5a (combined eastward and westward expansion). As in the single variable runs, little

change was noted in historical run of this cumulative test case while comparing with Option 7. Comparing the results to those of Option 7/5a, the changes were slightly greater in salinity, but less for all other parameters compared.

VI. REFERENCES

Blumberg, A. F., B. Galperin, and D. J. O'Connor (1992): Modeling vertical structure of open channel flows. Journal of Hydraulic Engineering, 118: 1119-1134.

Blumberg, A. F. and G. L. Mellor (1987): A description of a three-dimensional coastal ocean circulation model, in Three-dimensional Coastal Ocean Models, Vol. 4, edited by N. Heaps, American Geophysical Union, Washington, D. C. 208 pp.

Boon, J. D., A. Y. Kuo, H. V. Wang, and J. M. Brubaker (1999): Proposed third crossing of Hampton Roads, James River, Virginia: feature-based criteria for evaluation of model study results. In M. L. Spaulding and H. L. Butler (eds.), ASCE 6th international conference on estuarine and coastal modeling, New Orleans, LA. pp. 223-237.

Boon, J. D., H. V. Wang, S. C. Kim, A. Y. Kuo, and G. M. Sisson (1999): Three Dimensional Hydrodynamic-Sedimentation Modeling Study, Hampton Roads Crossing, Lower James River, Virginia: Report to the Virginia Department of Transportation. Special Report No. 354 in Applied Science and Ocean Engineering, Virginia Institute of Marine Science, Gloucester Point, Virginia. 36pp, 3 Appendices.

Casulli, V. and R. T. Cheng (1993): Semi-implicit finite difference methods for three-dimensional shallow water flow. Inter. J. for numerical Methods in Fluids, Vol. 15, pp 629-648.

CH2MHILL (2002): Elizabeth River Hydrodynamic and Water Quality Modeling: Flushing Analysis for APM Terminals Marine Container Terminal, Portsmouth, Virginia. Final Report prepared for the Williamsburg Environmental Group, 43 pp. and Appendices.

Fang, C. S., B. J. Neilson, A. Y. Kuo, R. J. Byrne, and C. S. Welch (1972): Physical and geological studies of the proposed bridge-tunnel crossing of Hampton Roads near Craney Island. Special Report in Applied Marine Science and Ocean Engineering No. 24, Virginia Institute of Marine Science, Gloucester Point, VA, pp. 199-241.

Galperin, B., L. H. Kantha, D. Hassid, and A. Rosati (1988): A quasi-equilibrium turbulent energy model for geophysical flow. Journal of Atmospheric Science, 45: 55-62.

Hamrick, J. M. (1996): User's manual for the environmental fluid dynamics computer code. Special report in Applied Marine Science and Ocean Engineering No. 331, Virginia Institute of Marine Science, Gloucester Point, VA, 223 pp.

Johnson, B. H., K. W. Kim, R. E. Heath, B. B. Hsieh, and H. L. Butler (1993): Validation of a three-dimensional hydrodynamic model of Chesapeake Bay. Journal of Hydraulic Engineering, 119: 2-20.

Kuo, A. Y., R. J. Byrne, J. M. Brubaker, and J. H. Posenau (1988): Vertical transport across an estuary front. In J. Dronkers and W. van Leussen (eds.), Physical Processes in Estuaries, Springer-Verlag, Berlin, pp. 93-109.

Kuo, A. Y., R. J. Byrne, P. V. Hyer, E. P. Ruzecki, and J. M. Brubaker (1990): Practical Application of Theory for Tidal-Intrusion Fronts. Journal of Waterway, Port, Coastal, and Ocean Engineering, 116(3): 341-361.

Maa, J. P-Y, C. H. Lee, F. J. Chen (1995): VIMS sea carousel: bed shear stress measurements. Marine Geology, 129: 129-136.

Miller, J. L. and A. Valle-Levinson (1996): The effect of bridge piles on stratification in the lower Chesapeake Bay. Estuaries, vol. 19, no. 3, pp. 526-539.

Neilson, B. J. (1975): A water quality study of the Elizabeth River: the effect of the Army Base and Lambert Point STP effluent. Special Report No. 75 in Applied Marine Science and Ocean Engineering, Virginia Institute of Marine Science, Gloucester Point, Virginia. 133 pp.

Nichols, M.M. (1977): Response and recovery of an estuary following a river flood. Journal of Sediment Petrol., vol. 47, pp. 1171-1186.

Oey, L. –Y., G. Mellor, and R. Hires (1985): Three-dimensional simulation of the Hudson-Raritan estuary. Part III: salt flux analyses. Journal of Physical Oceanography 14: 629-645.

Ruzecki, E. P., and W. J. Hargis, Jr. (1988): Interaction between circulation of the estuary of the James River and transport of oyster larvae, In B. J. Neilson, A. Y. Kuo and J. M. Brubaker (eds.), Estuarine Circulation. The Humana Press, Clifton, N. J., pp. 255-278.

Shen, J., J. D. Boon, and A. Y. Kuo (1999): A modeling study of a tidal intrusion front and its impact on larval dispersion in the James River estuary, Virginia. Estuaries 22(3a):681-692.

Shen, J., and A. Y. Kuo (1999): Numerical investigation of an estuarine front and its associated eddy. Journal of Waterway, Port, Coastal, and Ocean Engineering 125(3):127-135.

Sisson, G. M., J. D. Boon, and K. L. Farnsworth (1999): The use of GIS in 3D Hydrodynamic model pre- and post-processing for feature-specific applications. In M. L. Spaulding and H. L. Butler (eds.), ASCE 6th international conference on estuarine and coastal modeling, New Orleans, LA, pp. 538-548.

Stigebrandt, A. (1992): Bridge-induced flow reduction in sea straits with reference to effects of a planned bridge across Öresund, Ambio 21:130-134.

Wang, H. V. and S.-C. Kim (2000): Simulation of Tunnel Island and Bridge Piling Effects in a Tidal Estuary. Estuarine and coastal modeling, proceedings of the 6th International Conference, edited by M. L. Spaulding and H. L. Butler. pp. 250-269.

Wang, H. V., S. C. Kim, J. D. Boon, A. Y. Kuo, G. M. Sisson, J. M. Brubaker, and J. P-Y. Maa (2001): Three Dimensional Hydrodynamic Modeling Study, Craney Island Eastward Expansion, Lower James River and Elizabeth River, Virginia. Final Report to the U.S. Army Corps of Engineers, Norfolk District and the Virginia Port Authority. Special Report No. 372 in Applied Marine Science and Ocean Engineering, Virginia Institute of Marine Science. 158 pp. and Appendices.

APPENDIX to CHAPTER III, SECTION A.1

Global Comparisons of Single Variable Runs

Spatial Distributions

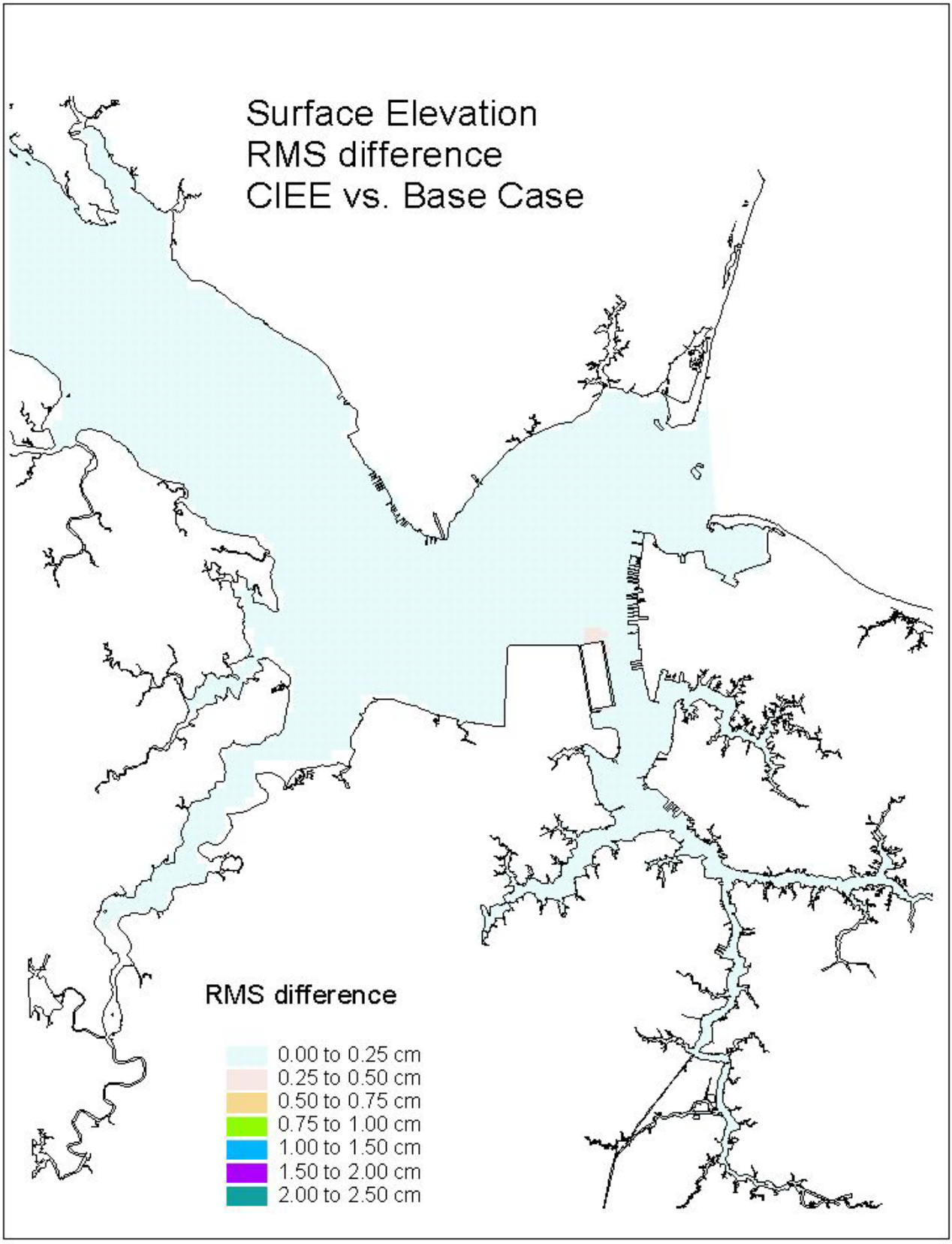

Figure 1. Single variable simulation comparison of surface elevation RMS difference for the Eastward Expansion versus the Base Case.

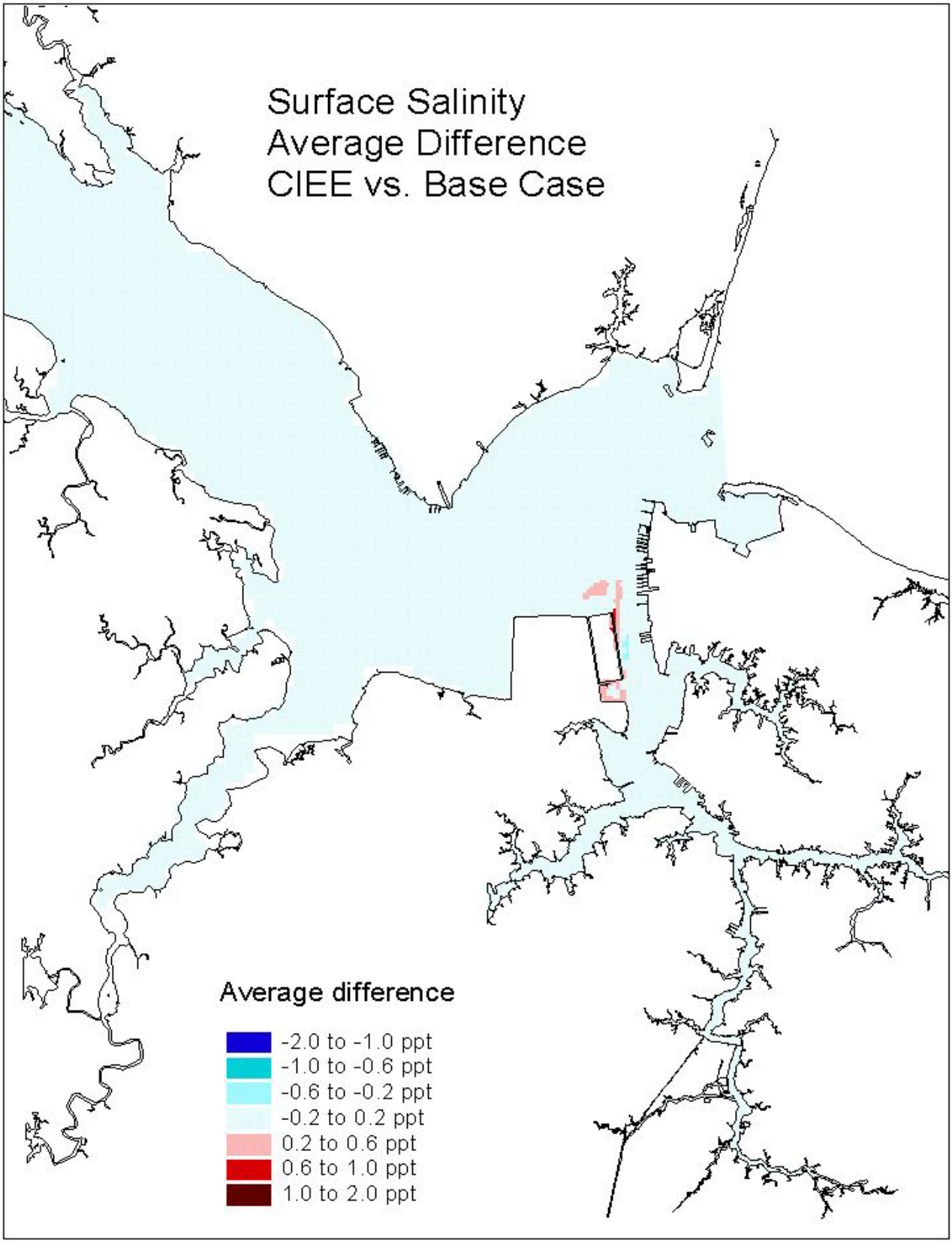

Figure 2. Single variable simulation comparison of the surface salinity average difference for the Eastward Expansion versus the Base Case.

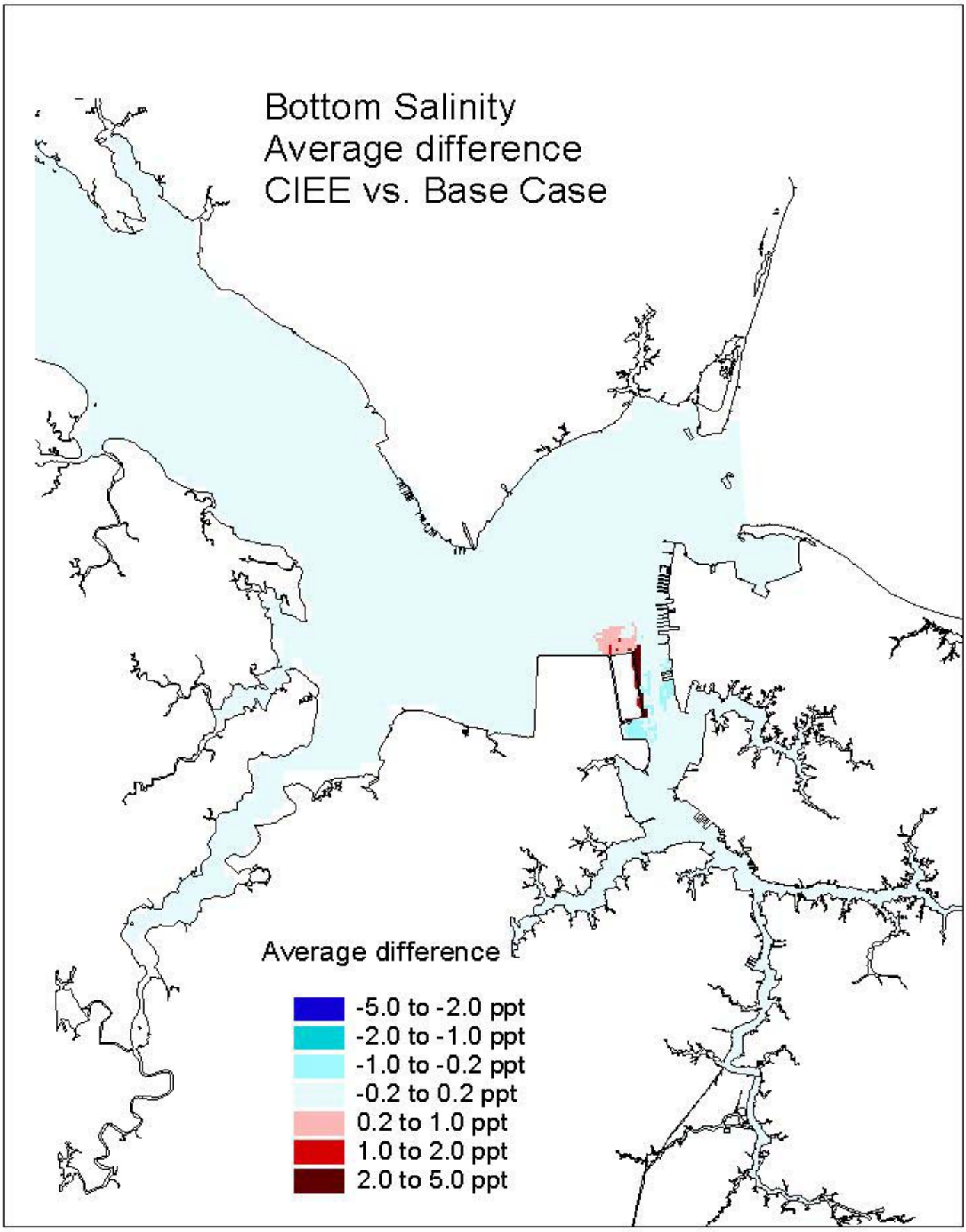

Figure 3. Single variable simulation comparison of the bottom salinity average difference for the Eastward Expansion versus the Base Case.

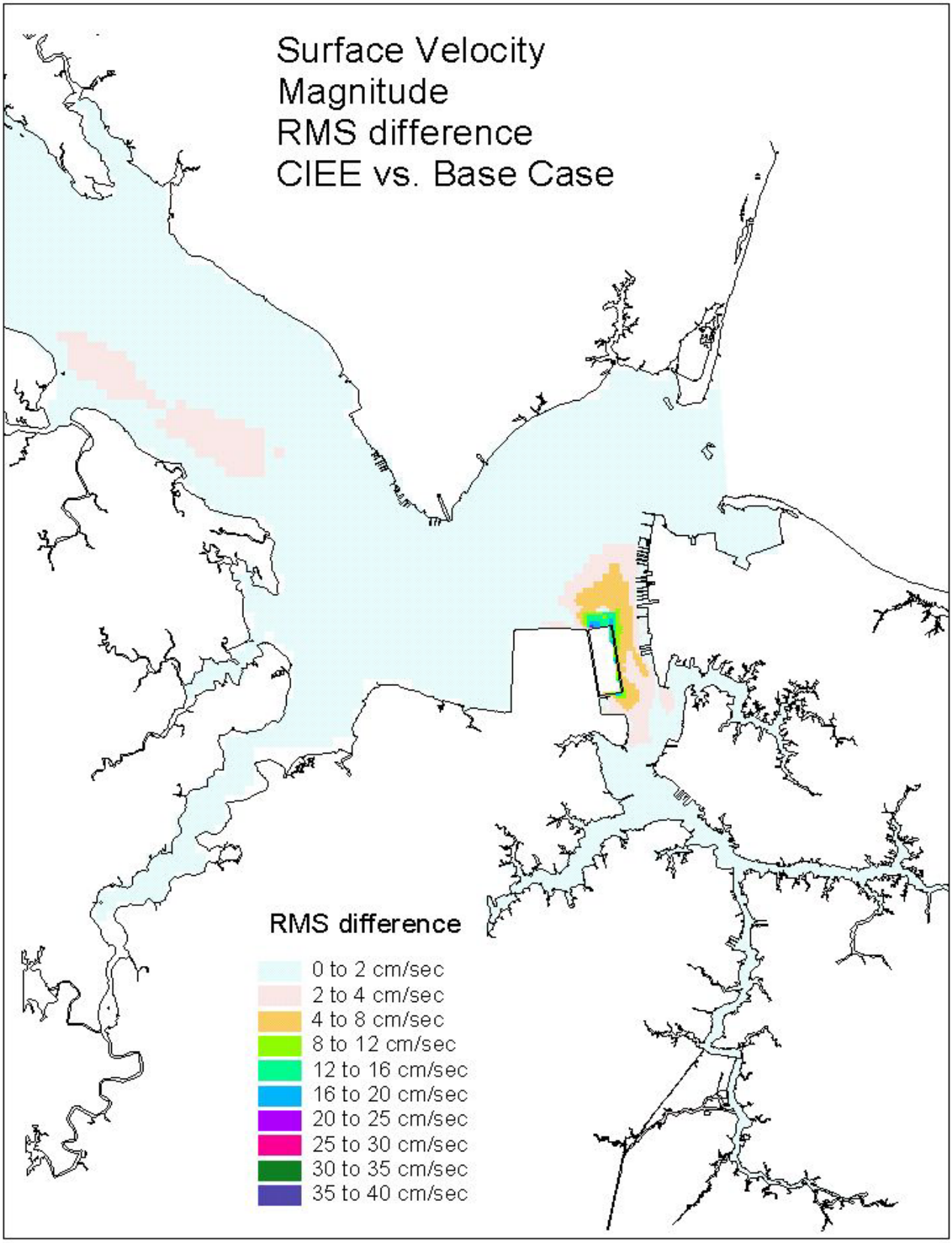

Figure 4. Single variable simulation comparison of the surface velocity RMS difference for the Eastward Expansion versus the Base Case.

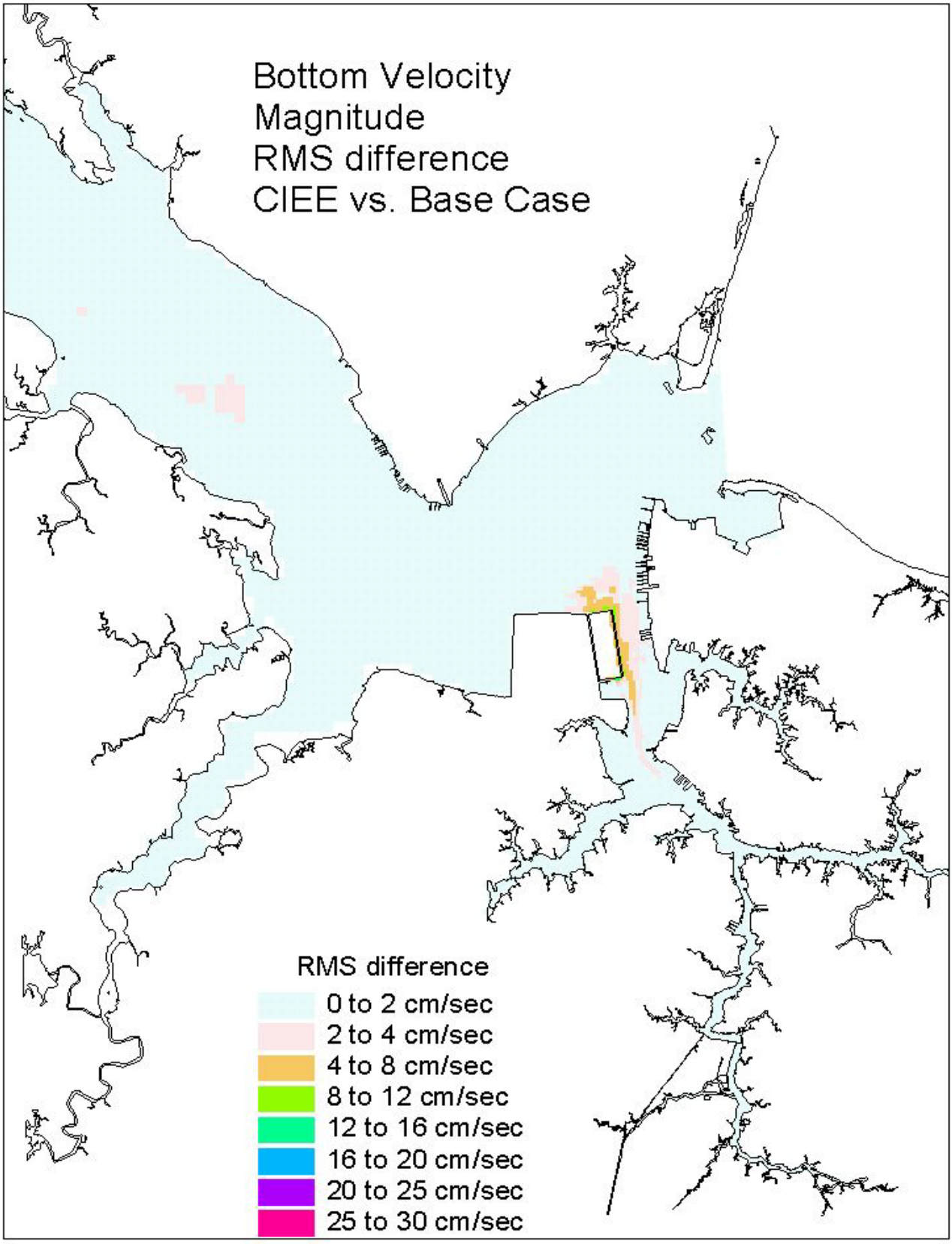

Figure 5. Single variable simulation comparison of the bottom velocity RMS difference for the Eastward Expansion versus the Base Case.

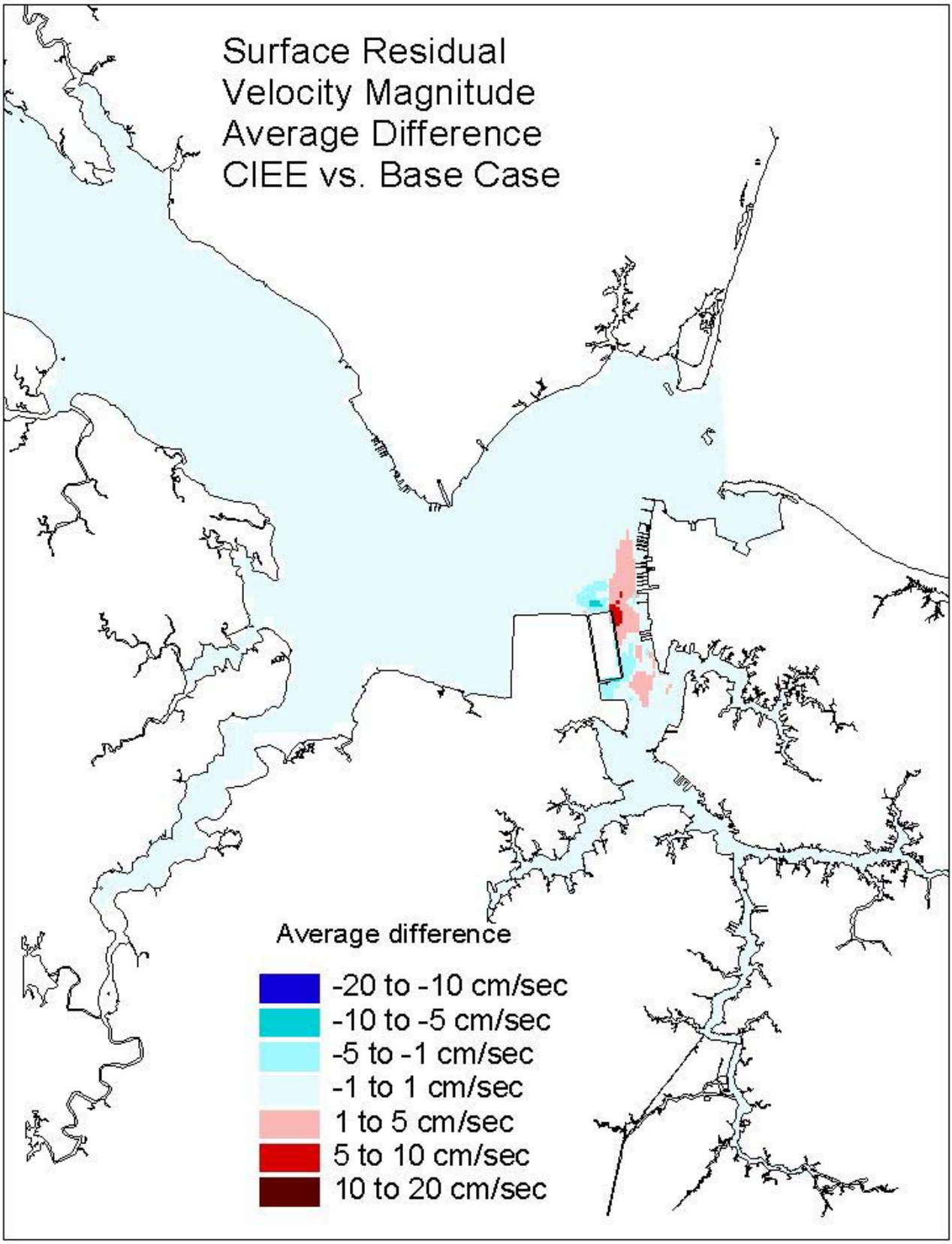

Figure 6. Single variable simulation comparison of the surface residual velocity average difference for the Eastward Expansion versus the Base Case.

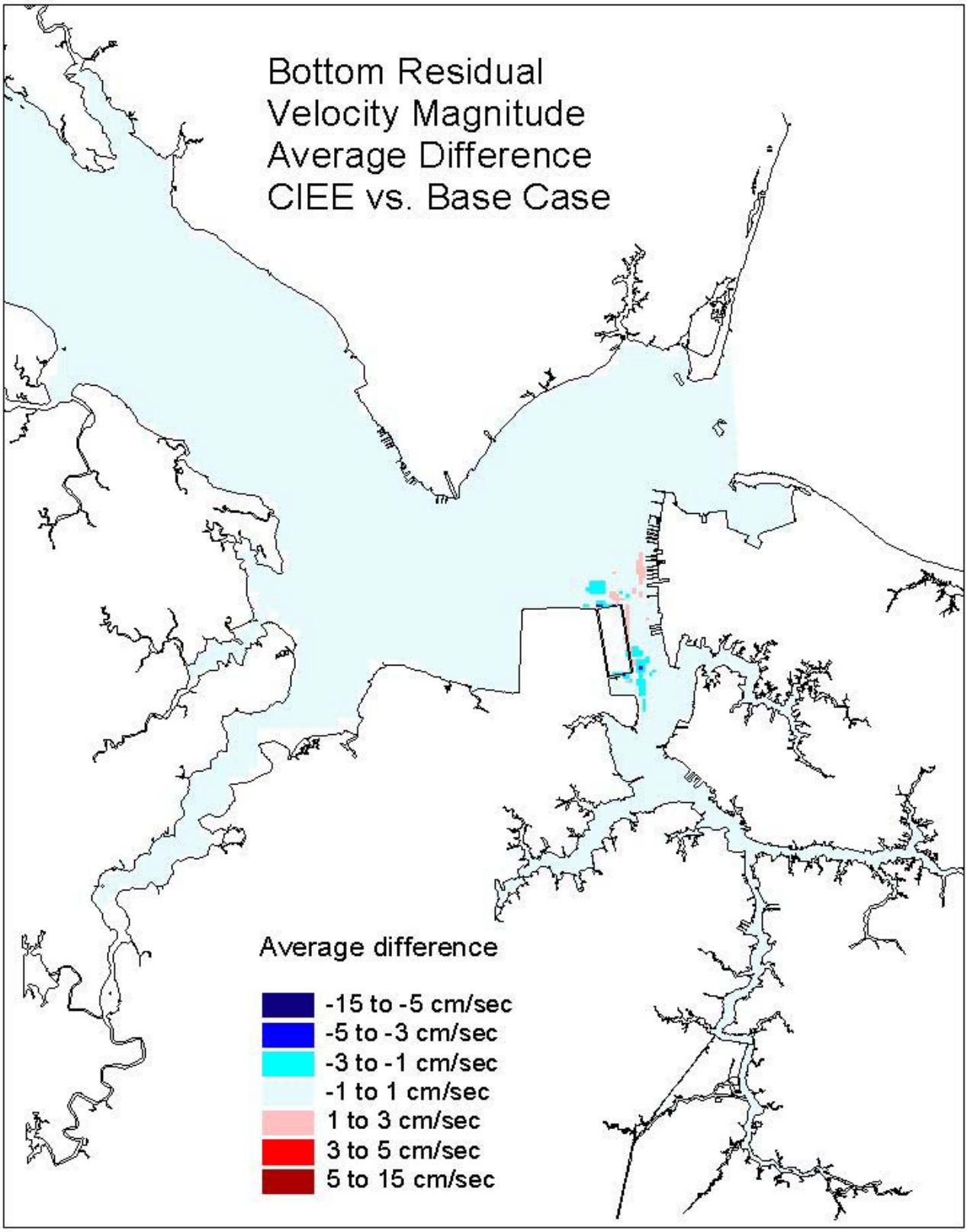

Figure 7. Single variable simulation comparison of the bottom residual velocity average difference for the Eastward Expansion versus the Base Case.

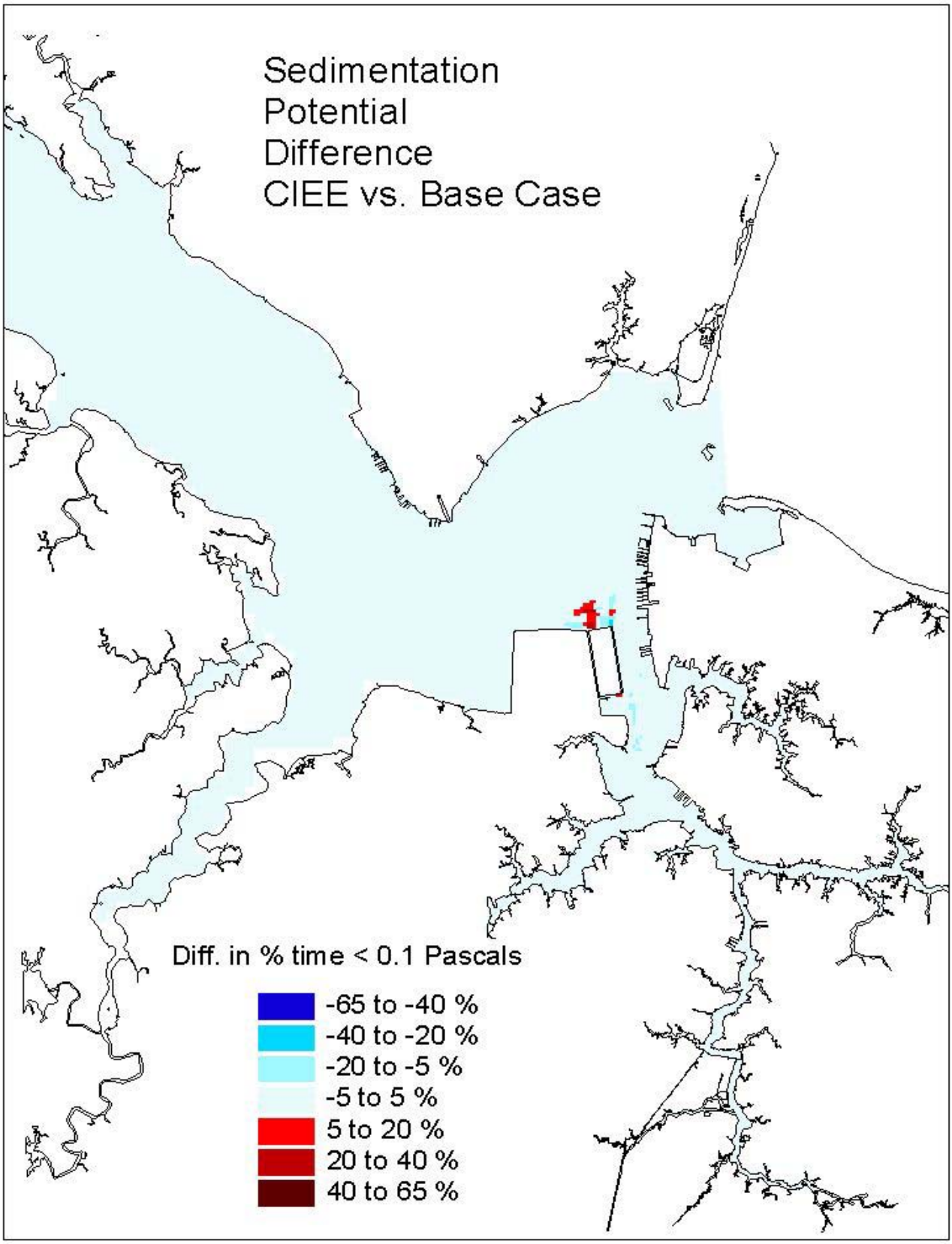

Figure 8. Single variable simulation comparison of the sedimentation potential difference for the Eastward Expansion versus the Base Case.

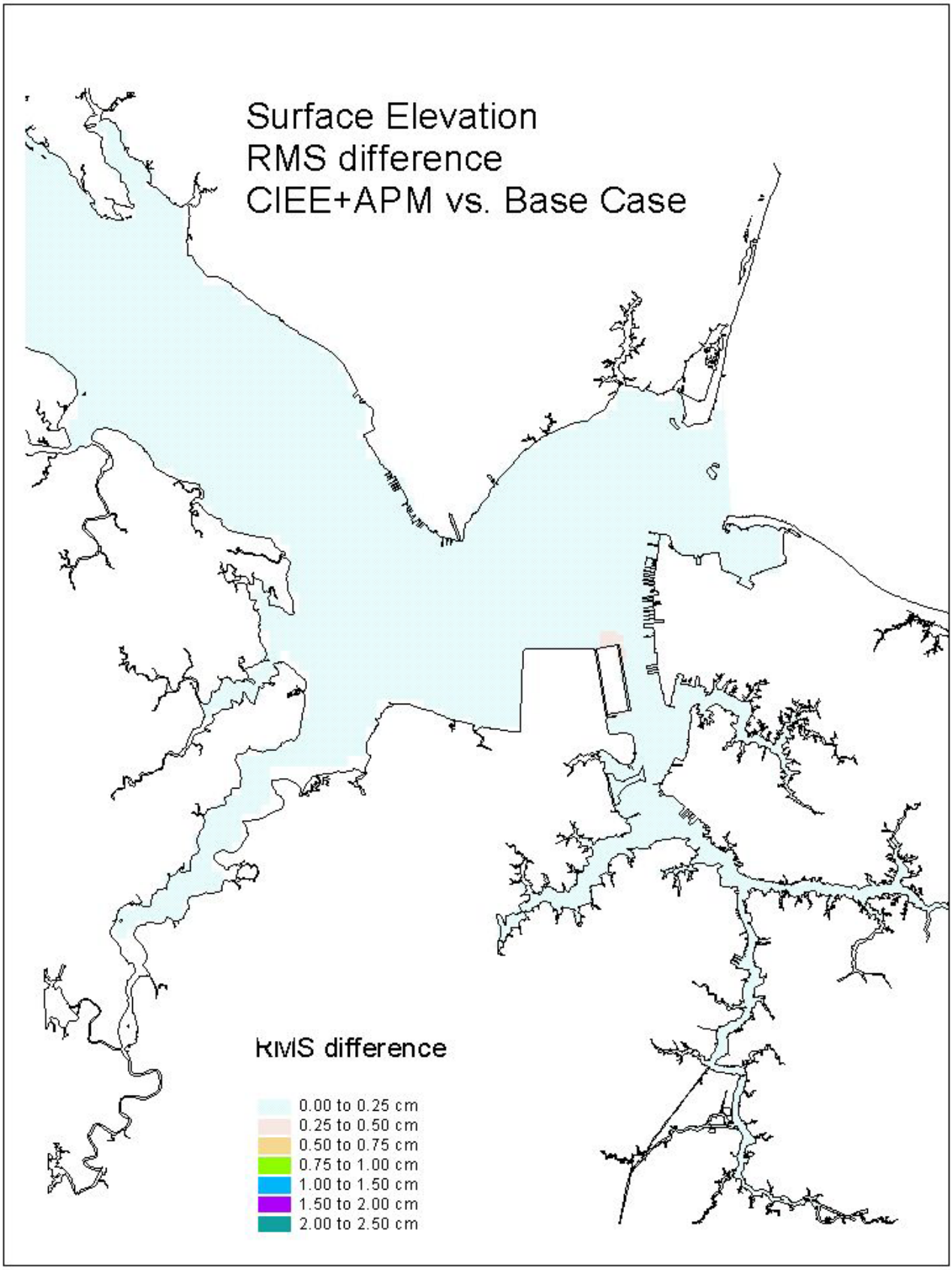

Figure 9. Single variable simulation comparison of the surface elevation RMS difference for the Eastward Expansion plus APM Terminal Dredging versus the Base Case.

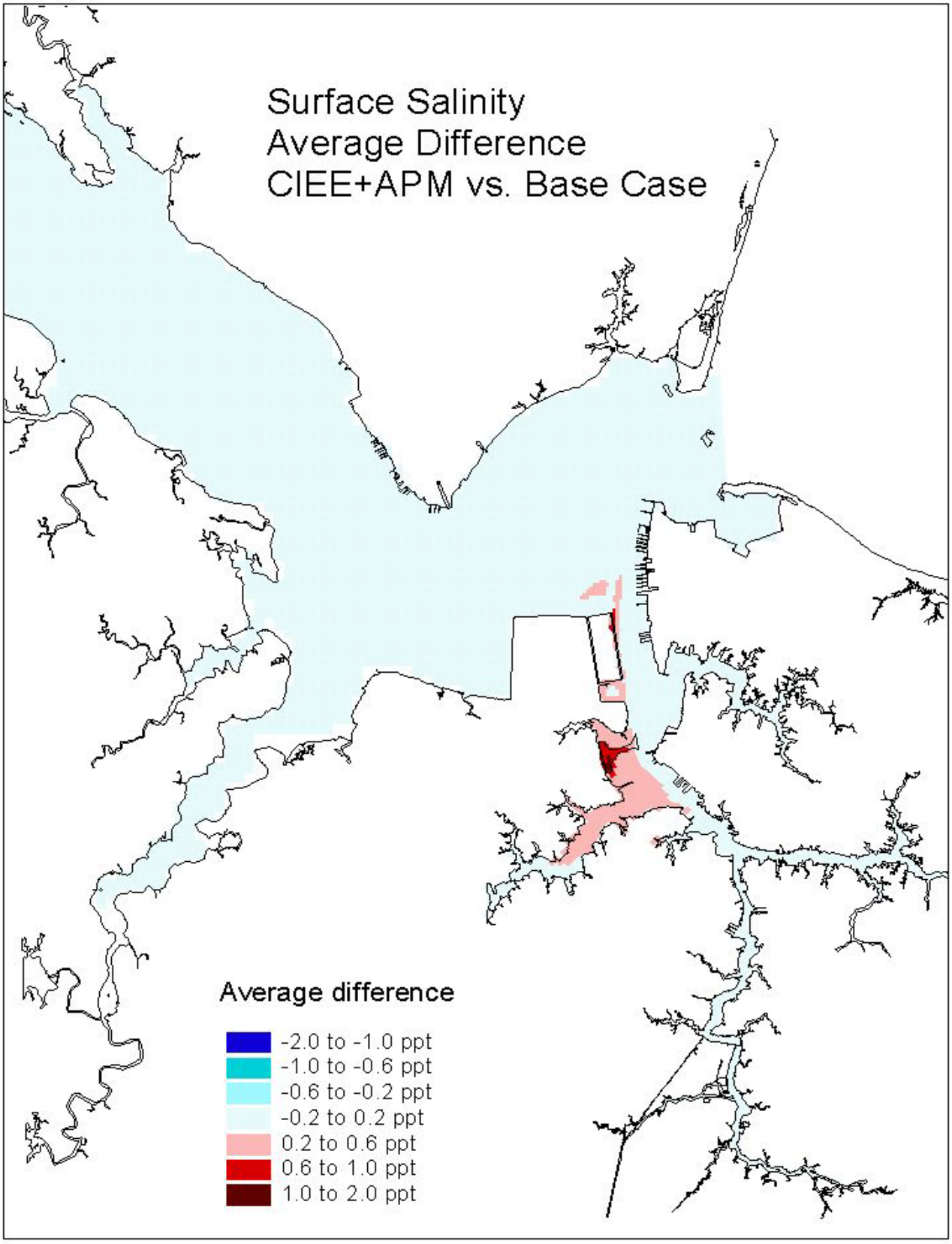

Figure 10. Single variable simulation comparison of the surface salinity average difference for the Eastward Expansion plus APM Terminal Dredging vs. the Base Case.

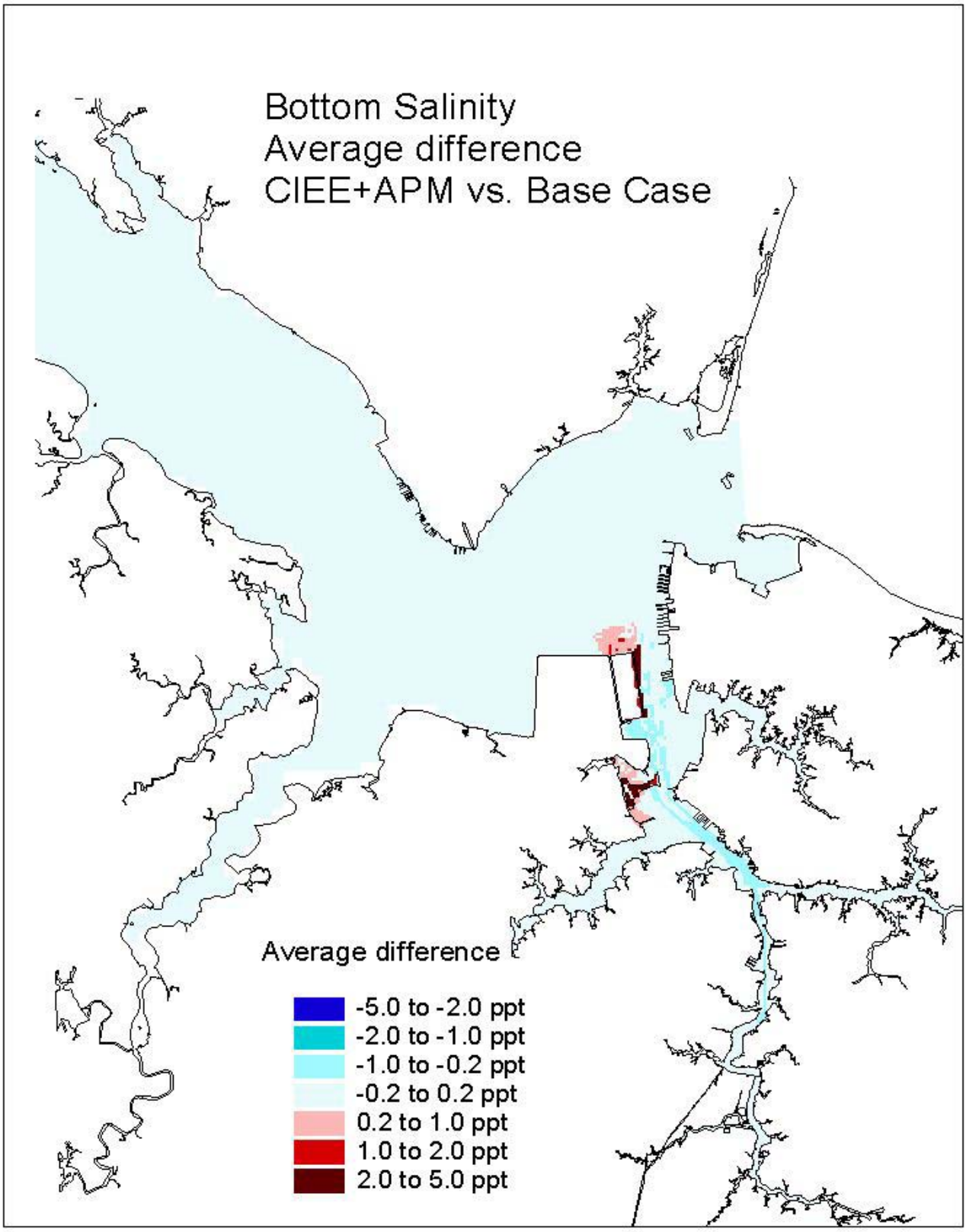

Figure 11. Single variable simulation comparison of the bottom salinity average difference for the Eastward Expansion plus APM Terminal Dredging vs. the Base Case.

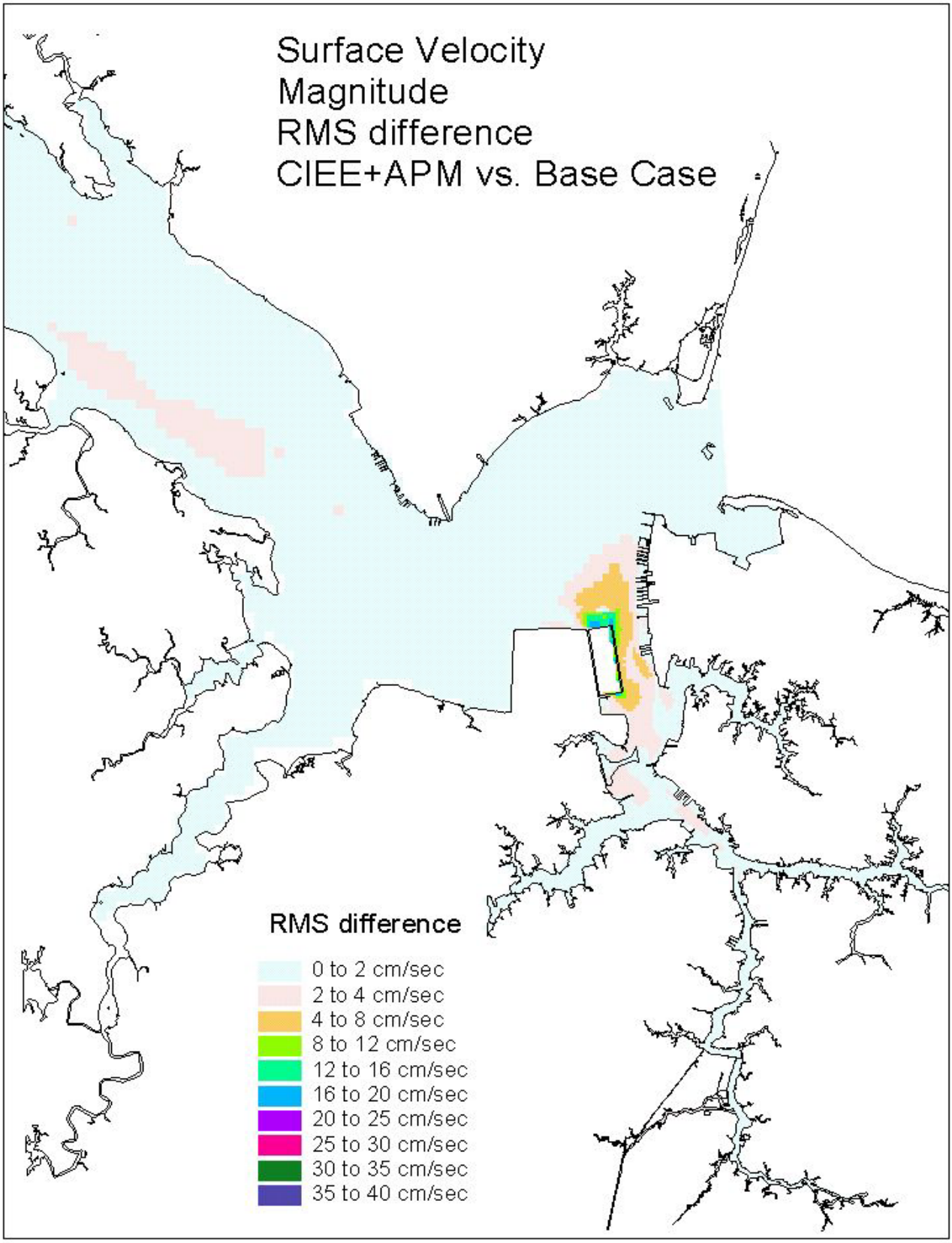

Figure 12. Single variable simulation comparison of the surface velocity RMS difference for the Eastward Expansion plus APM Terminal Dredging versus the Base Case.

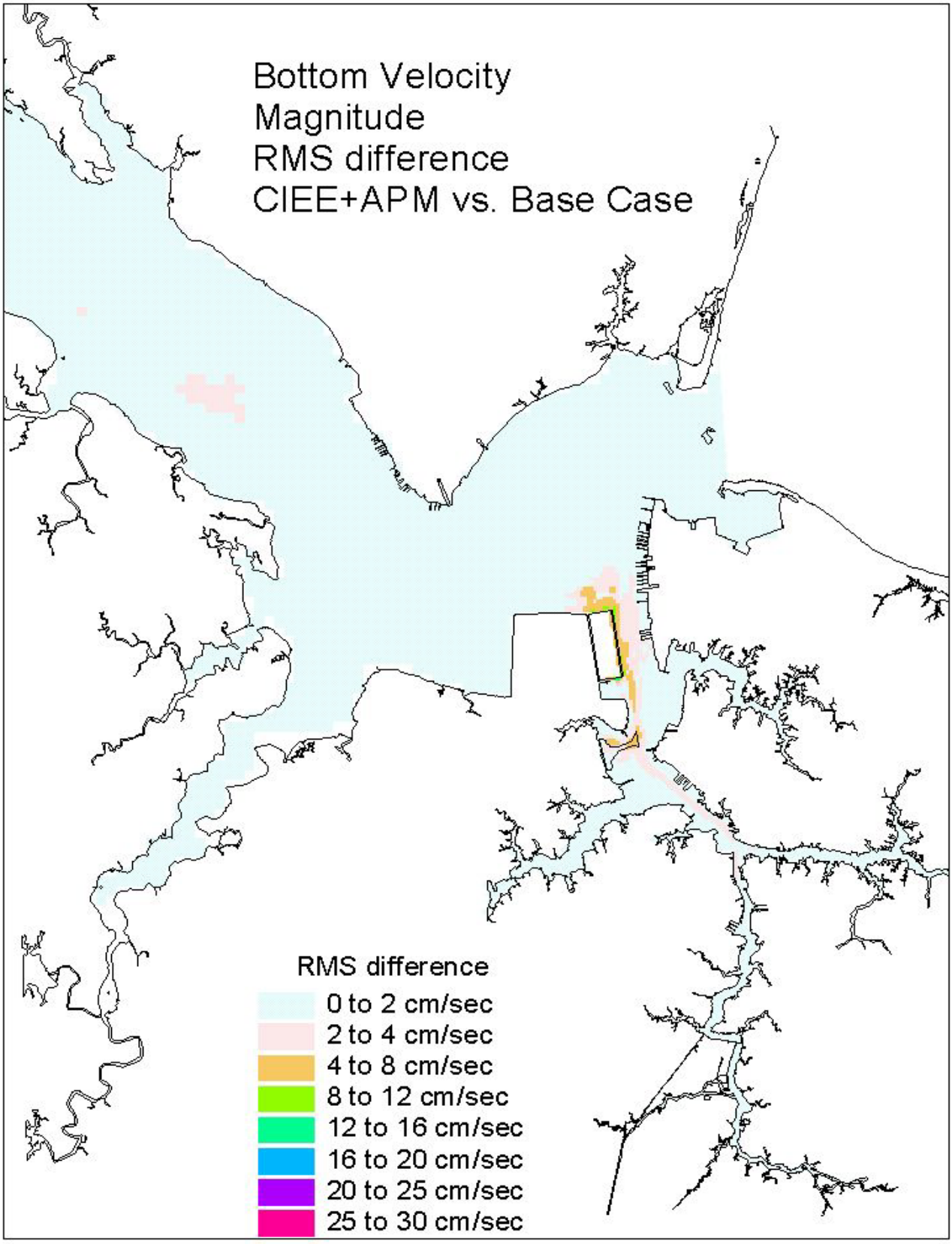

Figure 13. Single variable simulation comparison of the bottom velocity RMS difference for the Eastward Expansion plus APM Terminal Dredging versus the Base Case.

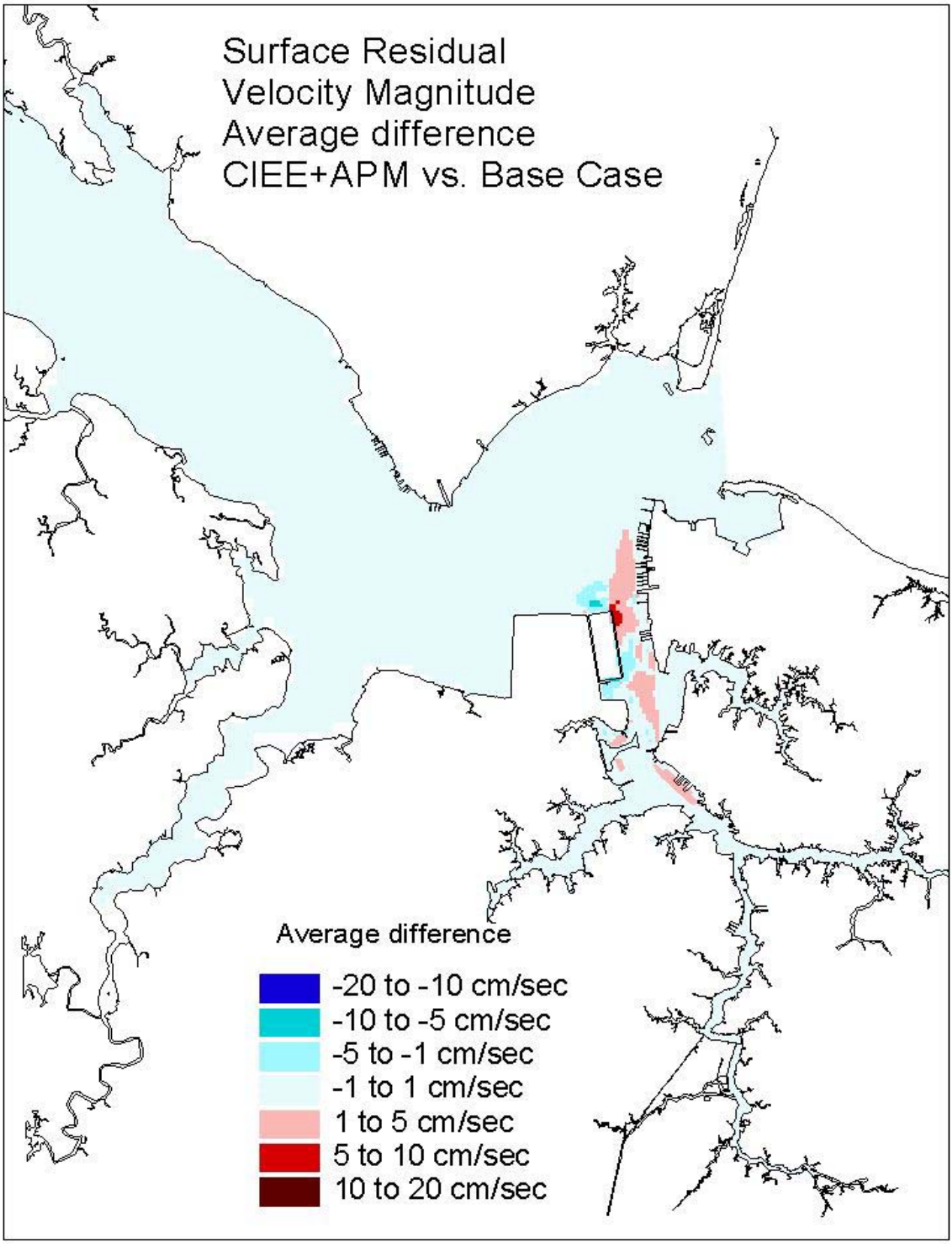

Figure 14. Single variable simulation comparison of the surface residual velocity average difference for the Eastward Expansion plus APM Terminal Dredging vs. the Base Case.

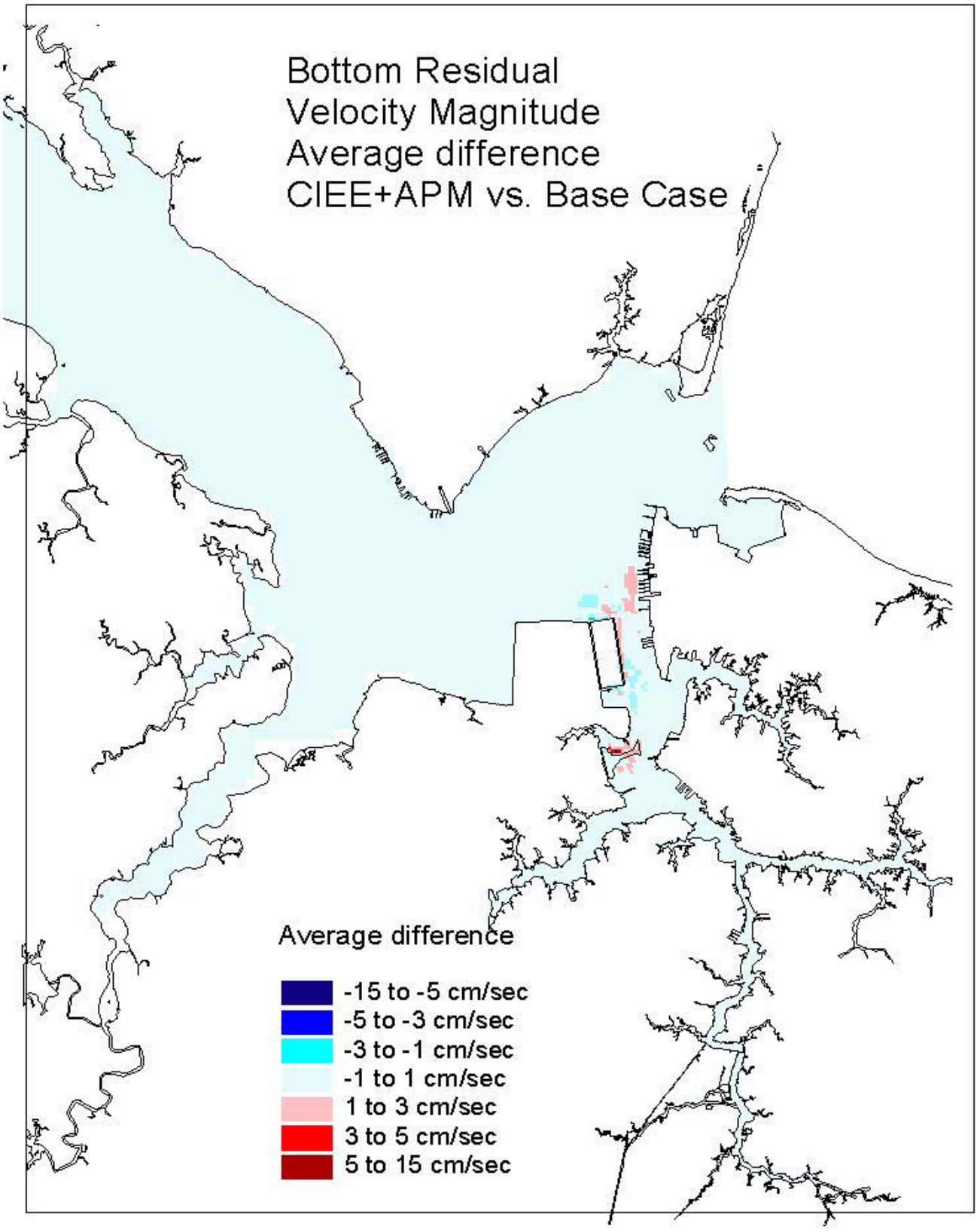

Figure 15. Single variable simulation comparison of the bottom residual velocity average difference for The Eastward Expansion plus APM Terminal Dredging vs. the Base Case.

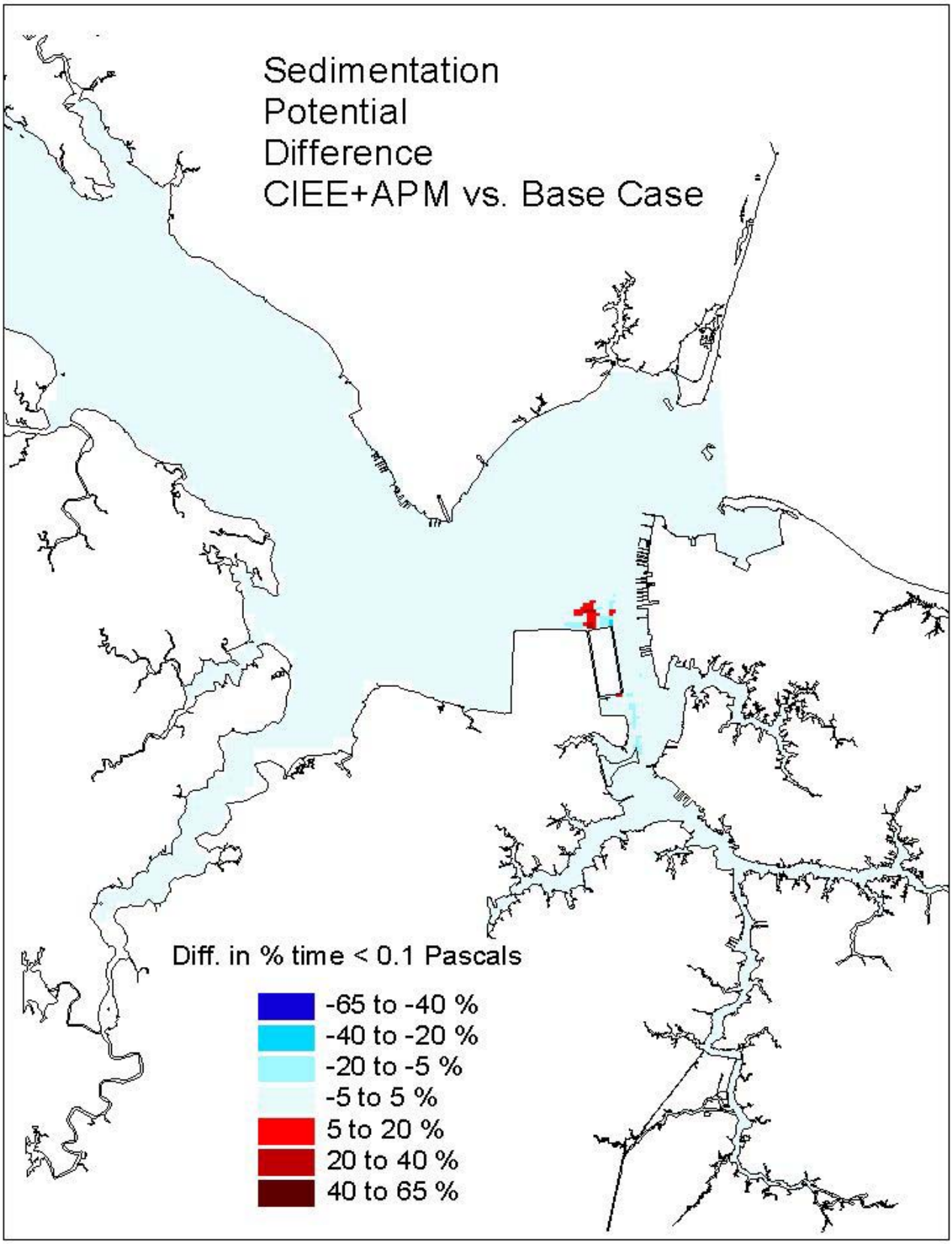

Figure 16. Single variable simulation comparison of the sedimentation potential difference for the Eastward Expansion plus APM Terminal Dredging vs. the Base Case.

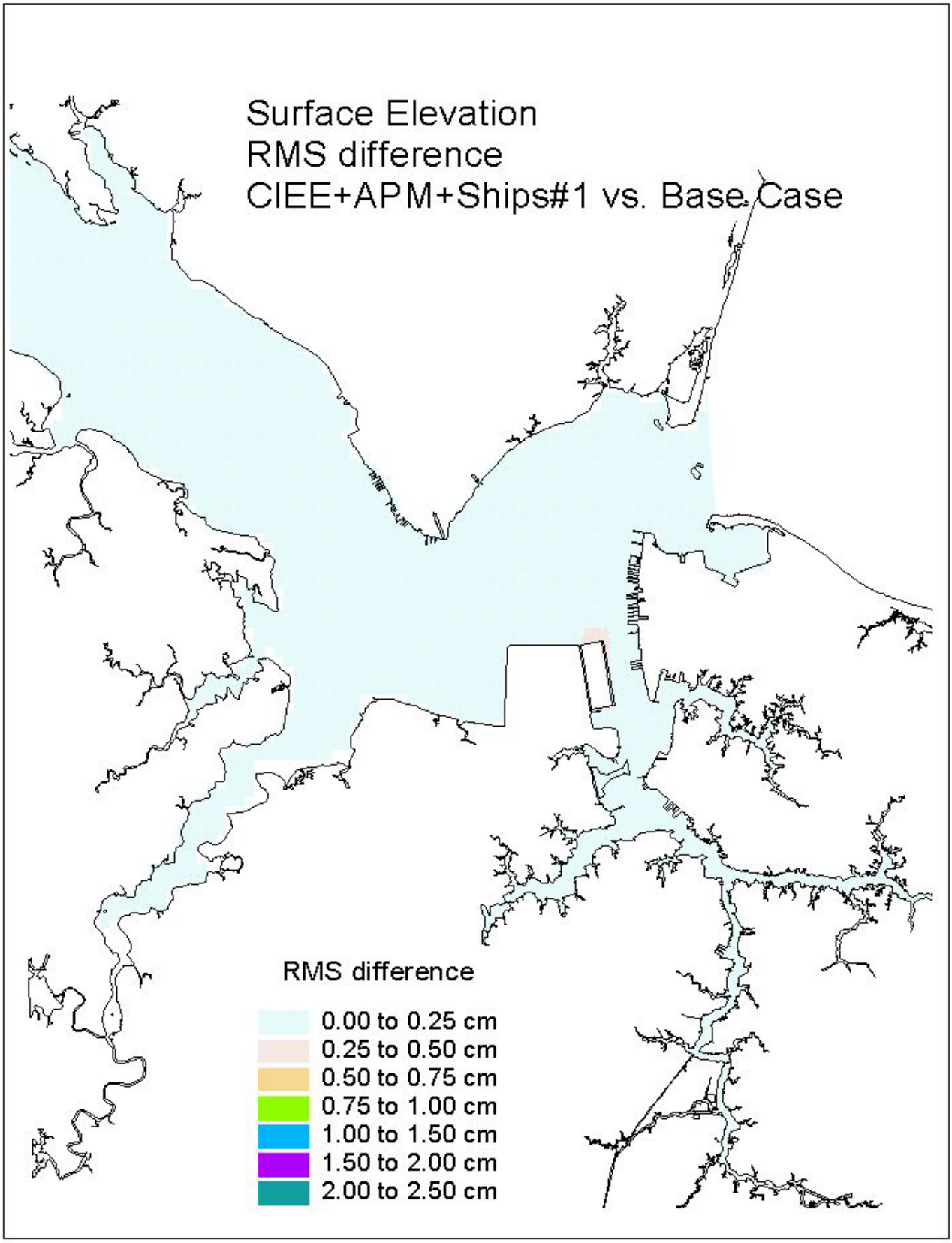

Figure 17. Single variable simulation comparison of the surface elevation RMS difference for the Eastward Expansion plus APM Terminal Dredging plus Ships (Case 2a) versus the Base Case.

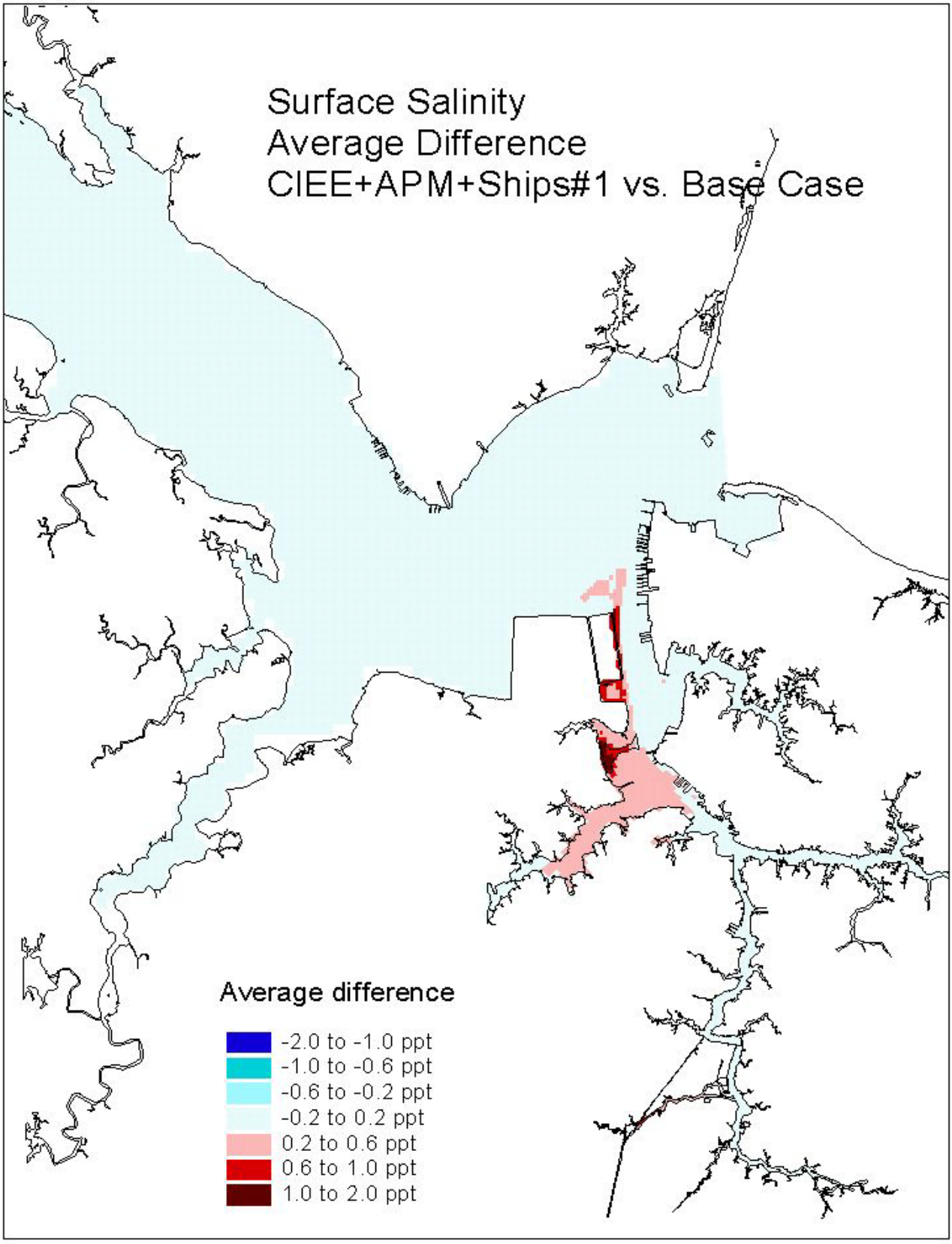

Figure 18. Single variable simulation comparison of the surface salinity average difference for the Westward Expansion plus APM Terminal Dredging plus Ships (Case 2a) versus the Base Case.

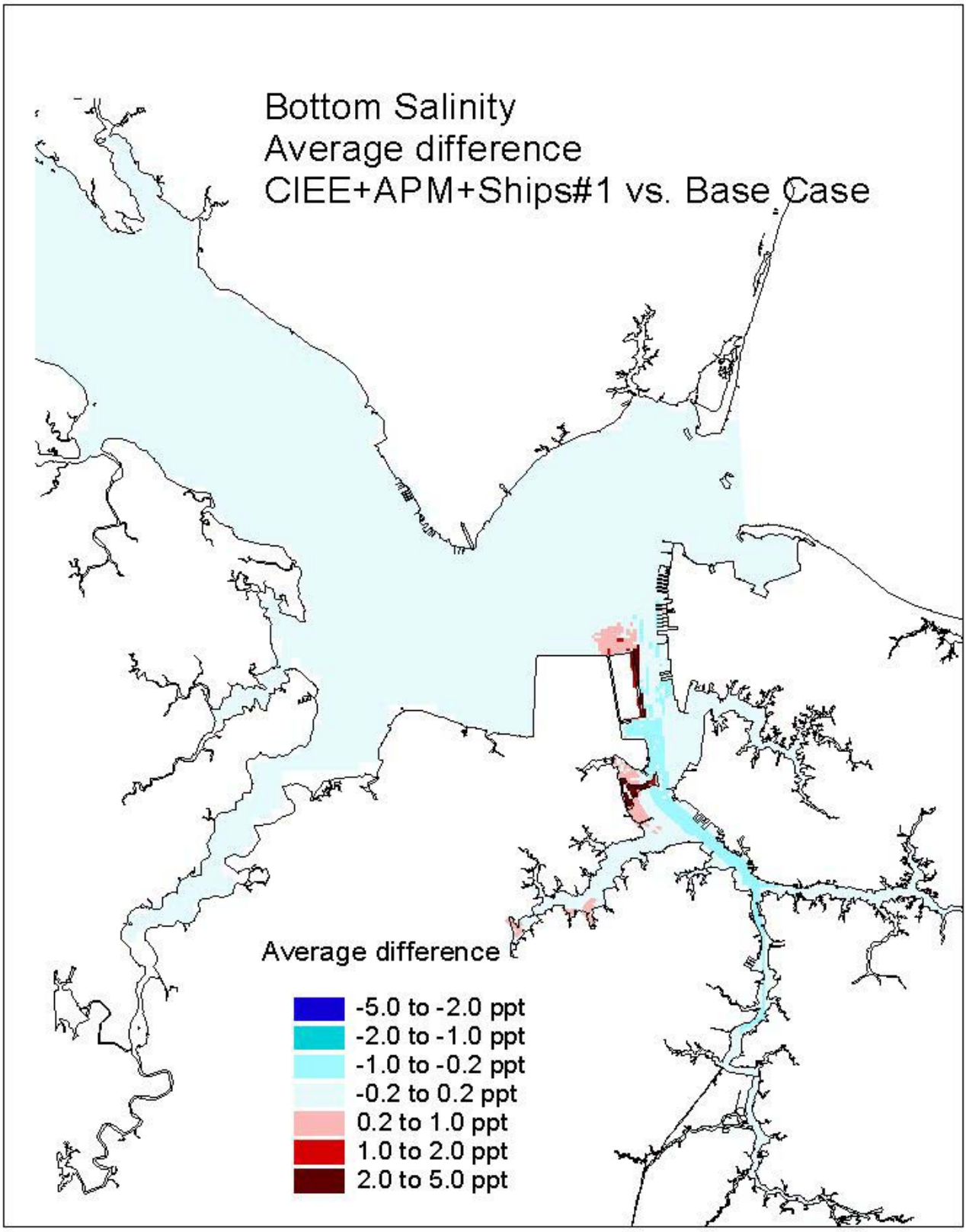

Figure 19. Single variable simulation comparison of the bottom salinity average difference for the Eastward Expansion plus APM Terminal Dredging plus Ships (Case 2a) versus the Base Case.

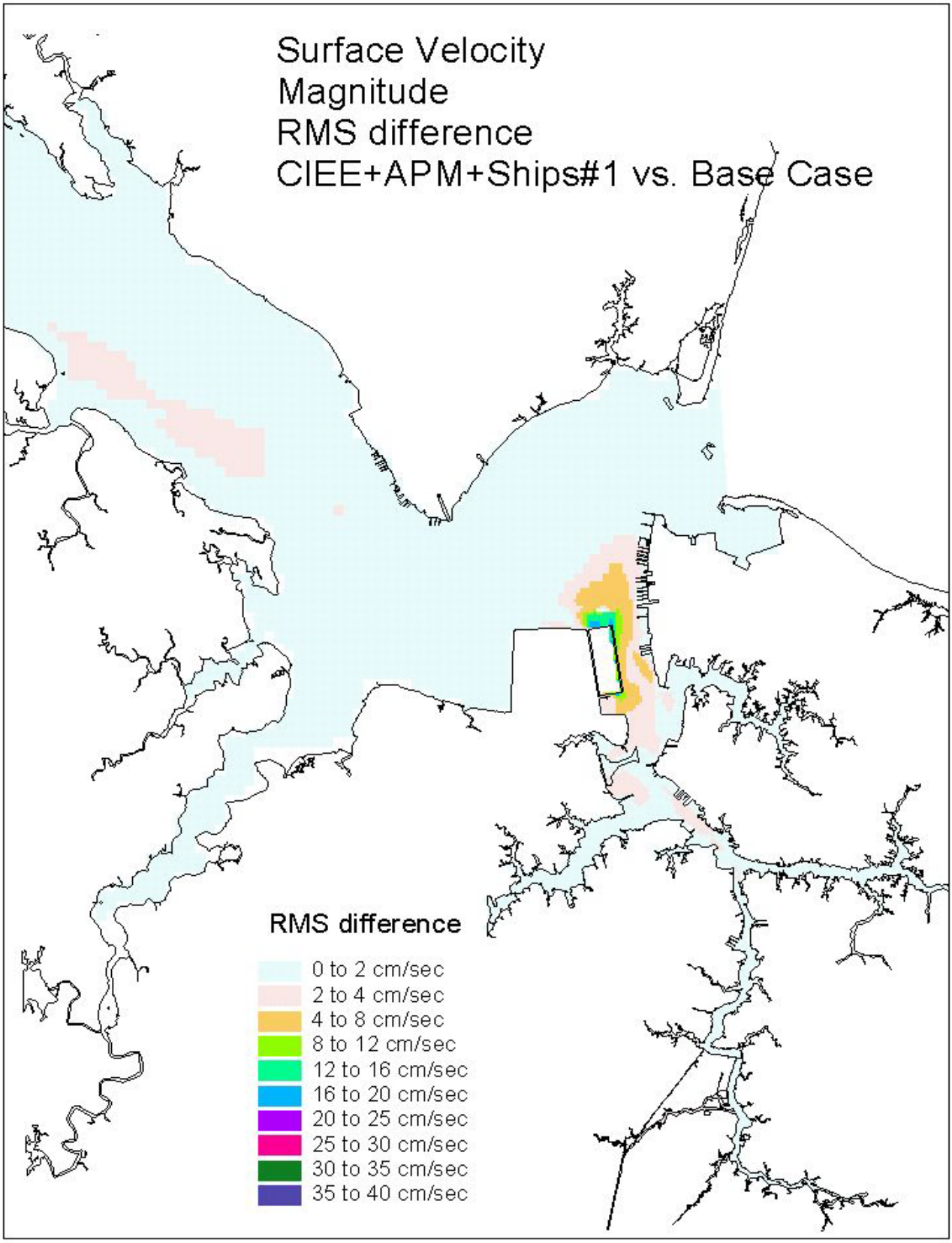

Figure 20. Single variable simulation comparison of the surface velocity RMS difference for the Eastward plus APM Terminal Dredging plus Ships (Case 2a) vs. the Base Case.

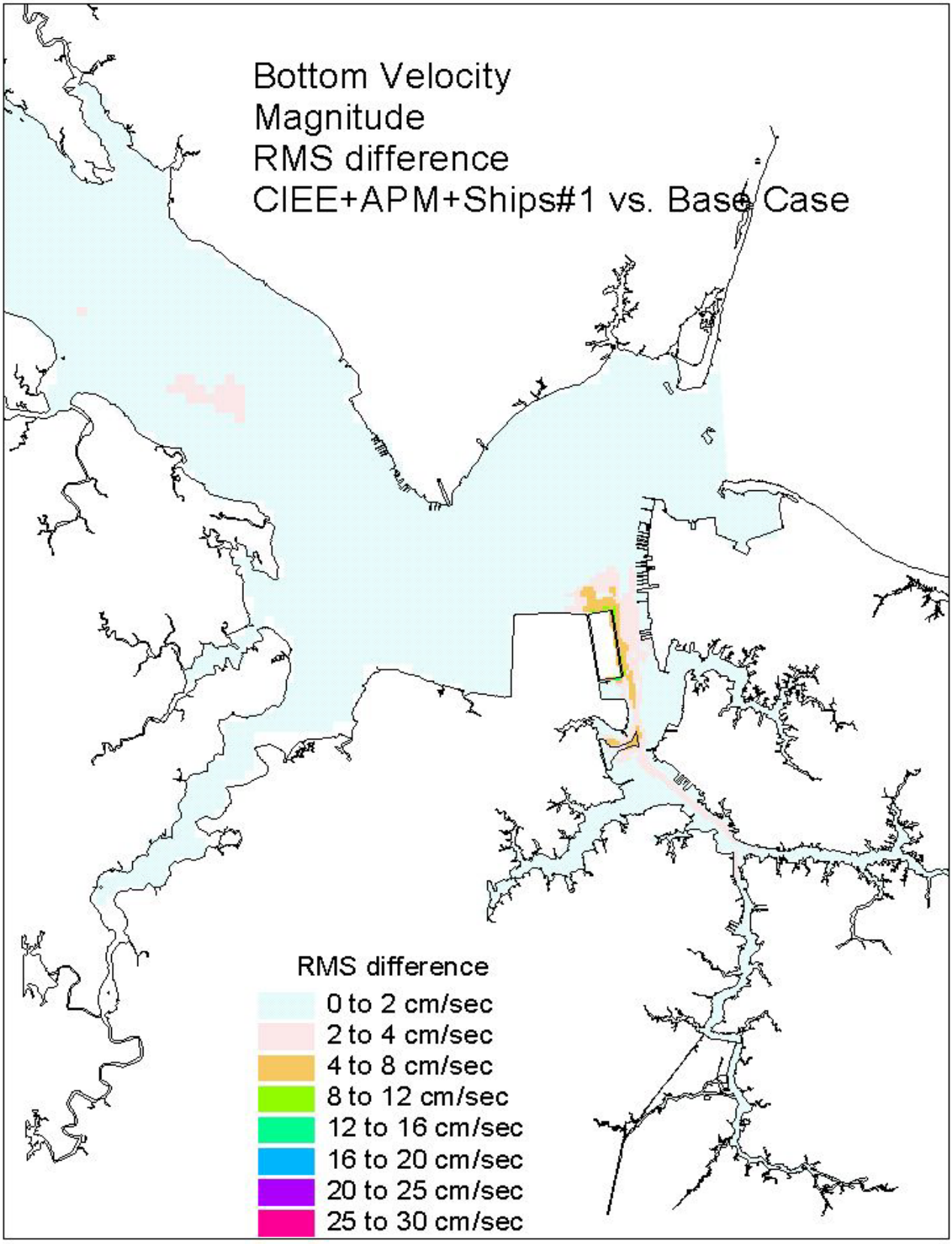

Figure 21. Single variable simulation comparison of the bottom velocity RMS difference for the Eastward Expansion plus APM Terminal Dredging plus Ships (Case 2a) versus the Base Case.

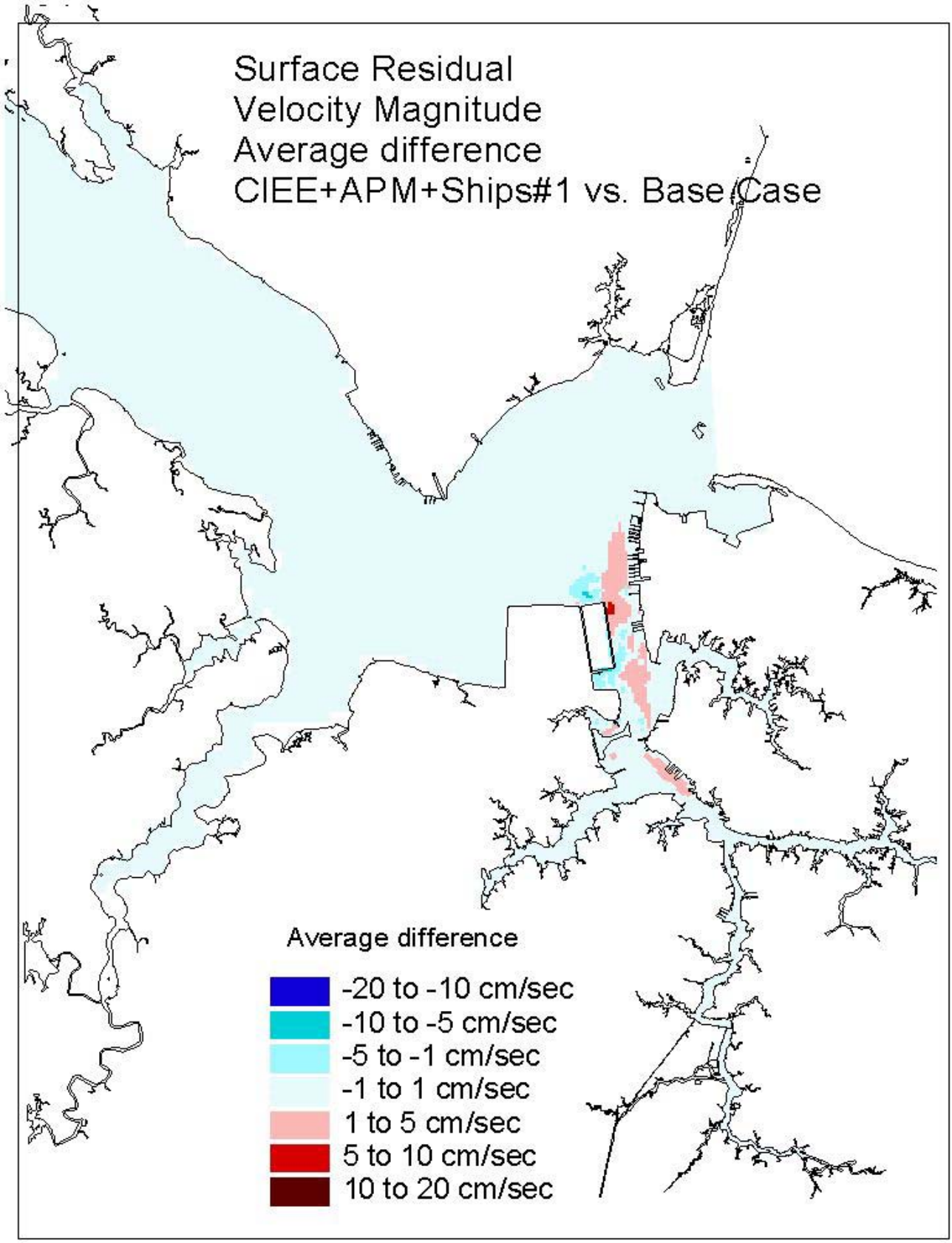

Figure 22. Single variable simulation comparison of the surface residual velocity average difference for the Eastward Expansion plus APM Terminal Dredging plus Ships (Case 2a) versus the Base Case.

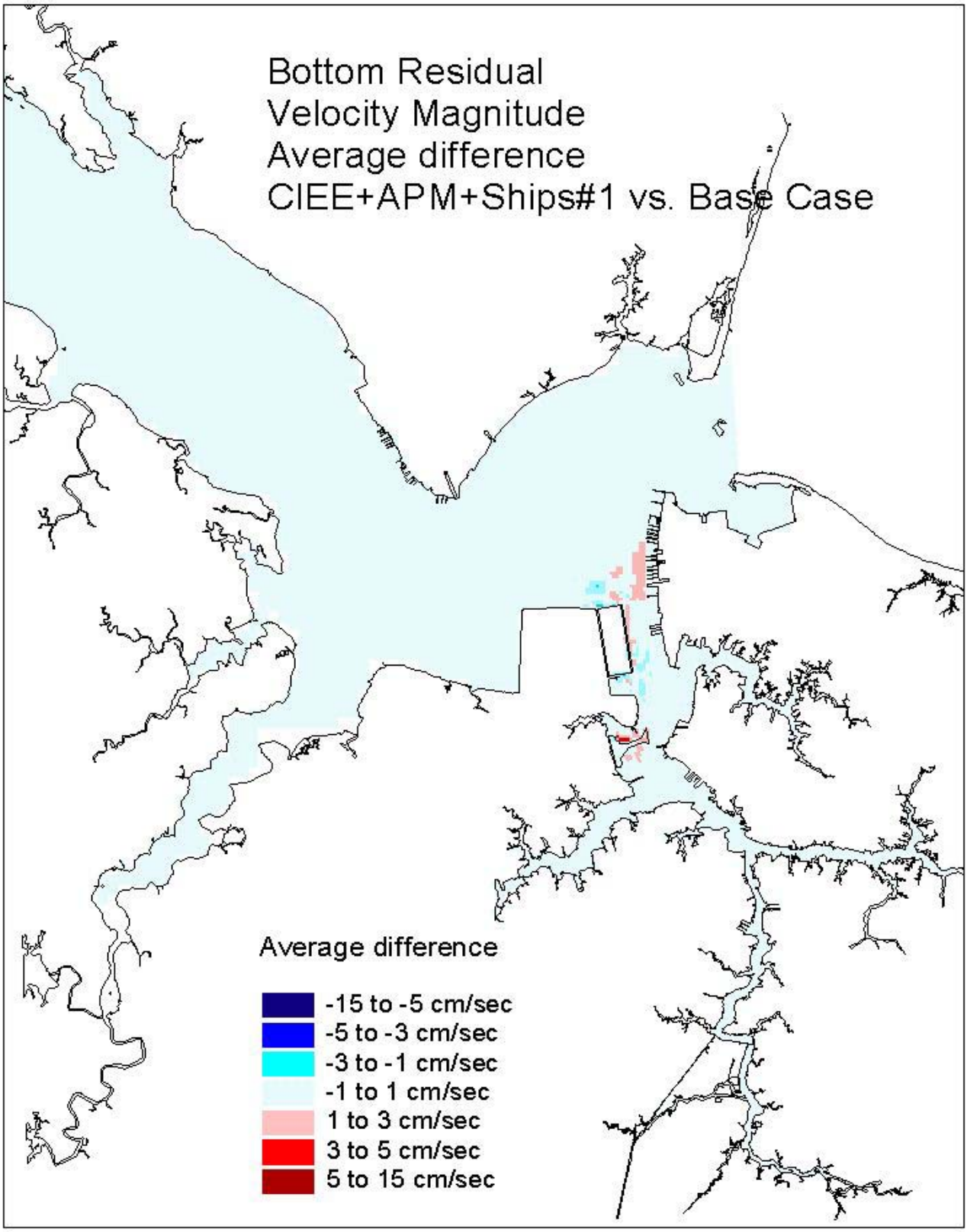

Figure 23. Single variable simulation comparison of the bottom residual velocity average difference for the Eastward Expansion plus APM Terminal Dredging plus Ships (Case 2a) versus the Base Case.

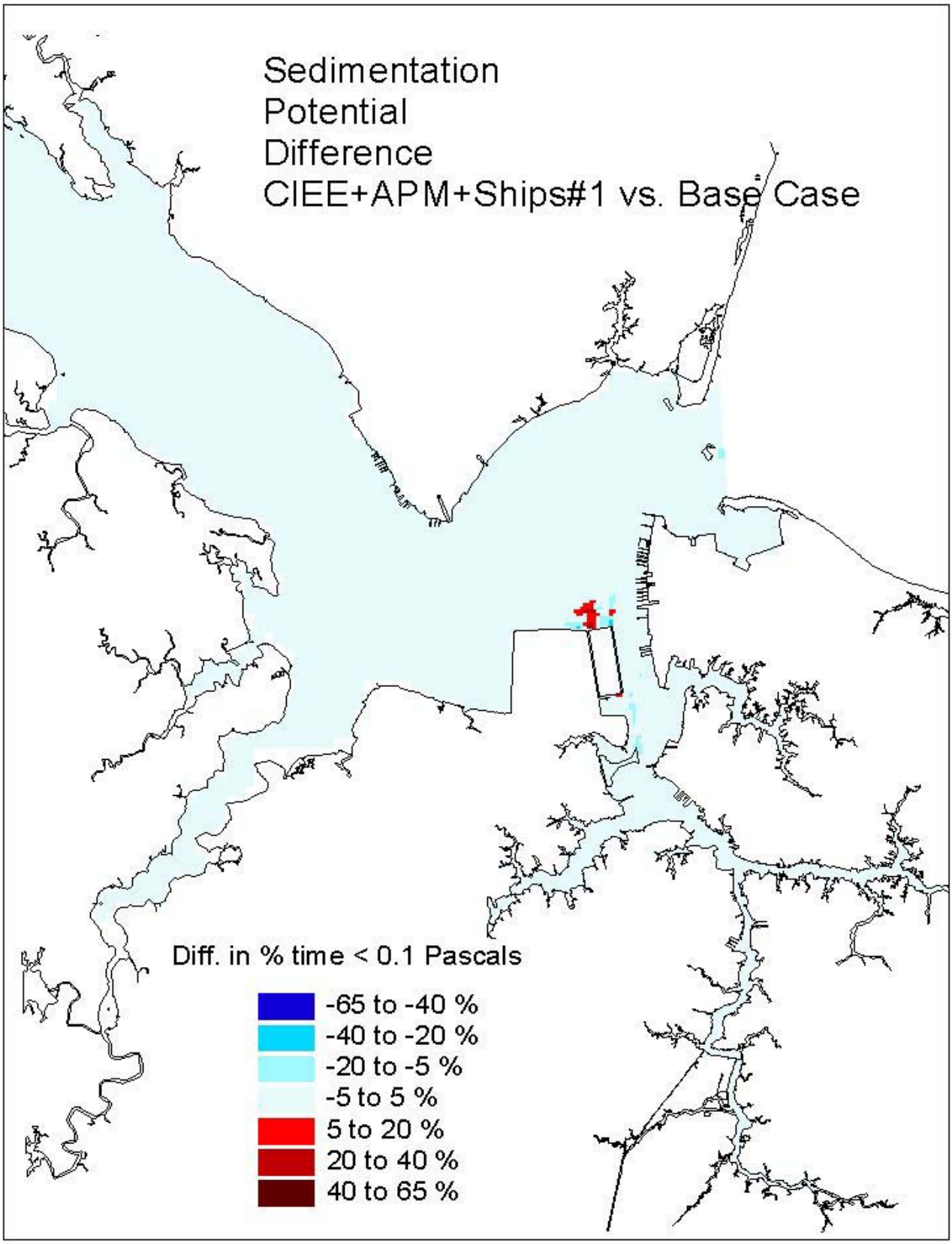

Figure 24. Single variable simulation comparison of the sedimentation potential difference for the Eastward Expansion plus APM Terminal Dredging plus Ships (Case 2a) versus the Base Case.

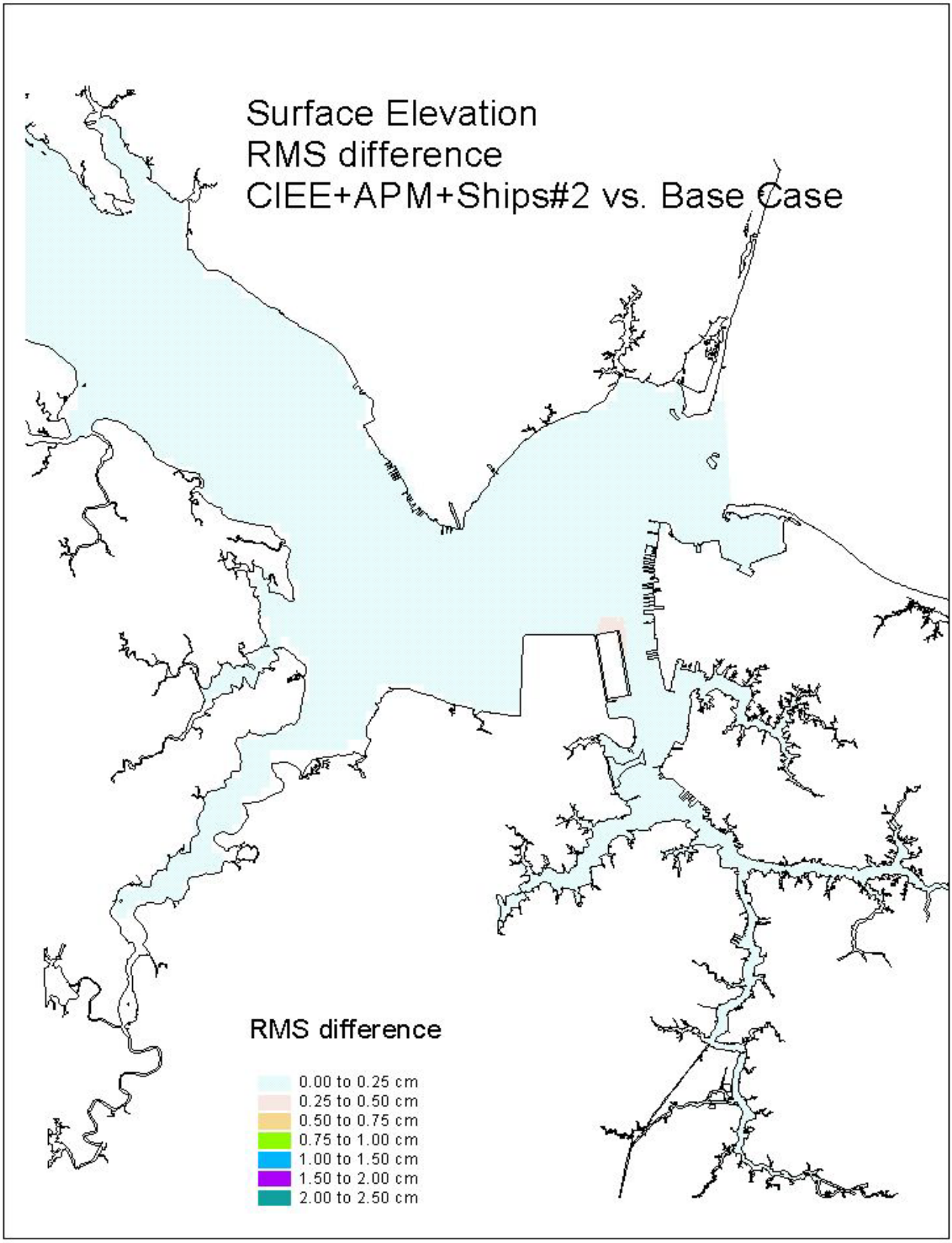

Figure 25. Single variable simulation comparison of the surface elevation RMS difference for the Eastward Expansion plus APM Terminal Dredging plus Ships (Case 2b) versus the Base Case

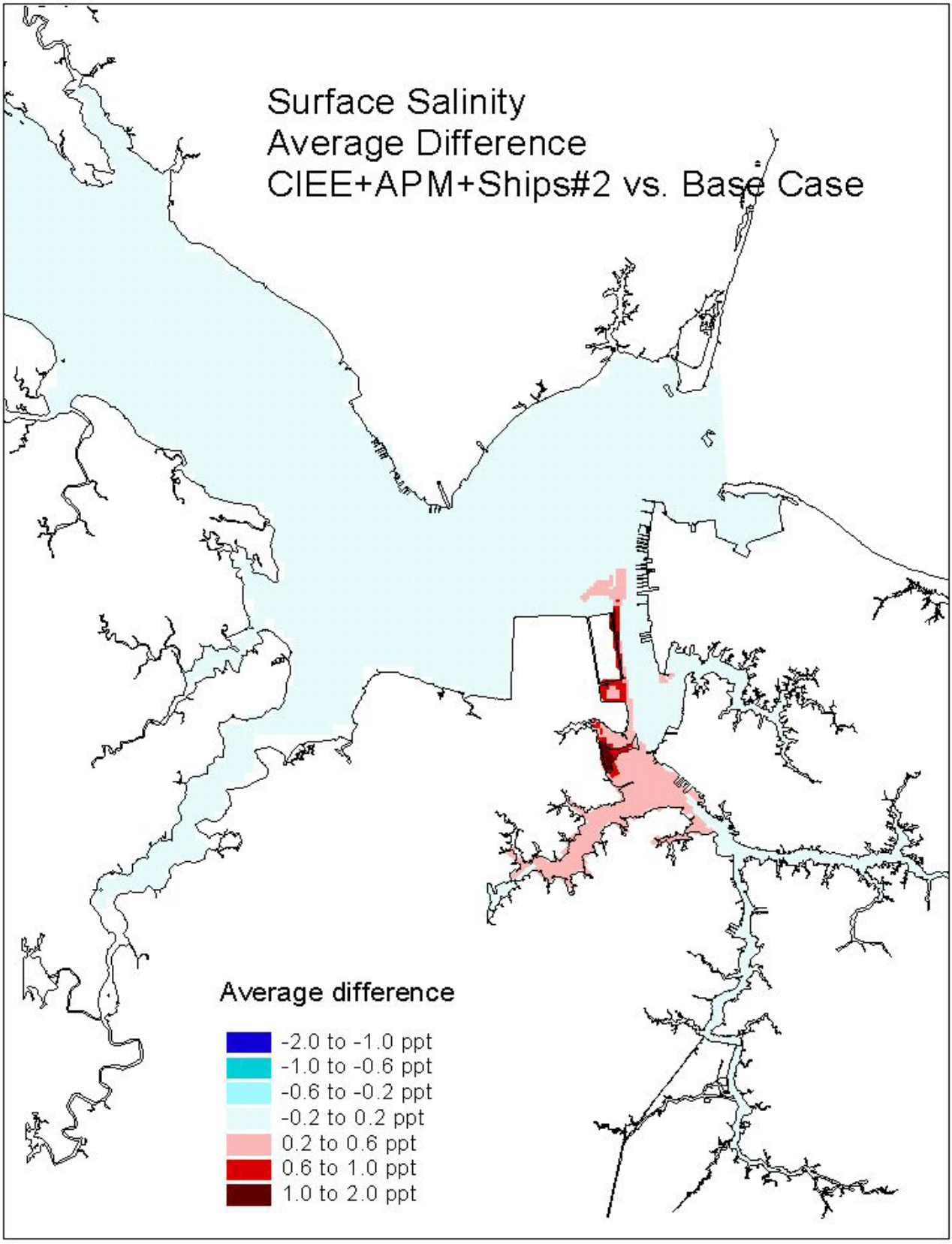

Figure 26. Single variable simulation comparison of the surface salinity average difference for the Eastward Expansion plus APM Terminal Dredging plus Ships (Case 2b) versus the Base Case

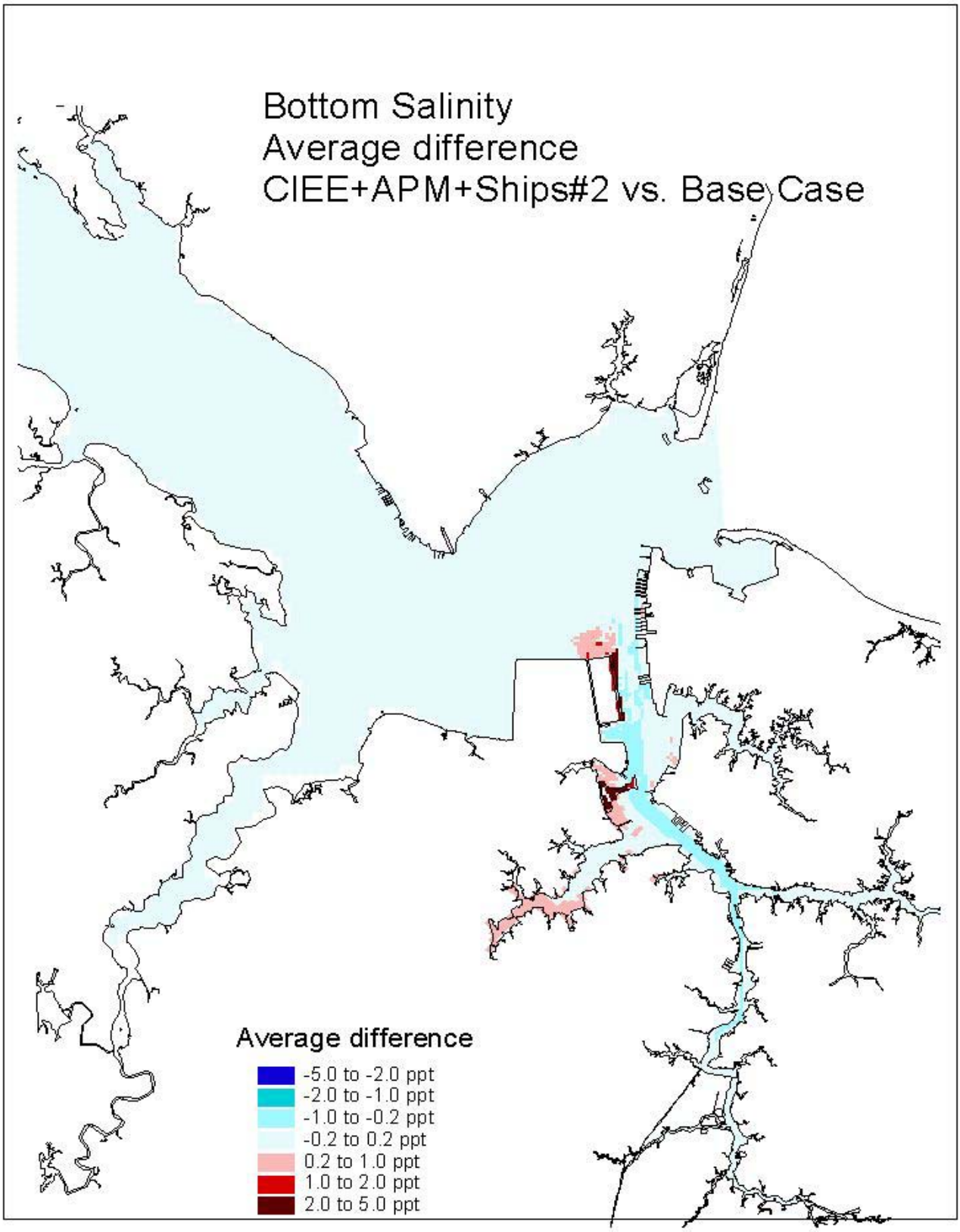

Figure 27. Single variable simulation comparison of the bottom salinity average difference for the Eastward Expansion plus APM Terminal Dredging plus Ships (Case 2b) versus the Base Case.

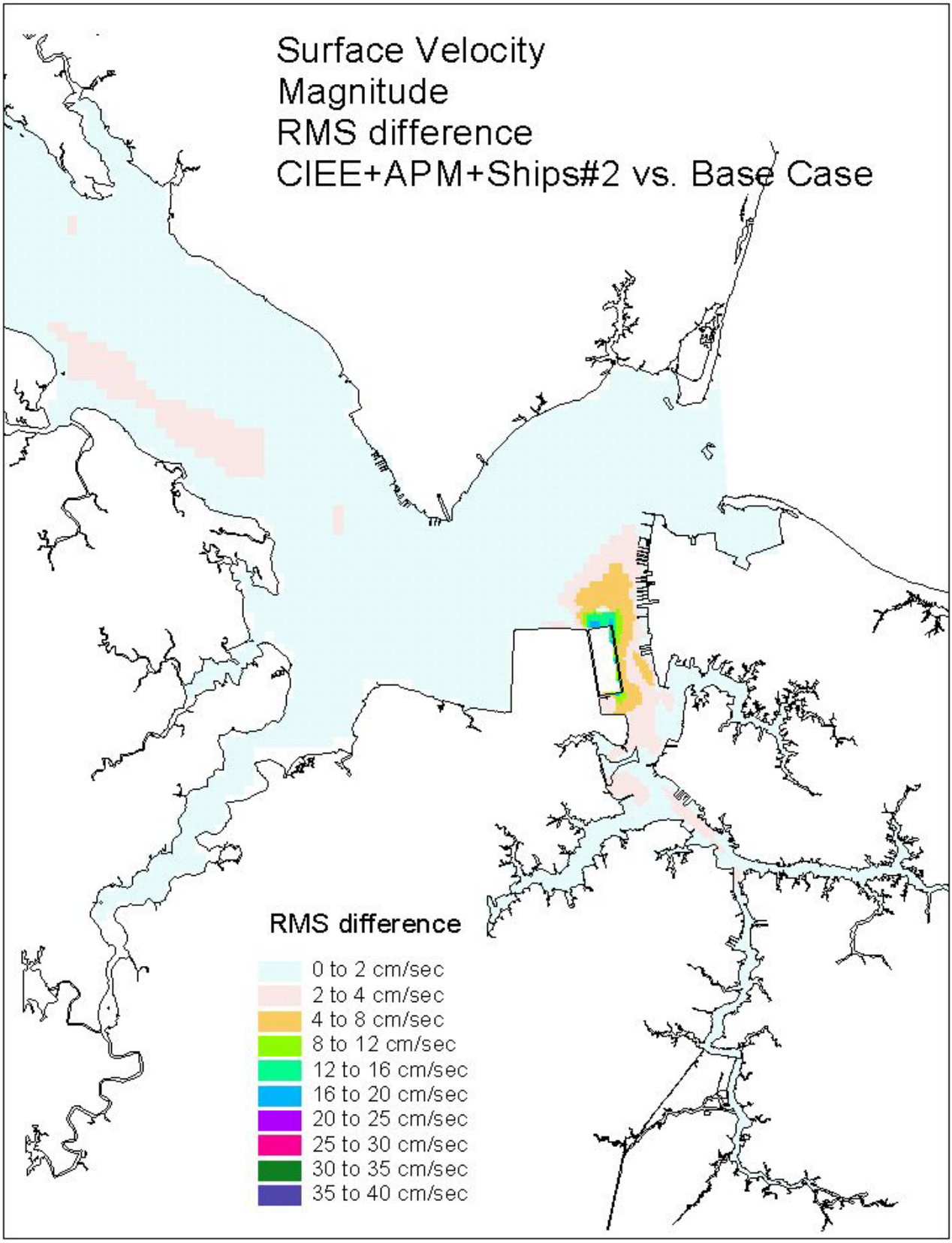

Figure 28. Single variable simulation comparison of the surface velocity RMS difference for the Eastward Expansion plus APM Terminal Dredging plus Ships (Case 2b) versus the Base Case.

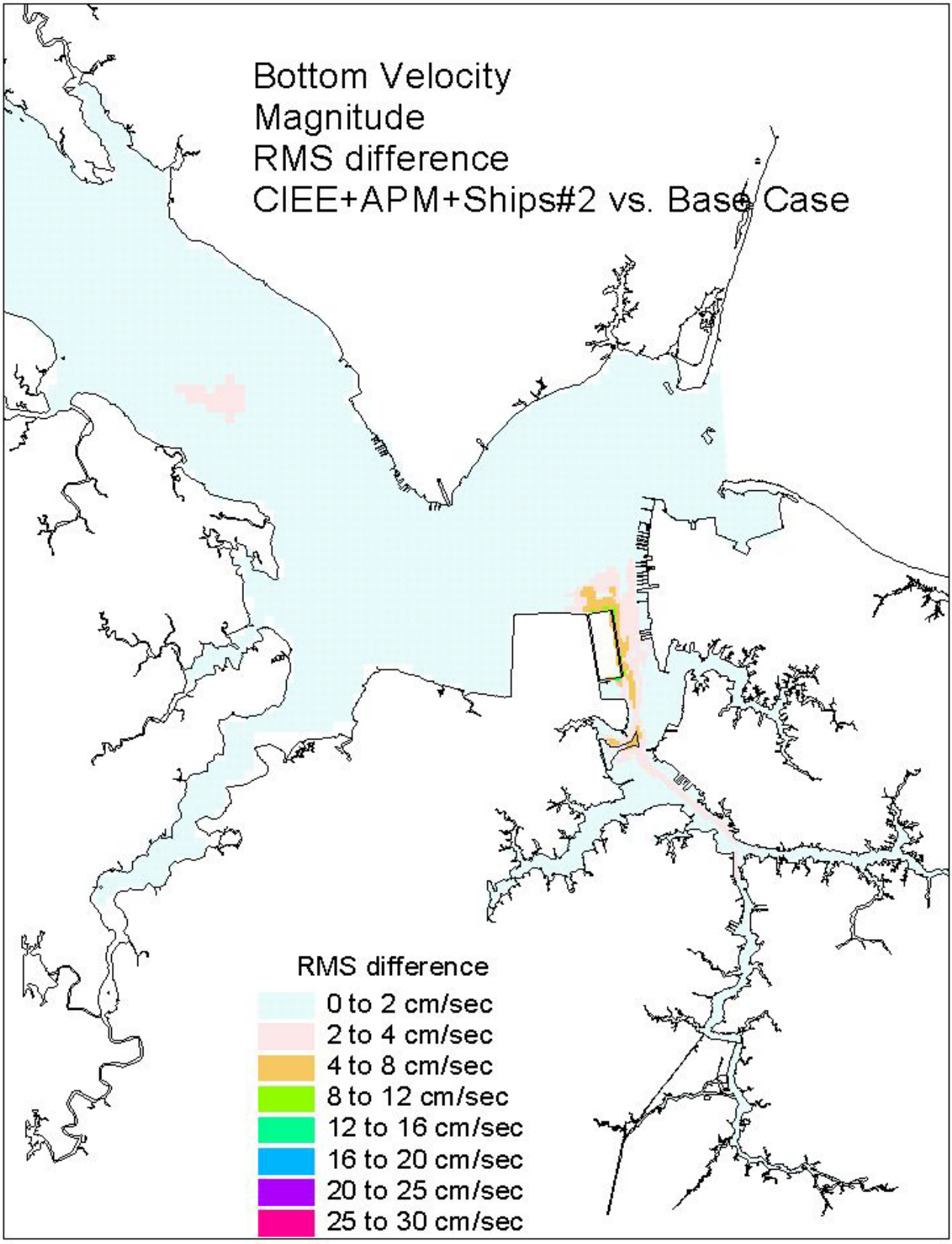

Figure 29. Single variable simulation comparison of the bottom velocity RMS difference for the Eastward Expansion plus APM Terminal Dredging plus Ships (Case 2b) versus the Base Case.

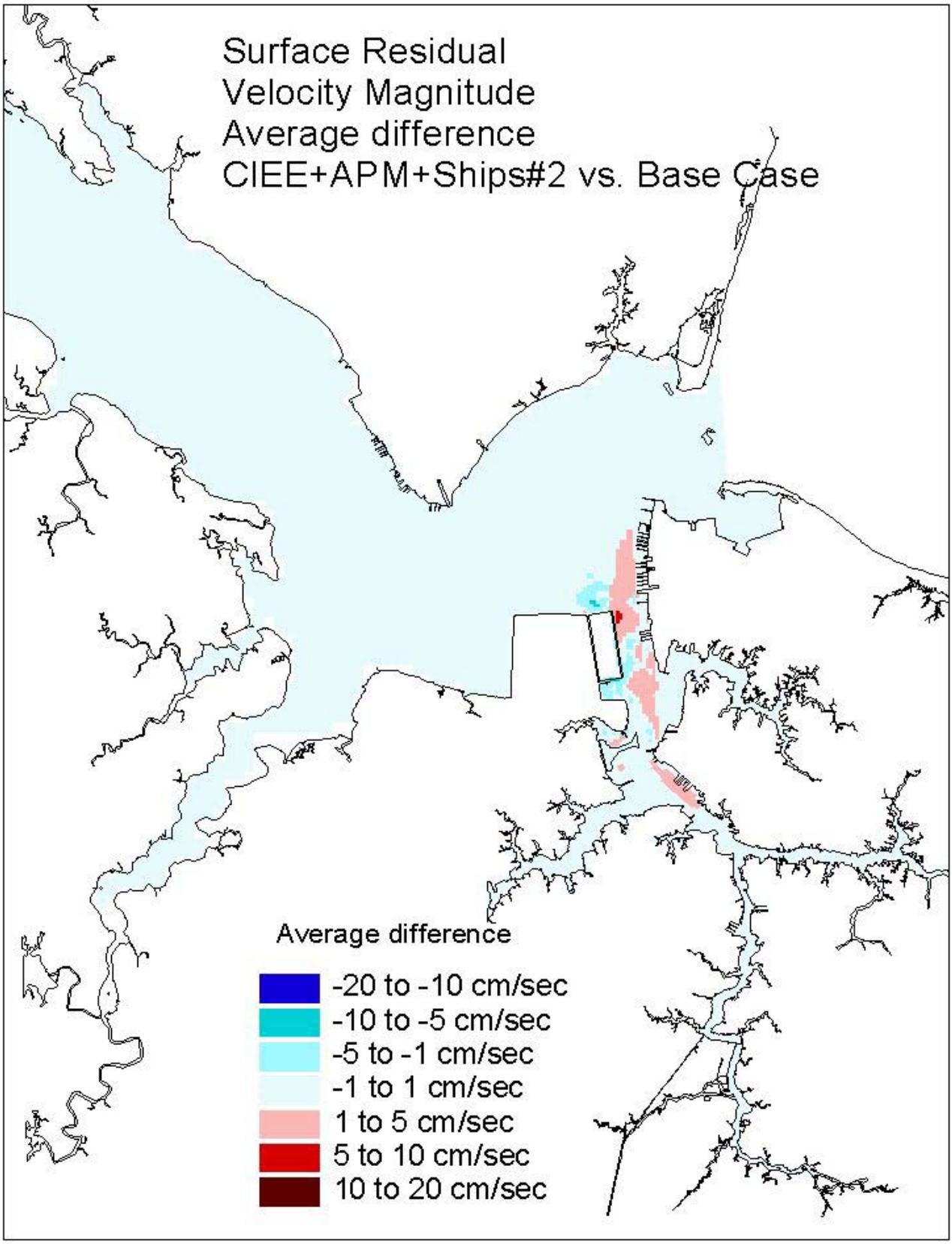

Figure 30. Single variable simulation comparison of the surface residual velocity average difference for the Eastward Expansion plus APM Terminal Dredging plus Ships (Case 2b) versus the Base Case.

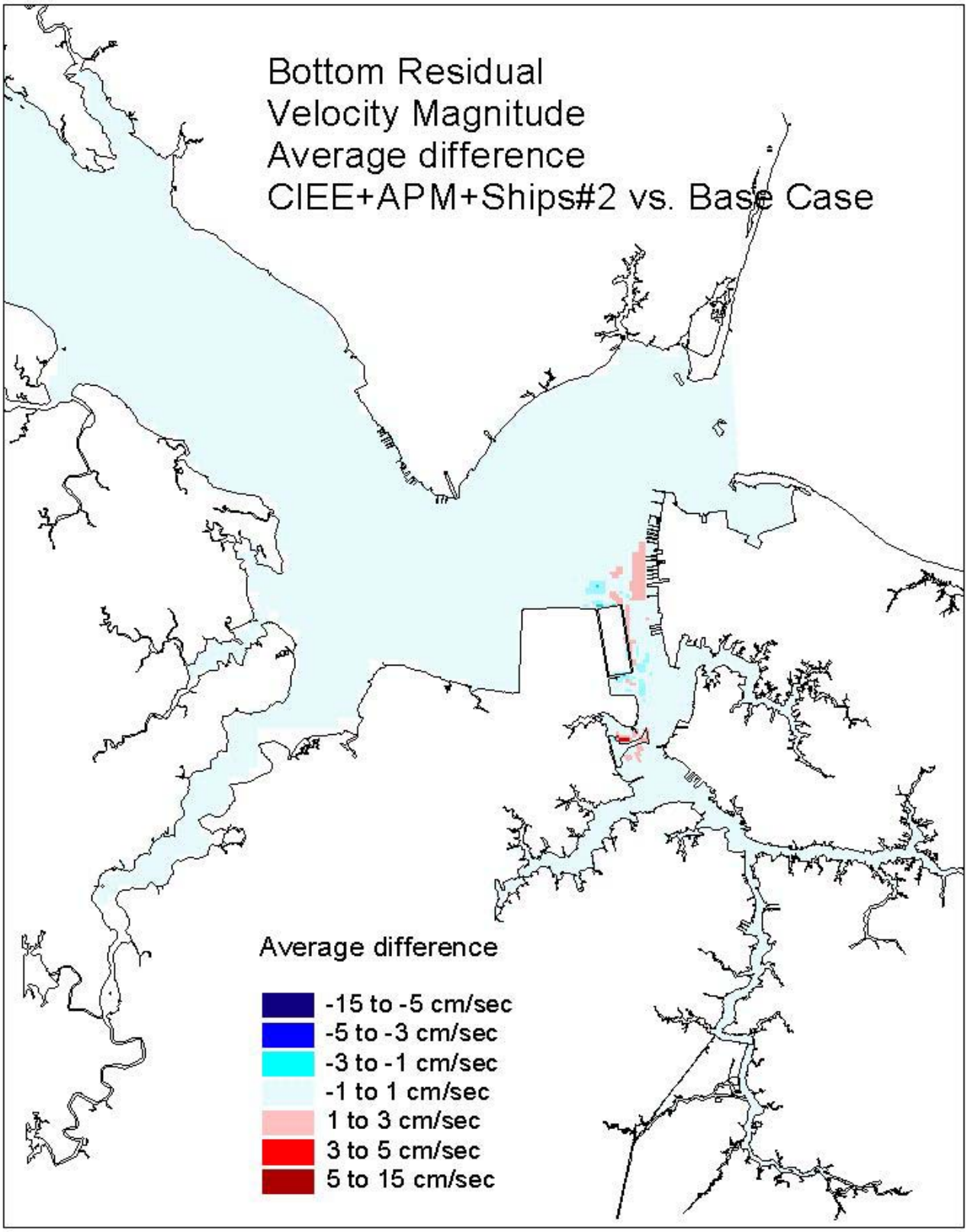

Figure 31. Single variable simulation comparison of the bottom residual velocity average difference for the Eastward Expansion plus APM Terminal Dredging plus Ships (Case 2b) versus the Base Case.

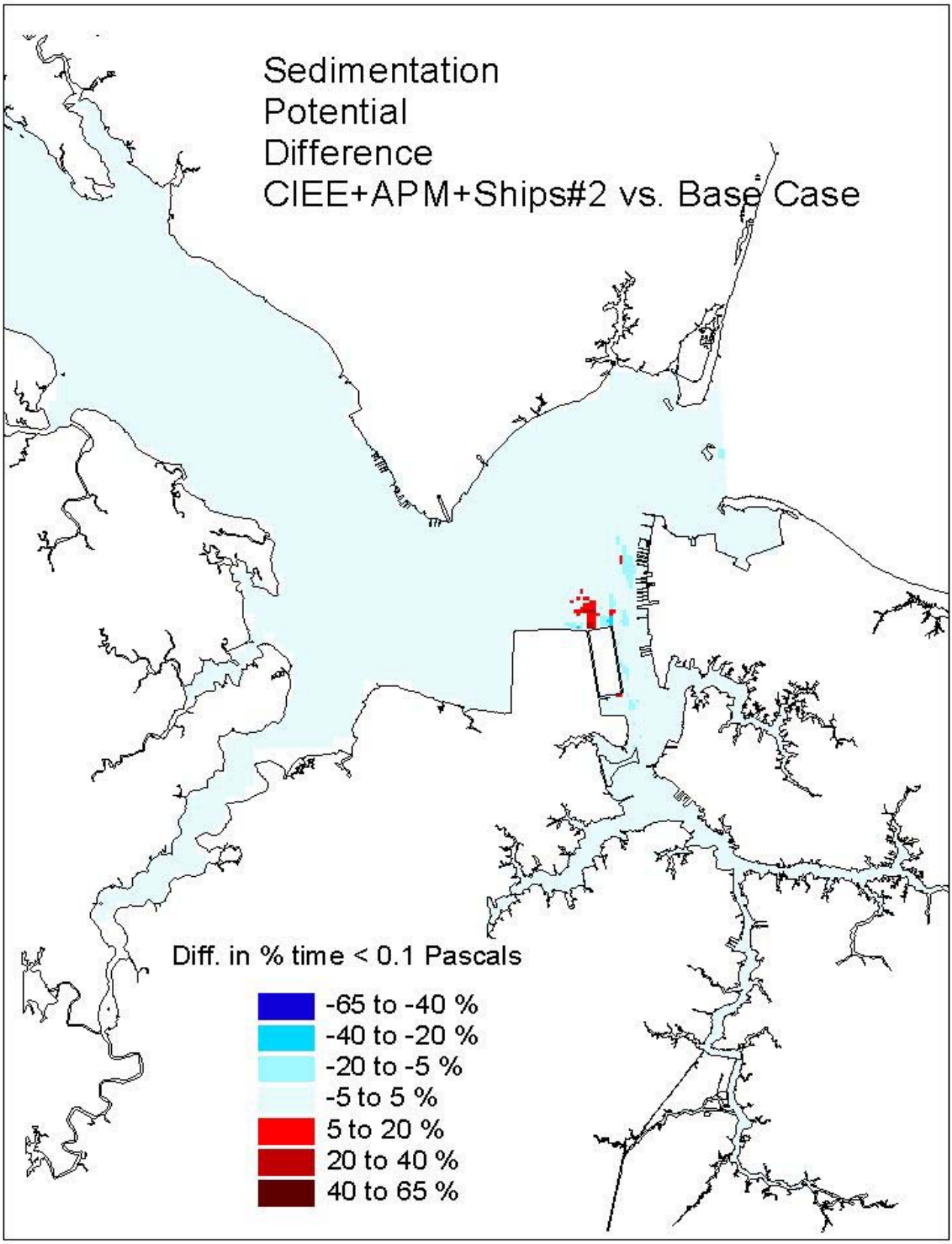

Figure 32. Single variable simulation comparison of the sedimentation potential difference for the Eastward Expansion plus APM Terminal Dredging plus Ships (Case 2b) versus the Base Case.

APPENDIX to CHAPTER III, SECTION A.2

Global Comparisons of Single Variable Runs

Percentile Analysis

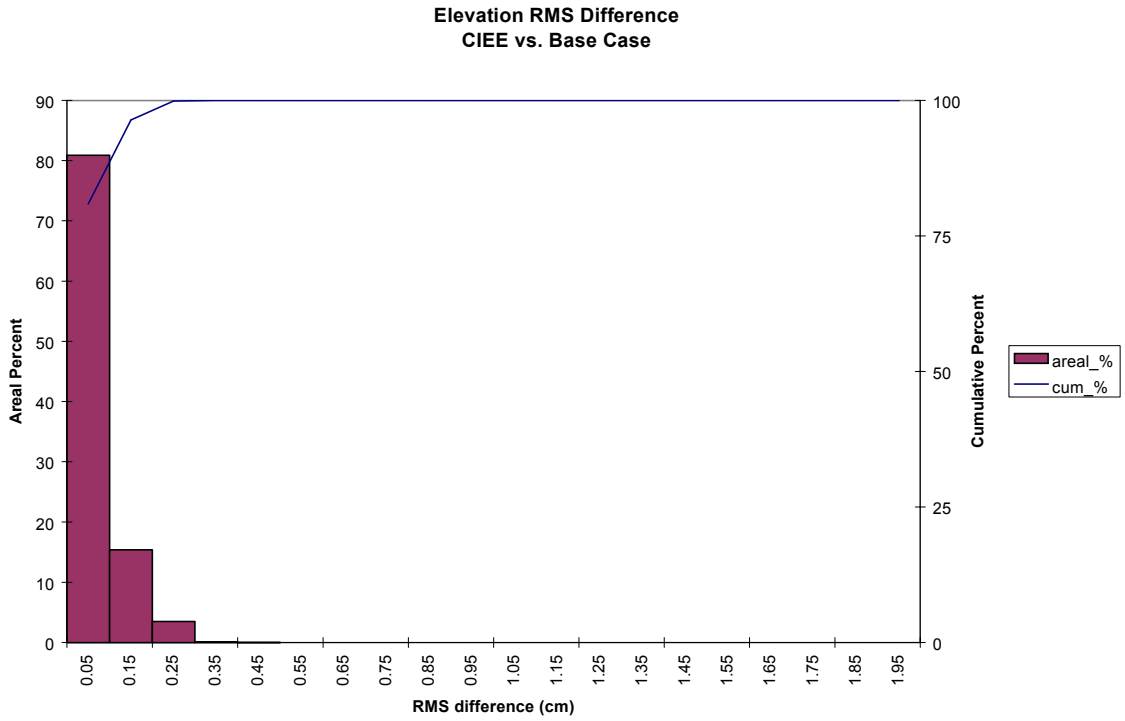

Figure 1. Frequency distribution of elevation RMS difference for the Eastward Expansion versus the Base Case.

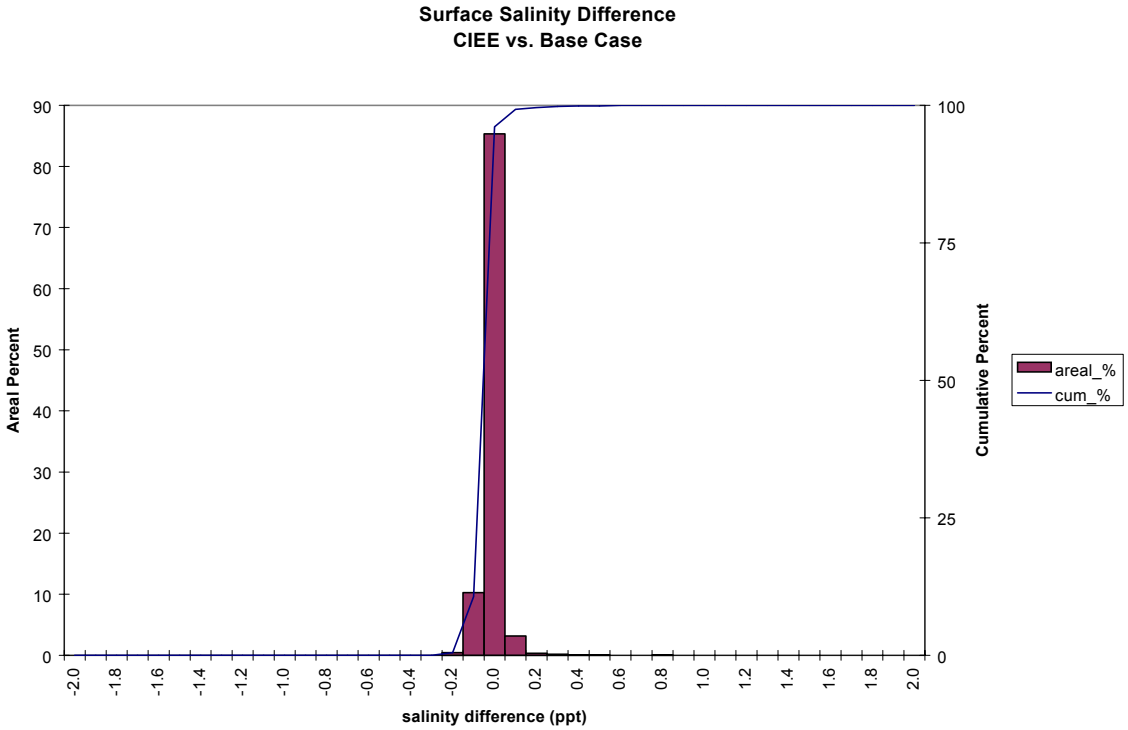

Figure 2. Frequency distribution of surface salinity average difference for the Eastward Expansion versus the Base Case.

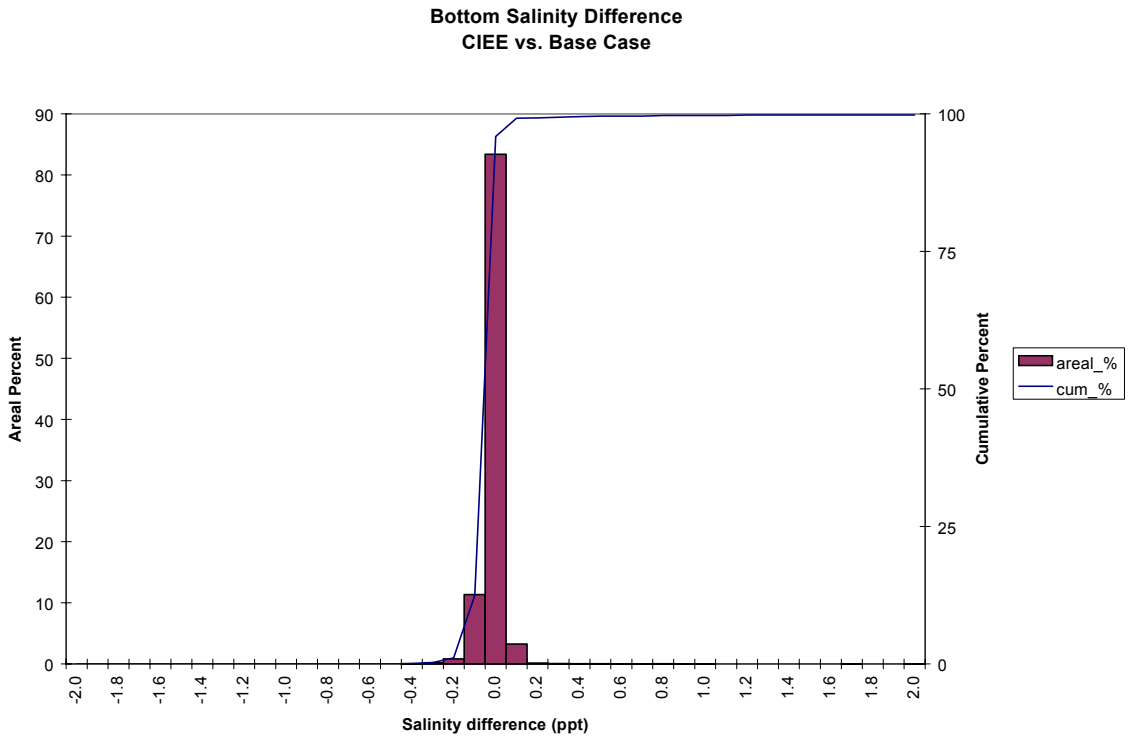

Figure 3. Frequency distribution of bottom salinity average difference for the Eastward Expansion versus the Base Case.

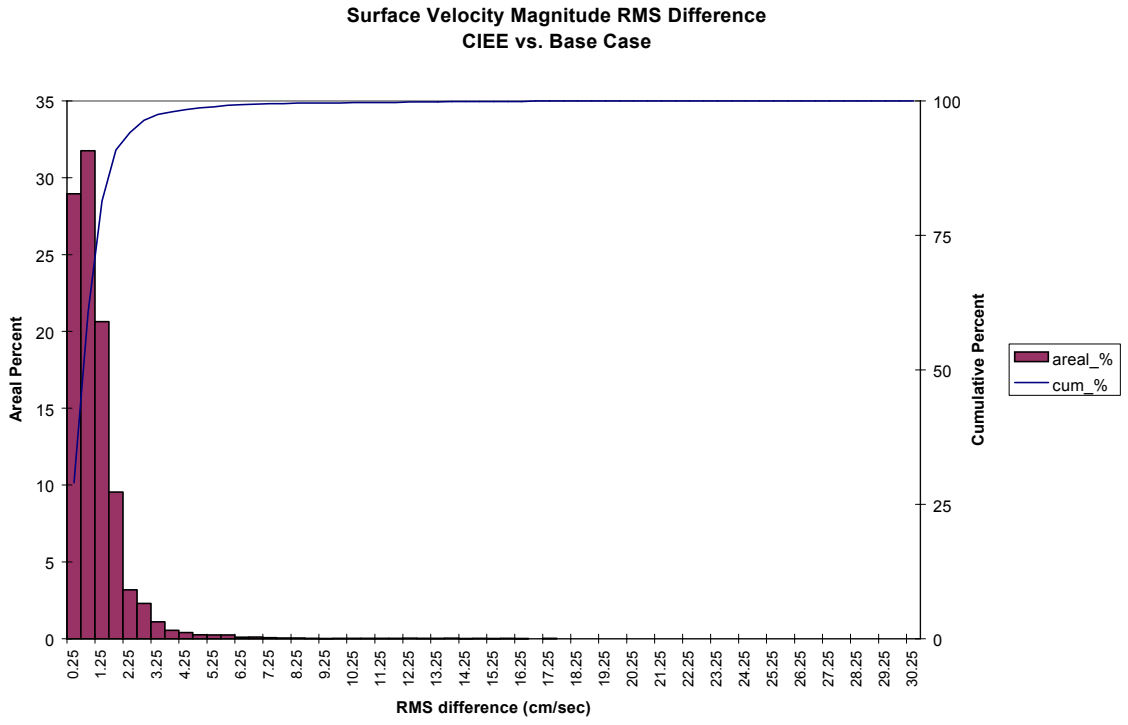

Figure 4. Frequency distribution of surface velocity RMS difference for the Eastward Expansion versus the Base Case.

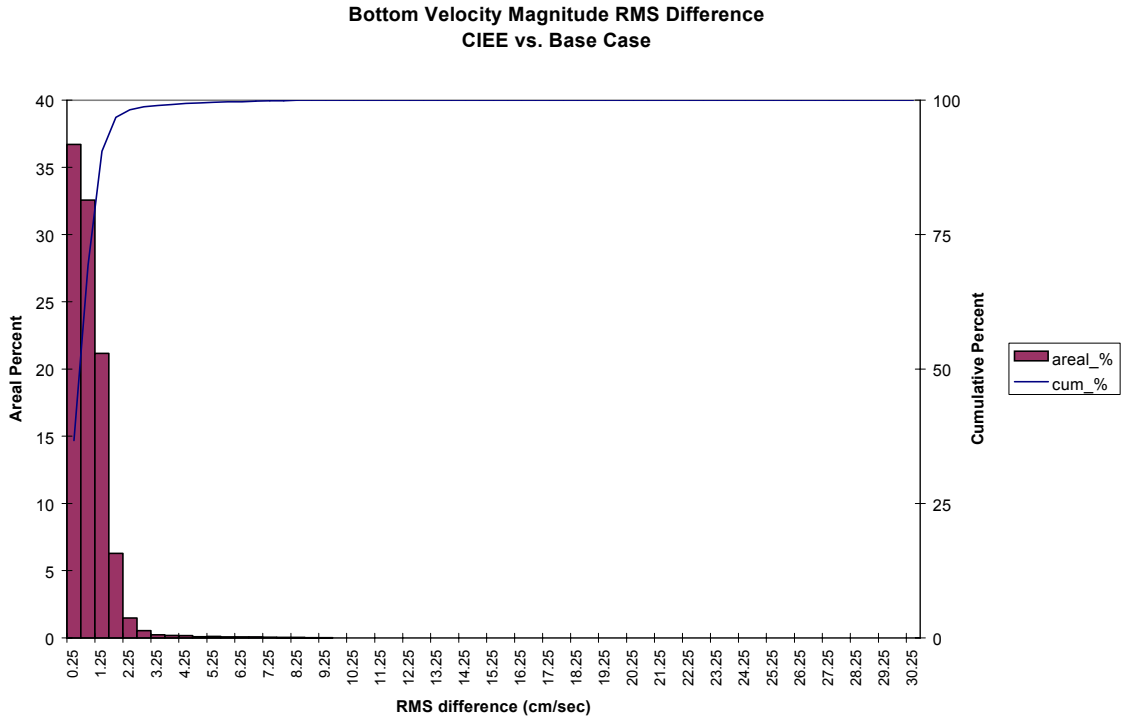

Figure 5. Frequency distribution of bottom velocity RMS difference for the Eastward Expansion versus the Base Case.

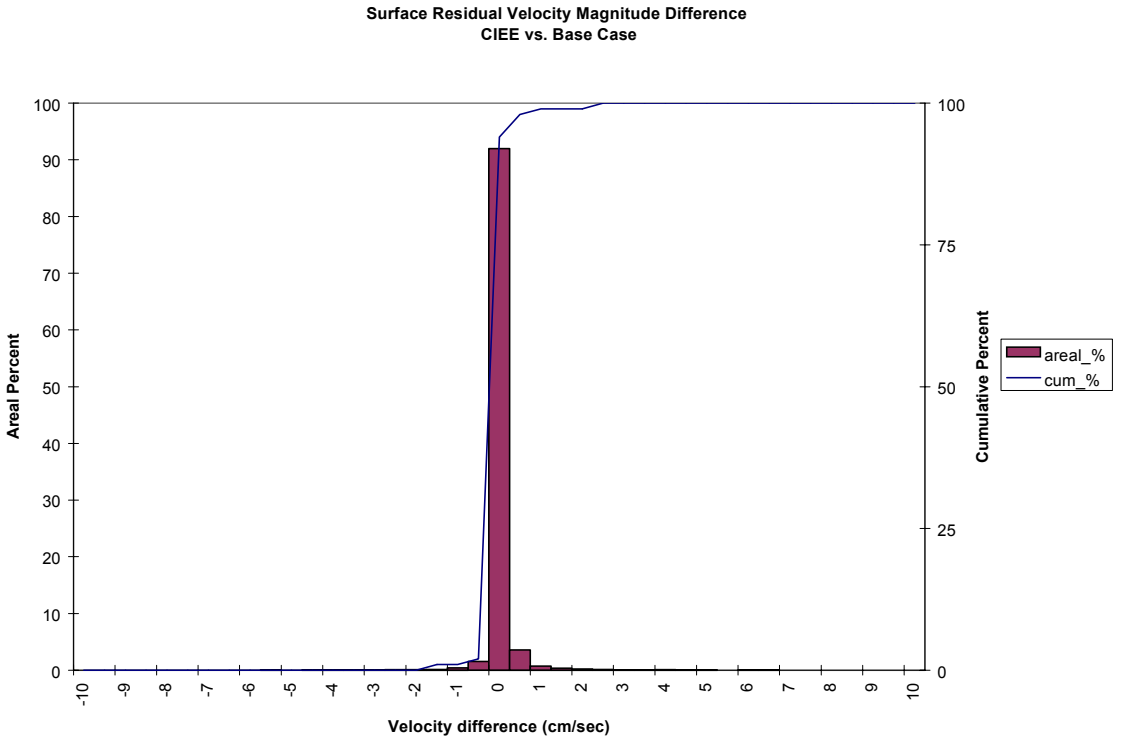

Figure 6. Frequency distribution of surface residual velocity magnitude average difference for the Eastward Expansion versus the Base Case.

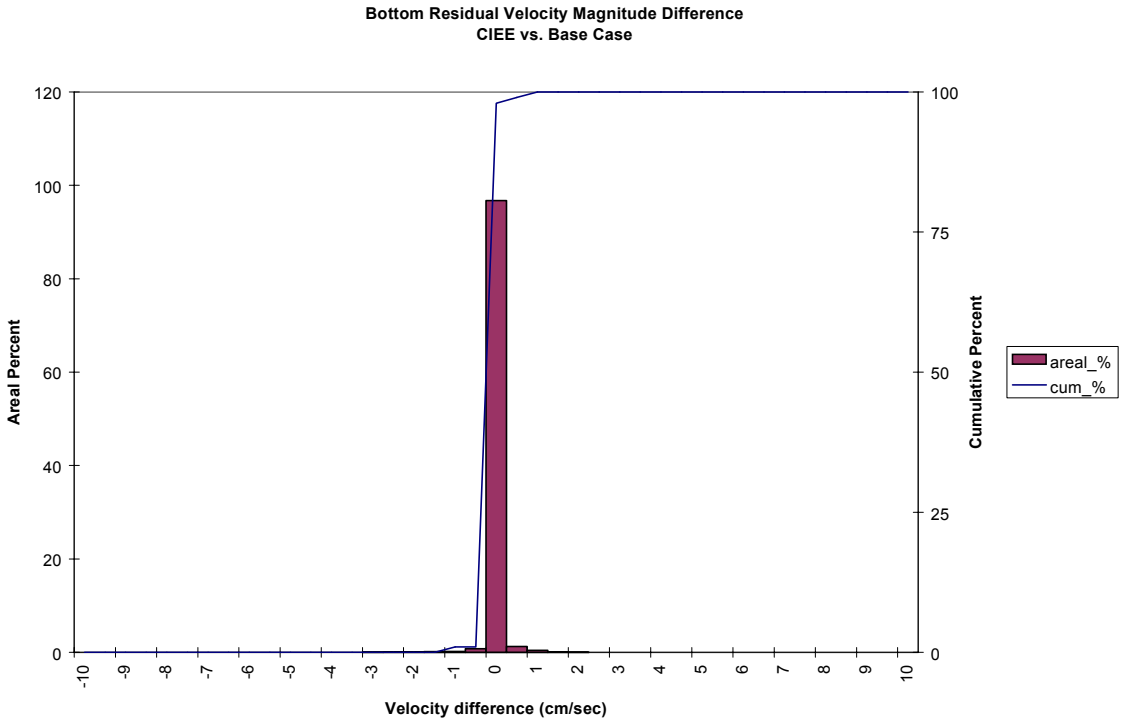

Figure 7. Frequency distribution of bottom residual velocity magnitude average difference for the Eastward Expansion versus the Base Case.

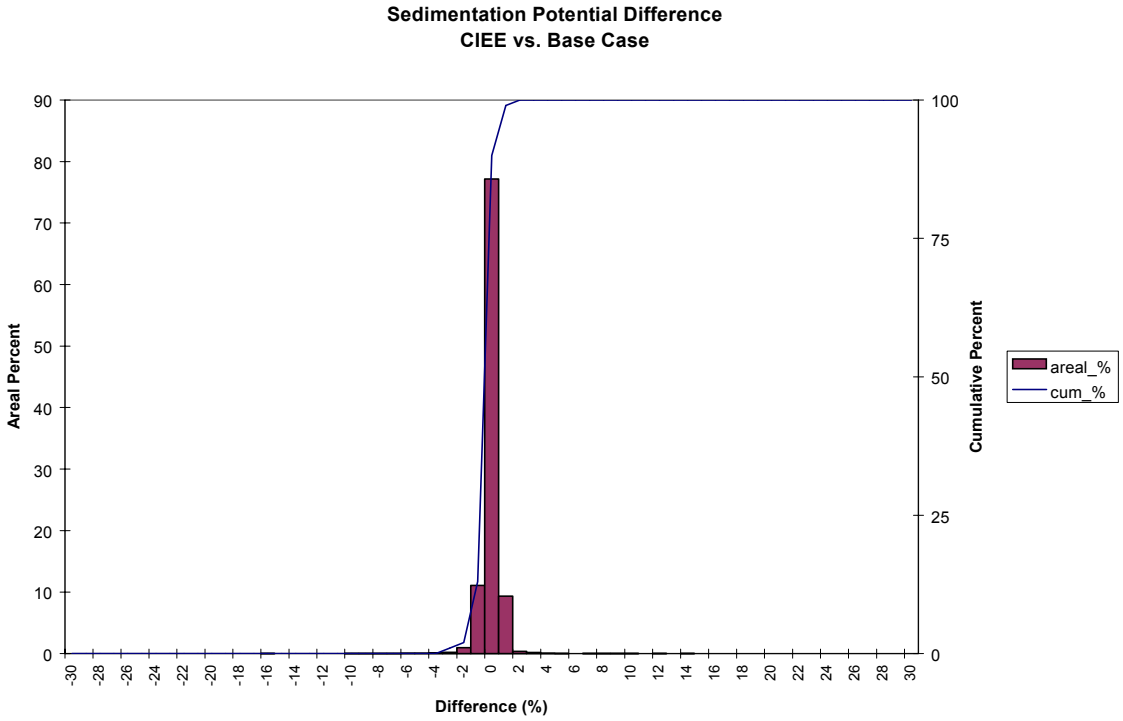

Figure 8. Frequency distribution of sedimentation potential difference for the Eastward Expansion versus the Base Case.

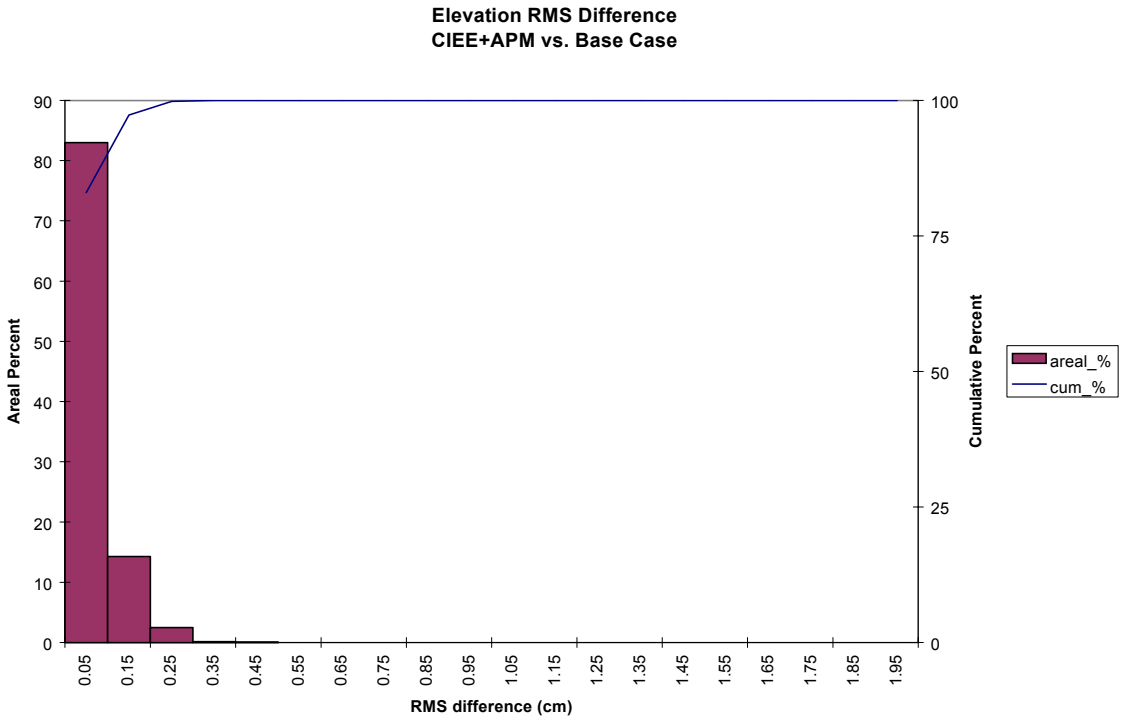

Figure 9. Frequency distribution of elevation RMS difference for the Eastward Expansion plus APM Terminal Dredging versus the Base Case.

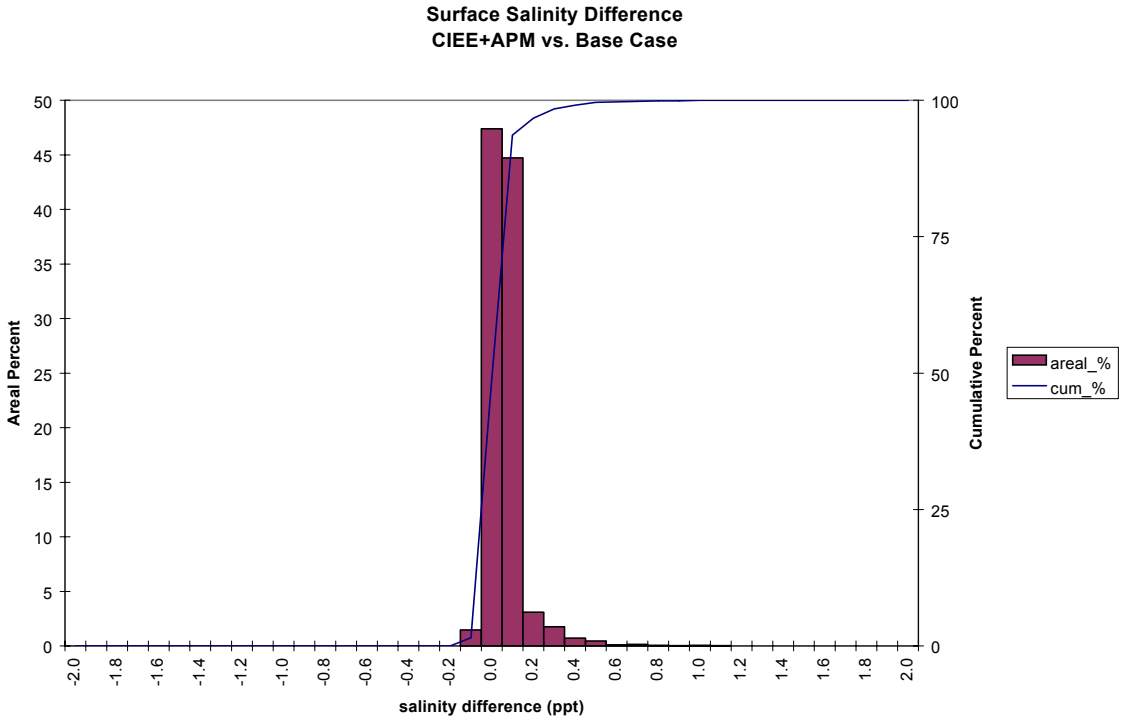

Figure 10. Frequency distribution of surface salinity average difference for the Eastward Expansion plus APM Terminal Dredging versus the Base Case.

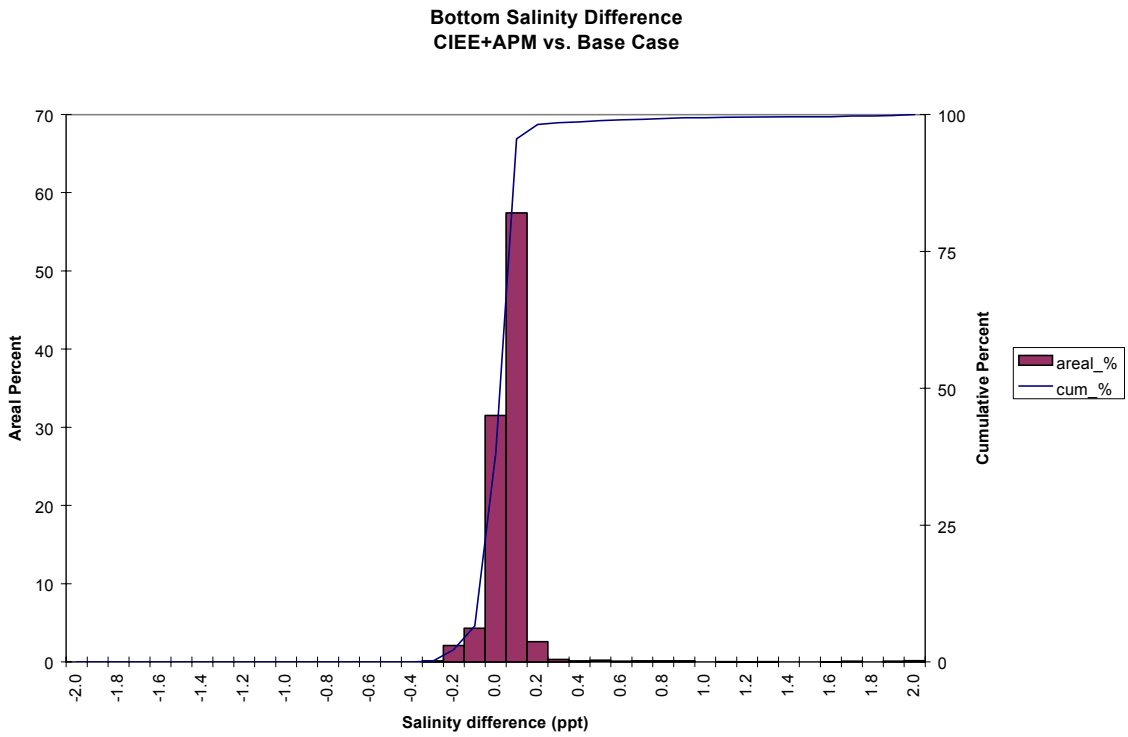

Figure 11. Frequency distribution of bottom salinity average difference for the Eastward Expansion plus APM Terminal Dredging versus the Base Case.

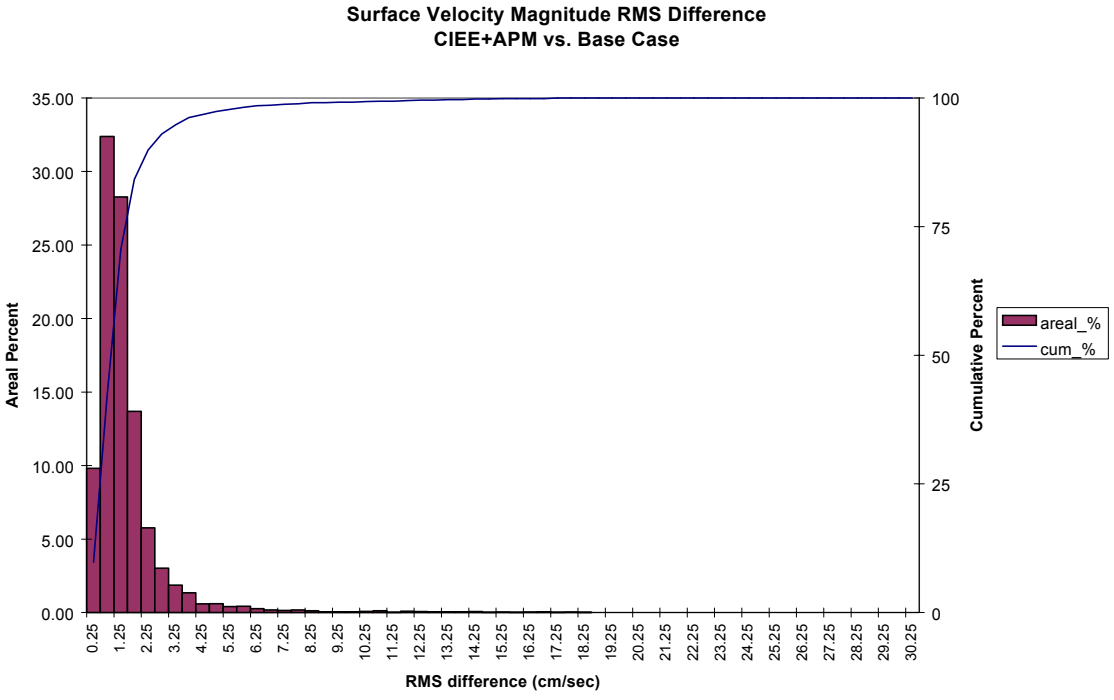

Figure 12. Frequency distribution of surface velocity RMS difference for the Eastward Expansion plus APM Terminal Dredging versus the Base Case.

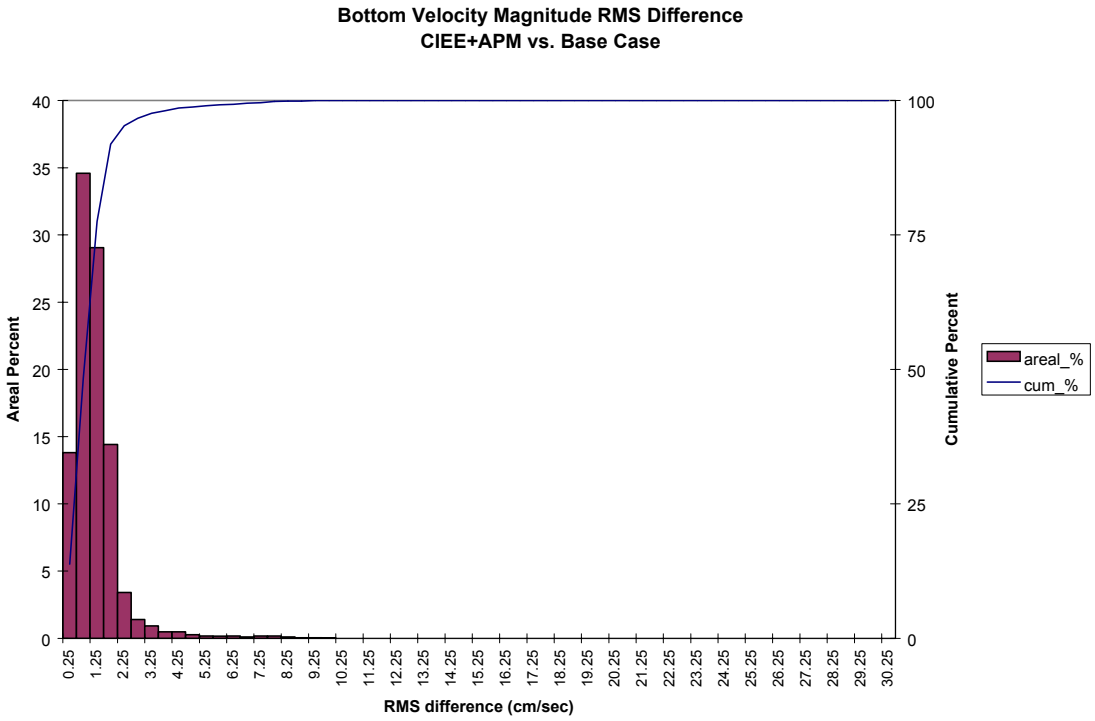

Figure 13. Frequency distribution of bottom velocity RMS difference for the Eastward Expansion plus APM Terminal Dredging versus the Base Case.

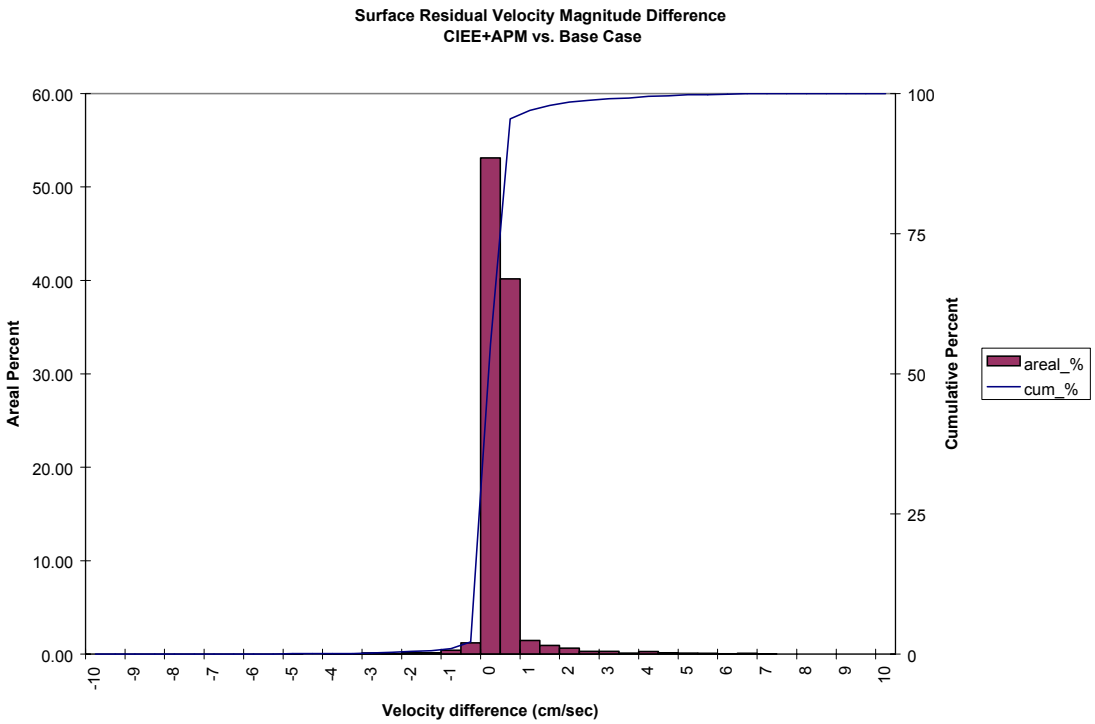

Figure 14. Frequency distribution of surface residual velocity magnitude average difference for the Eastward Expansion plus APM Terminal Dredging versus the Base Case.

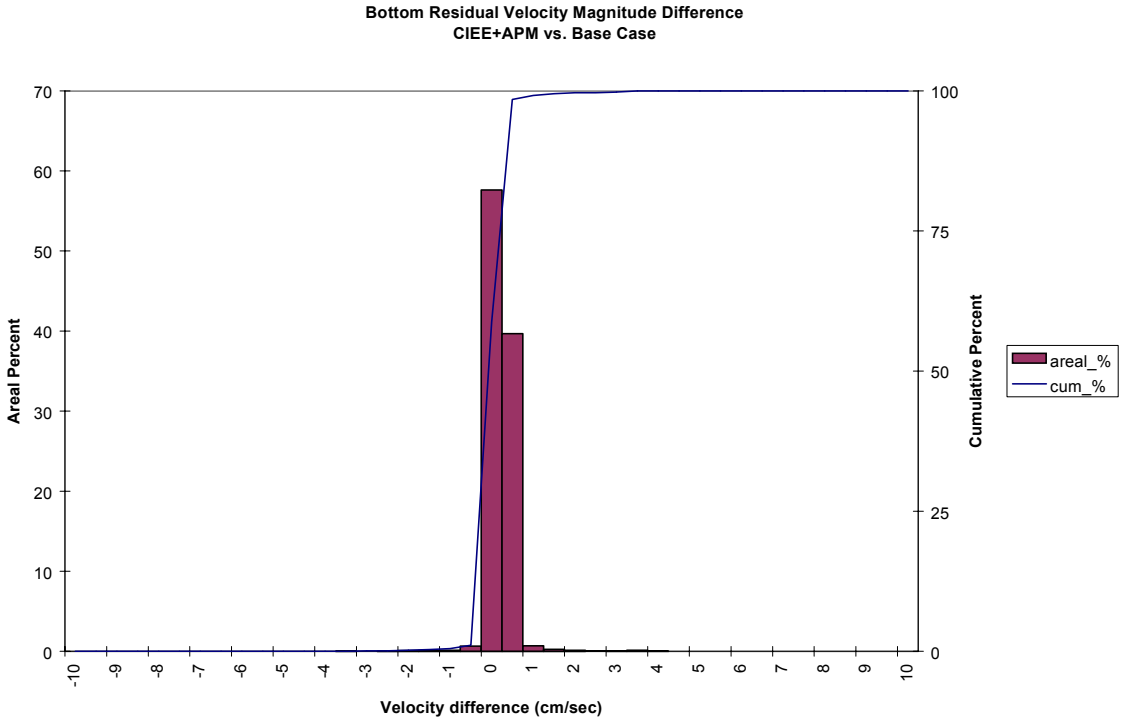

Figure 15. Frequency distribution of bottom residual velocity magnitude average difference for the Eastward Expansion plus APM Terminal Dredging versus the Base Case.

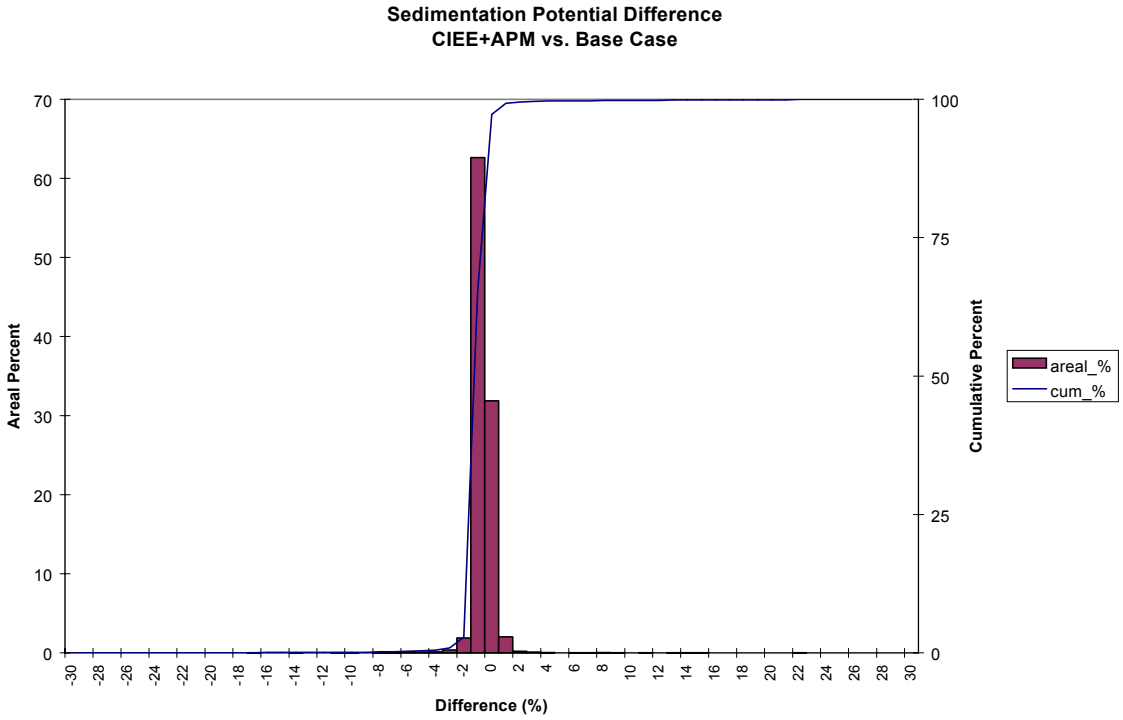

Figure 16. Frequency distribution of sedimentation potential difference for the Eastward Expansion plus APM Terminal Dredging versus the Base Case.

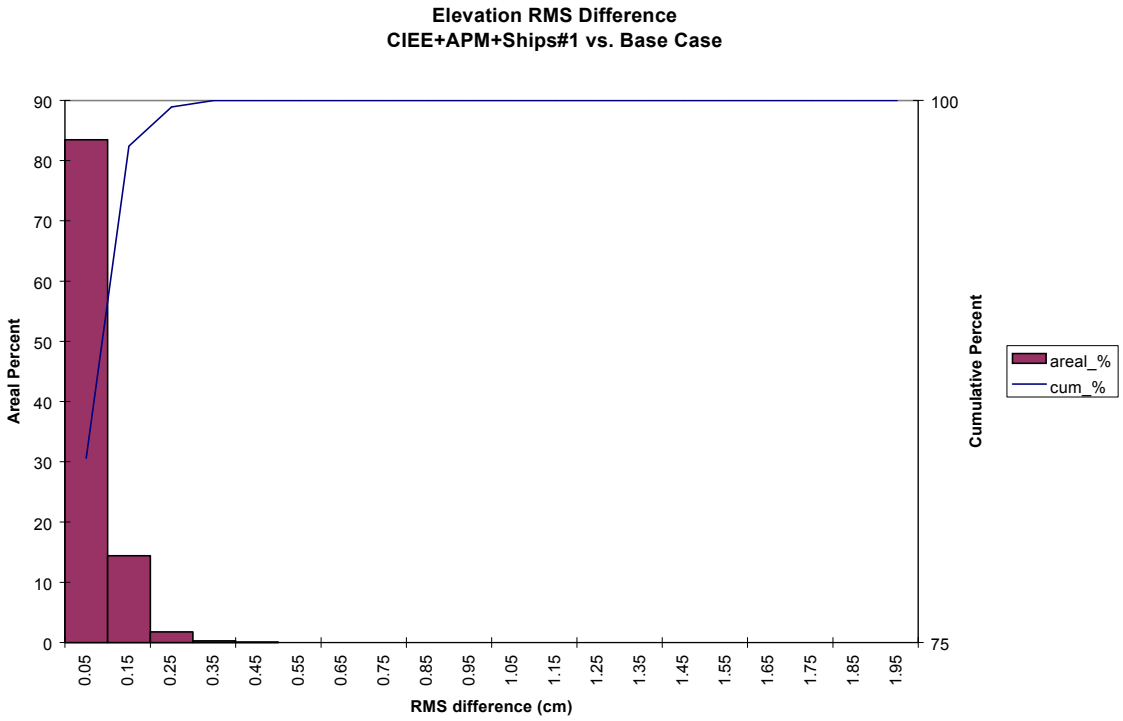

Figure 17. Frequency distribution of elevation RMS difference for the Eastward Expansion plus APM Terminal Dredging plus Ships (Case 2a) versus the Base Case.

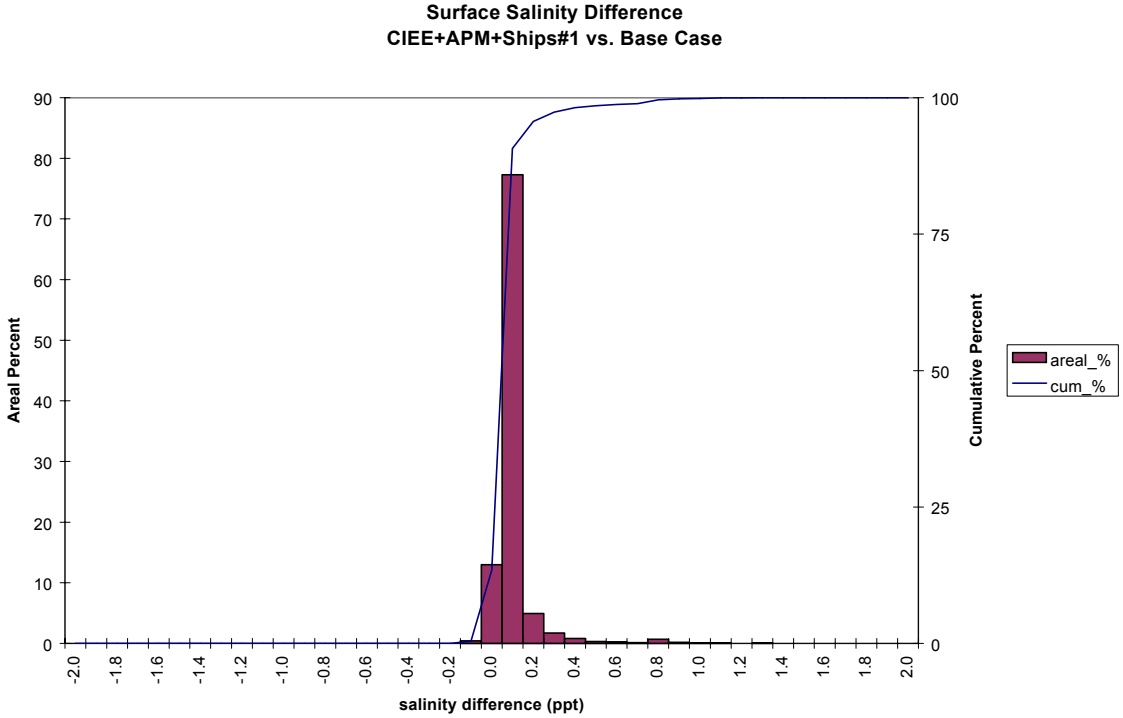

Figure 18. Frequency distribution of surface salinity difference for the Eastward Expansion plus APM Terminal Dredging plus Ships (Case 2a) versus the Base Case.

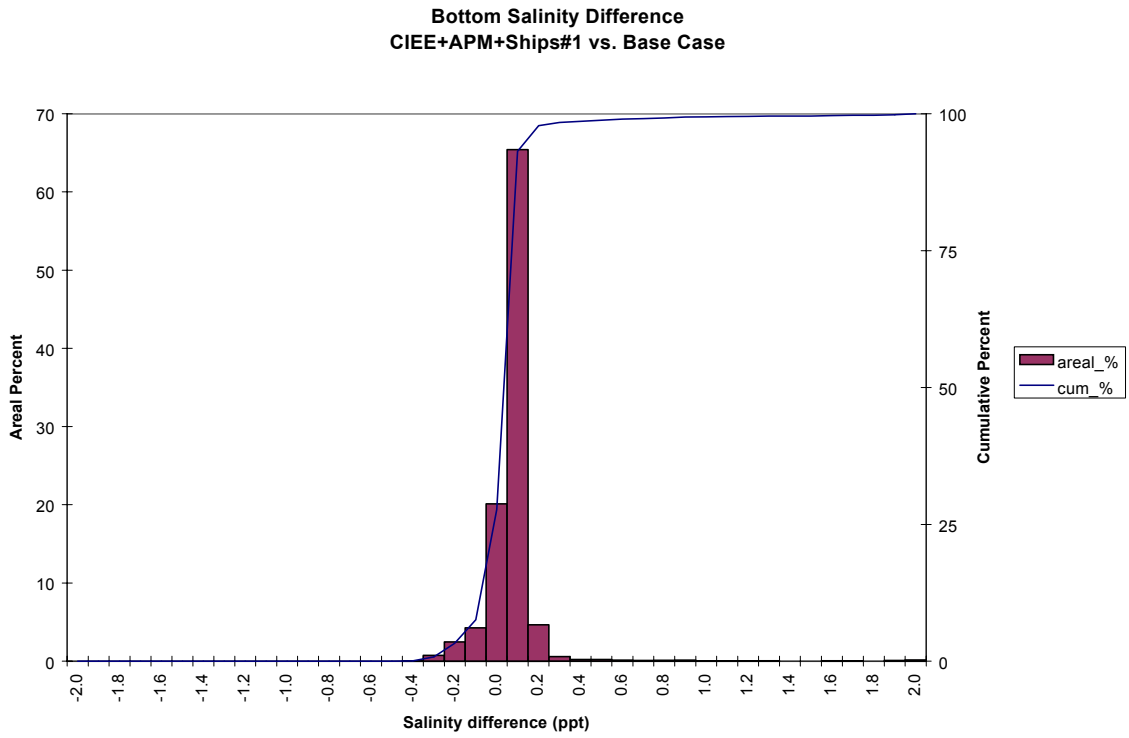

Figure 19. Frequency distribution of bottom salinity average difference for the Eastward Expansion plus APM Terminal Dredging plus Ships (Case 2a) versus the Base Case.

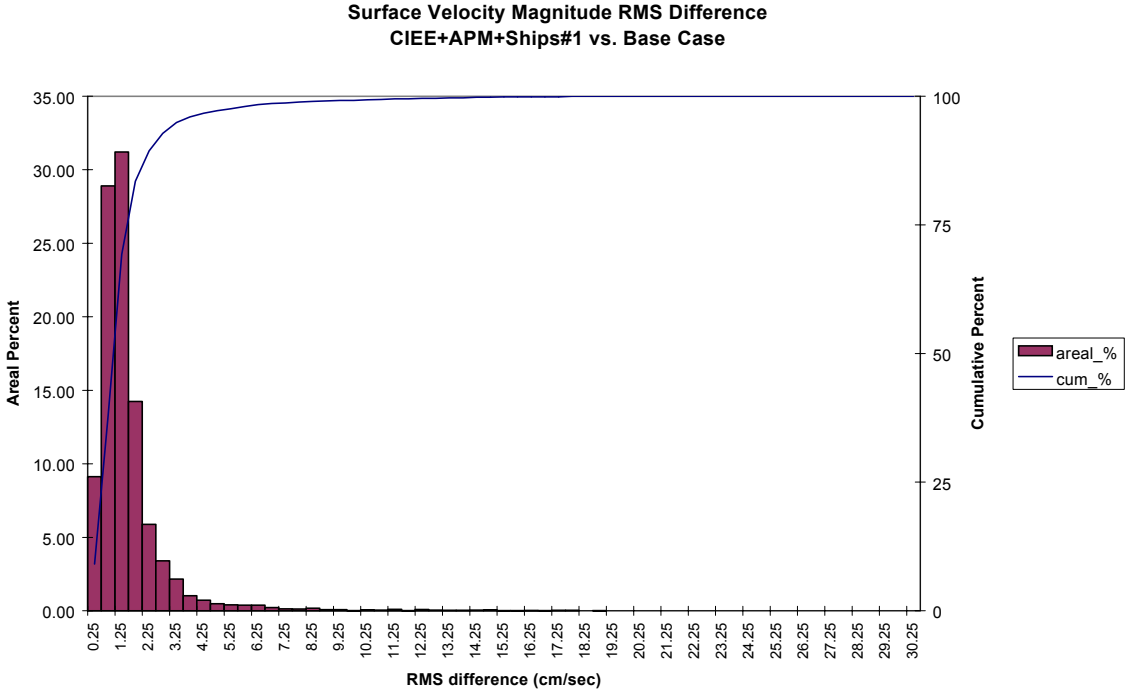

Figure 20. Frequency distribution of surface velocity RMS difference for the Eastward Expansion plus APM Terminal Dredging plus Ships (Case 2a) versus the Base Case.

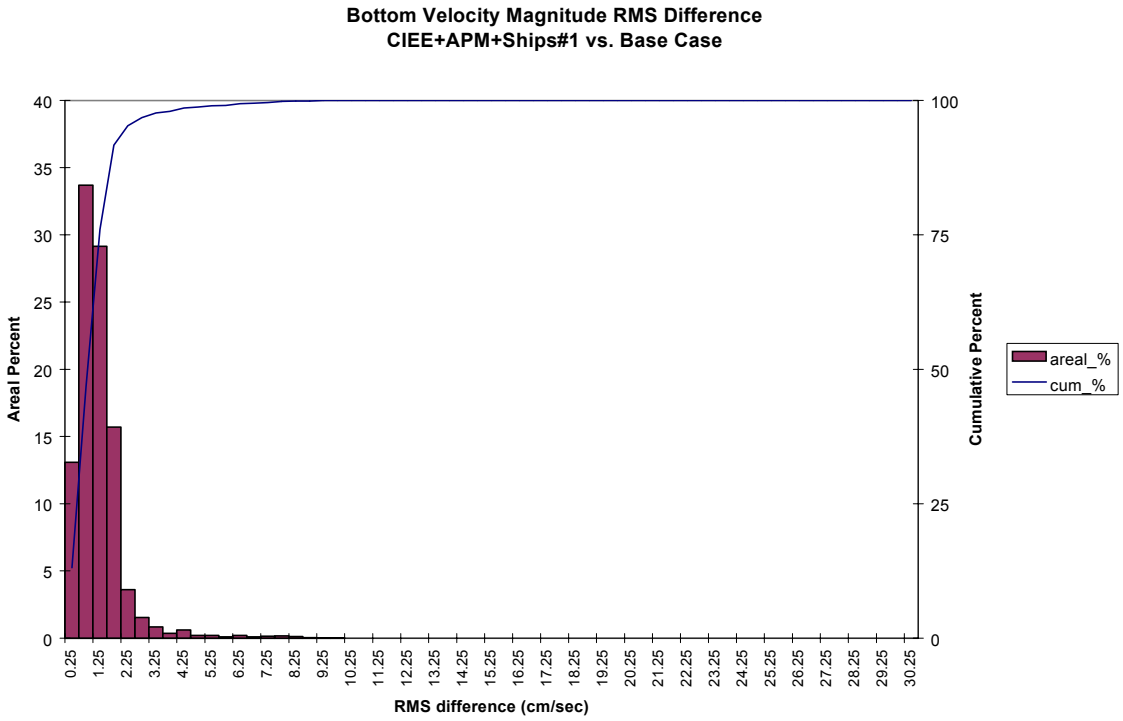

Figure 21. Frequency distribution of bottom velocity RMS difference for the Eastward plus APM Terminal Dredging plus Ships (Case 2a) versus the Base Case.

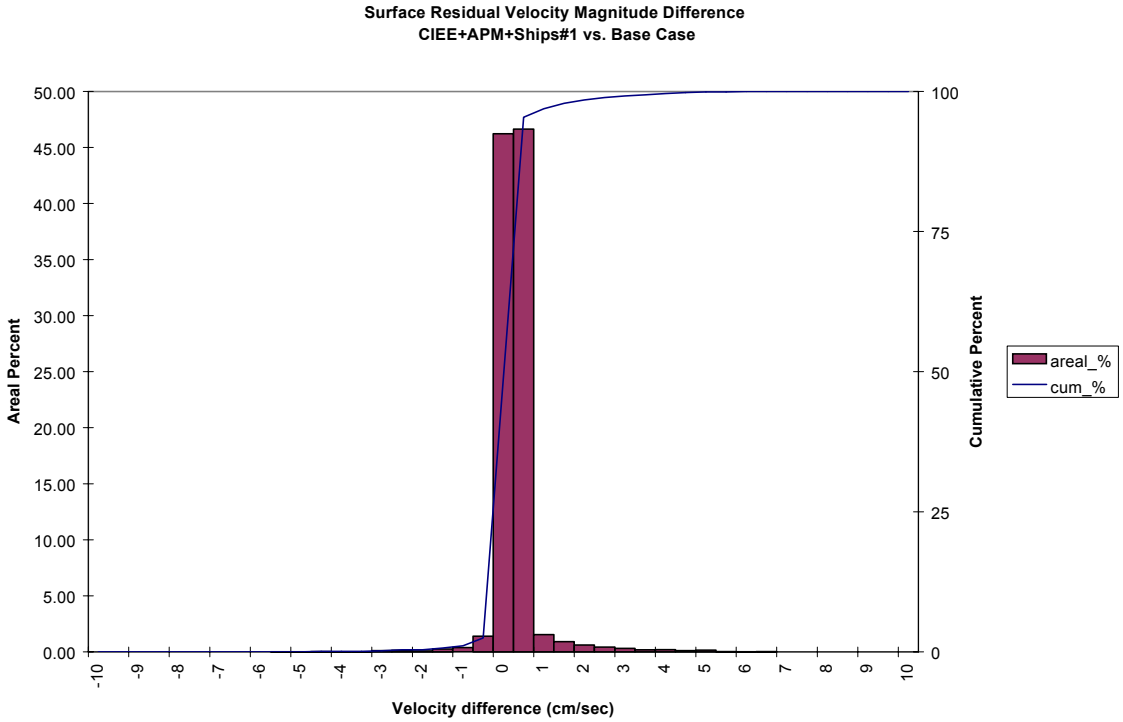

Figure 22. Frequency distribution of surface residual velocity magnitude average difference for the Eastward Expansion plus APM Terminal Dredging plus Ships (Case 2a) versus the Base Case.

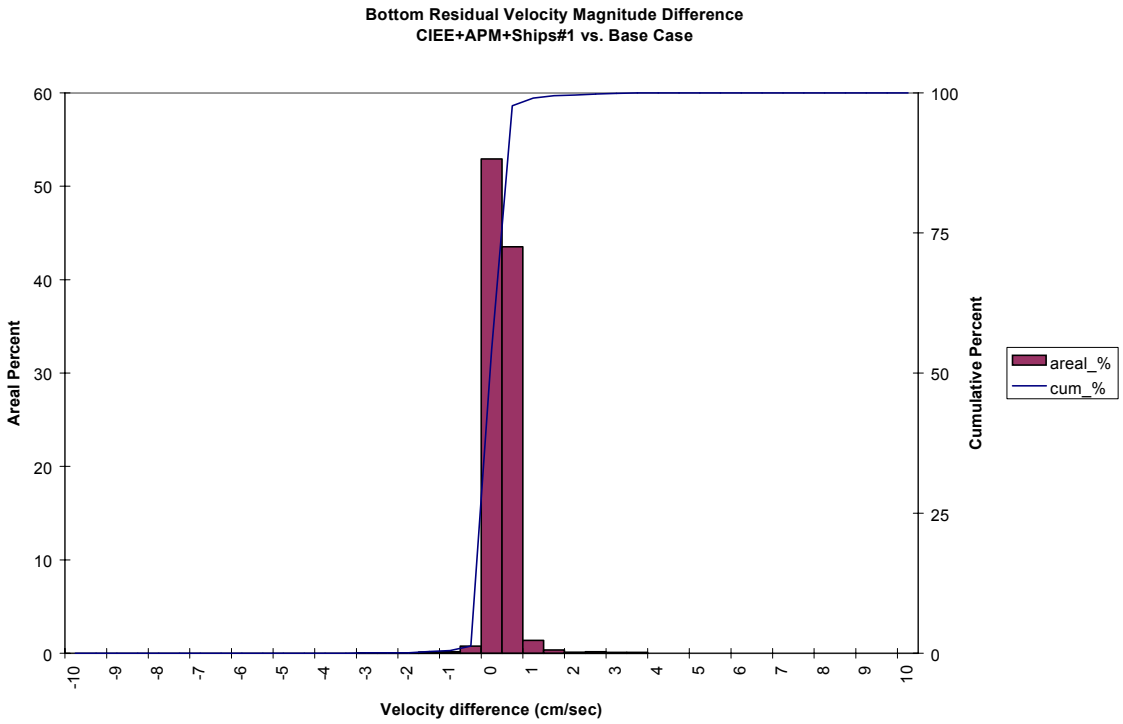

Figure 23. Frequency distribution of bottom residual velocity magnitude difference for the Eastward Expansion plus APM Terminal Dredging plus Ships (Case 2a) versus the Base Case.

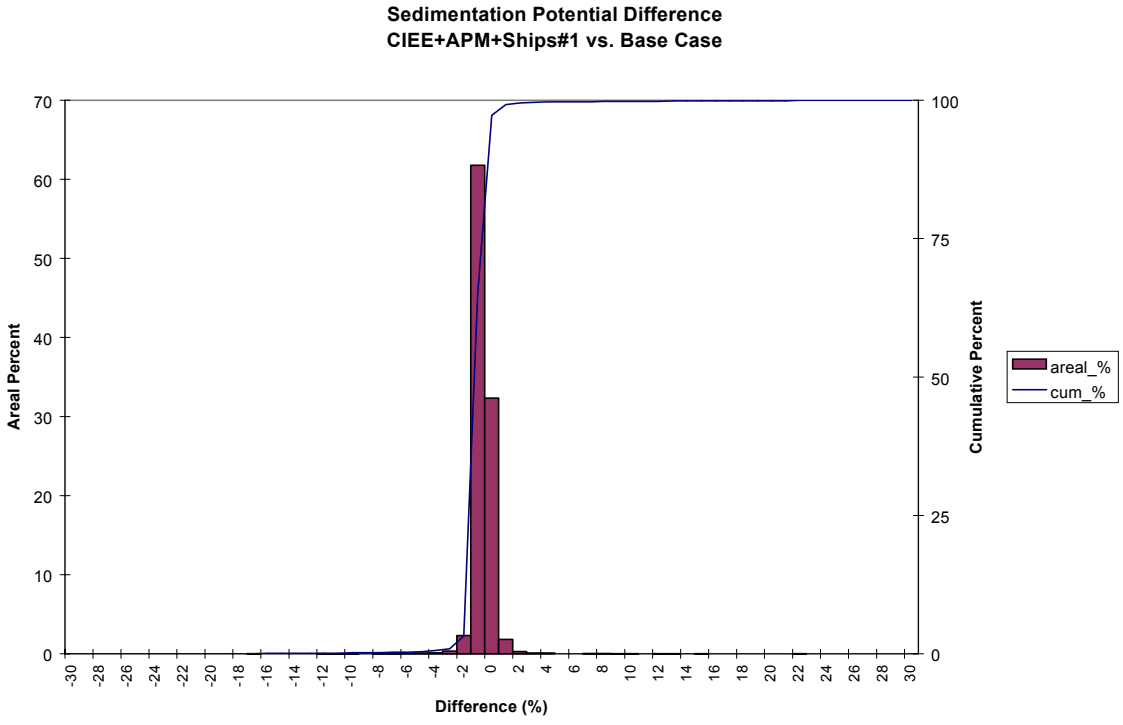

Figure 24. Frequency distribution of sedimentation potential difference for the Eastward Expansion plus APM Terminal Dredging plus Ships (Case 2a) versus the Base Case.

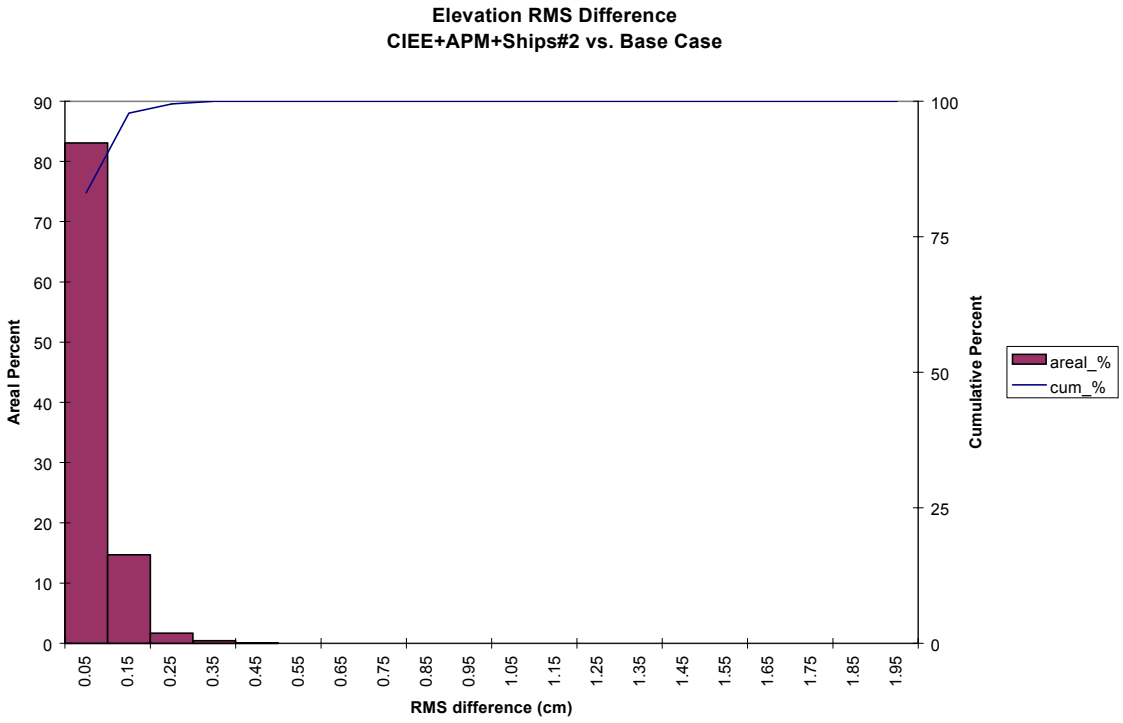

Figure 25. Frequency distribution of elevation RMS difference for the Eastward Expansion plus APM Terminal Dredging plus Ships (Case 2b) versus the Base Case.

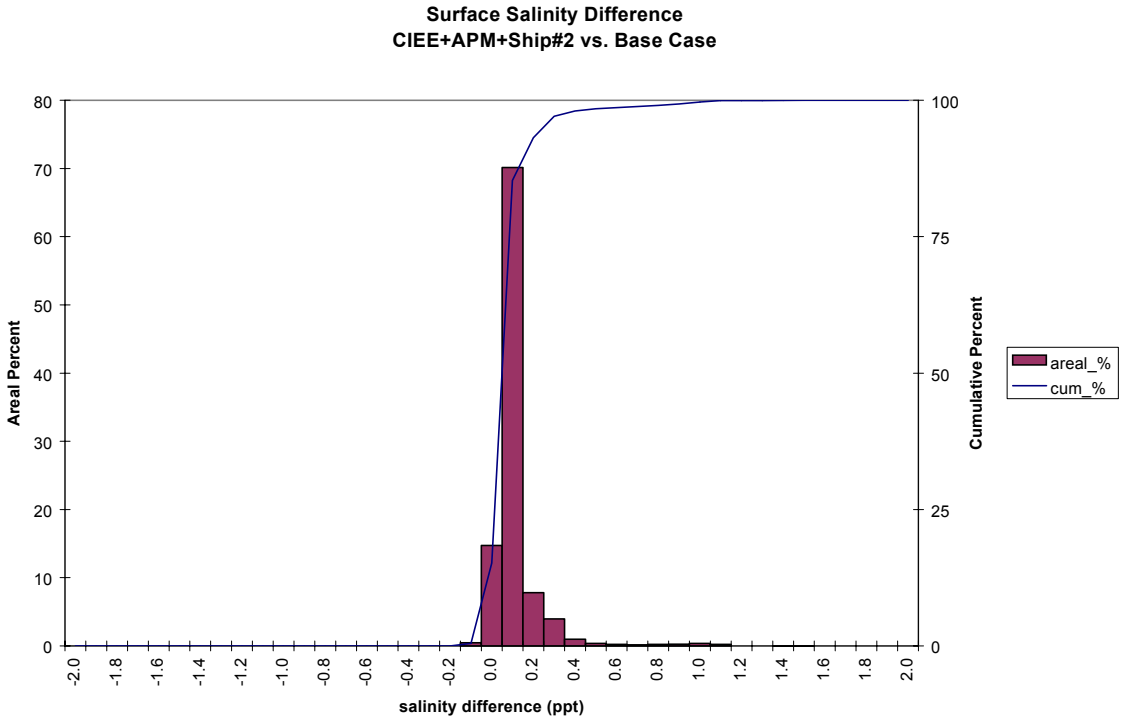

Figure 26. Frequency distribution of surface salinity difference for the Eastward Expansion plus APM Terminal Dredging plus Ships (Case 2b) versus the Base Case.

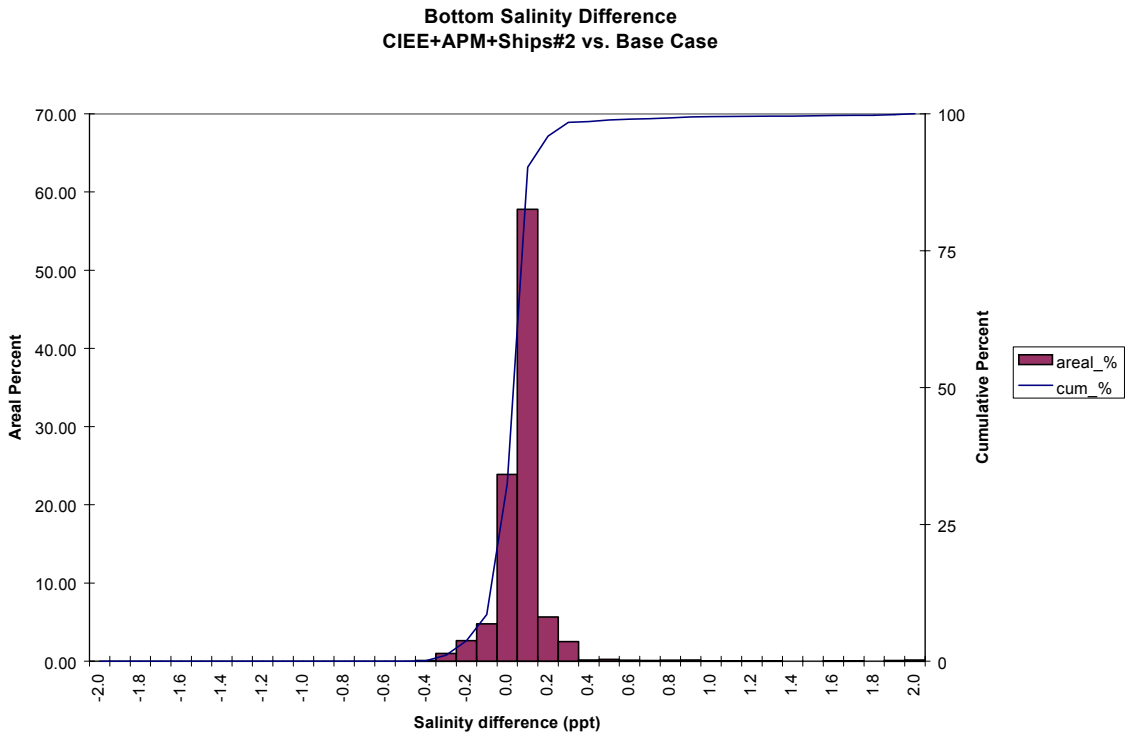

Figure 27. Frequency distribution of bottom salinity average difference for the Eastward Expansion plus APM Terminal Dredging plus Ships (Case 2b) versus the Base Case.

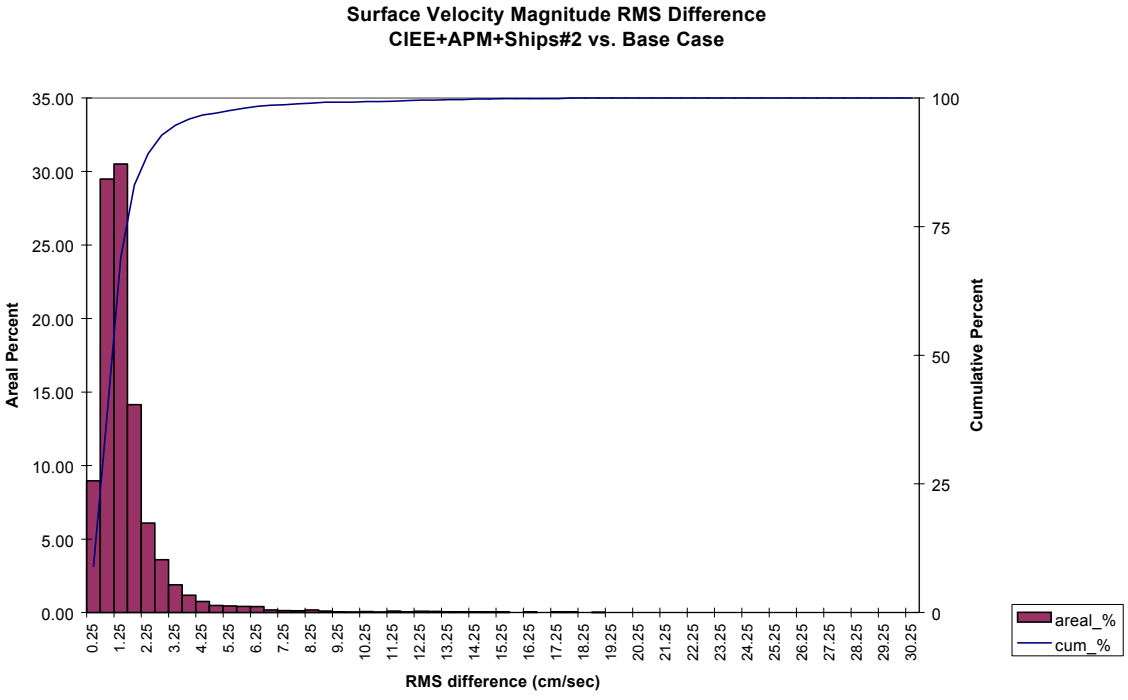

Figure 28. Frequency distribution of surface velocity RMS difference for the Eastward Expansion plus APM Terminal Dredging plus Ships (Case 2b) versus the Base Case.

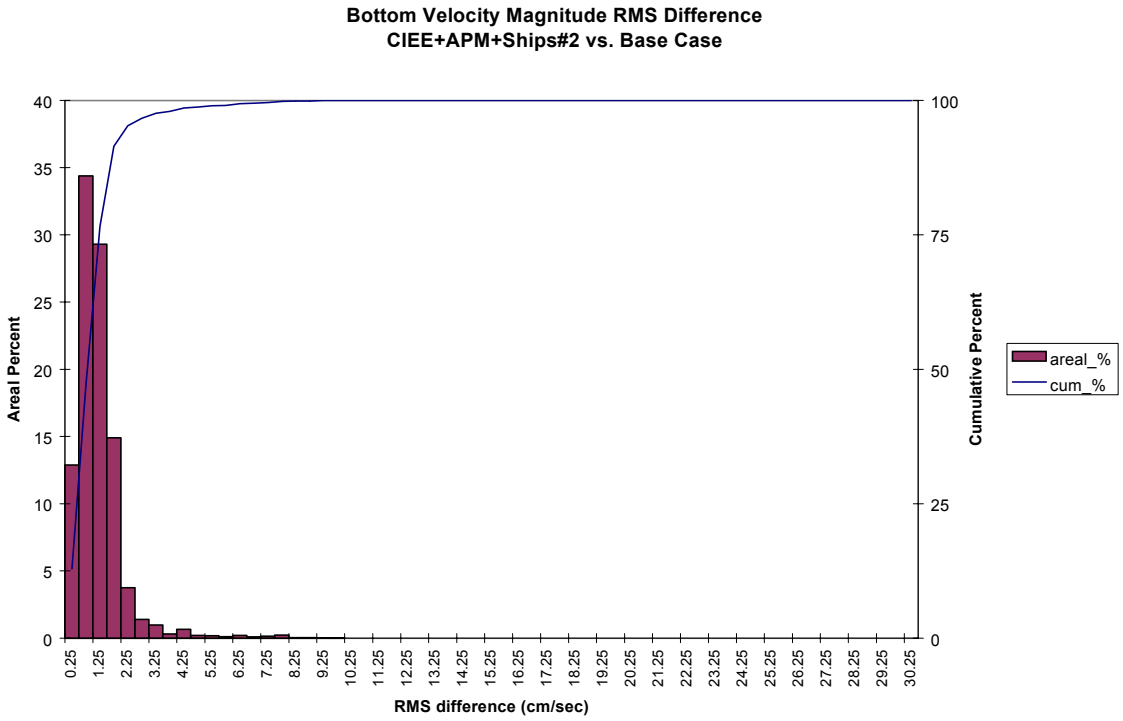

Figure 29. Frequency distribution of bottom velocity RMS difference for the Eastward Expansion plus APM Terminal Dredging plus Ships (Case 2b) versus the Base Case.

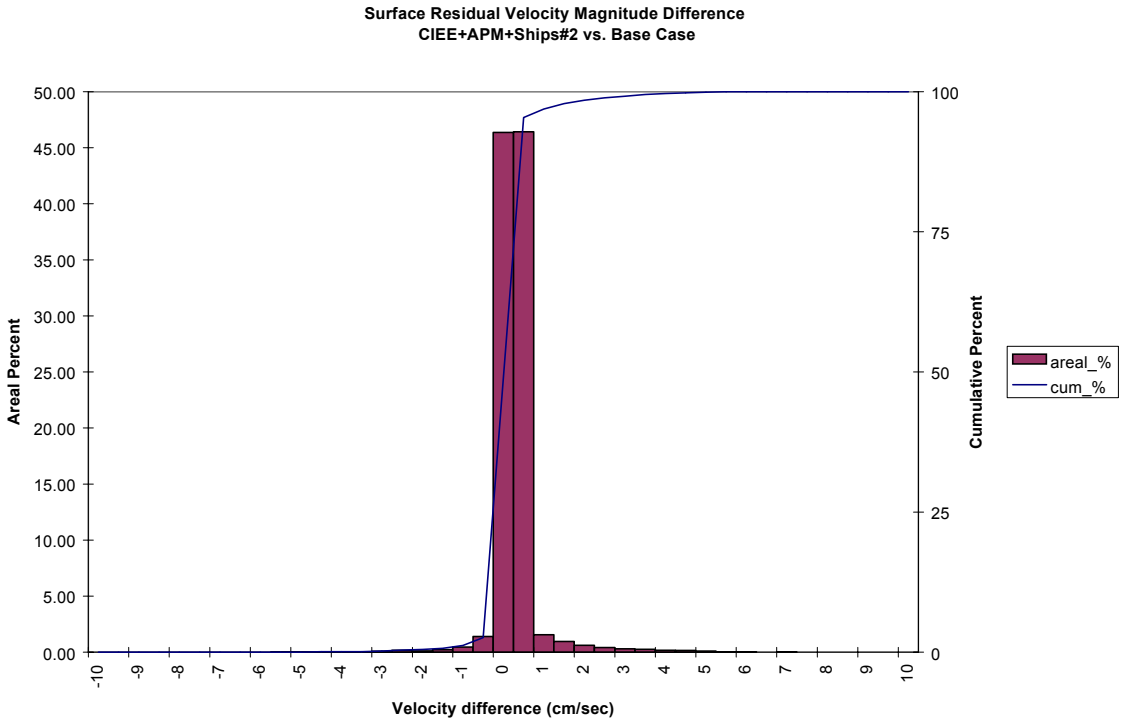

Figure 30. Frequency distribution of surface residual velocity magnitude average Difference for the Eastward Expansion plus APM Terminal Dredging plus Ships (Case 2b) versus the Base Case.

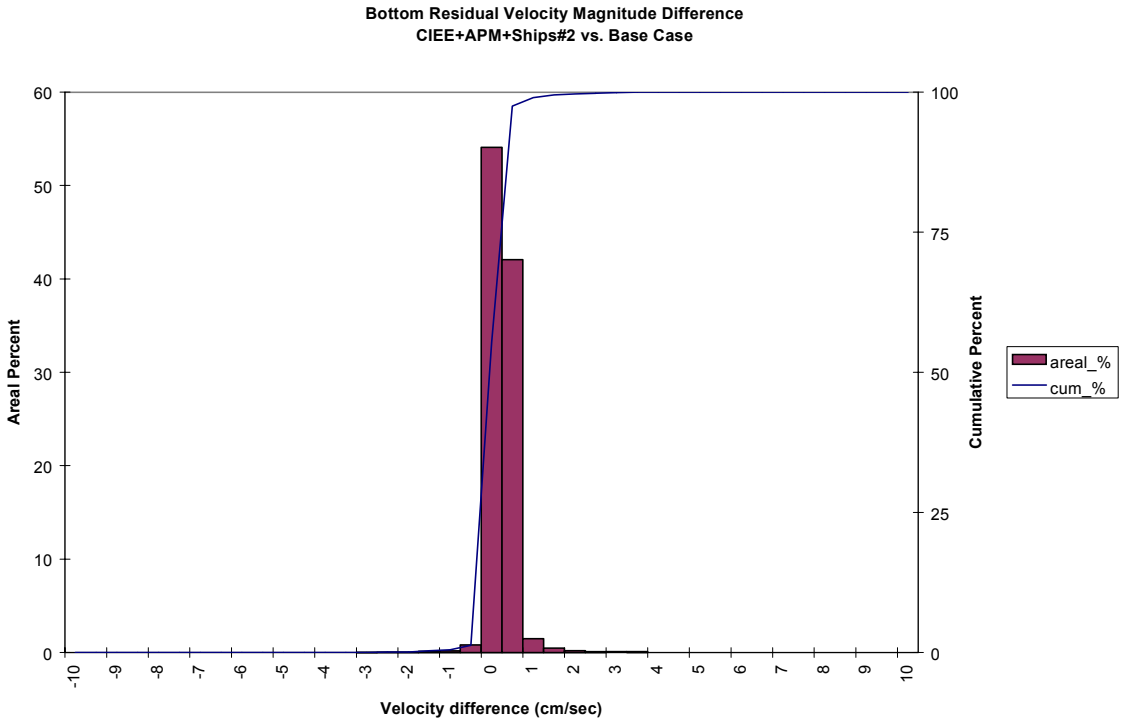

Figure 31. Frequency distribution of bottom residual velocity magnitude difference for the Eastward Expansion plus APM Terminal Dredging plus Ships (Case 2b) versus the Base Case.

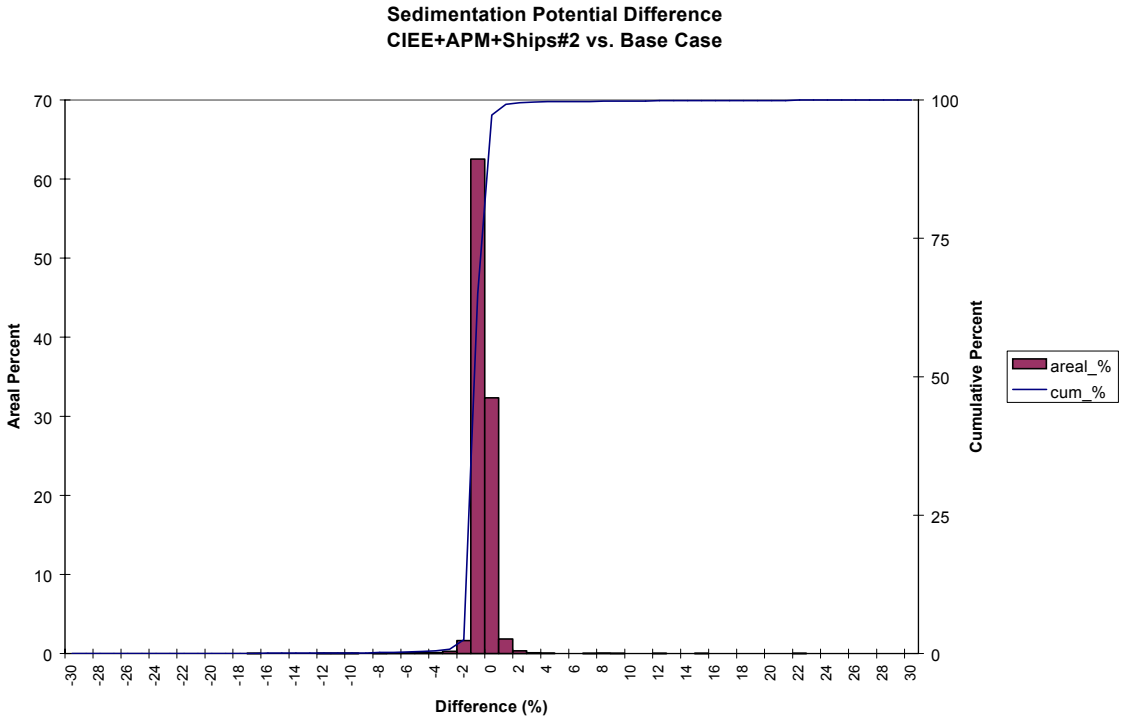

Figure 32. Frequency distribution of sedimentation potential difference for the Eastward Expansion plus APM Terminal Dredging plus Ships (Case 2b) versus the Base Case.

APPENDIX to CHAPTER IV, SECTION A.1

Global Comparisons of Historical Runs

Spatial Distributions

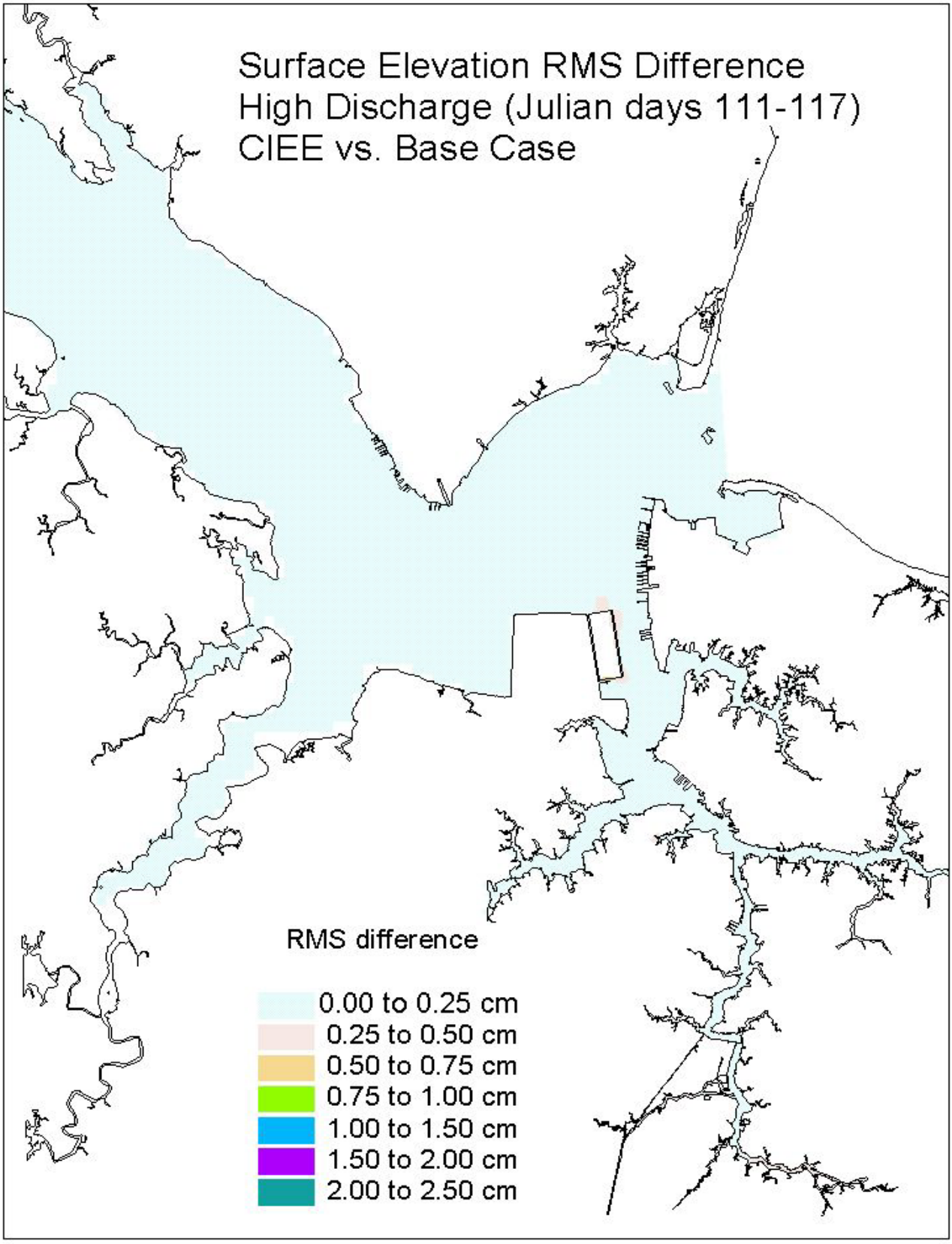

Figure 1. Historical simulation comparison (high discharge) of the surface elevation RMS difference for the Eastward Expansion versus the Base Case.

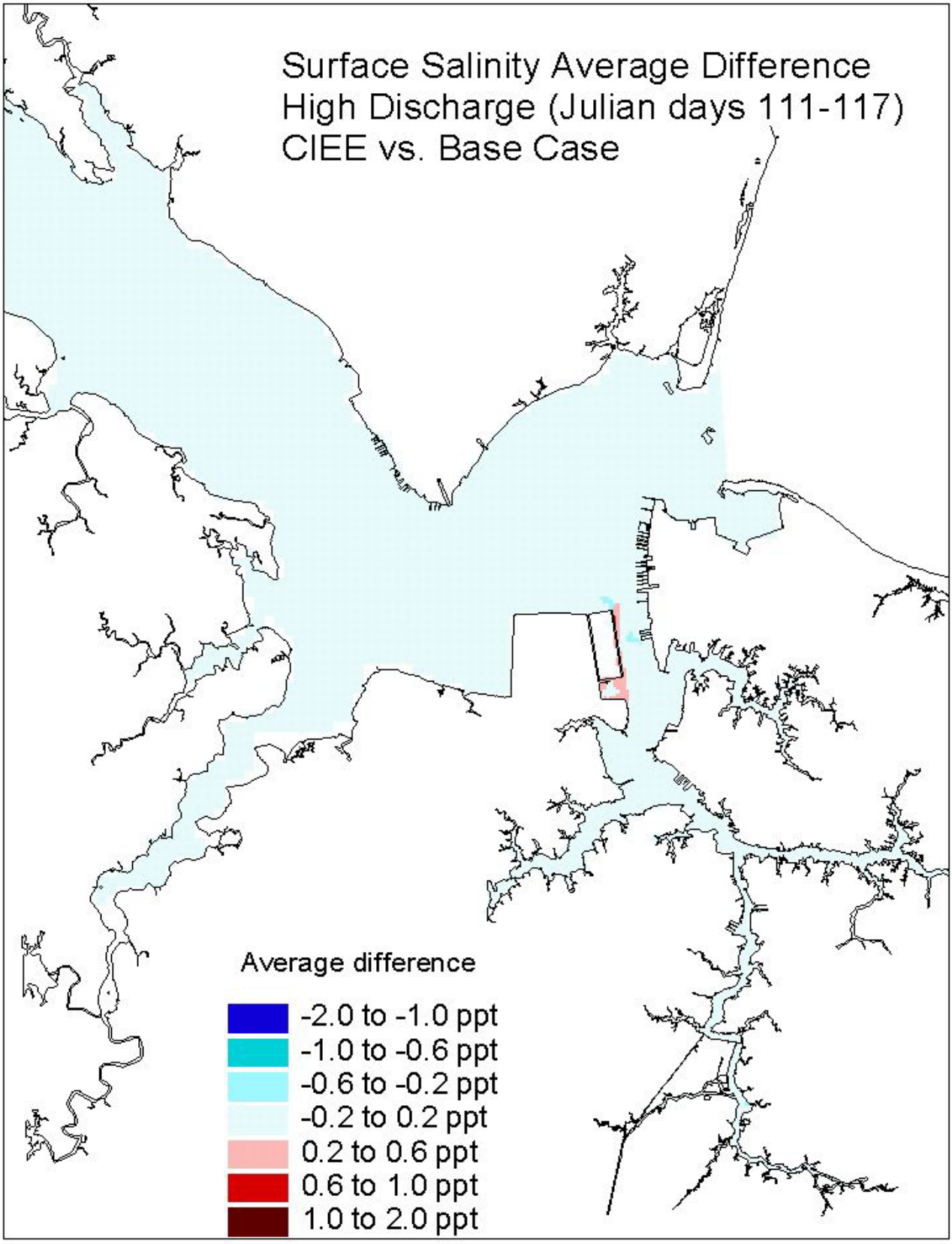

Figure 2. Historical simulation comparison (high discharge) of the surface salinity average difference for the Eastward Expansion versus the Base Case.

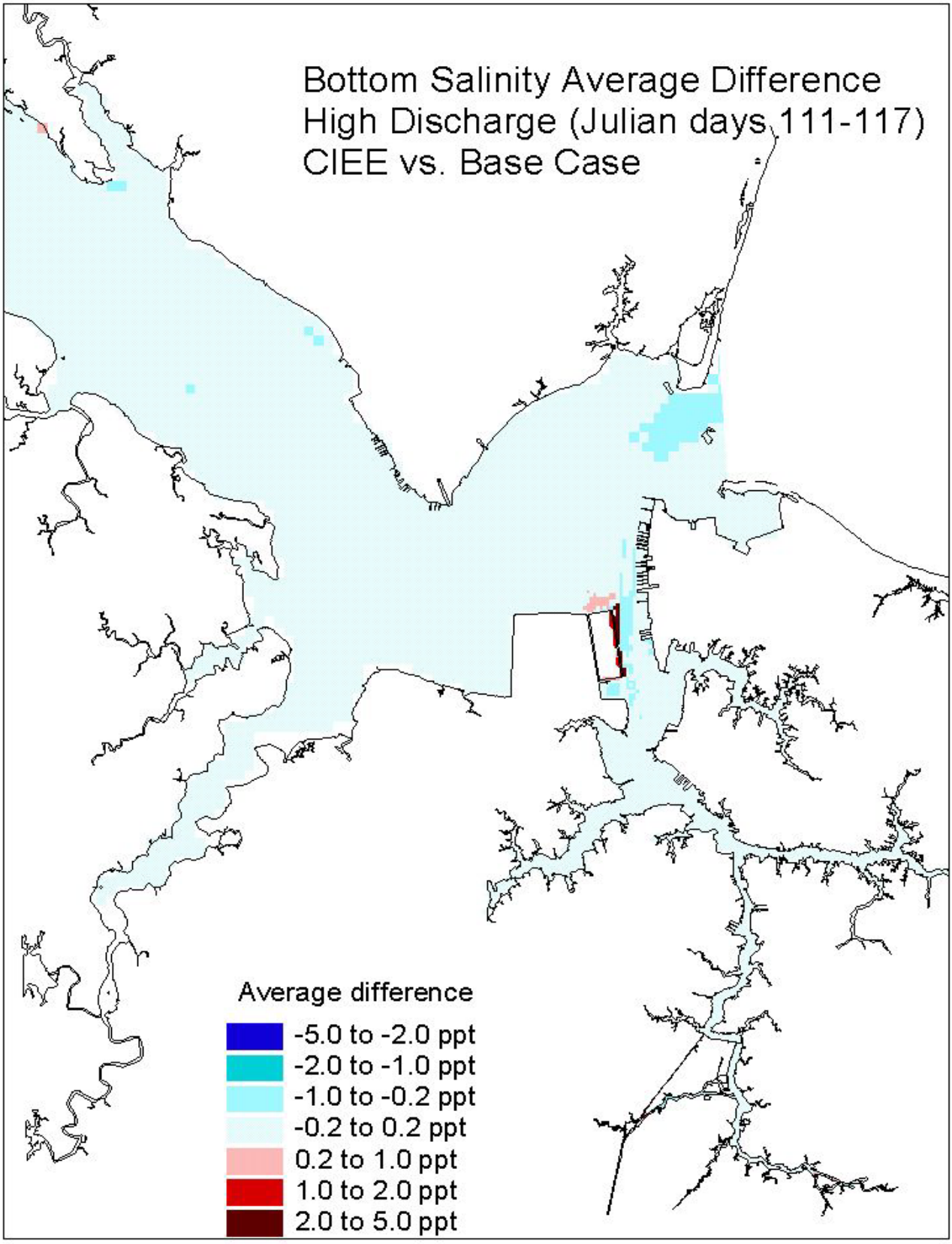

Figure 3. Historical simulation comparison (high discharge) of the bottom salinity average difference for the Eastward Expansion versus the Base Case.

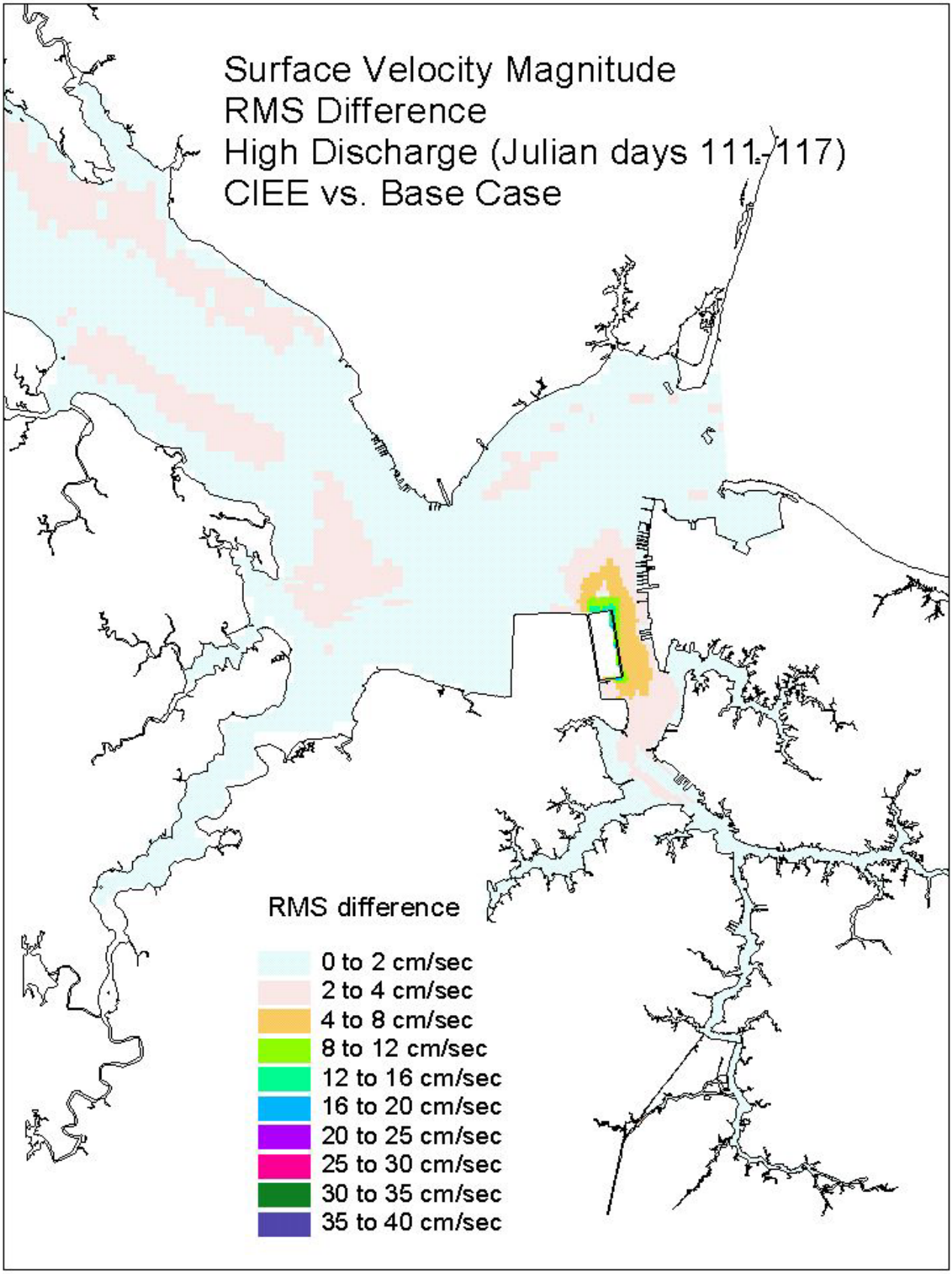

Figure 4. Historical simulation comparison (high discharge) of the surface velocity RMS difference for the Eastward Expansion versus the Base Case.

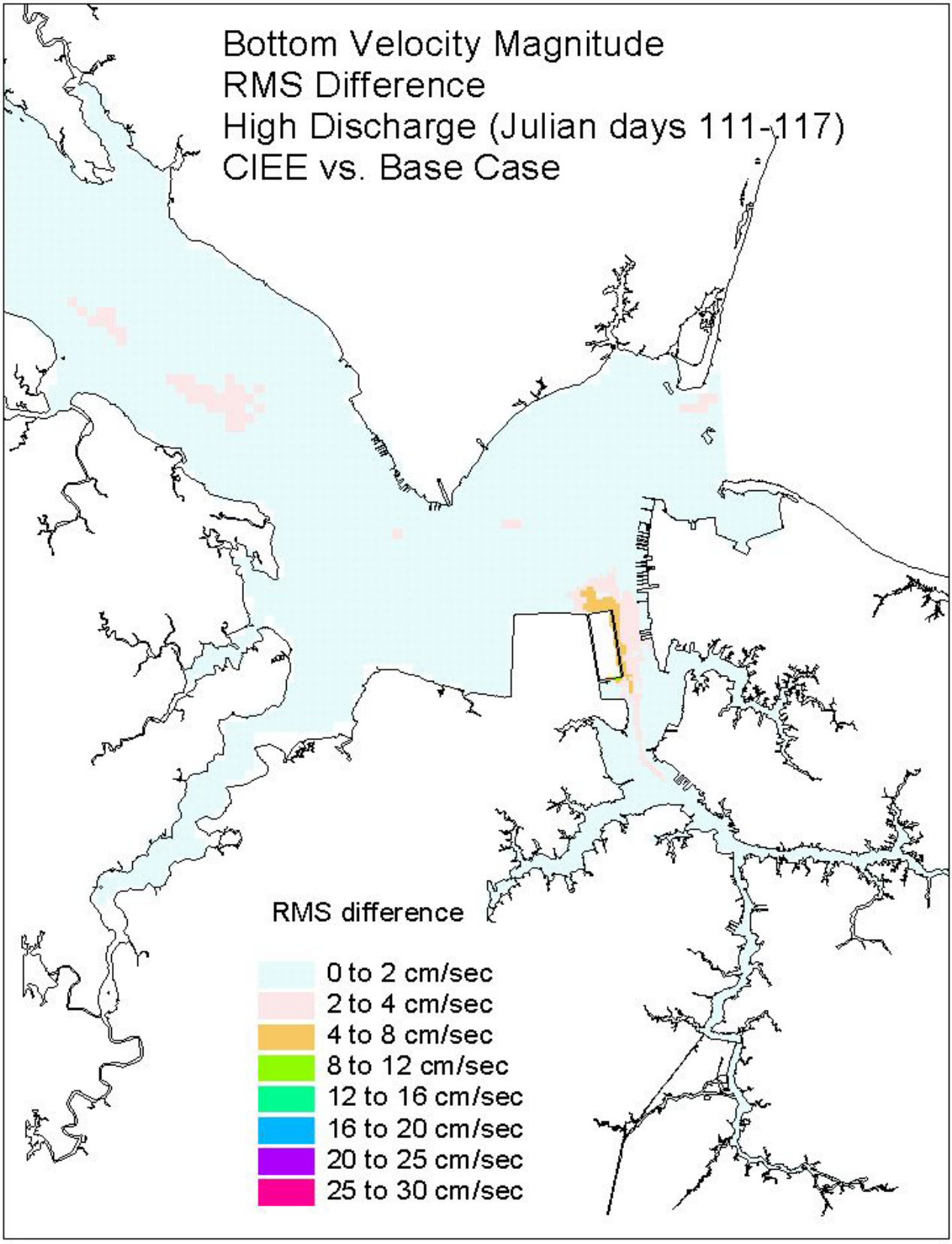

Figure 5. Historical simulation comparison (high discharge) of the bottom velocity RMS difference for the Eastward Expansion versus the Base Case.

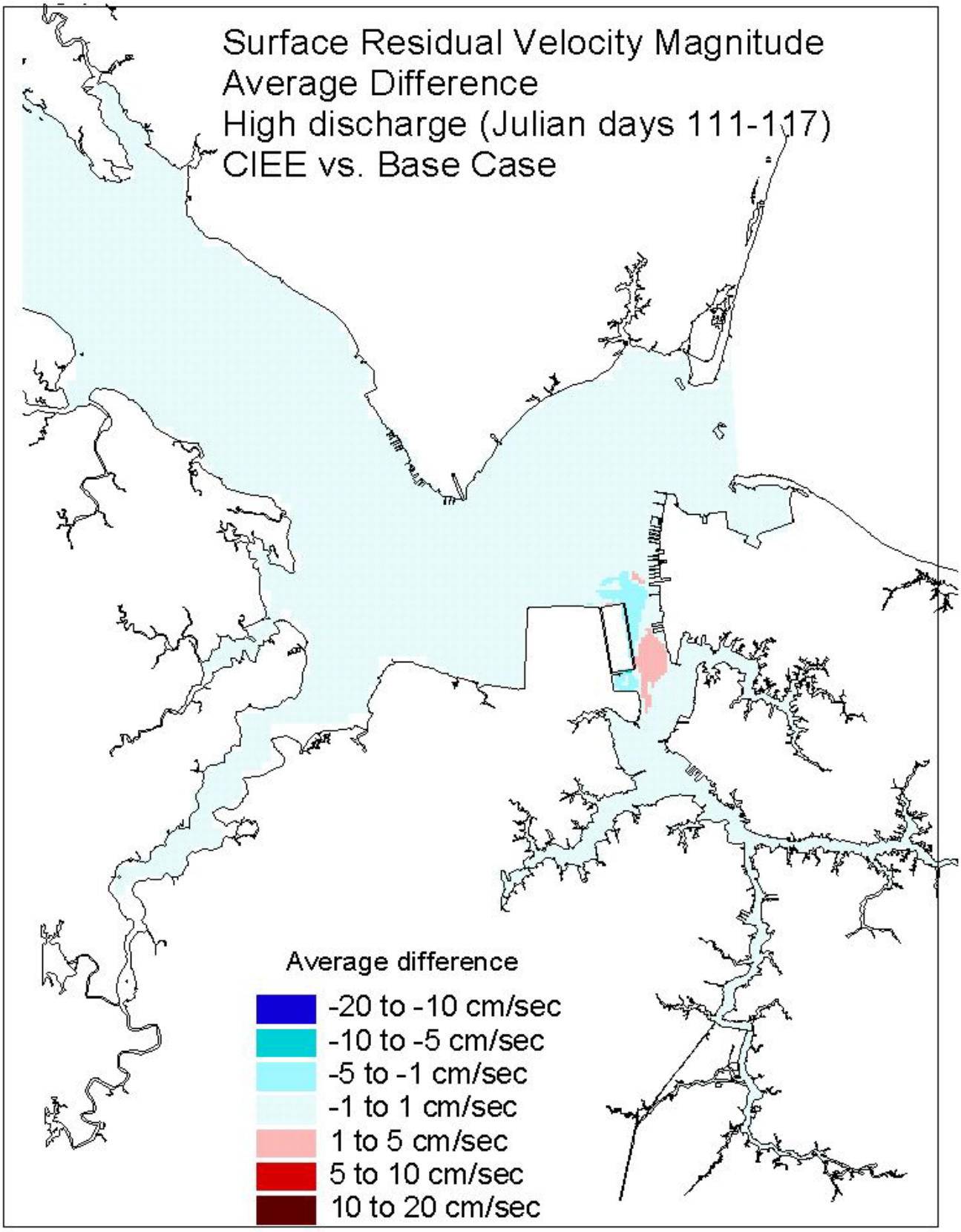

Figure 6. Historical simulation comparison (high discharge) of the surface residual velocity average difference for the Eastward Expansion versus the Base Case.

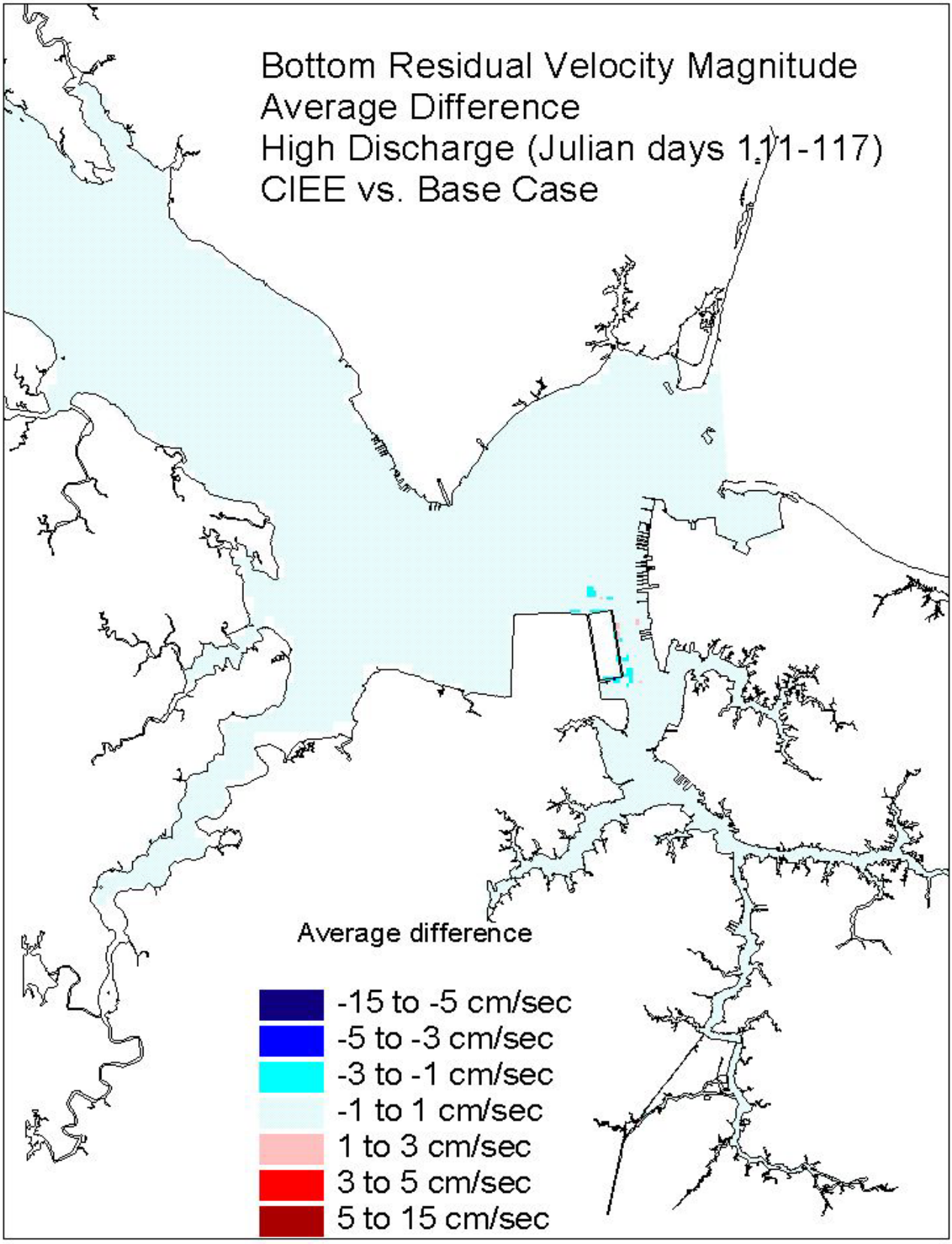

Figure 7. Historical simulation comparison (high discharge) of the bottom residual velocity average difference for the Eastward Expansion versus the Base Case.

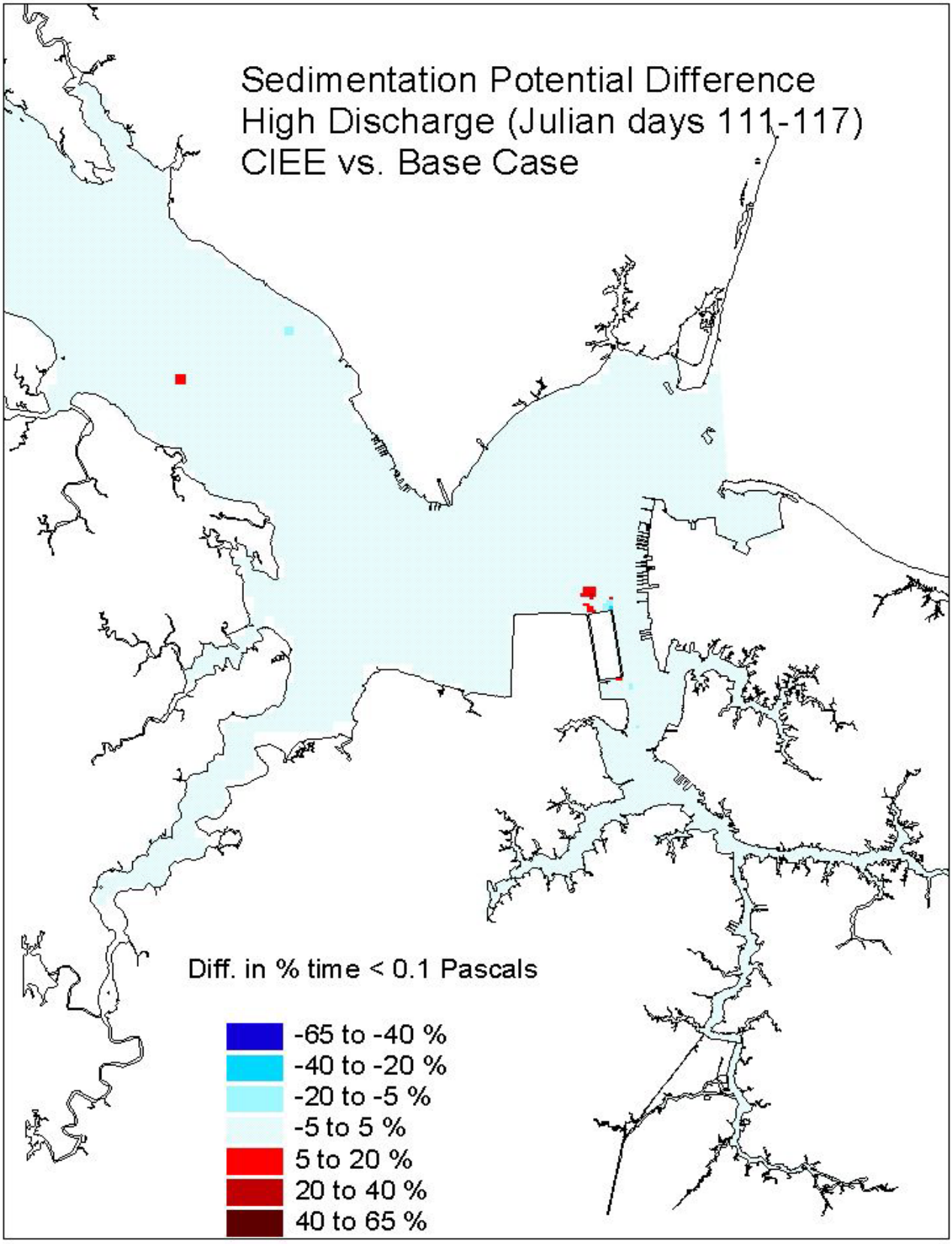

Figure 8. Historical simulation comparison (high discharge) of the sedimentation potential difference for the Eastward Expansion versus the Base Case.

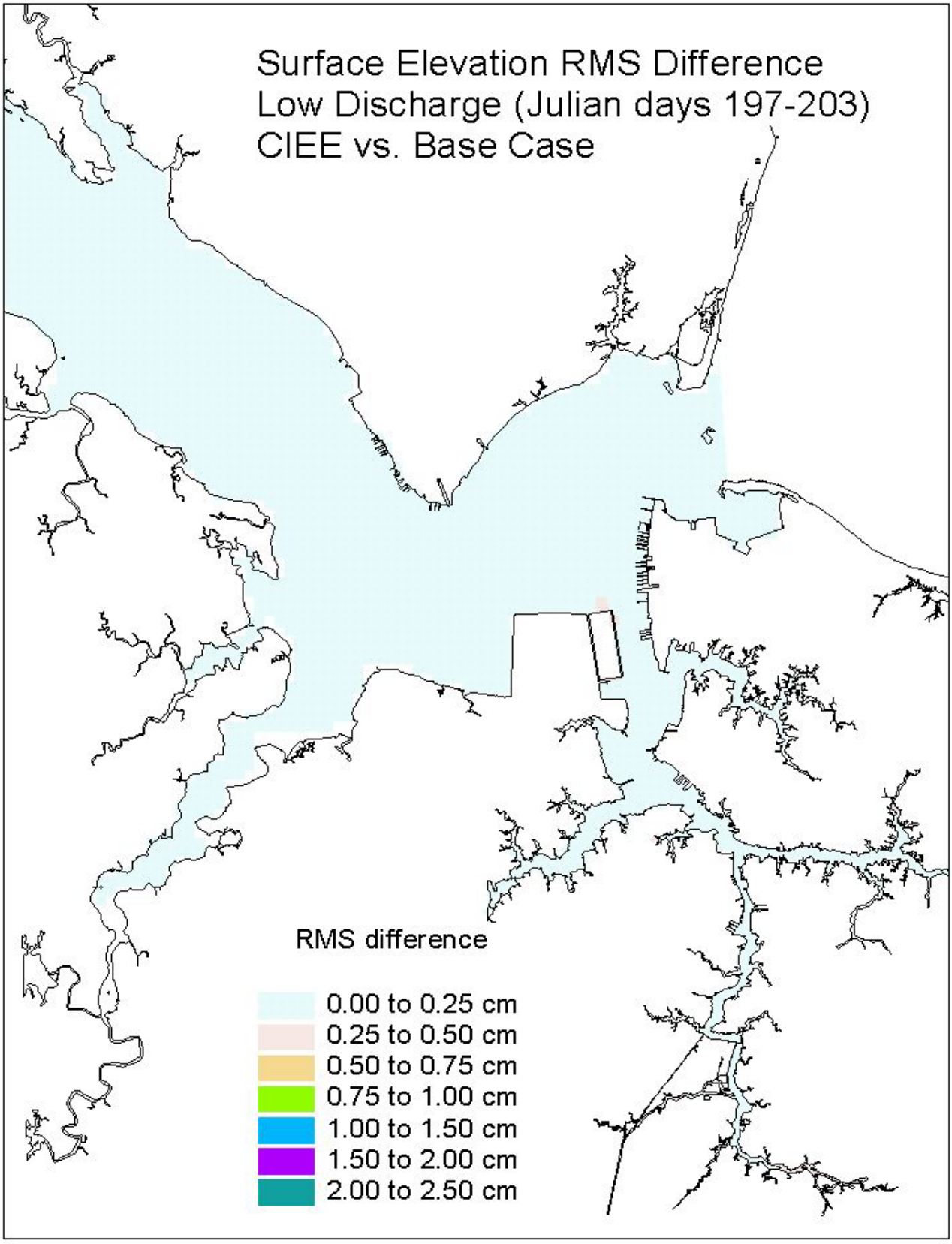

Figure 9. Historical simulation comparison (low discharge) of the surface elevation RMS difference for the Eastward Expansion versus the Base Case.

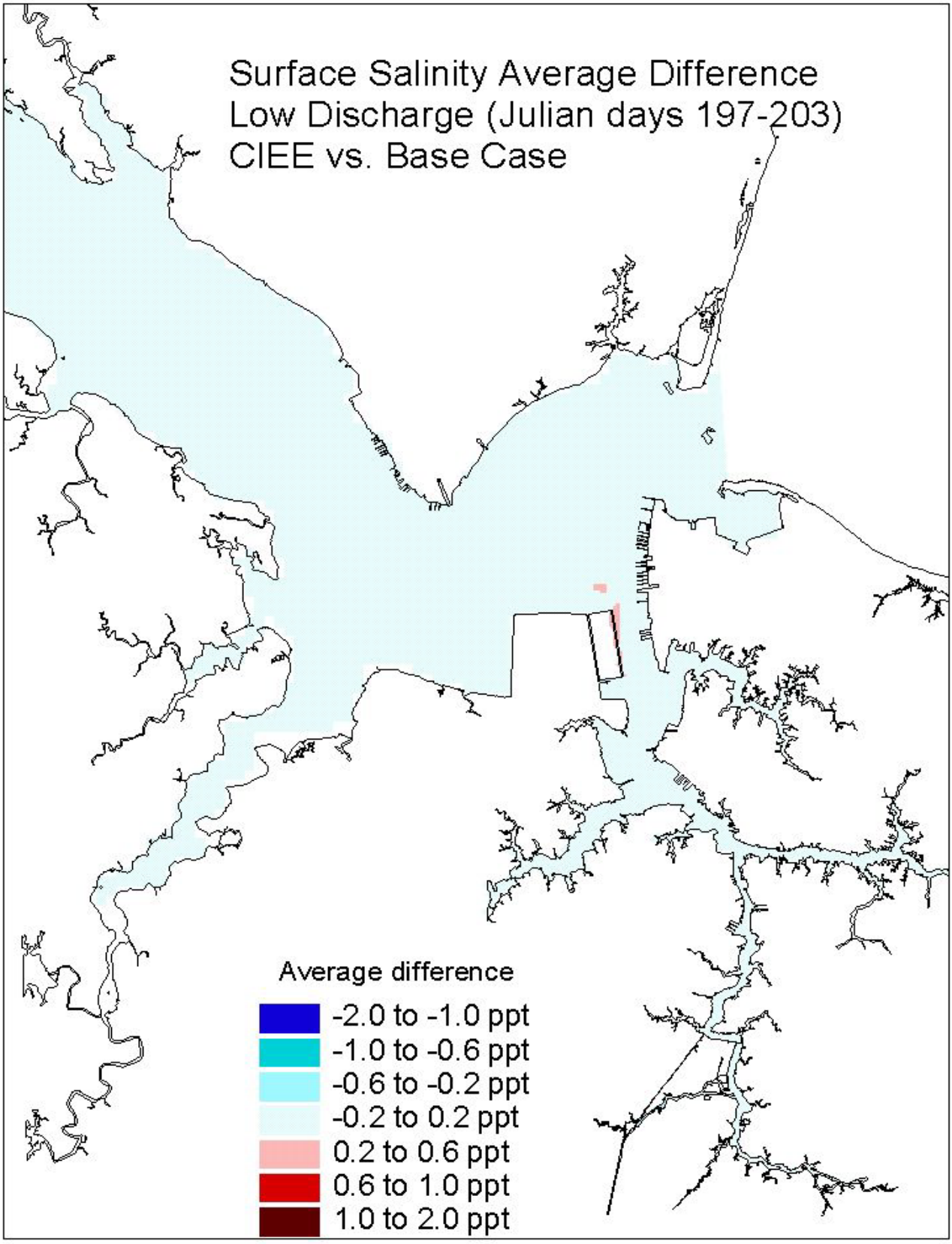

Figure 10. Historical simulation comparison (low discharge) of the surface salinity average difference for the Eastward Expansion versus the Base Case.

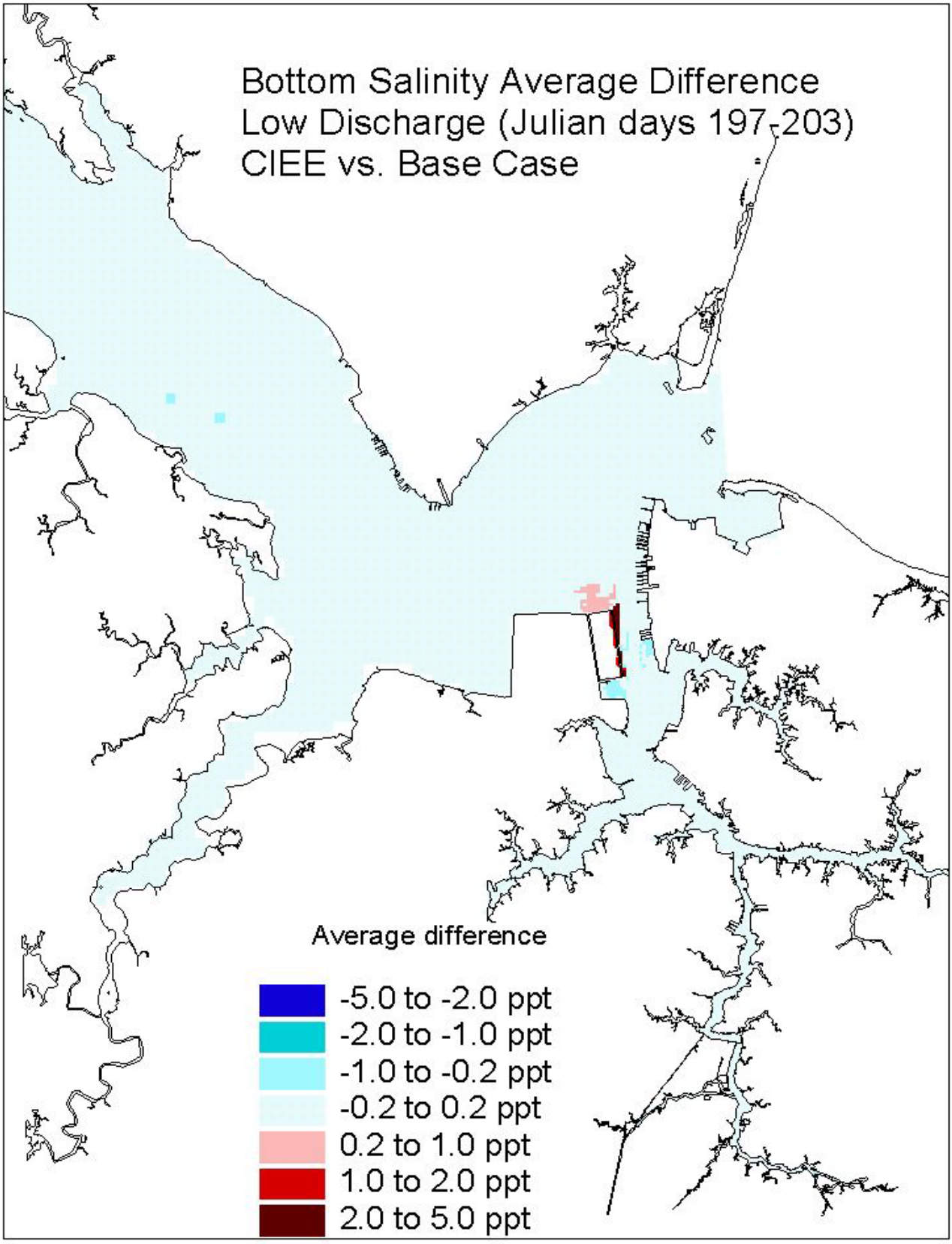

Figure 11. Historical simulation comparison (low discharge) of the bottom salinity average difference for the Eastward Expansion versus the Base Case.

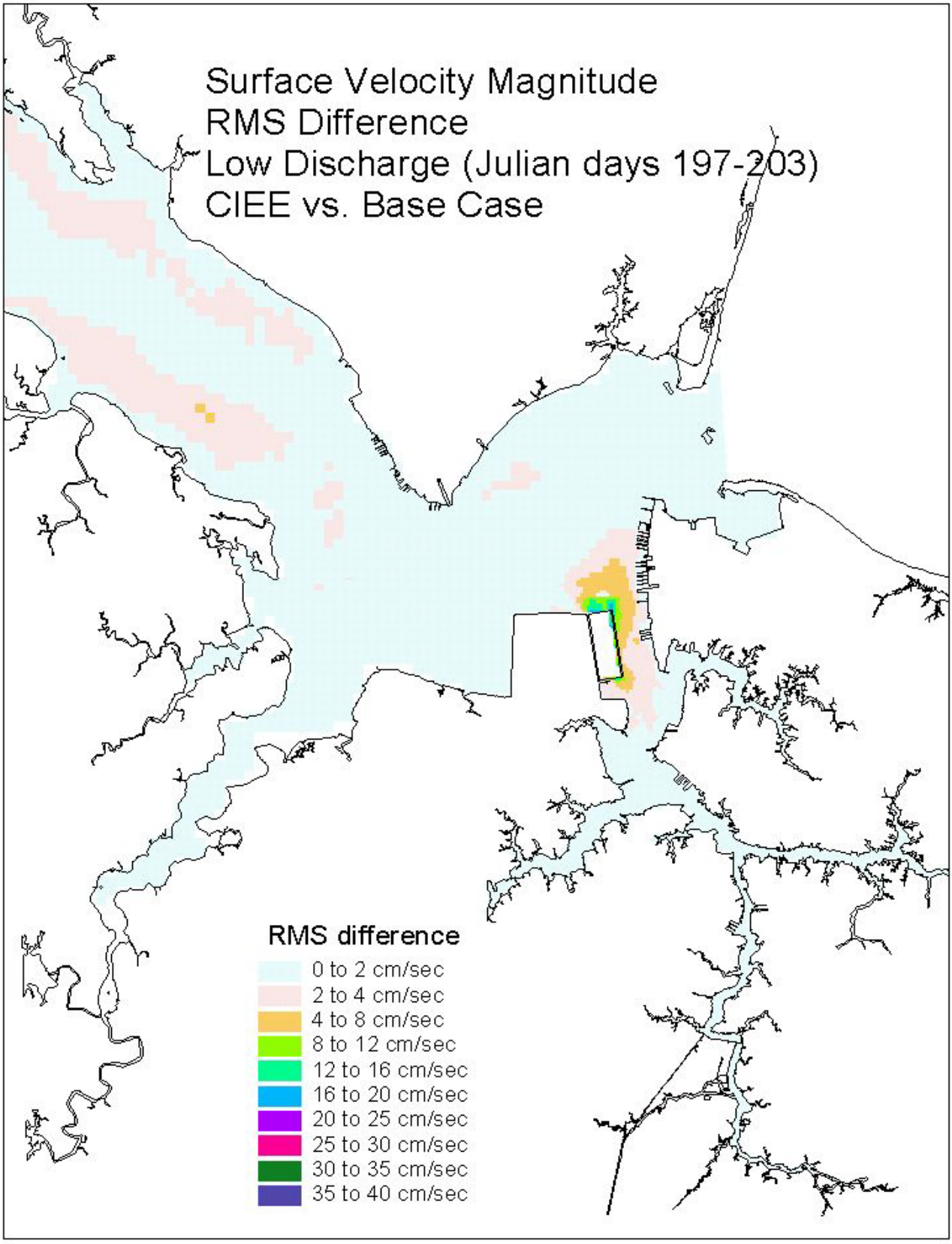

Figure 12. Historical simulation comparison (low discharge) of the surface velocity RMS difference for the Eastward Expansion versus the Base Case.

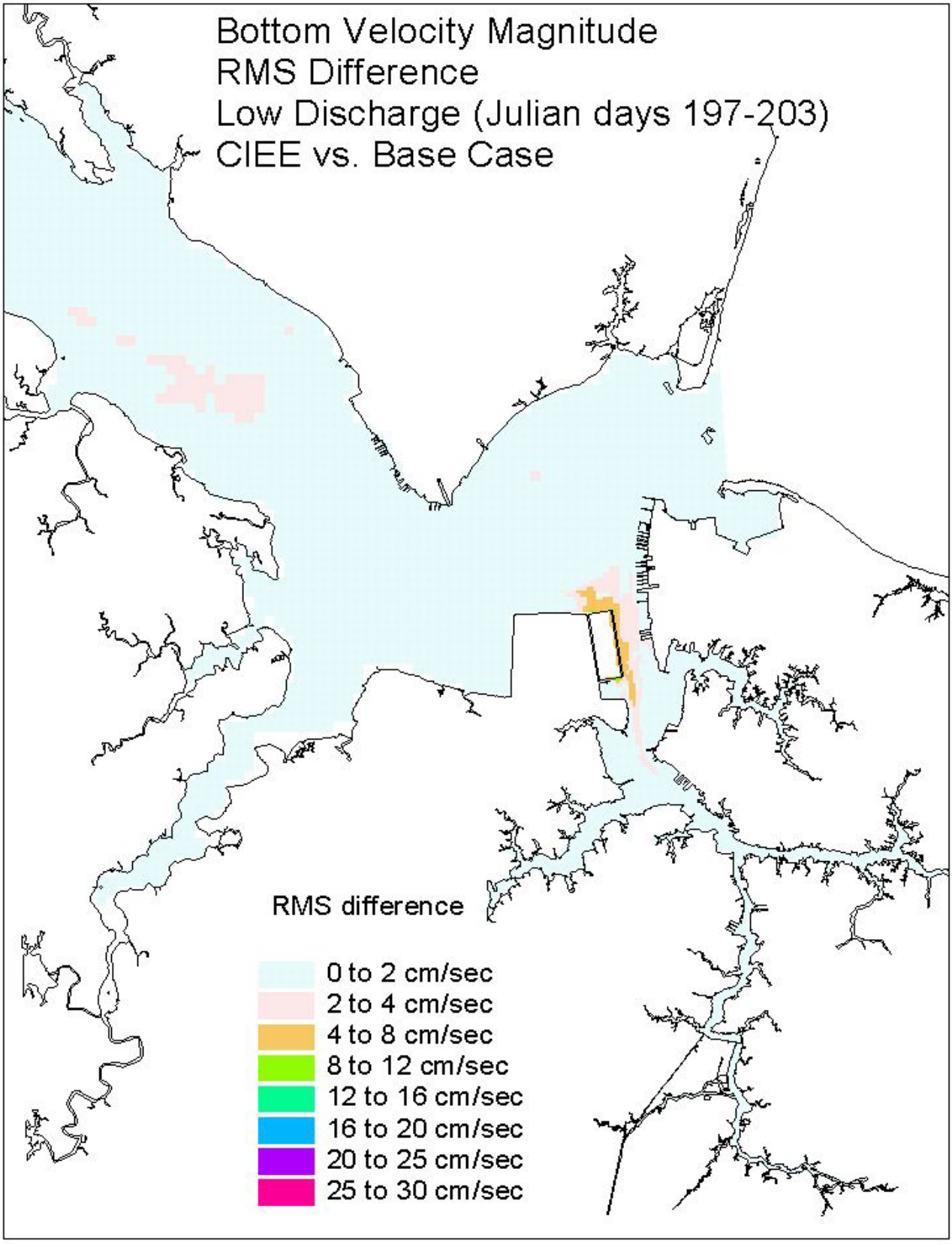

Figure 13. Historical simulation comparison (low discharge) of the bottom velocity RMS difference for the Eastward Expansion versus the Base Case.

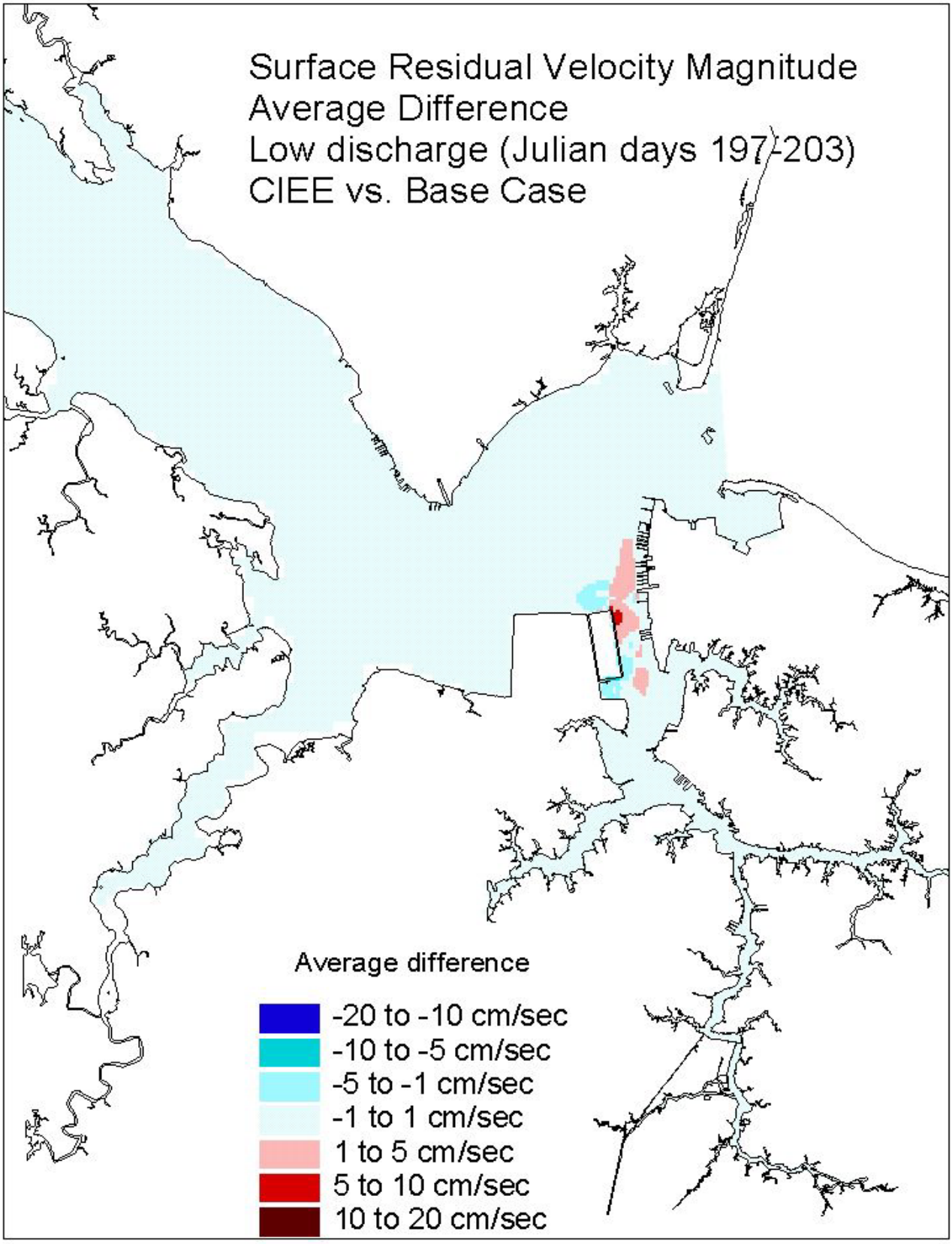

Figure 14. Historical simulation comparison (low discharge) of the surface residual velocity average difference for the Eastward Expansion versus the Base Case.

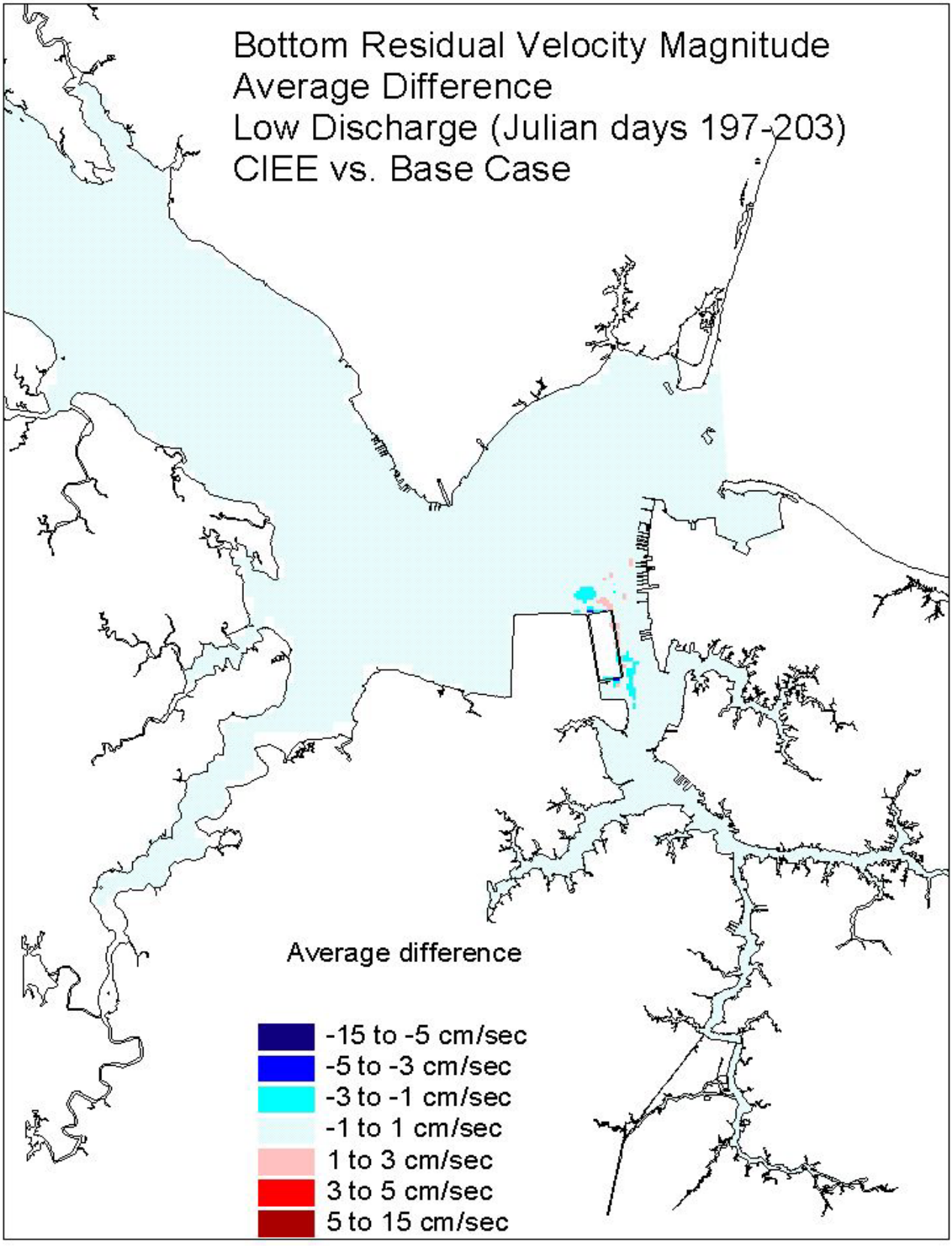

Figure 15. Historical simulation comparison (low discharge) of the bottom residual velocity average difference for the Eastward Expansion versus the Base Case.

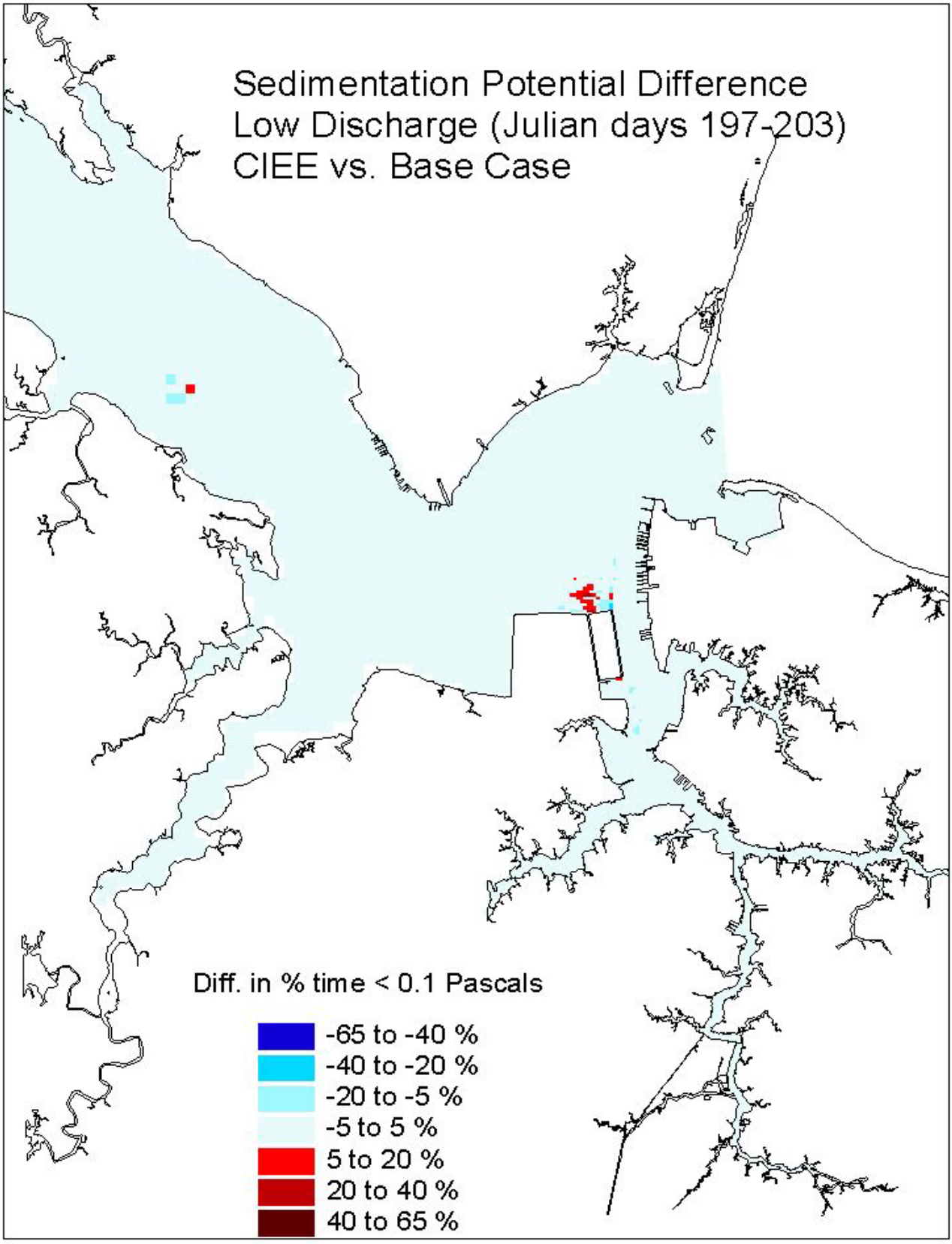

Figure 16. Historical simulation comparison (low discharge) of the sedimentation potential difference for the Eastward Expansion versus the Base Case.

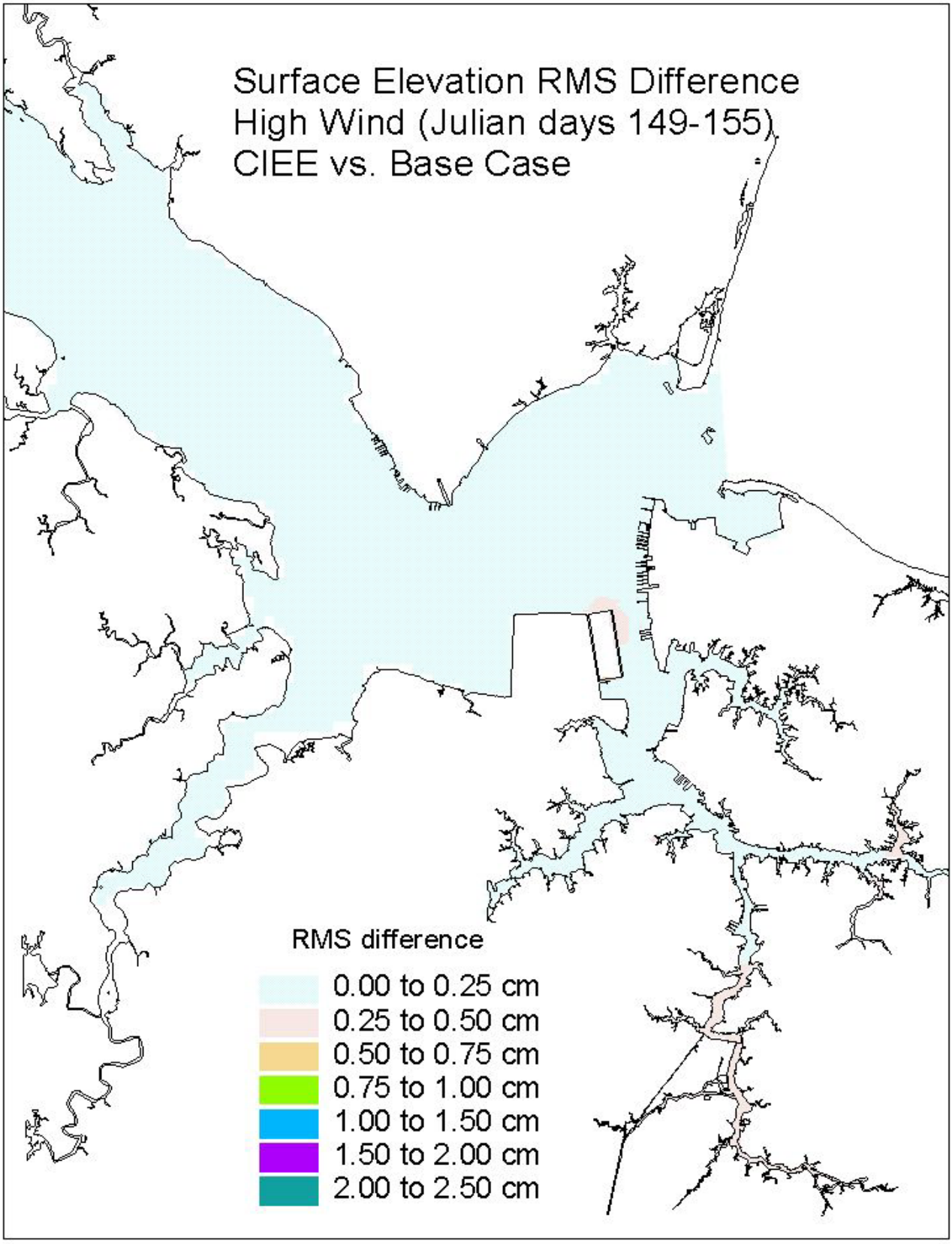

Figure 17. Historical simulation comparison (high wind) of the surface elevation RMS difference for the Eastward Expansion versus the Base Case.

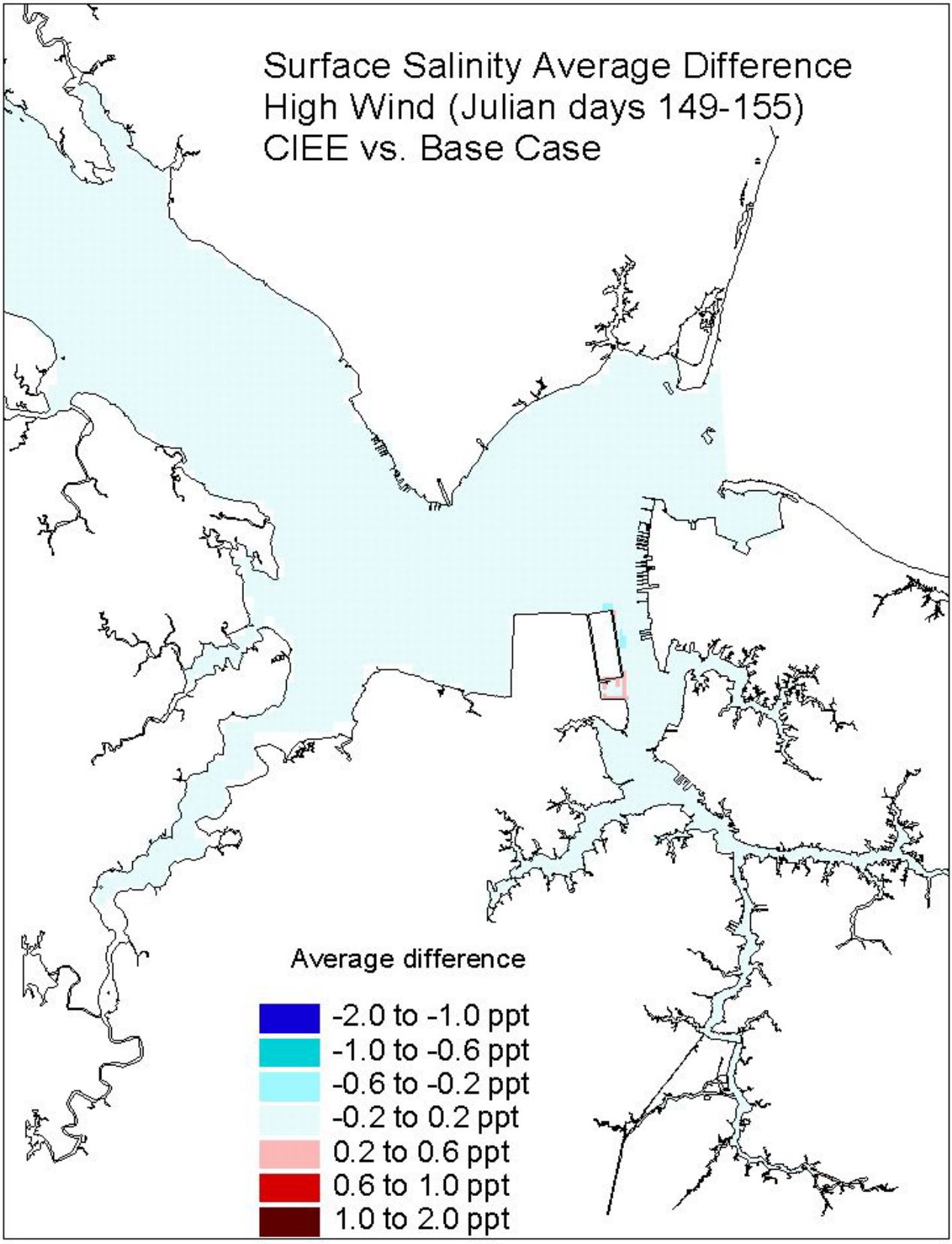

Figure 18. Historical simulation comparison (high wind) of the surface salinity average difference for the Eastward Expansion versus the Base Case.

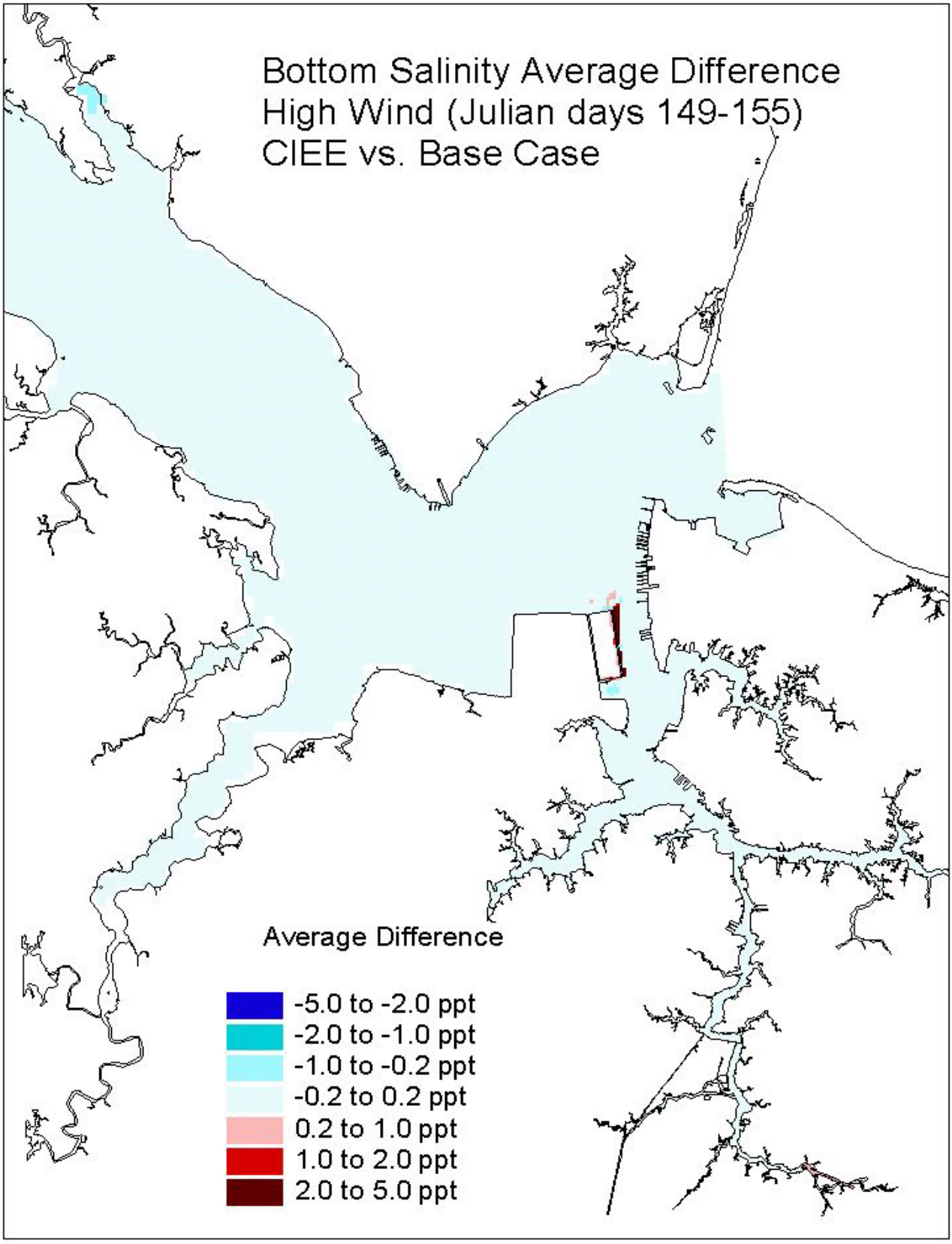

Figure 19. Historical simulation comparison (high wind) of the bottom salinity average difference for the Eastward Expansion versus the Base Case.

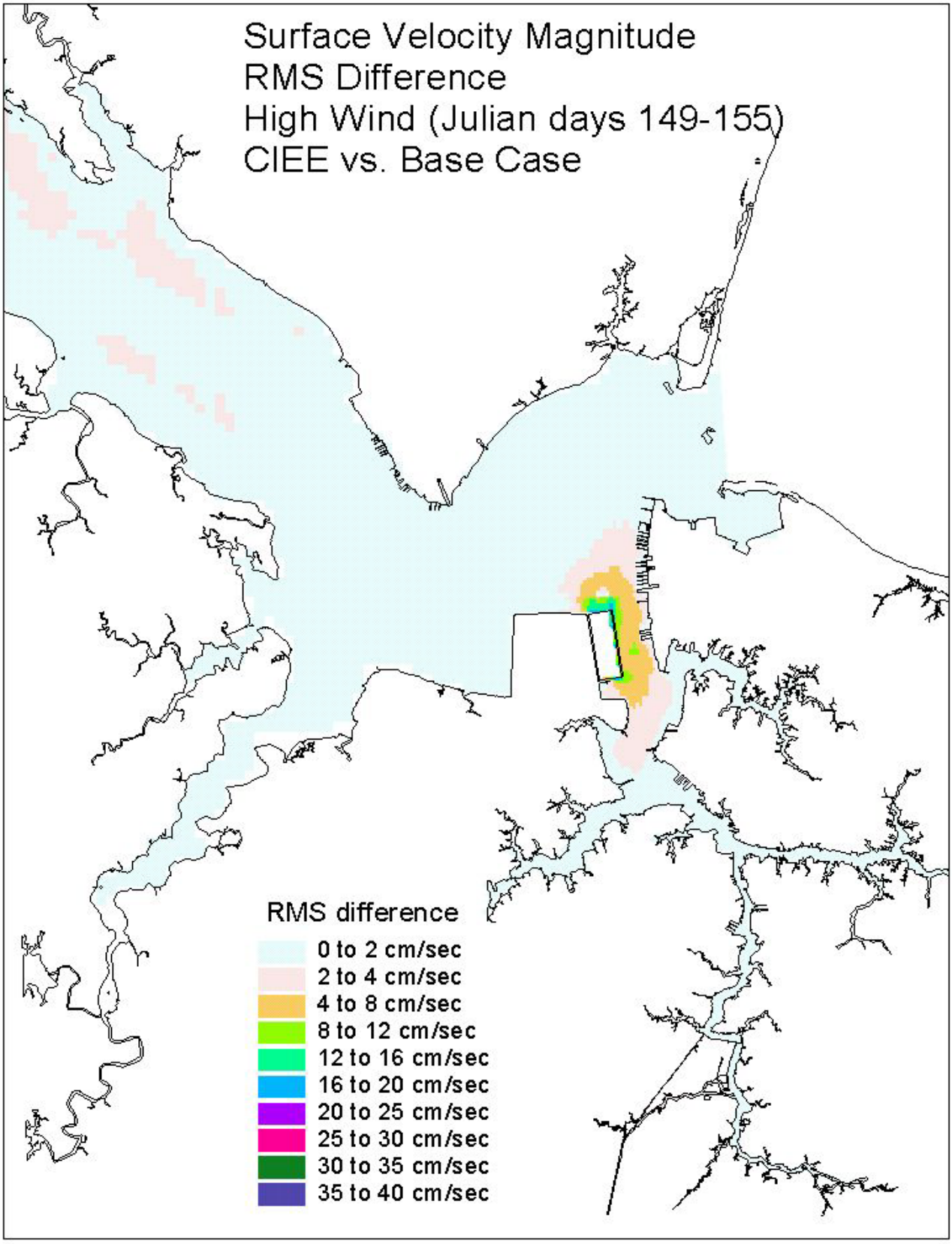

Figure 20. Historical simulation comparison (high wind) of the surface velocity RMS difference for the Eastward Expansion versus the Base Case.

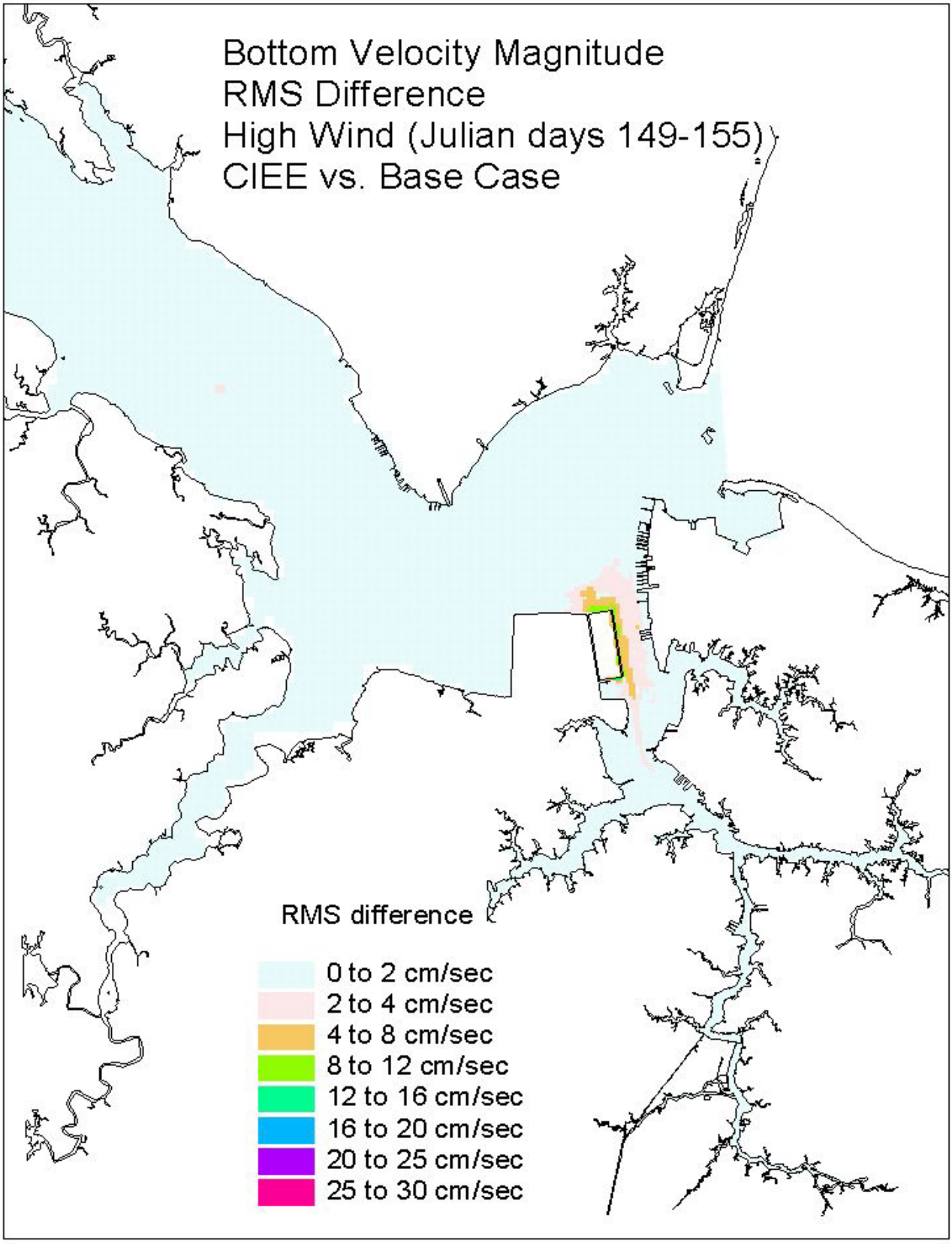

Figure 21. Historical simulation comparison (high wind) of the bottom velocity RMS difference for the Eastward Expansion versus the Base Case.

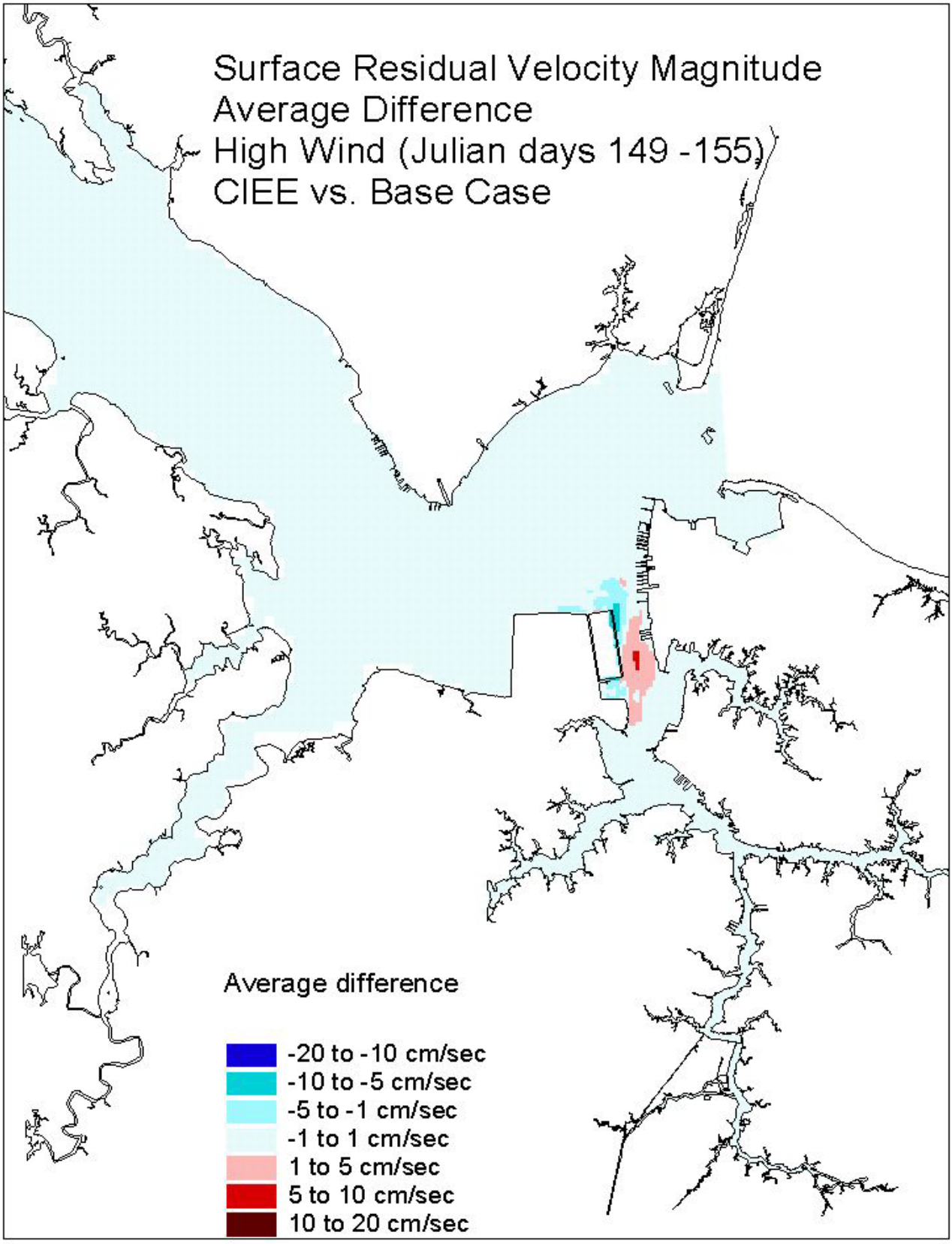

Figure 22. Historical simulation comparison (high wind) of the surface residual velocity average difference for the Eastward Expansion versus the Base Case.

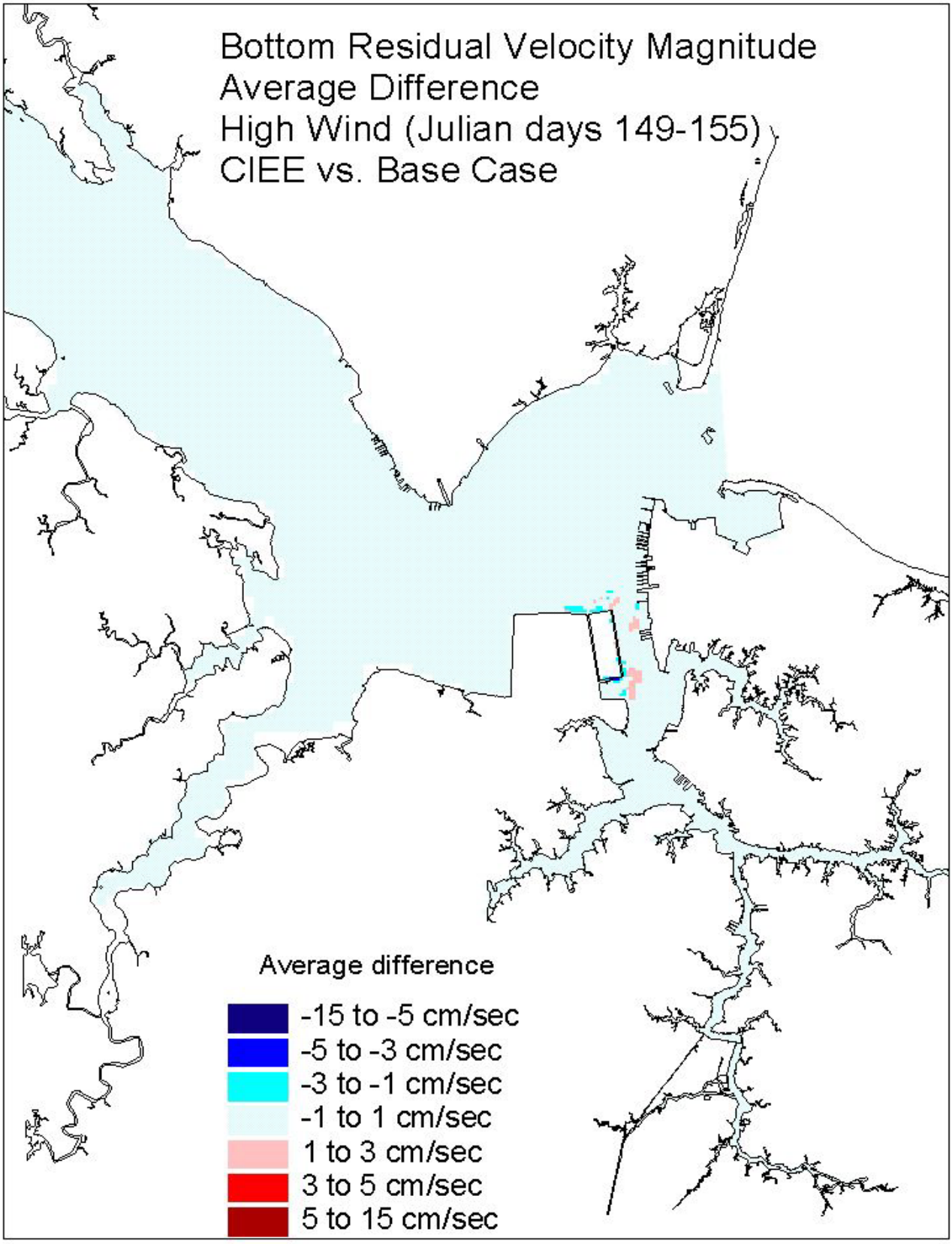

Figure 23. Historical simulation comparison (high wind) of the bottom residual velocity average difference for the Eastward Expansion versus the Base Case.

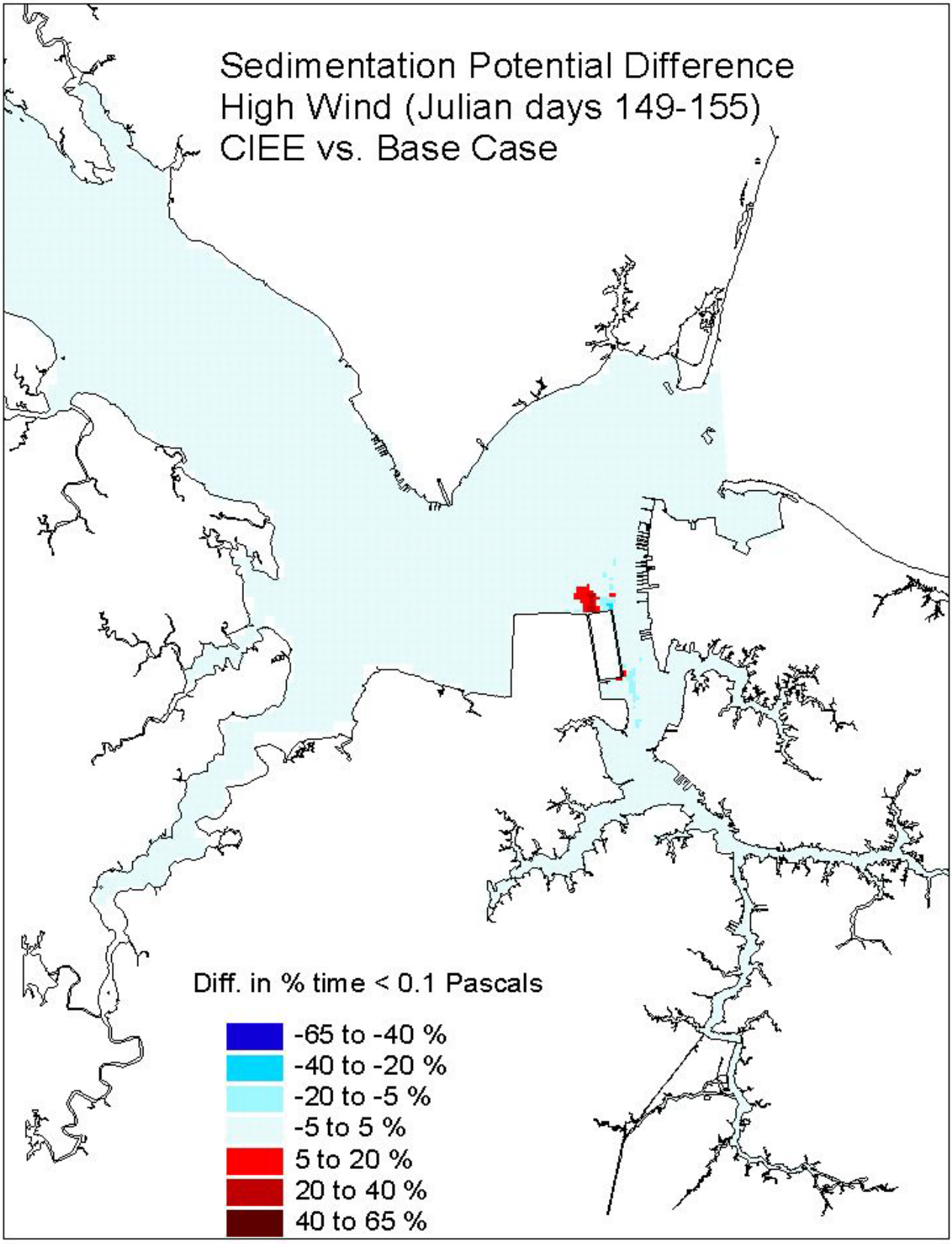

Figure 24. Historical simulation comparison (high wind) of the sedimentation potential difference for the Eastward Expansion versus the Base Case.

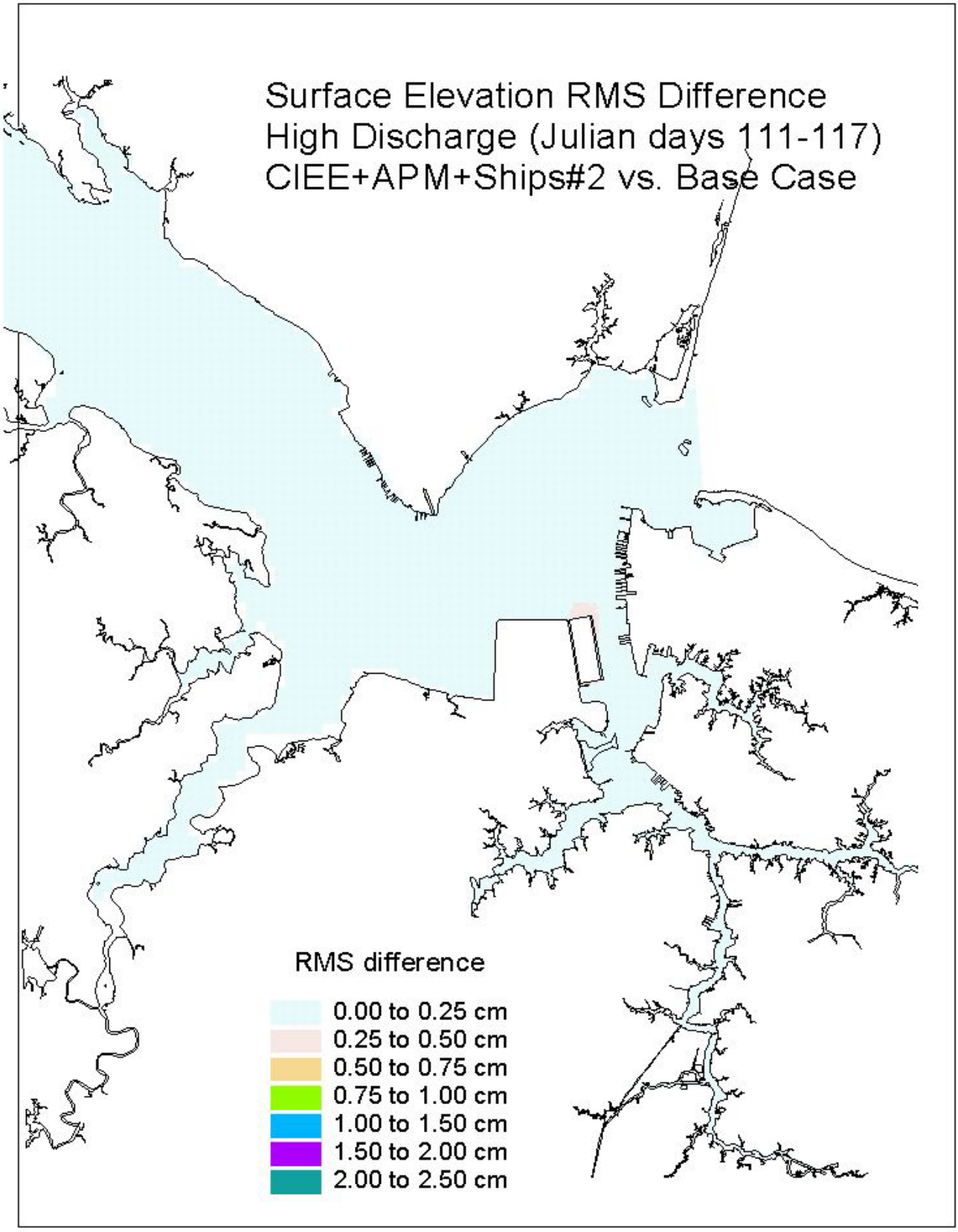

Figure 25. Historical simulation comparison (high discharge) of the surface elevation RMS difference for the Eastward Expansion plus APM Terminal Dredging plus Ships (Case 2b) versus the Base Case.

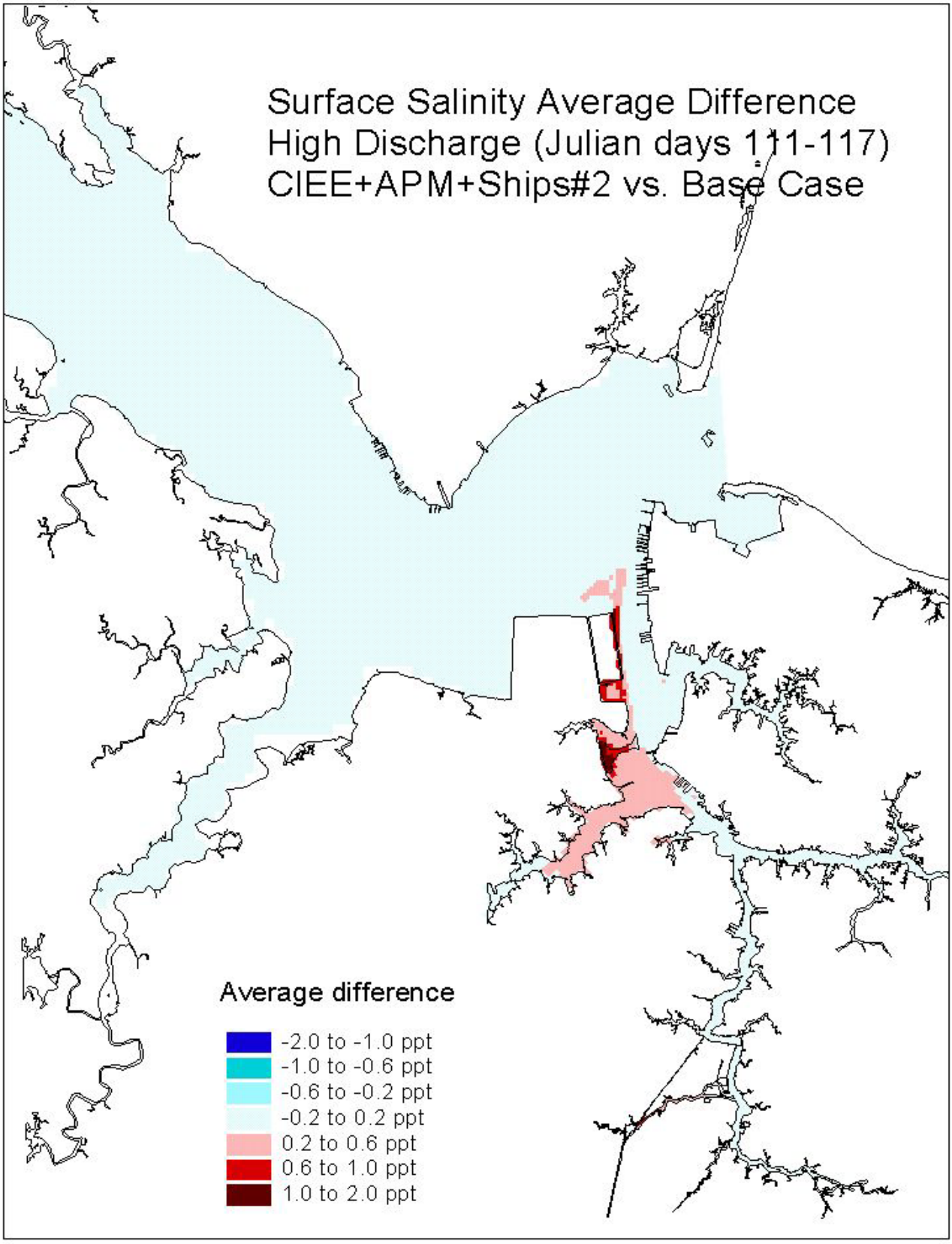

Figure 26. Historical simulation comparison (high discharge) of the surface salinity average difference for the Eastward Expansion APM Terminal Dredging plus Ships (Case 2b) versus the Base Case.

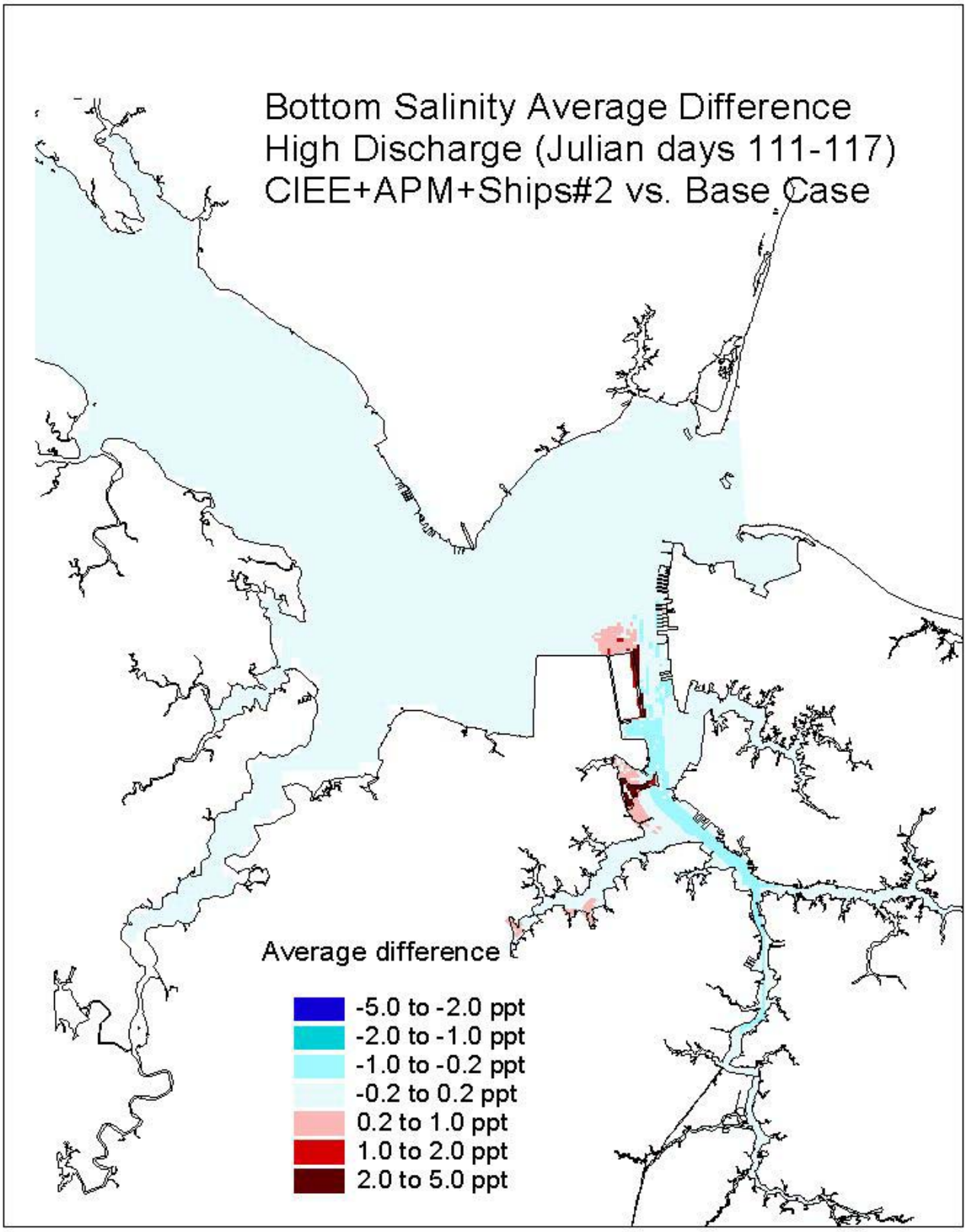

Figure 27. Historical simulation comparison (high discharge) of the bottom salinity average difference for the Eastward Expansion APM Terminal Dredging plus Ships (Case 2b) versus the Base Case.

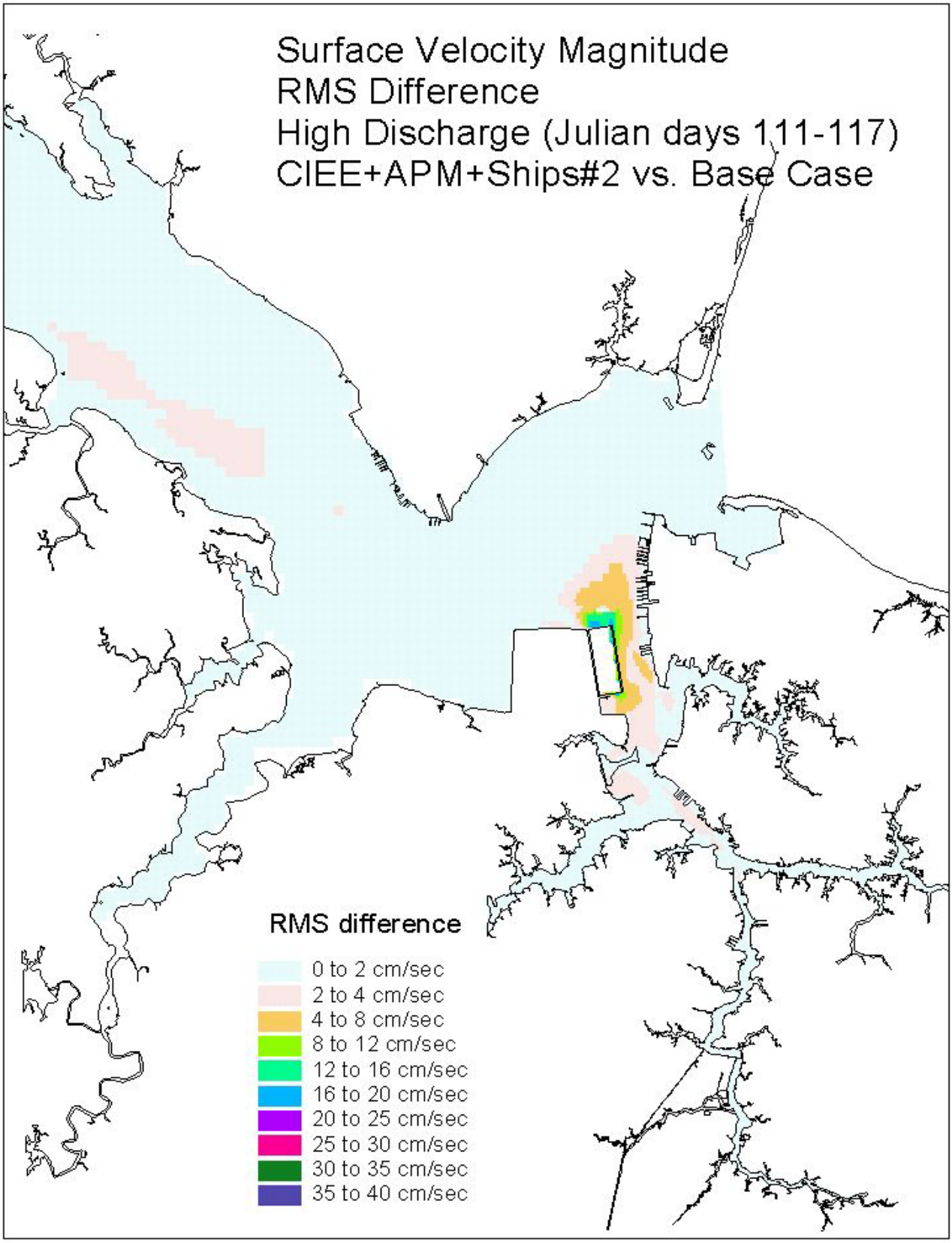

Figure 28. Historical simulation comparison (high discharge) of the surface velocity RMS difference for the Eastward Expansion APM Terminal Dredging plus Ships (Case 2b) versus the Base Case.

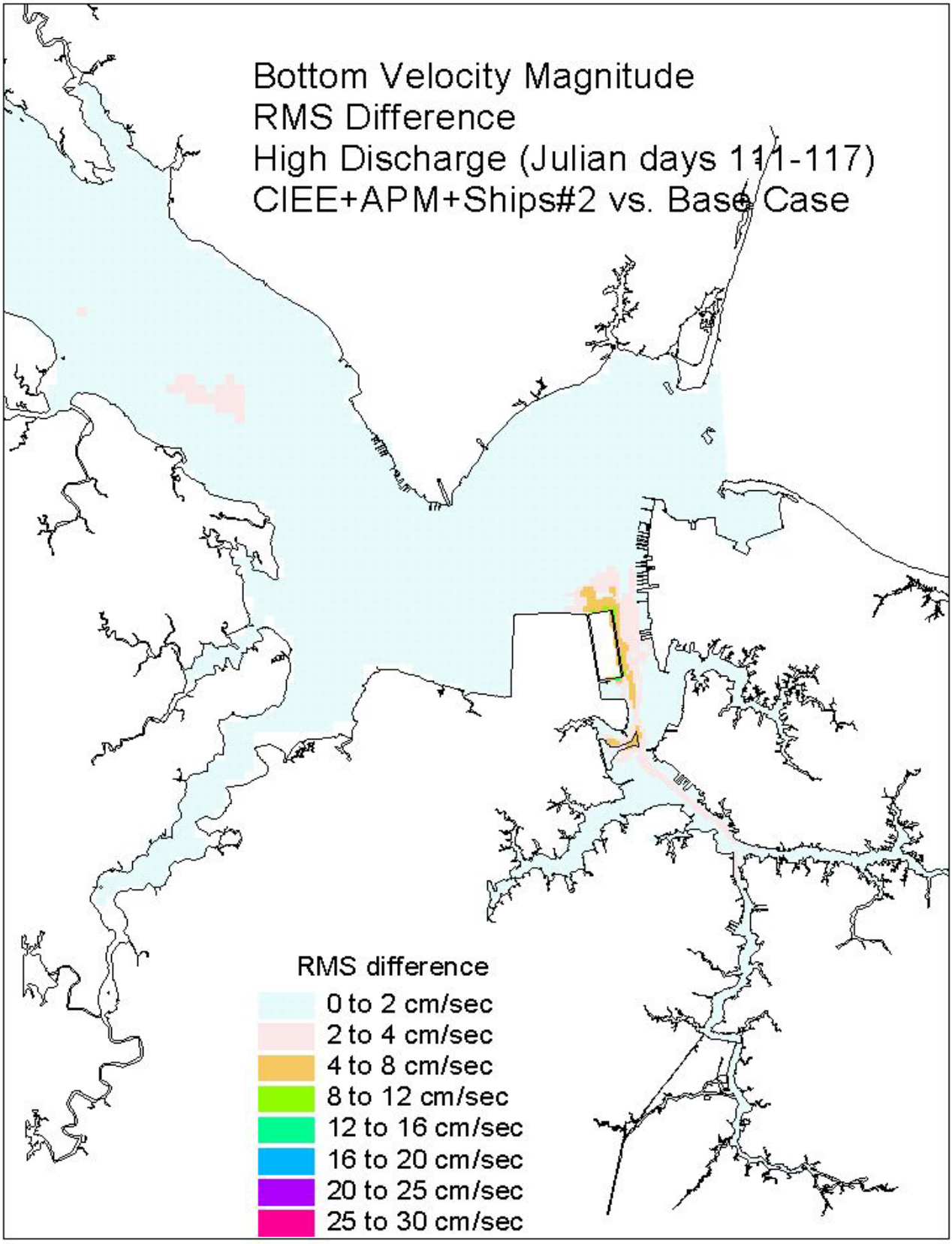

Figure 29. Historical simulation comparison (high discharge) of the bottom velocity RMS difference for the Eastward Expansion plus APM Terminal Dredging plus Ships (Case 2b) versus the Base Case.

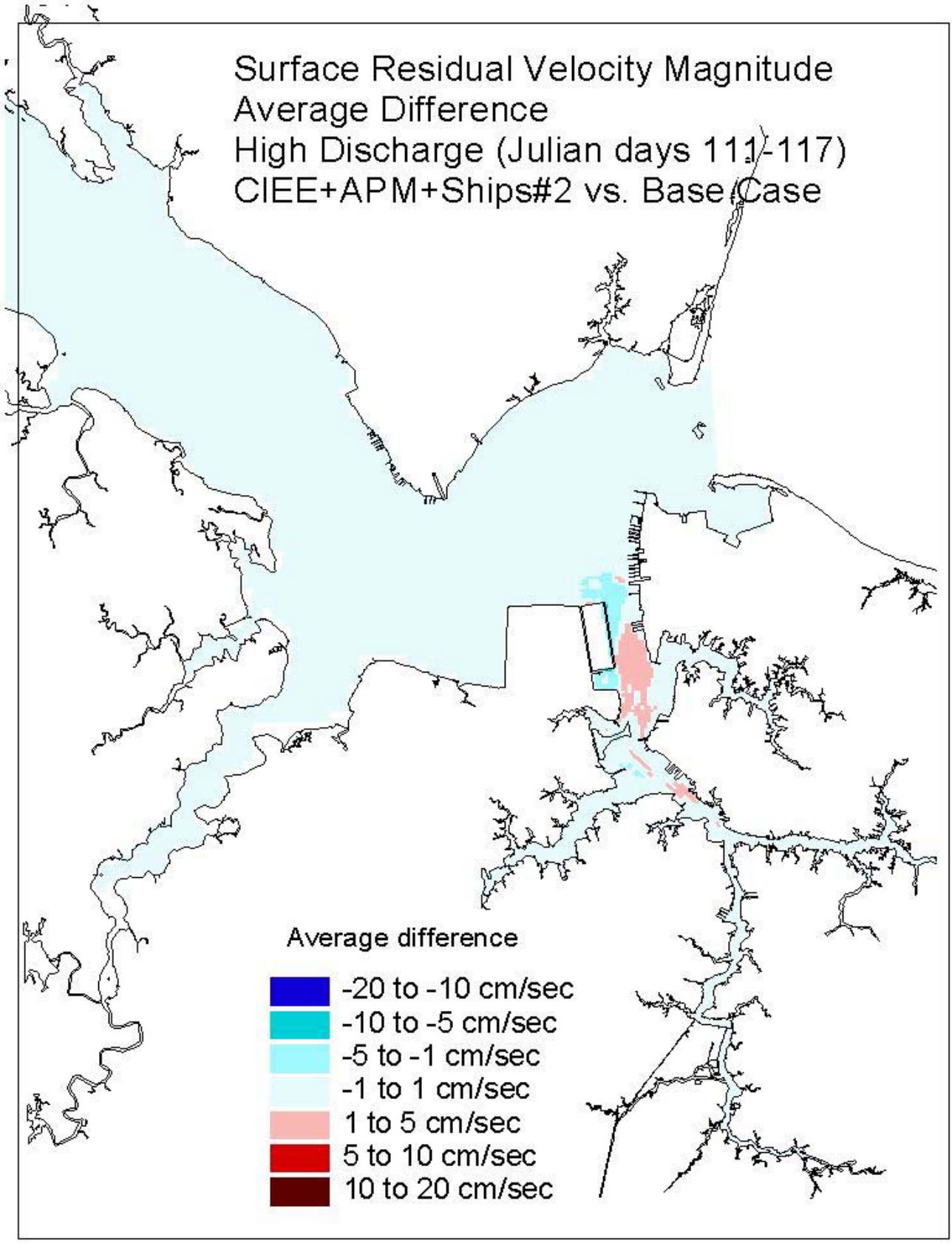

Figure 30. Historical simulation comparison (high discharge) of the surface residual velocity average difference for the Eastward Expansion plus APM Terminal Dredging plus Ships (Case 2b) versus the Base Case.

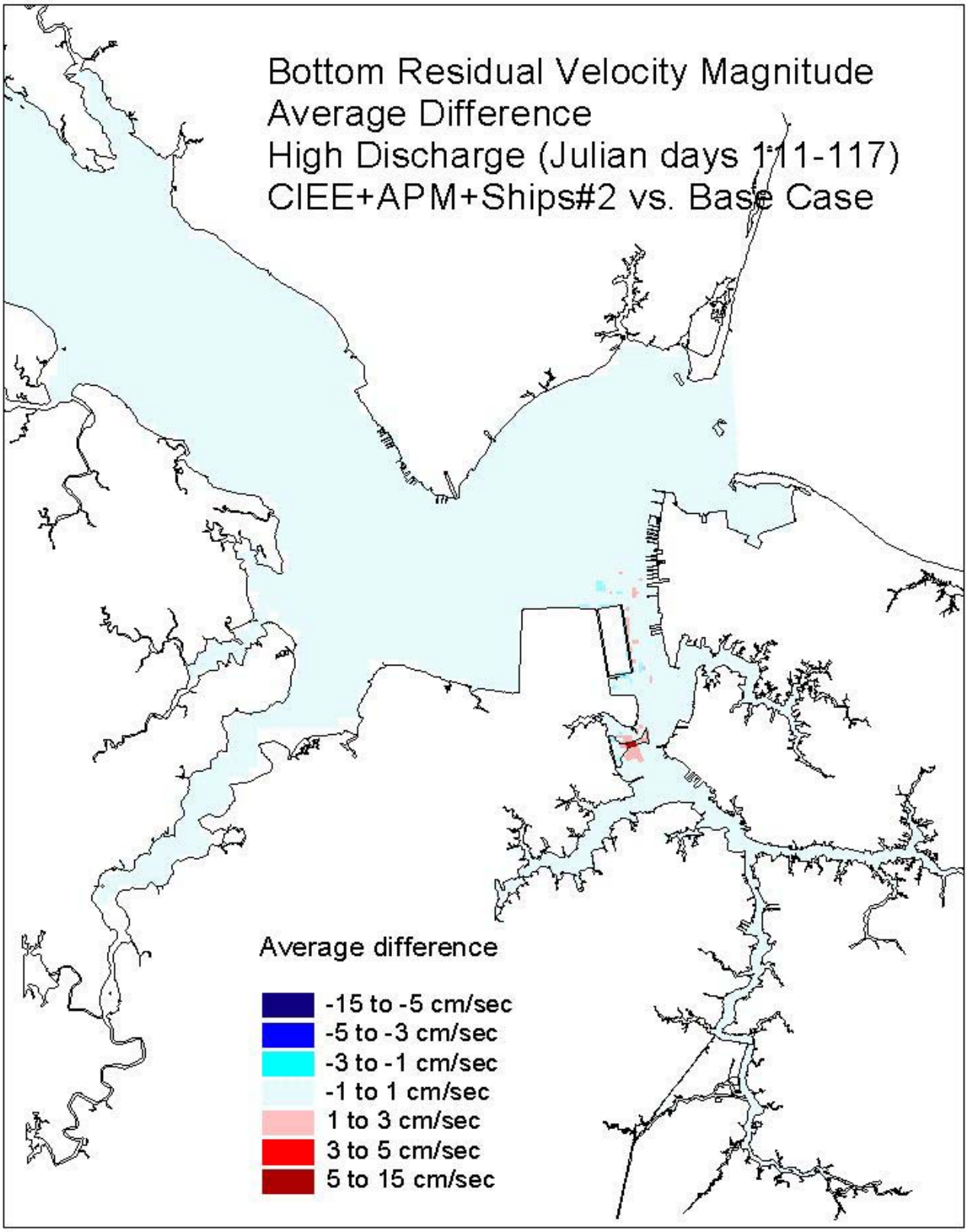

Figure 31. Historical simulation comparison (high discharge) of the bottom residual velocity average difference for the Eastward Expansion plus APM Terminal Dredging plus Ships (Case 2b) versus the Base Case.

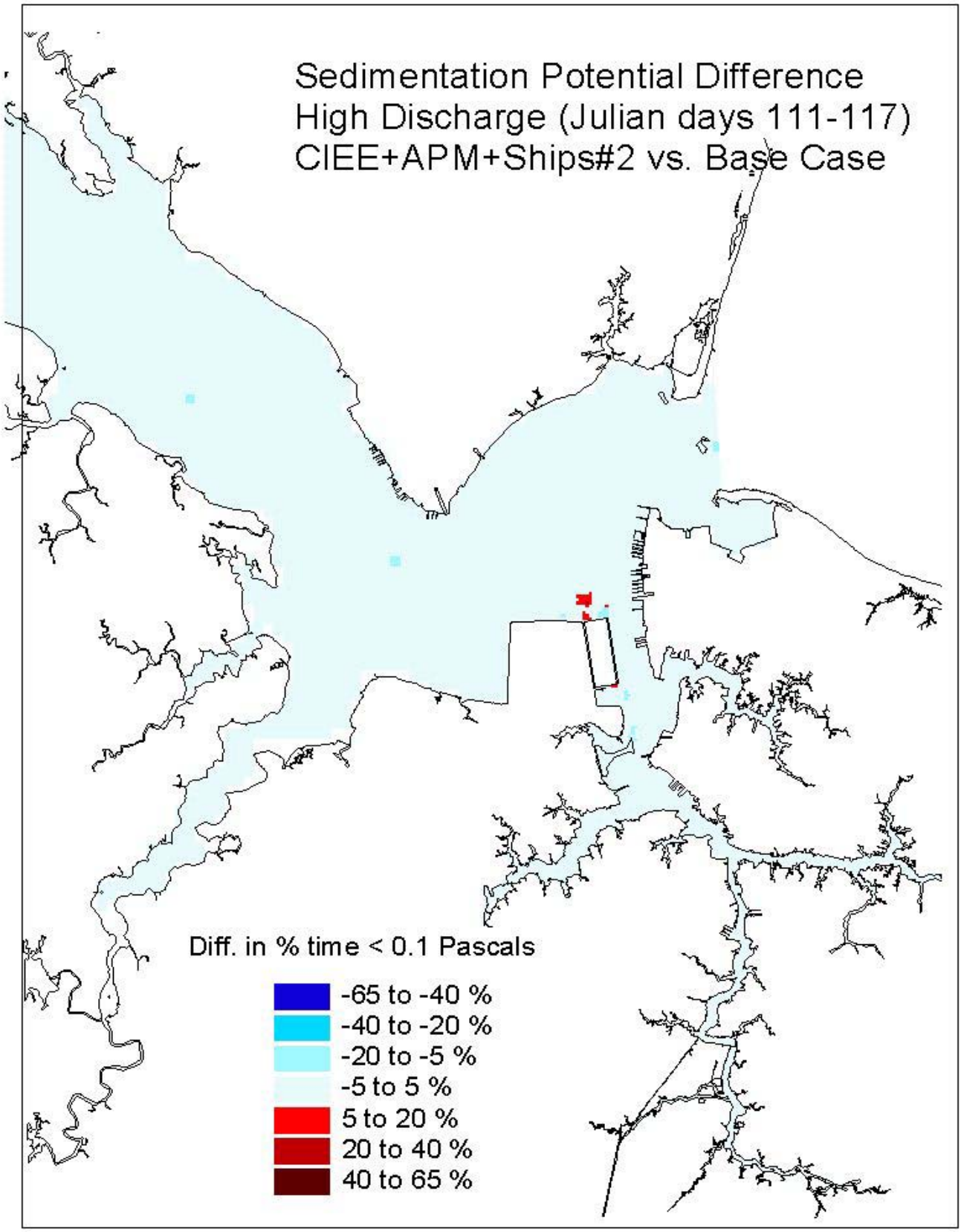

Figure 32. Historical simulation comparison (high discharge) of the sedimentation potential difference for the Eastward Expansion plus APM Terminal Dredging plus Ships (Case 2b) versus the Base Case.

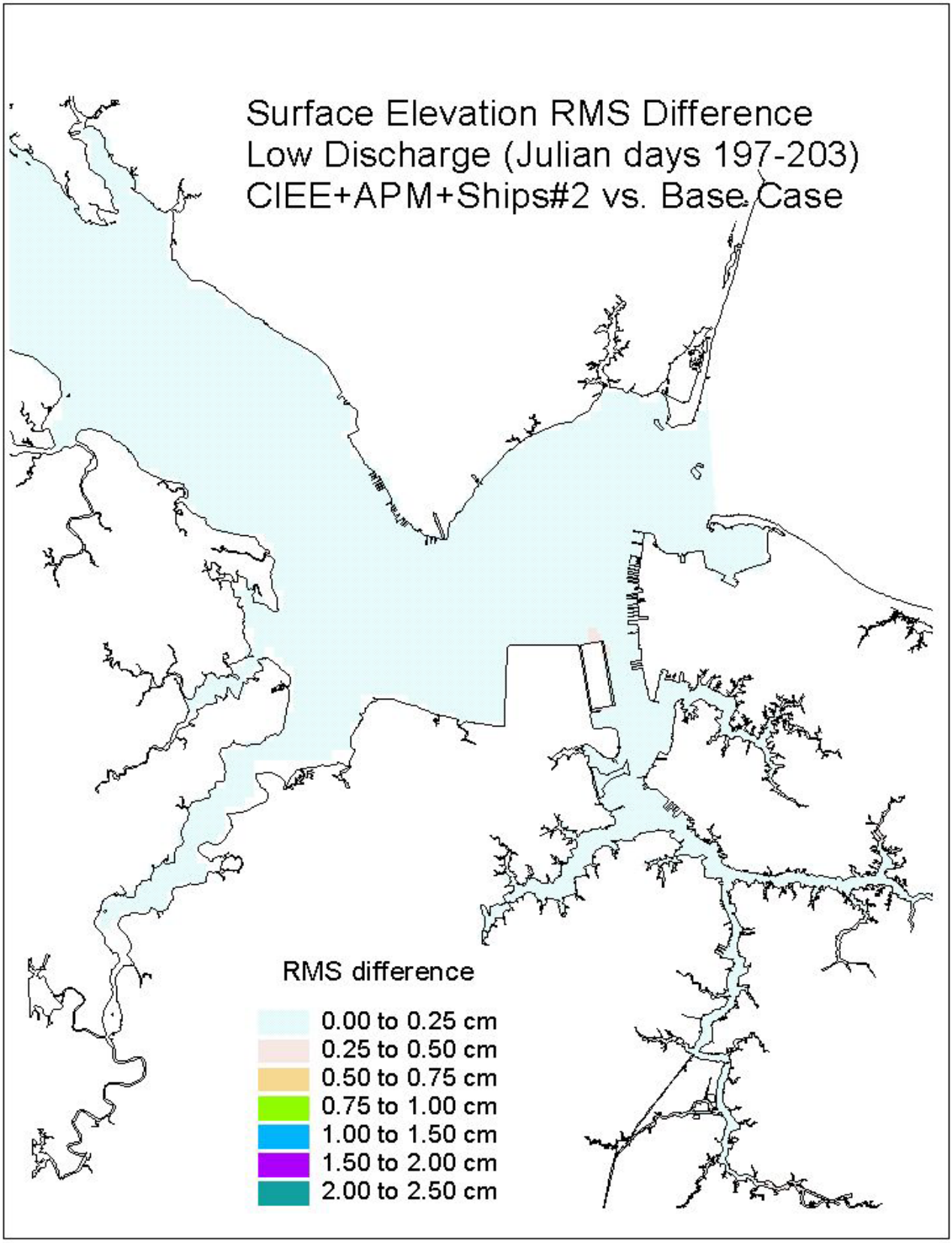

Figure 33. Historical simulation comparison (low discharge) of the surface elevation RMS difference for the Eastward Expansion plus APM Terminal Dredging plus Ships (Case 2b) versus the Base Case.

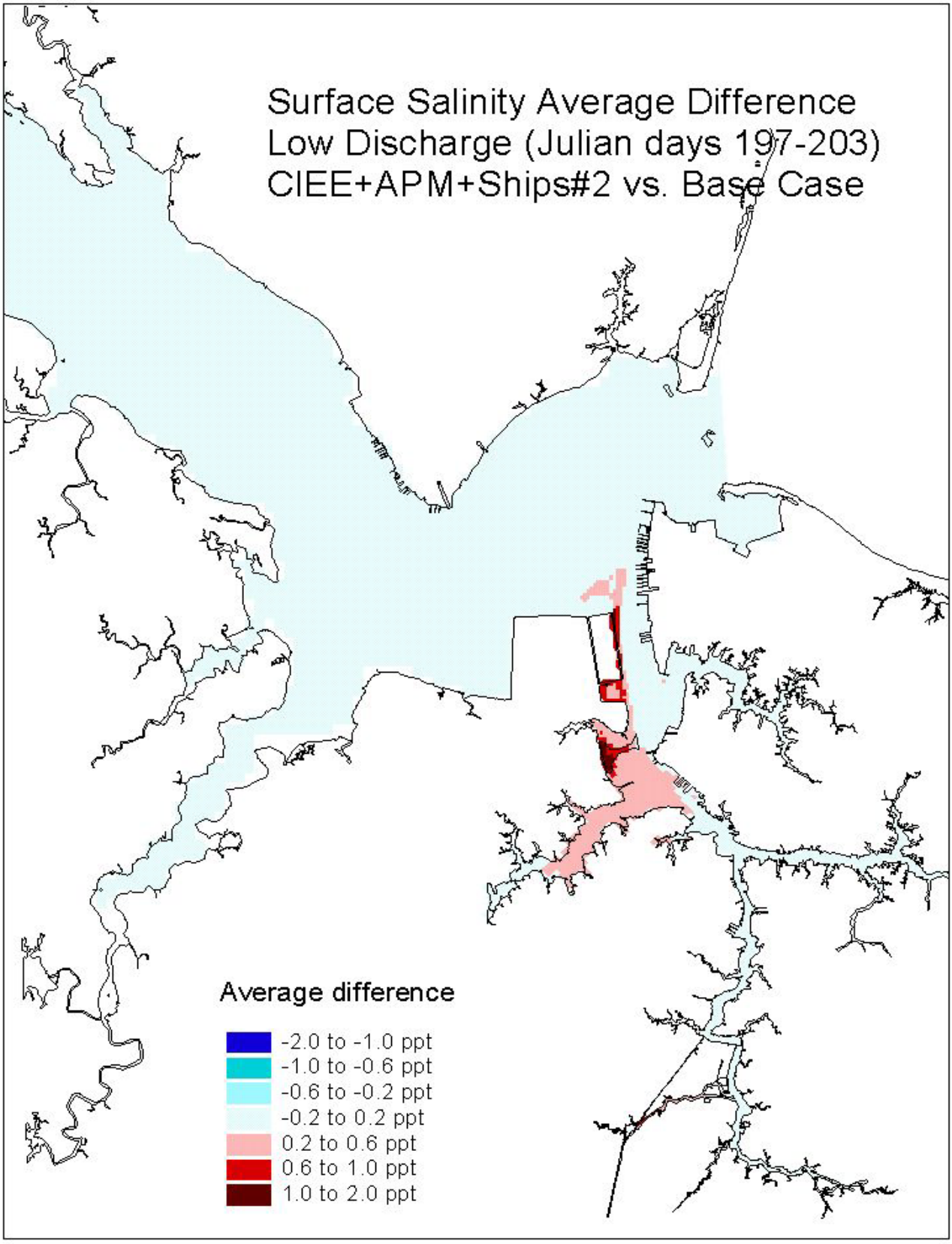

Figure 34. Historical simulation comparison (low discharge) of the surface salinity average difference for the Eastward Expansion plus APM Terminal Dredging plus Ships (Case 2b) versus the Base Case.

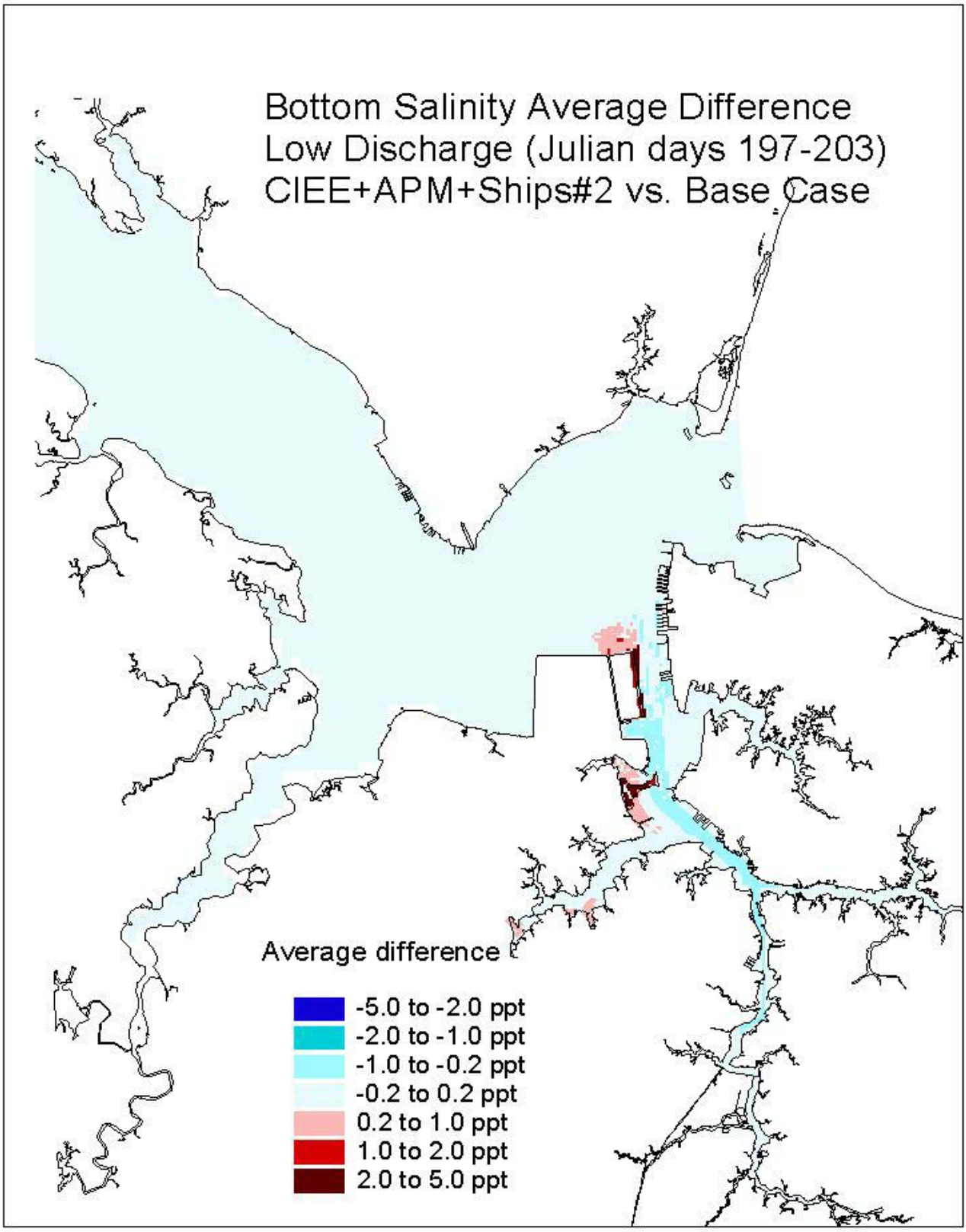

Figure 35. Historical simulation comparison (low discharge) of the bottom salinity average difference for the Eastward Expansion plus APM Terminal Dredging plus Ships (Case 2b) versus the Base Case.

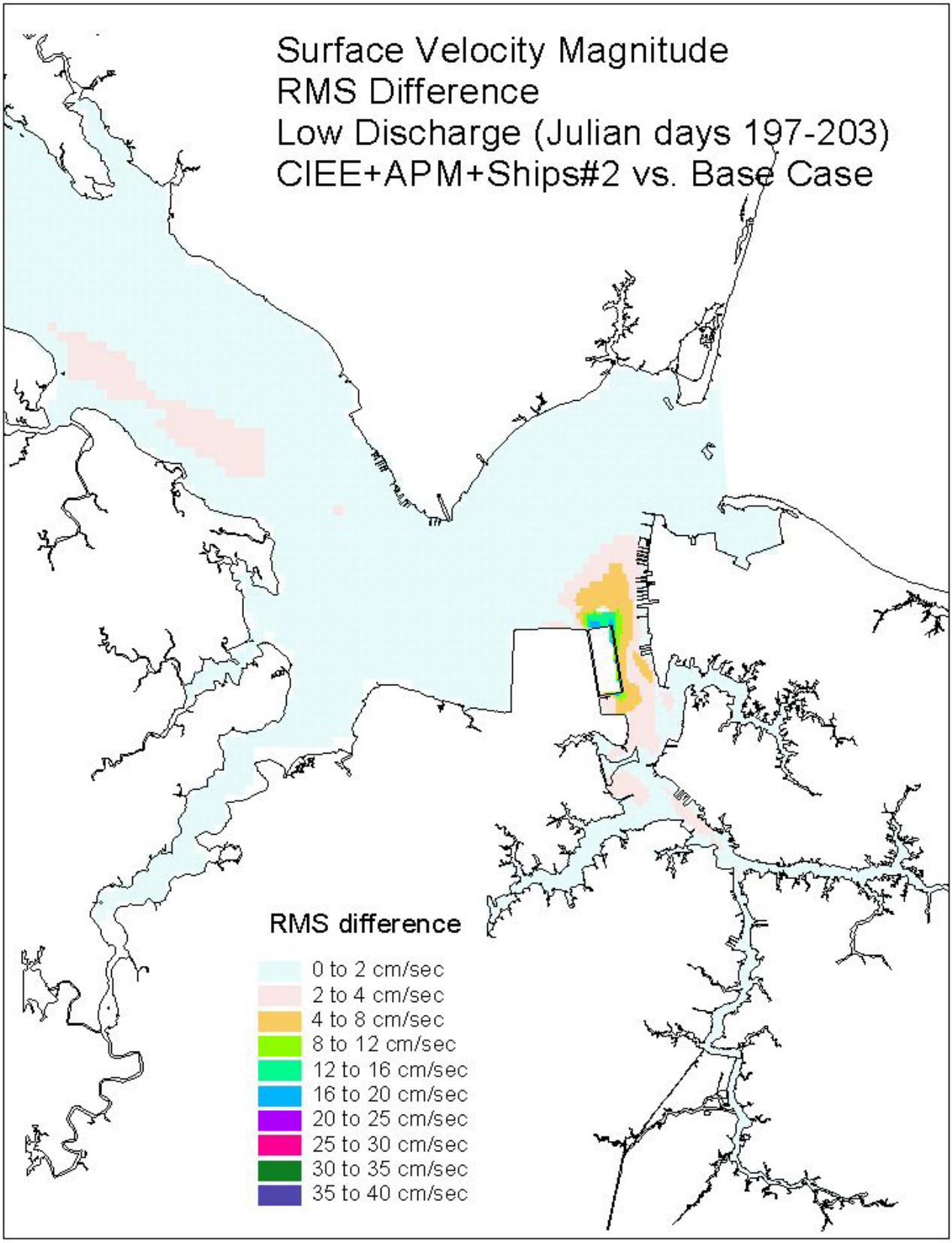

Figure 36. Historical simulation comparison (low discharge) of the surface velocity RMS difference for the Eastward Expansion plus APM Terminal Dredging plus Ships (Case 2b) versus the Base Case.

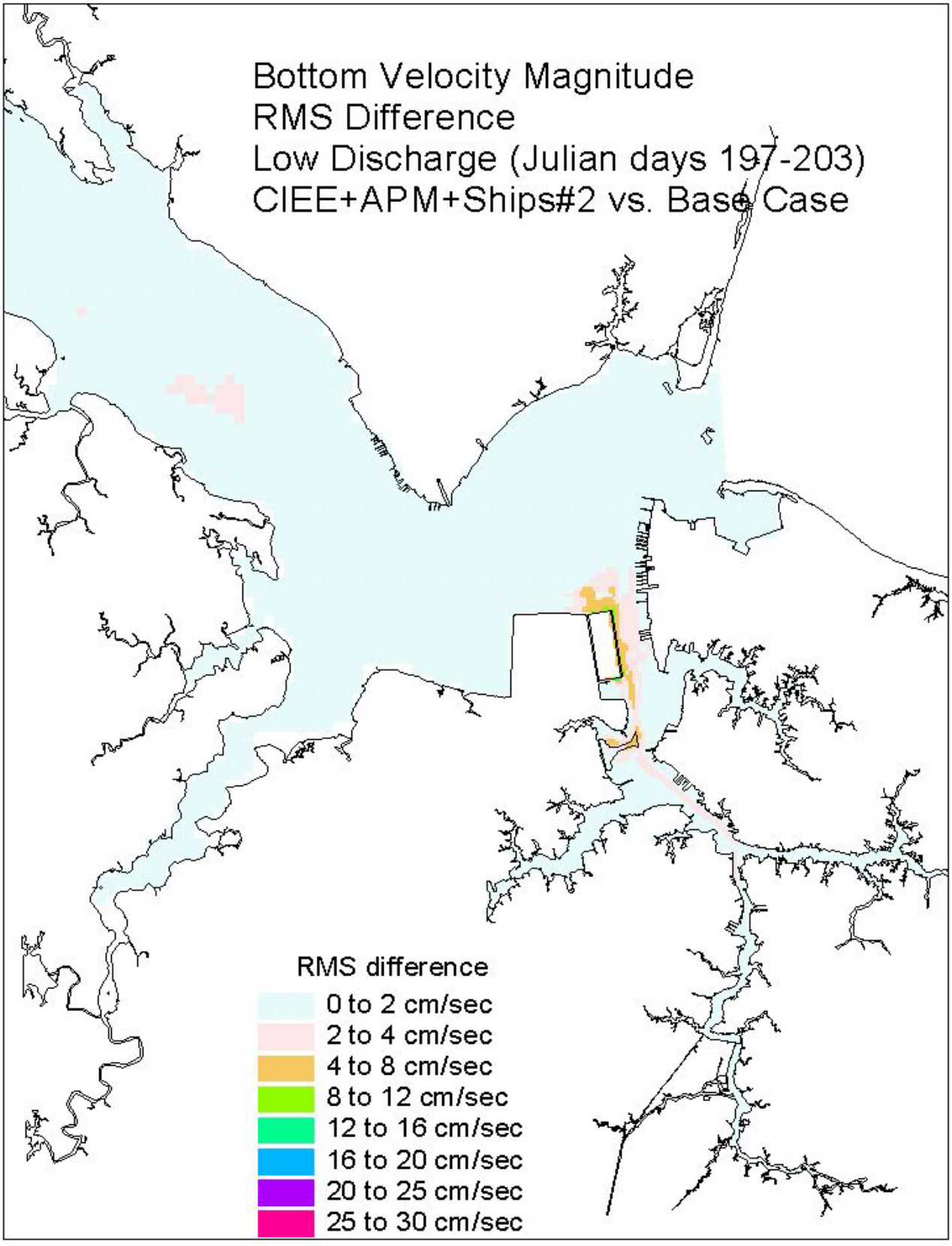

Figure 37. Historical simulation comparison (low discharge) of the bottom velocity RMS difference for the Eastward Expansion plus APM Terminal Dredging plus Ships (Case 2b) versus the Base Case.

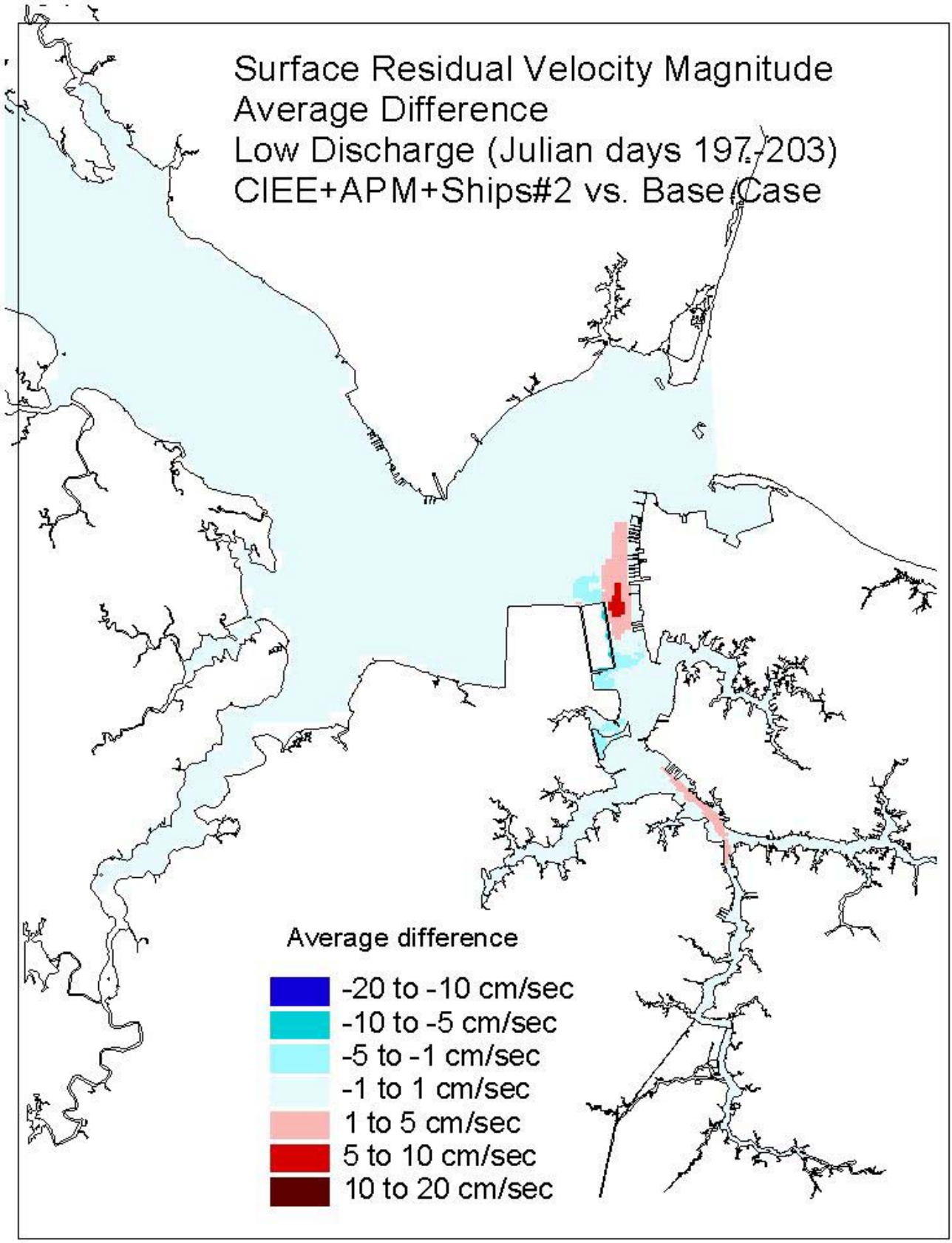

Figure 38. Historical simulation comparison (low discharge) of the surface residual velocity average difference for the Eastward Expansion plus APM Terminal Dredging plus Ships (Case 2b) versus the Base Case.

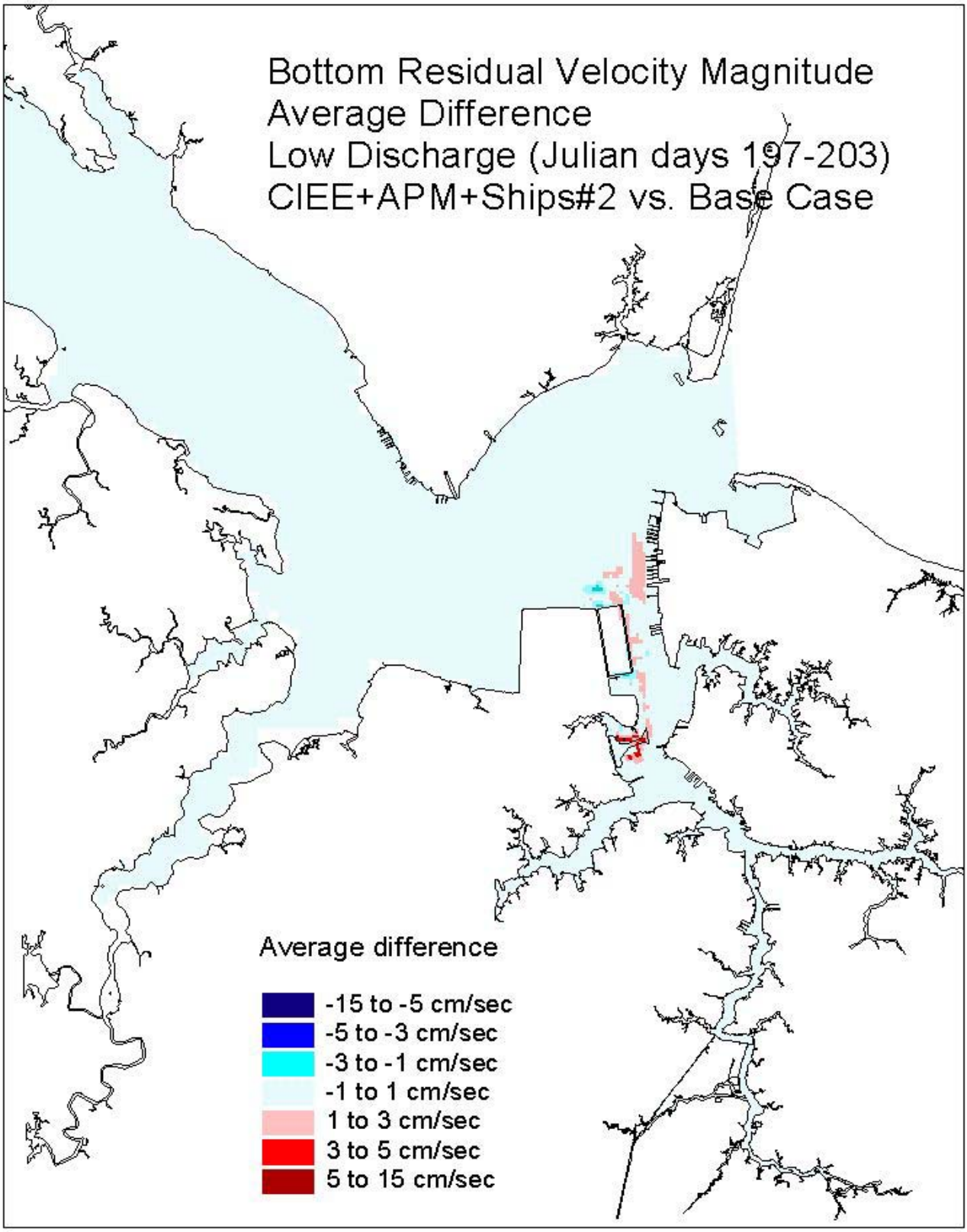

Figure 39. Historical simulation comparison (low discharge) of the bottom residual velocity average difference for the Eastward Expansion plus APM Terminal Dredging plus Ships (Case 2b) versus the Base Case.

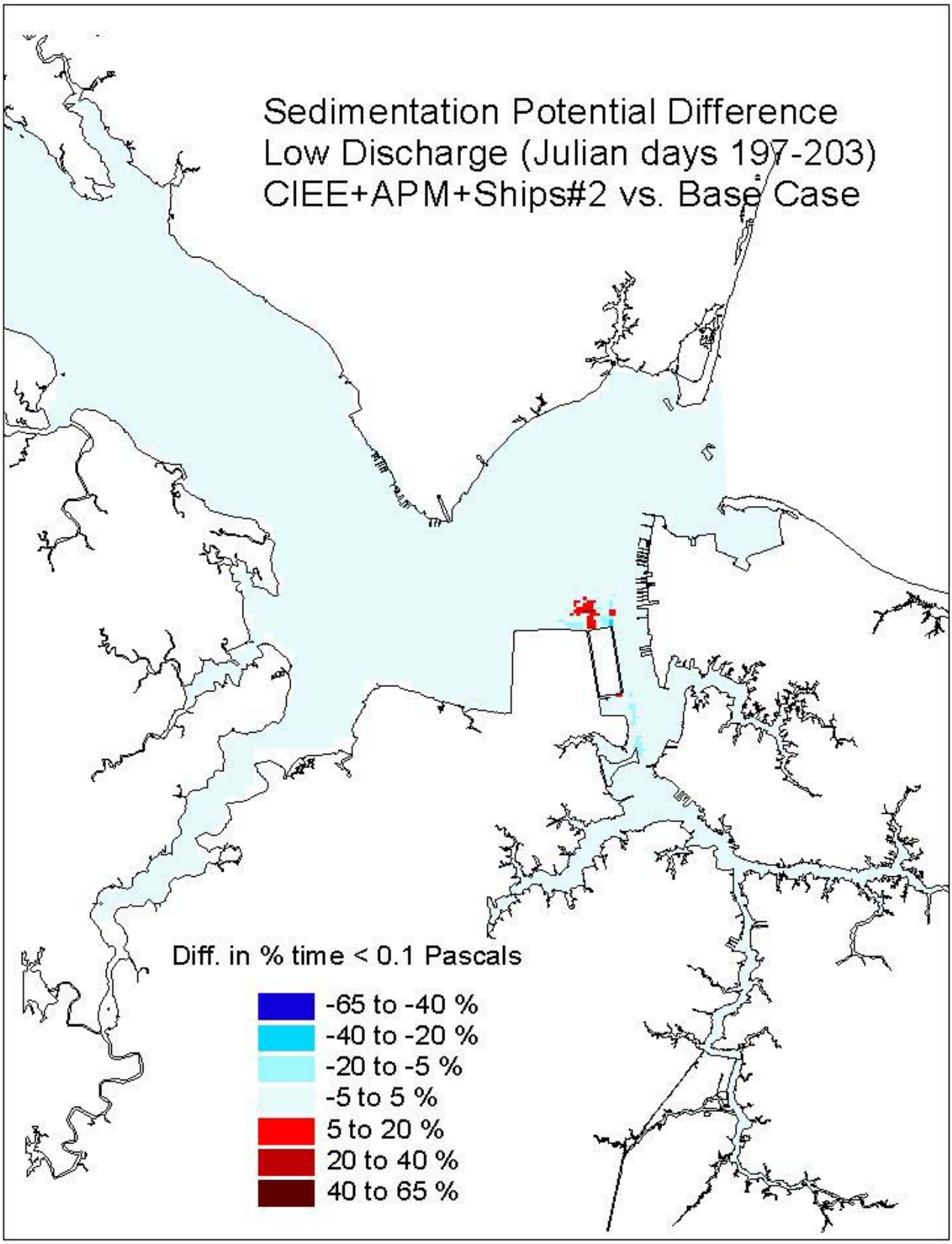

Figure 40. Historical simulation comparison (low discharge) of the sedimentation potential for the Eastward Expansion plus APM Terminal Dredging plus Ships (Case 2b) versus the Base Case.

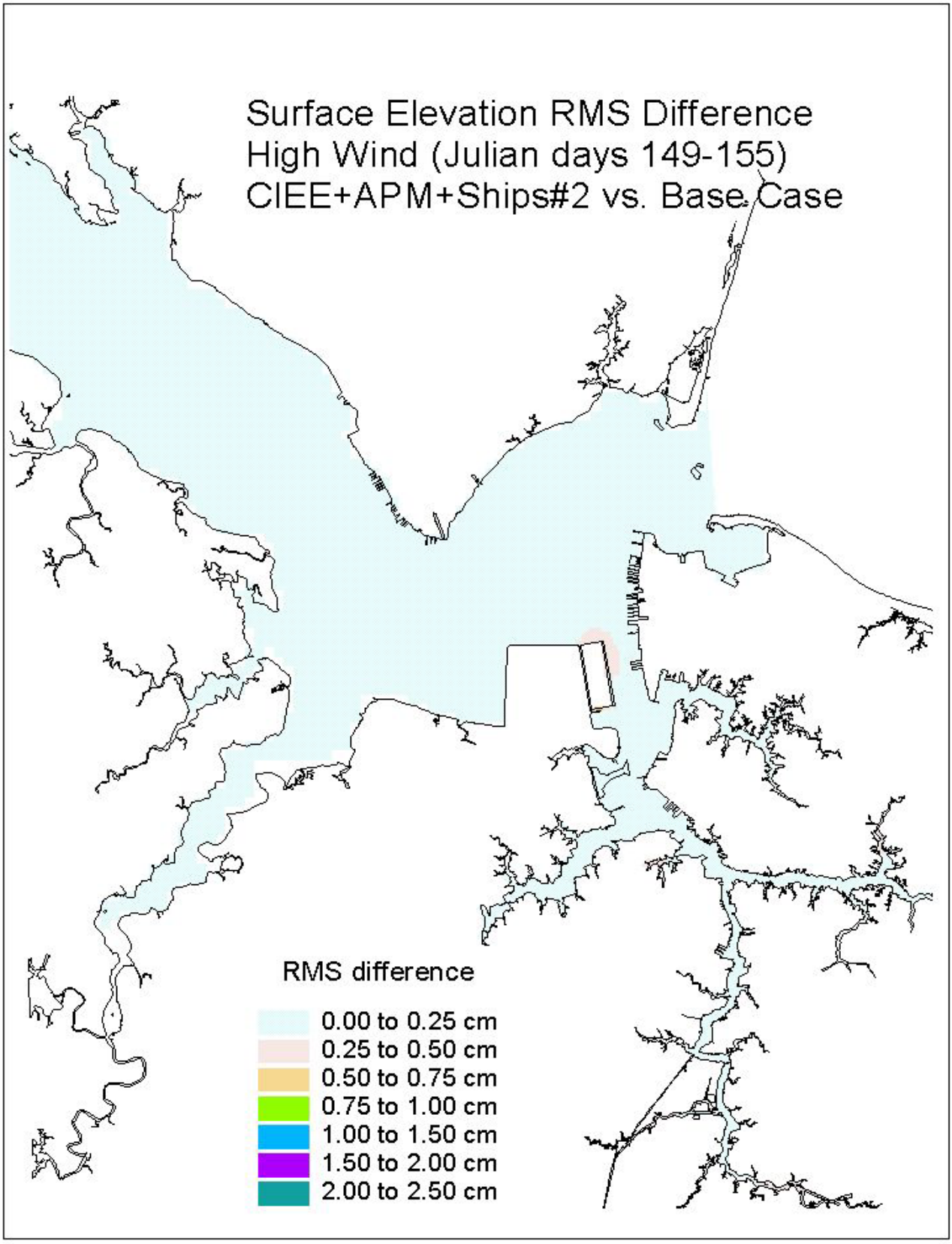

Figure 41. Historical simulation comparison (high wind) of the surface elevation RMS difference for the Eastward Expansion plus APM Terminal Dredging plus Ships (Case 2b) versus the Base Case.

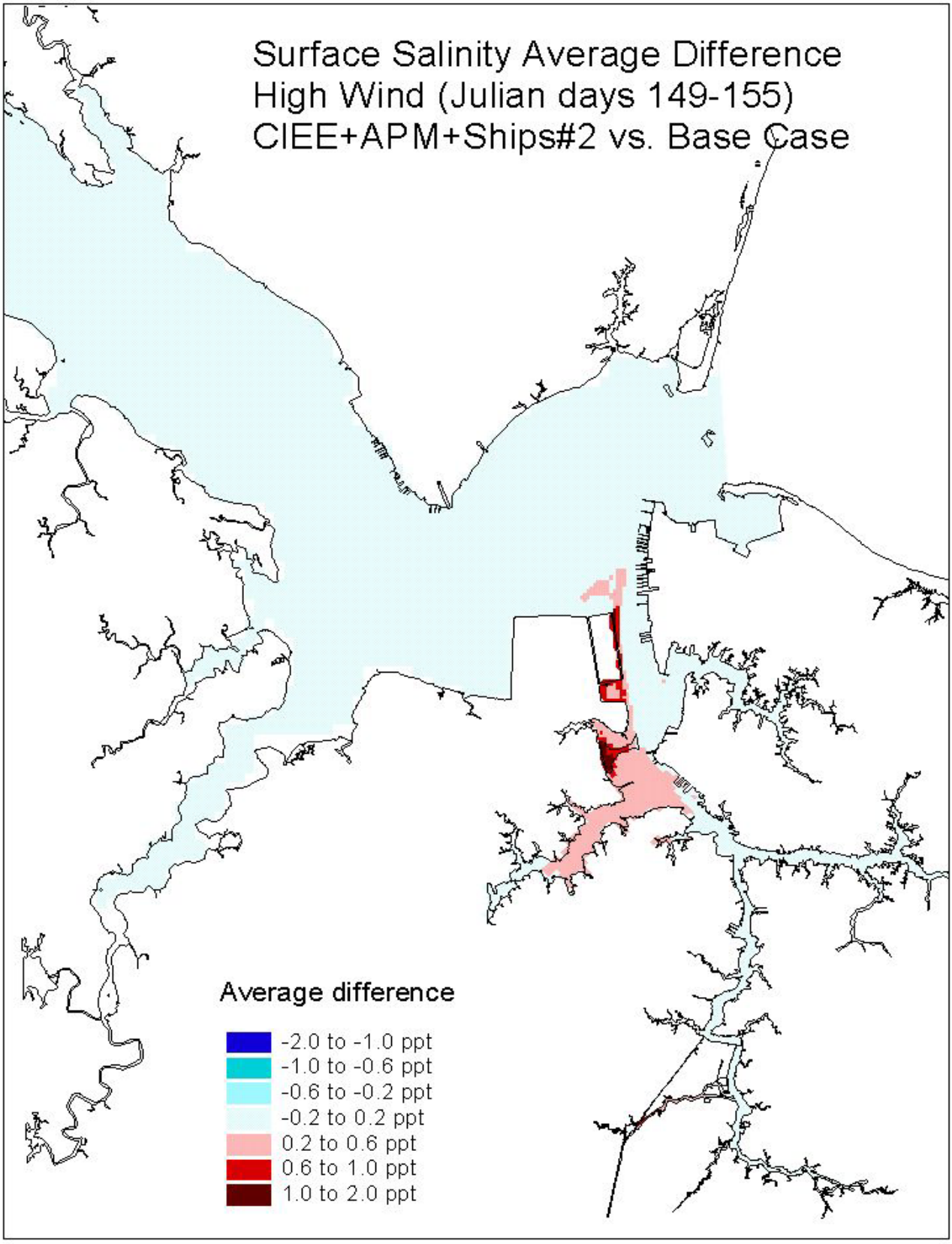

Figure 42. Historical simulation comparison (high wind) of the surface salinity average difference for the Eastward Expansion plus APM Terminal Dredging plus Ships (Case 2b) versus the Base Case.

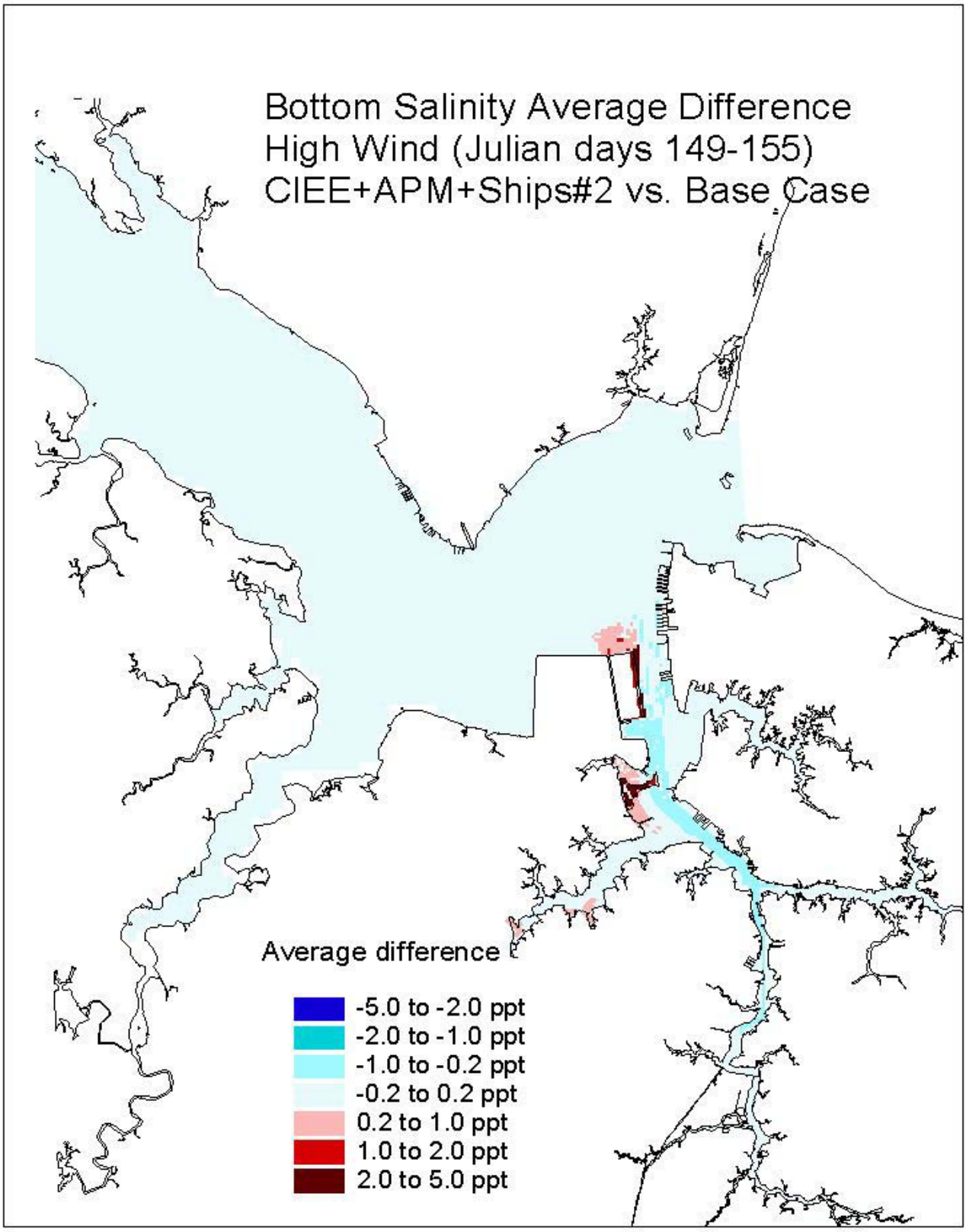

Figure 43. Historical simulation comparison (high wind) of the bottom salinity average difference for the Eastward Expansion plus APM Terminal Dredging plus Ships (Case 2b) versus the Base Case.

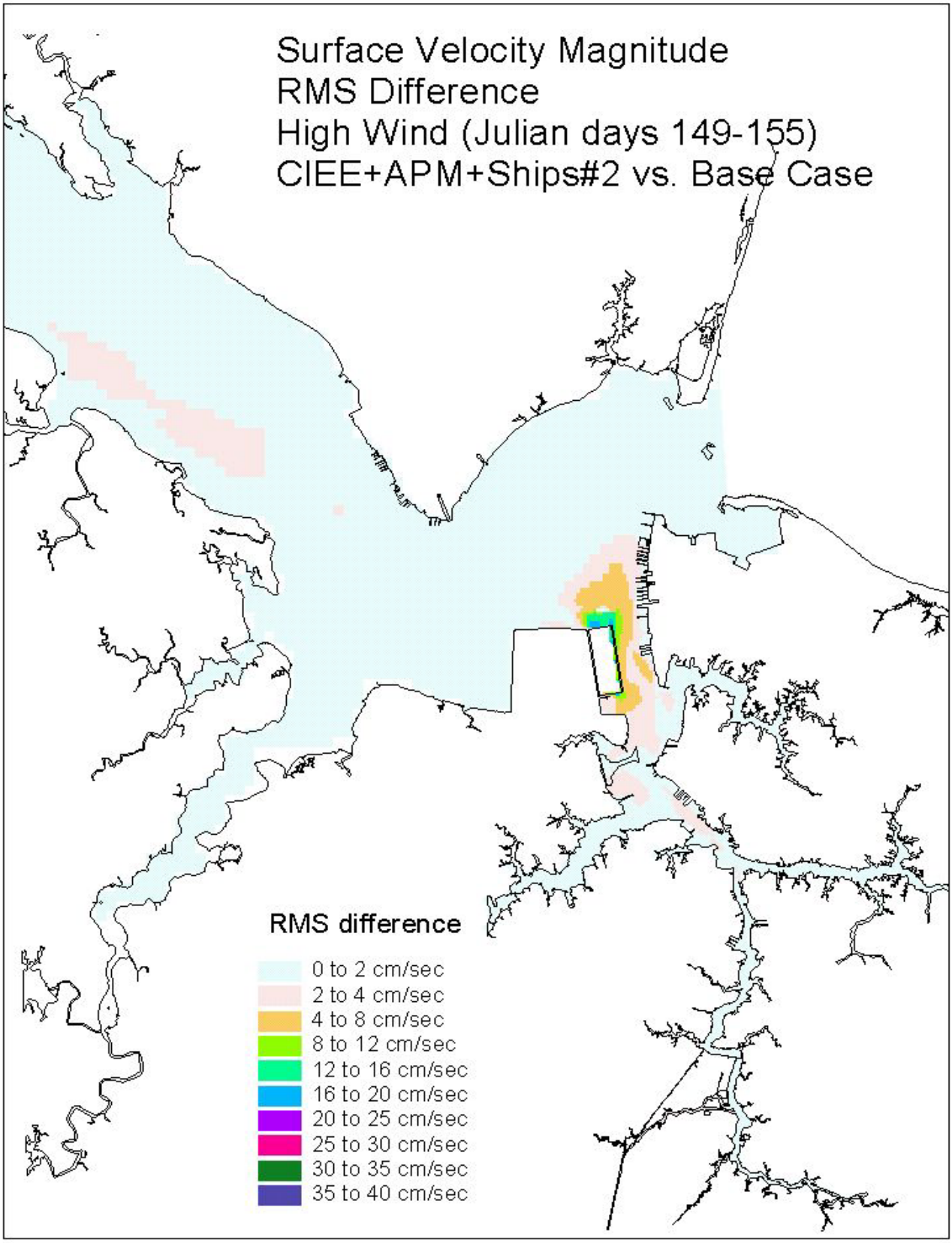

Figure 44. Historical simulation comparison (high wind) of the surface velocity RMS difference for the Eastward Expansion plus APM Terminal Dredging plus Ships (Case 2b) versus the Base Case.

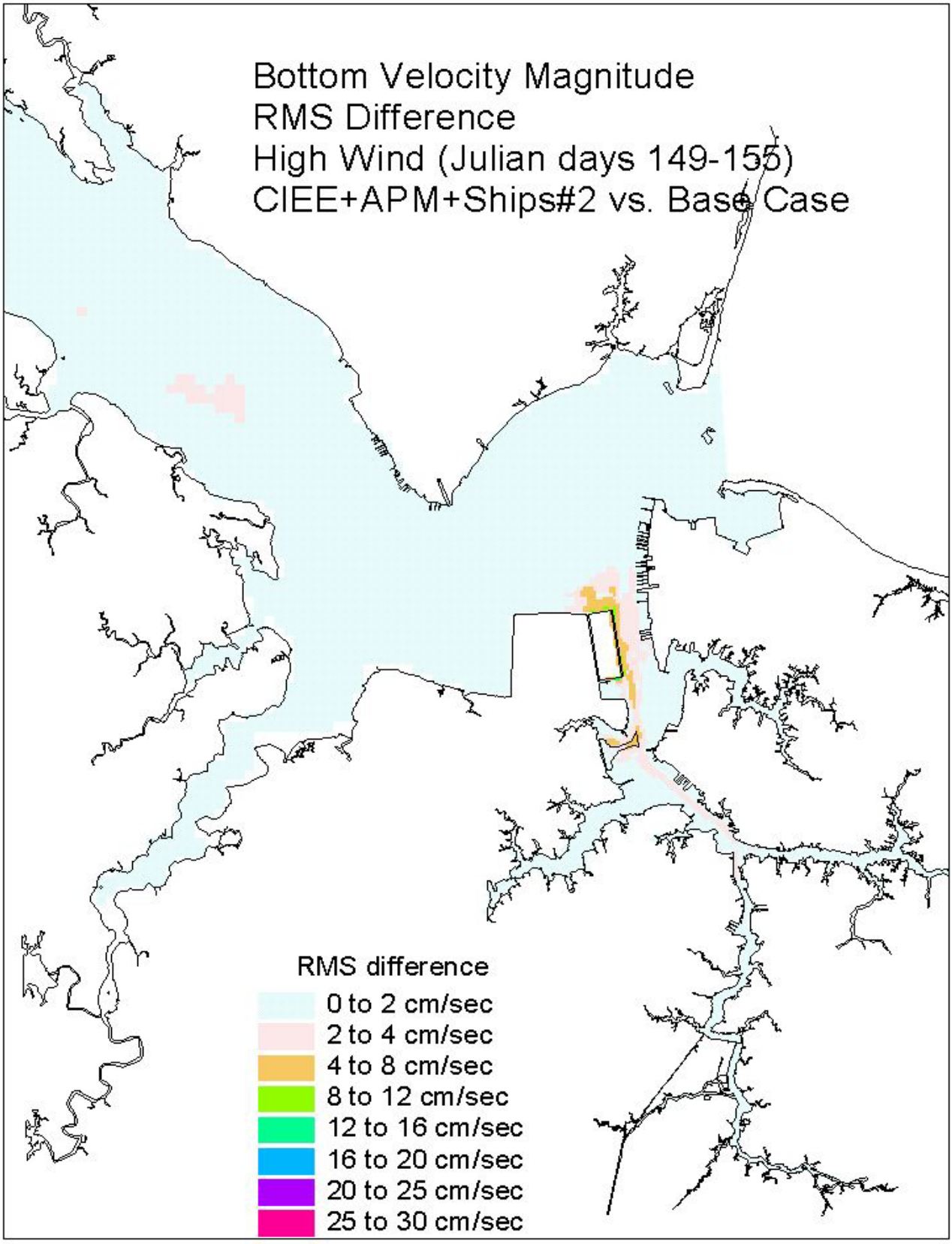

Figure 45. Historical simulation comparison (high wind) of the bottom velocity RMS difference for the Eastward Expansion plus APM Terminal Dredging plus Ships (Case 2b) versus the Base Case.

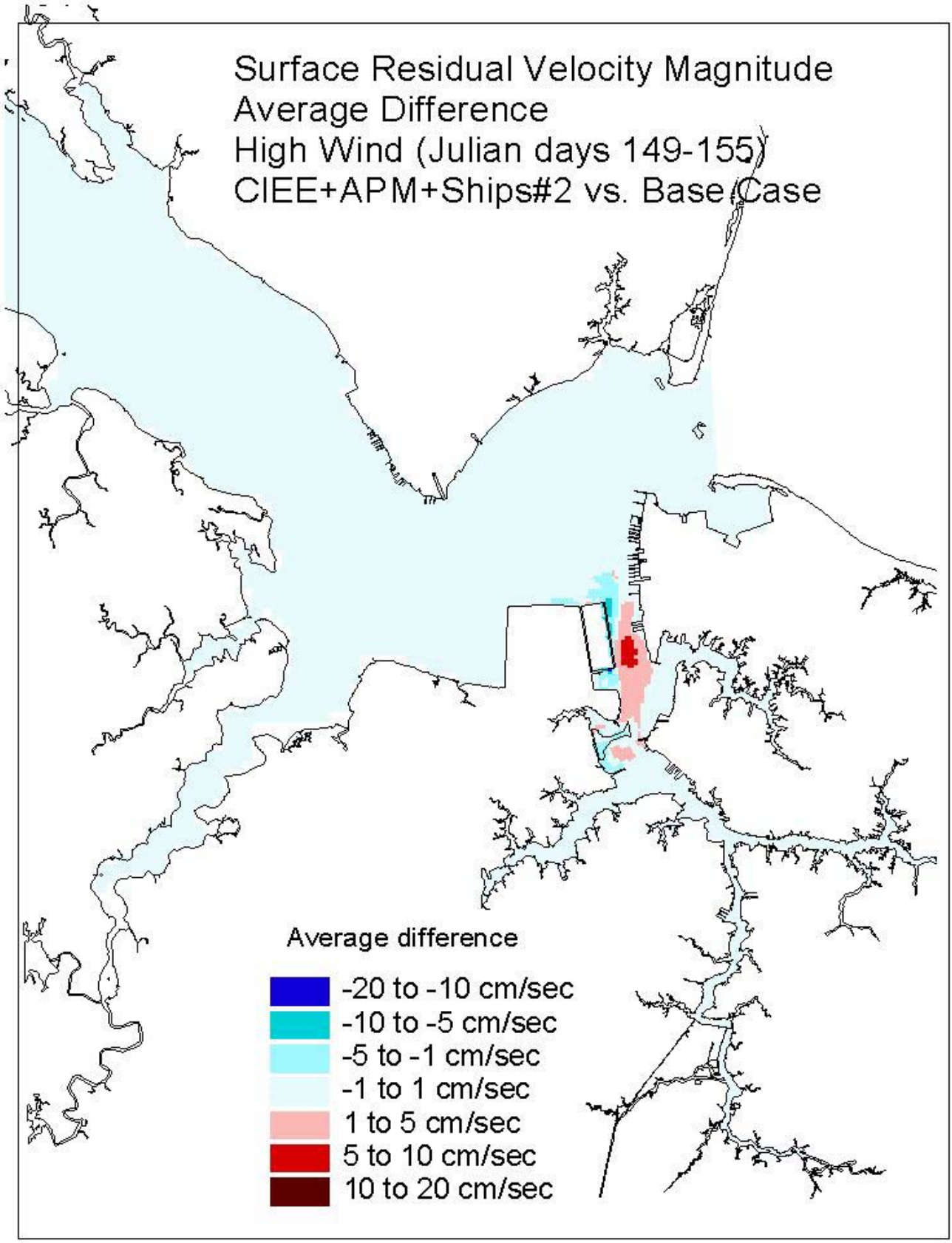

Figure 46. Historical simulation comparison (high wind) of the surface residual velocity average difference for the Eastward Expansion plus APM Terminal Dredging plus Ships (Case 2b) versus the Base Case.

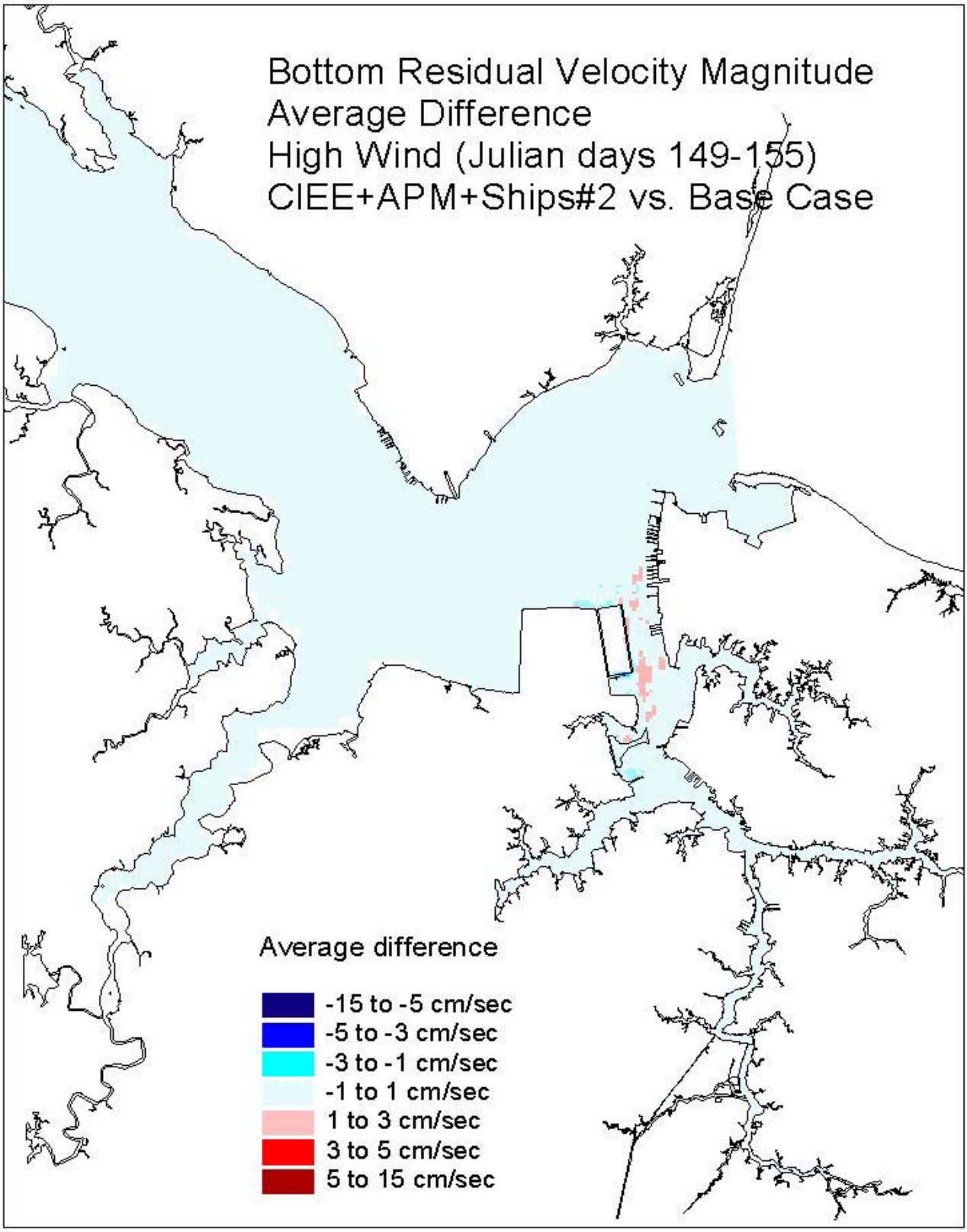

Figure 47. Historical simulation comparison (high wind) of the bottom residual velocity average difference for the Eastward Expansion plus APM Terminal Dredging plus Ships (Case 2b) versus the Base Case.

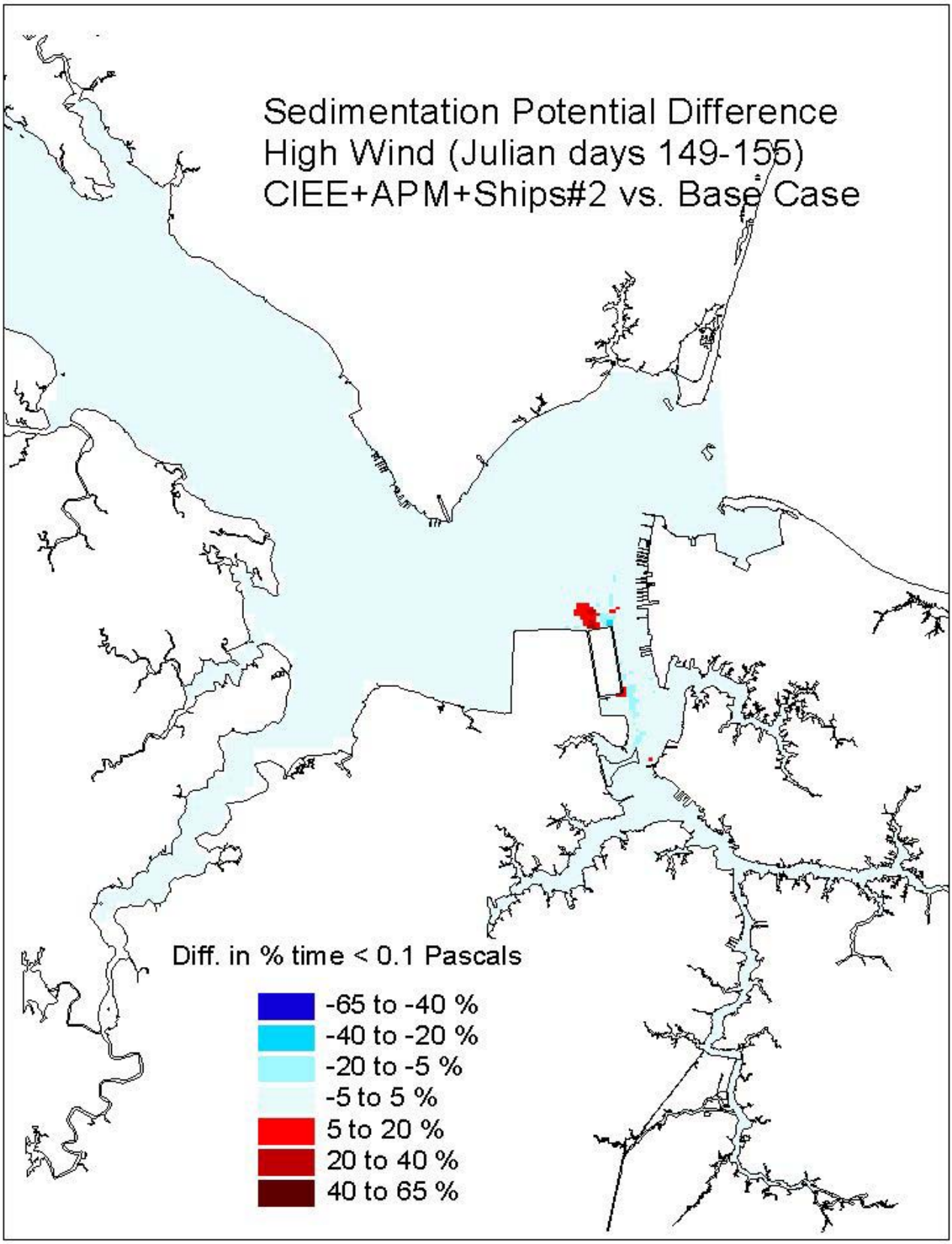

Figure 48. Historical simulation comparison (high wind) of the sedimentation potential difference for the Eastward Expansion plus APM Terminal Dredging plus Ships (Case 2b) versus the Base Case.

APPENDIX to CHAPTER IV, SECTION A.2

Global Comparisons of Historical Runs

Percentile Analysis

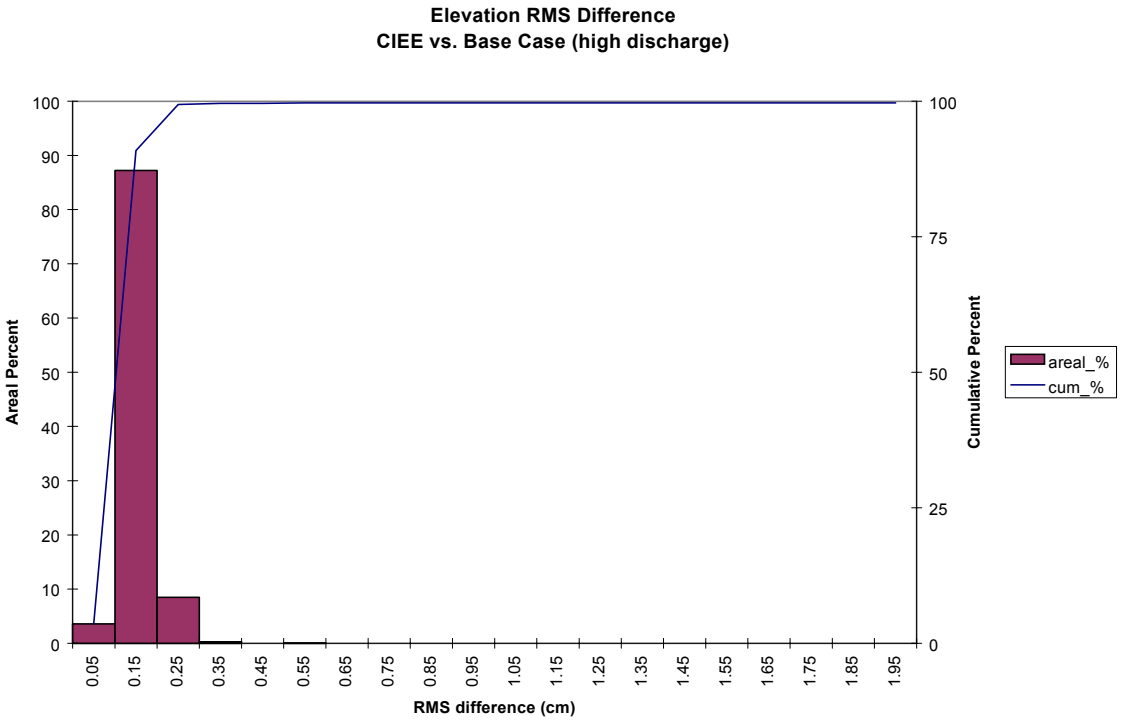

Figure 1. Frequency distribution of elevation RMS difference for the Eastward Expansion versus the Base Case during the high discharge event of historical simulation.

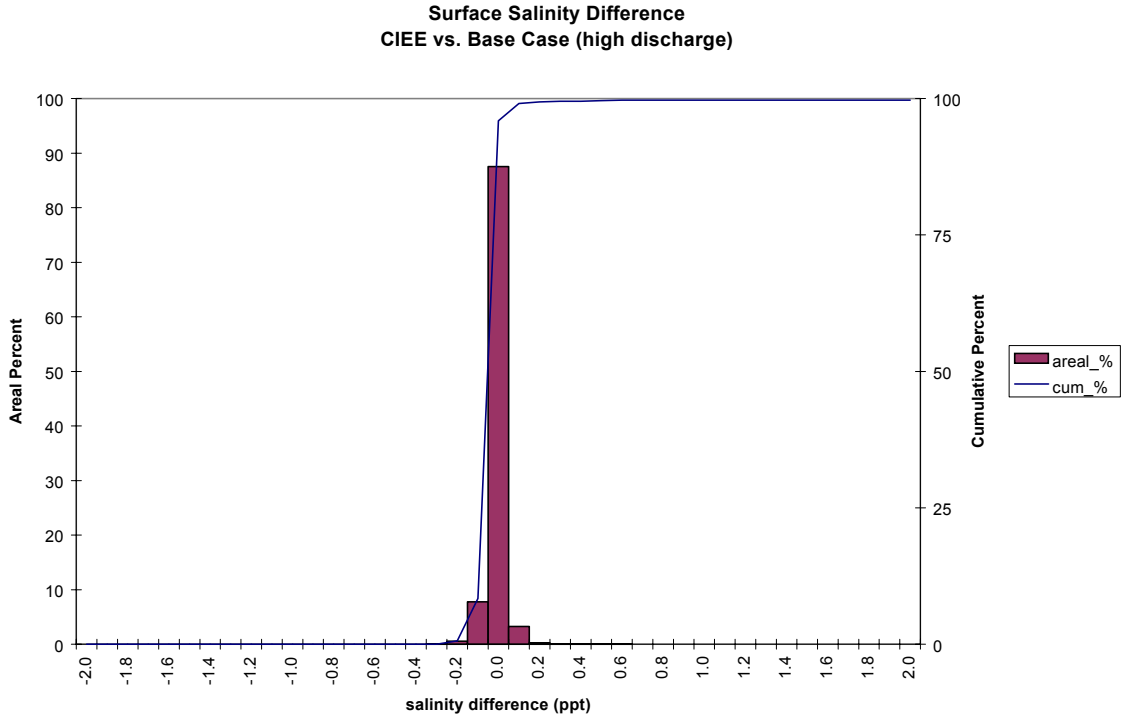

Figure 2. Frequency distribution of surface salinity average difference for the Eastward Expansion versus the Base Case during the high discharge event of historical simulation.

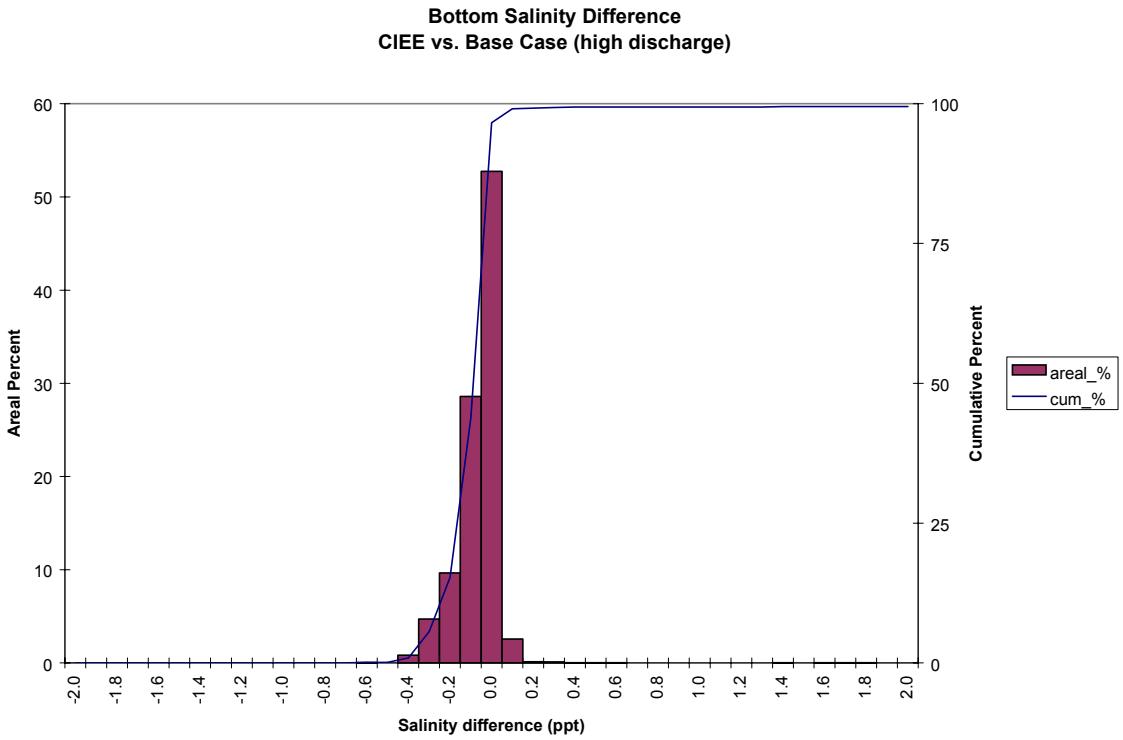

Figure 3. Frequency distribution of bottom salinity average difference for the Eastward Expansion versus the Base Case during the high discharge event of historical simulation.

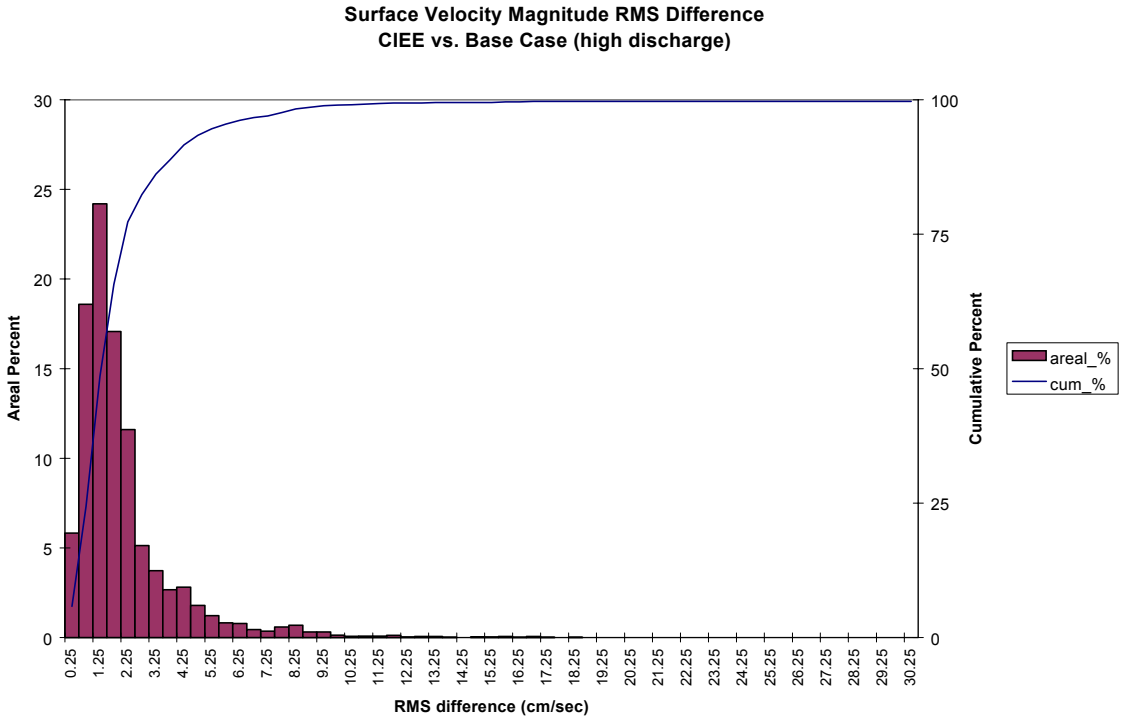

Figure 4. Frequency distribution of surface velocity RMS difference for the Eastward Expansion versus the Base Case during the high discharge event of historical simulation.

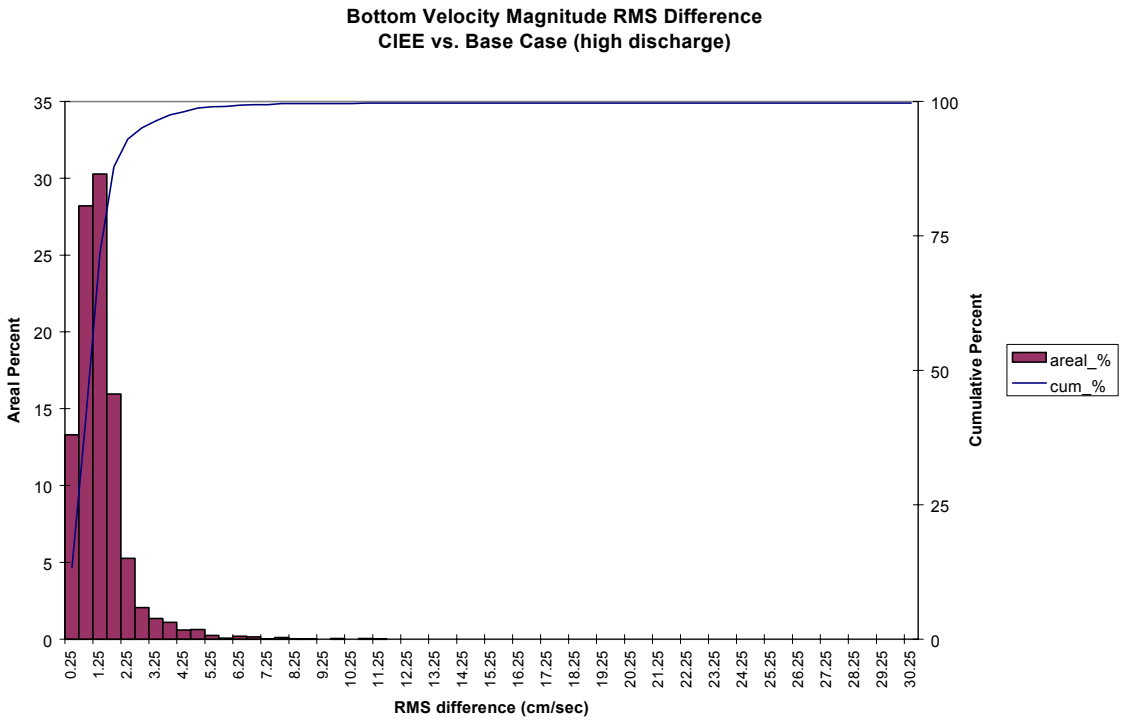

Figure 5. Frequency distribution of bottom velocity RMS difference for the Eastward Expansion versus the Base Case during the high discharge event of historical simulation.

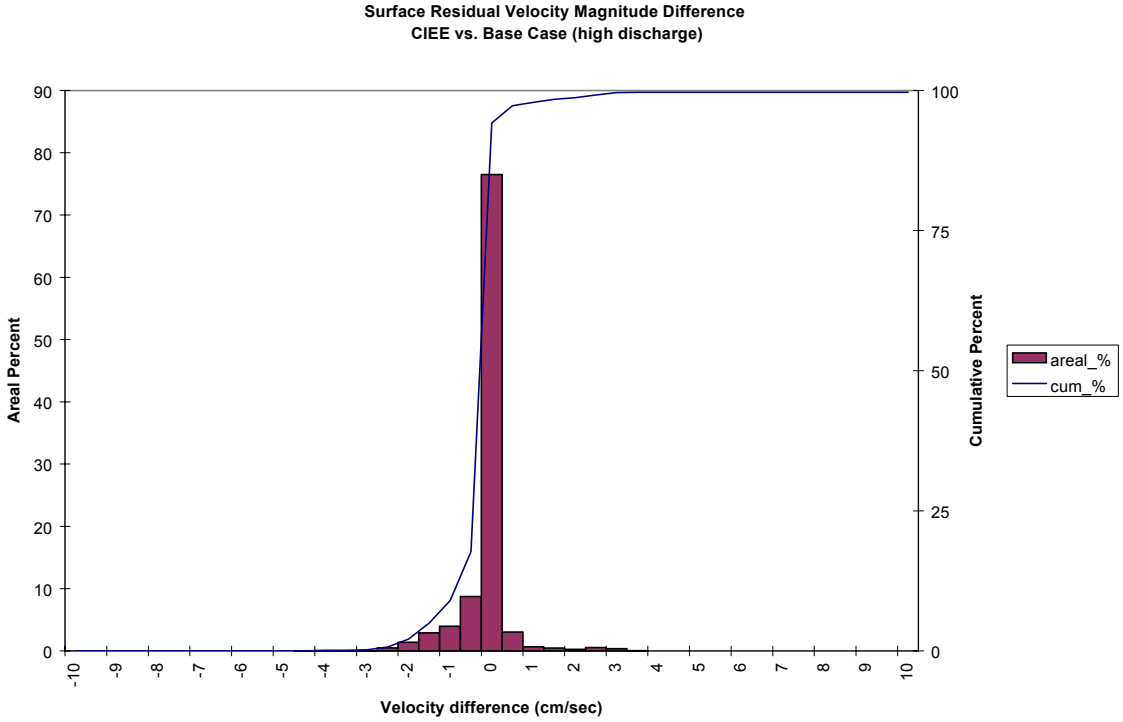

Figure 6. Frequency distribution of surface residual velocity magnitude average difference for the Eastward Expansion versus the Base Case during the high discharge event of historical simulation.

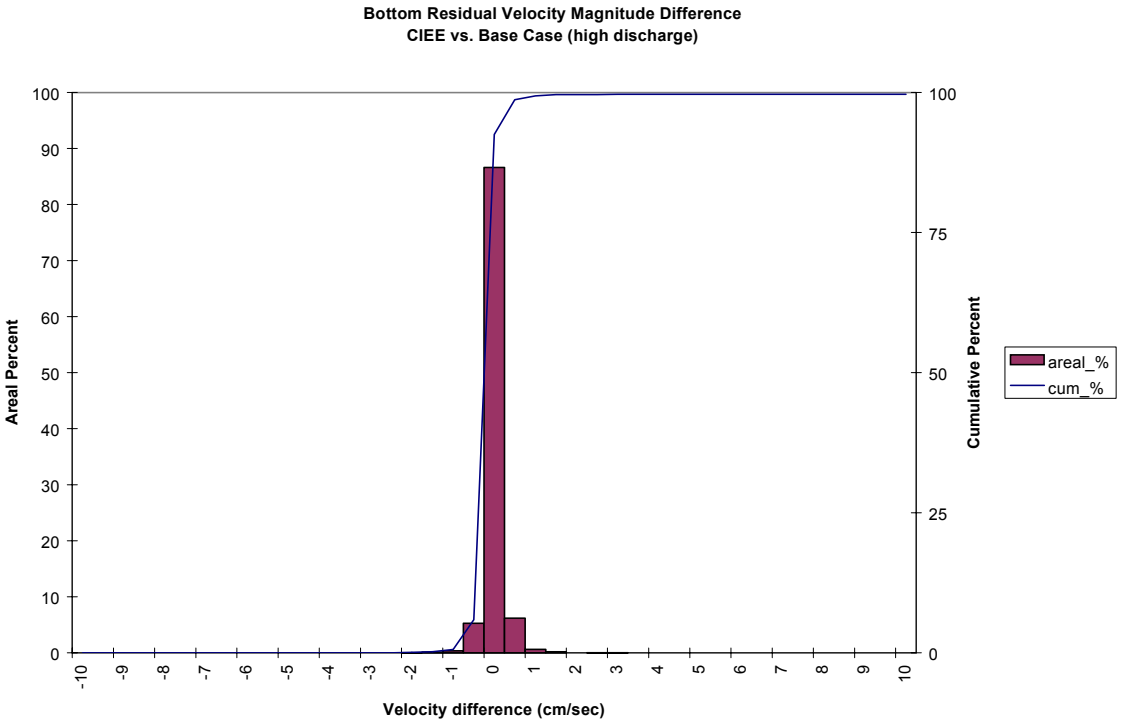

Figure 7. Frequency distribution of bottom residual velocity magnitude average difference for the Eastward Expansion versus the Base Case during the high discharge event of historical simulation.

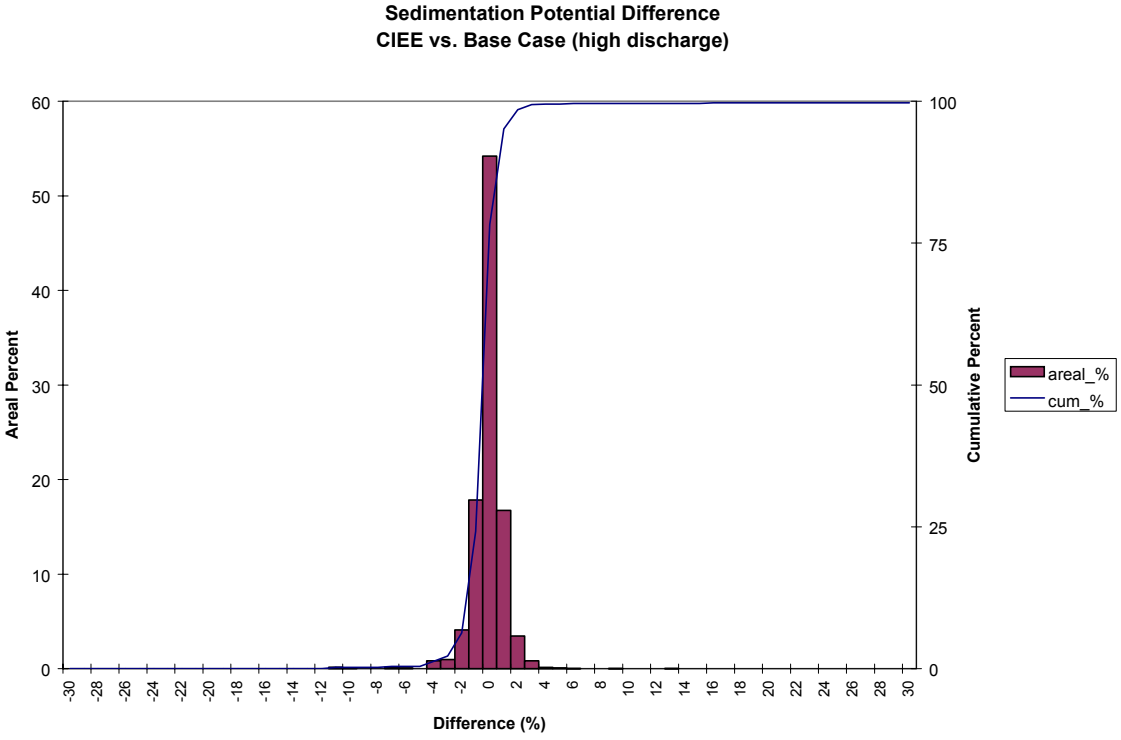

Figure 8. Frequency distribution of sedimentation potential difference for the Eastward Expansion versus the Base Case during the high discharge event of historical simulation.

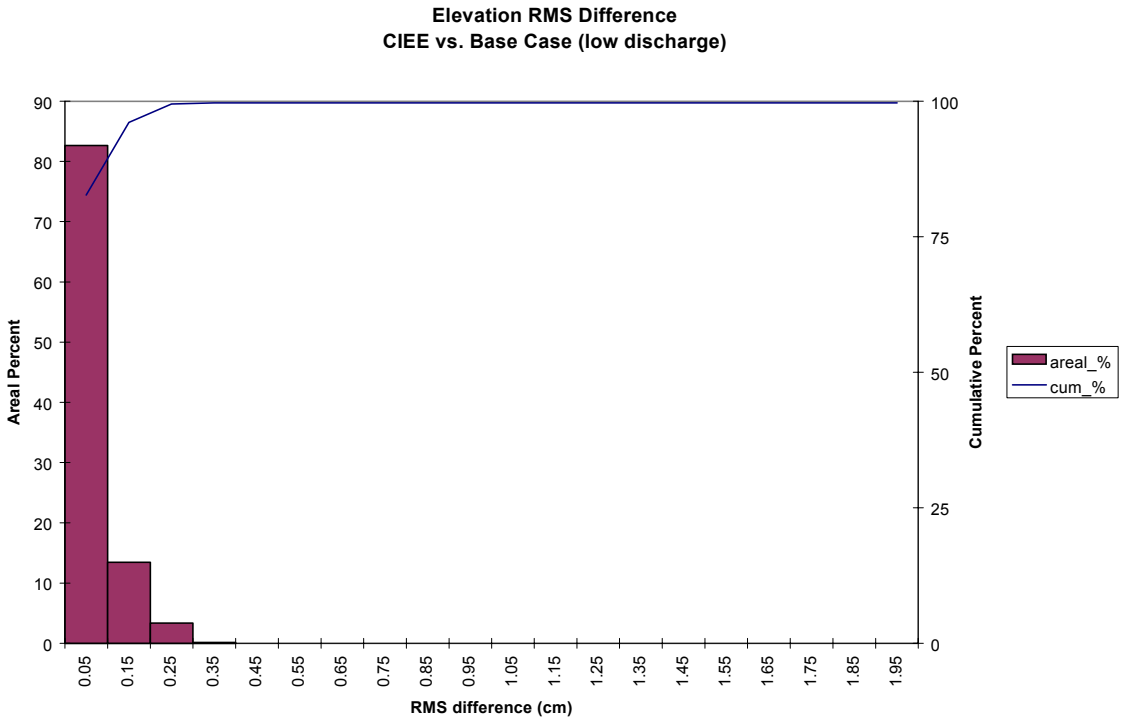

Figure 9. Frequency distribution of elevation RMS difference for the Eastward Expansion versus the Base Case during the low discharge event of historical simulation.

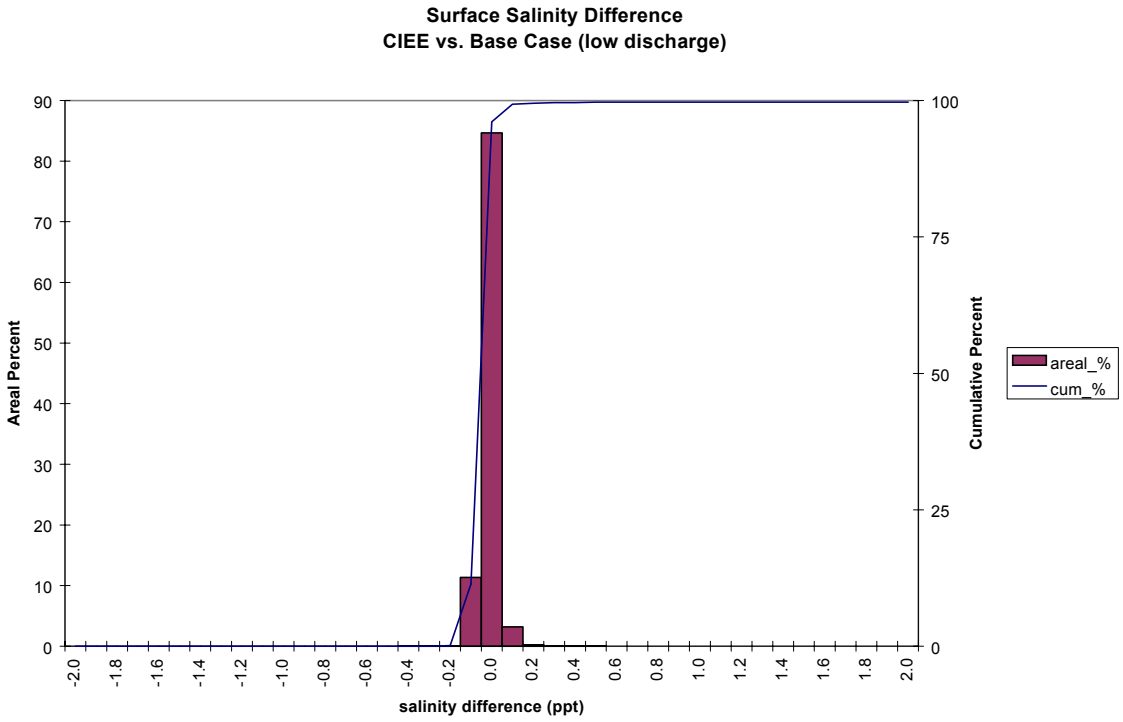

Figure 10. Frequency distribution of surface salinity average difference for the Eastward Expansion versus the Base Case during the low discharge event of historical simulation.

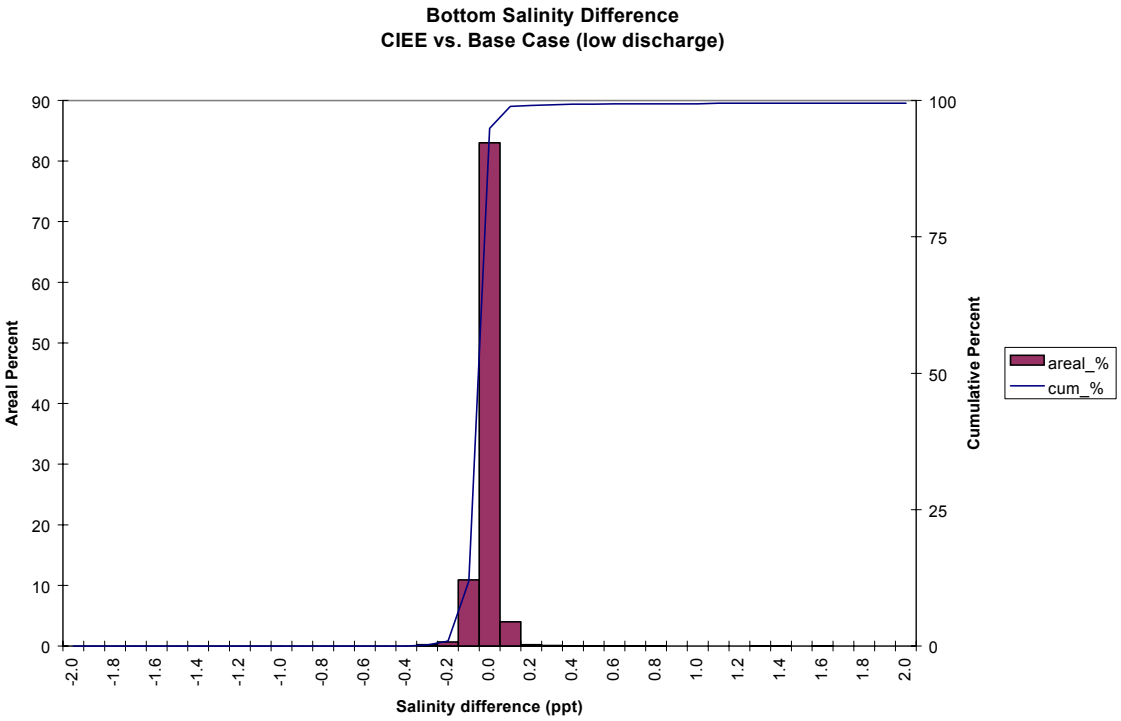

Figure 11. Frequency distribution of bottom salinity average difference for the Eastward Expansion versus the Base Case during the low discharge event of historical simulation.

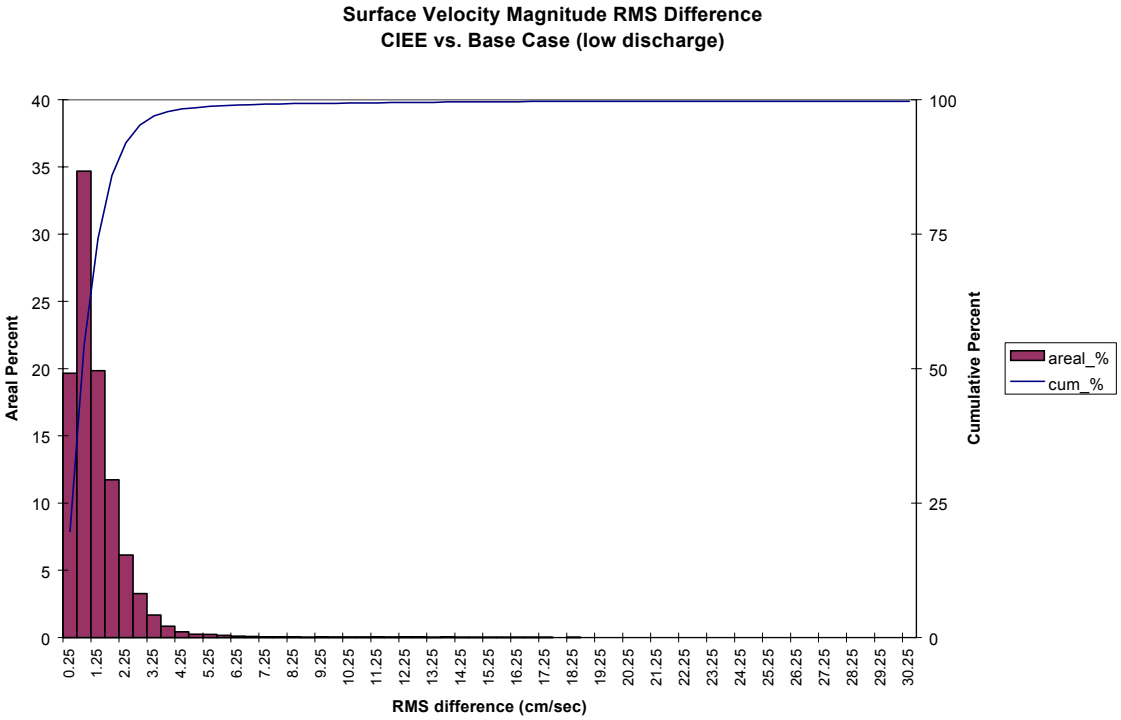

Figure 12. Frequency distribution of surface velocity RMS difference for the Eastward Expansion versus the Base Case during the low discharge event of historical simulation.

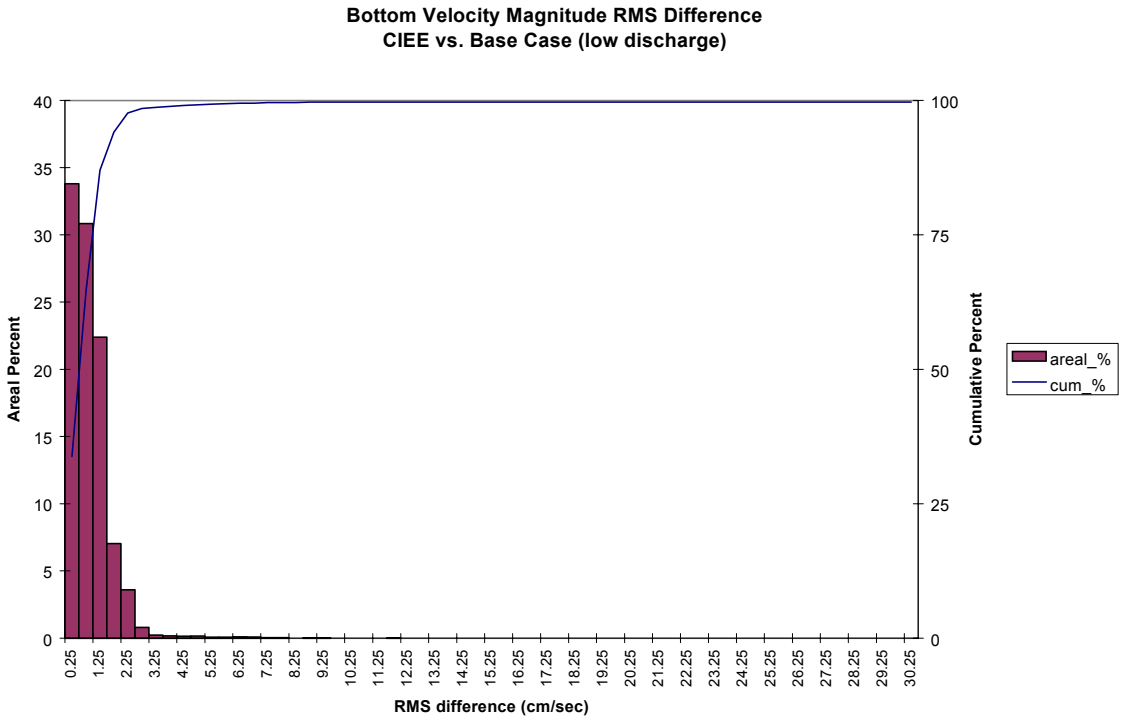

Figure 13. Frequency distribution of bottom velocity RMS difference for the Eastward Expansion versus the Base Case during the low discharge event of historical simulation.

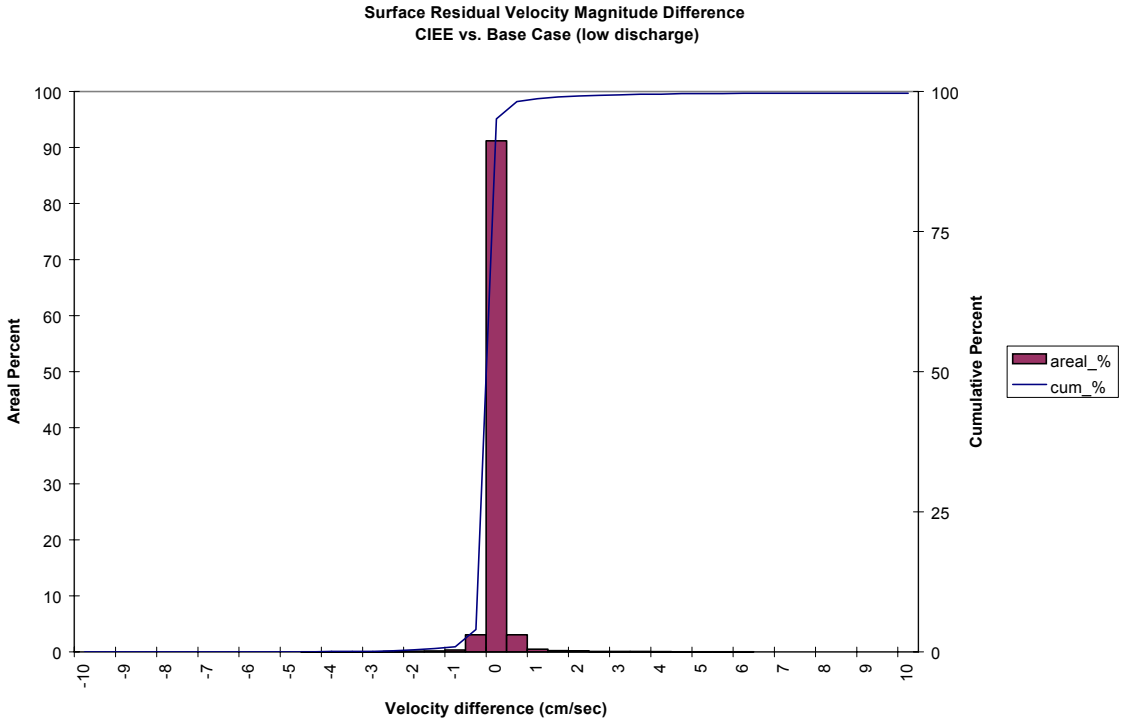

Figure 14. Frequency distribution of surface residual velocity magnitude average difference for the Eastward Expansion versus the Base Case during the low discharge event of historical simulation.

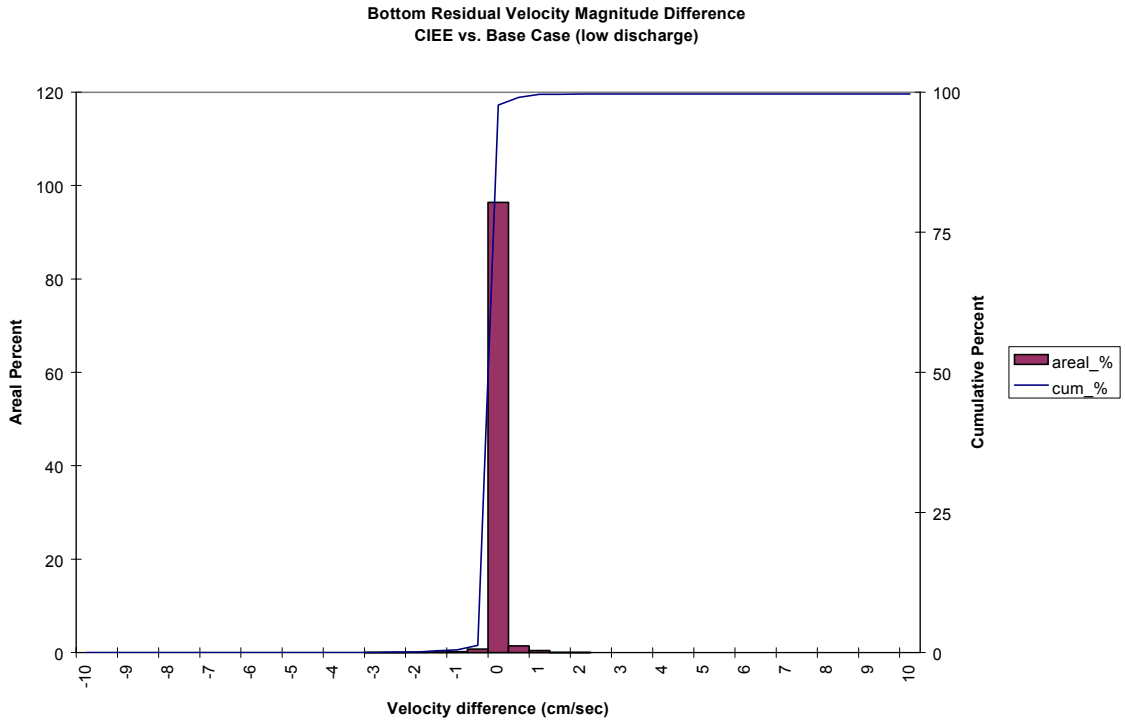

Figure 15. Frequency distribution of bottom residual velocity magnitude average difference for the Eastward Expansion versus the Base Case during the low discharge event of historical simulation.

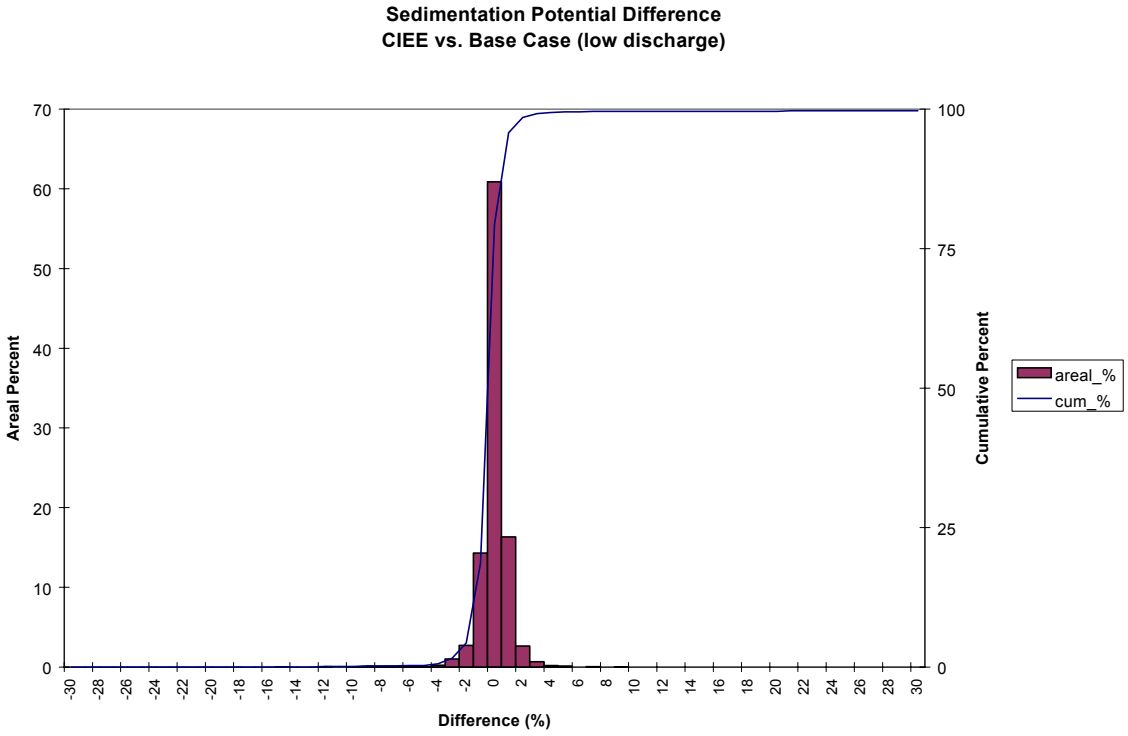

Figure 16. Frequency distribution of sedimentation potential difference for the Eastward Expansion versus the Base Case during the low discharge event of historical simulation.

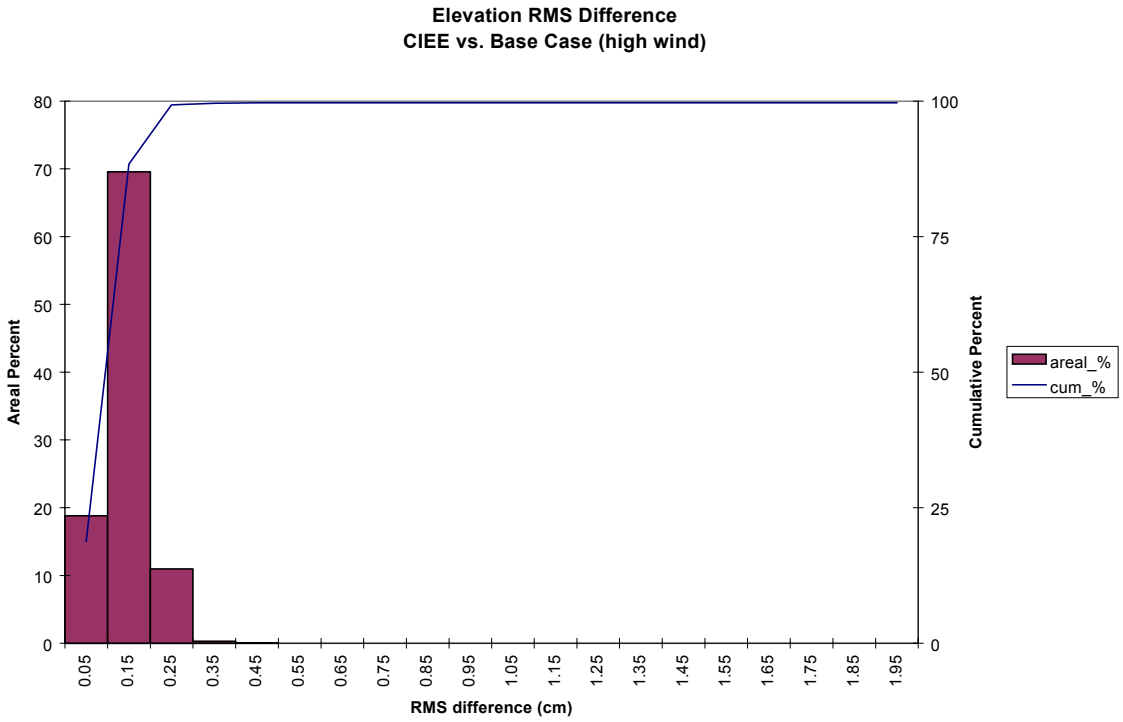

Figure 17. Frequency distribution of elevation RMS difference for the Eastward Expansion versus the Base Case during the high wind event of historical simulation.

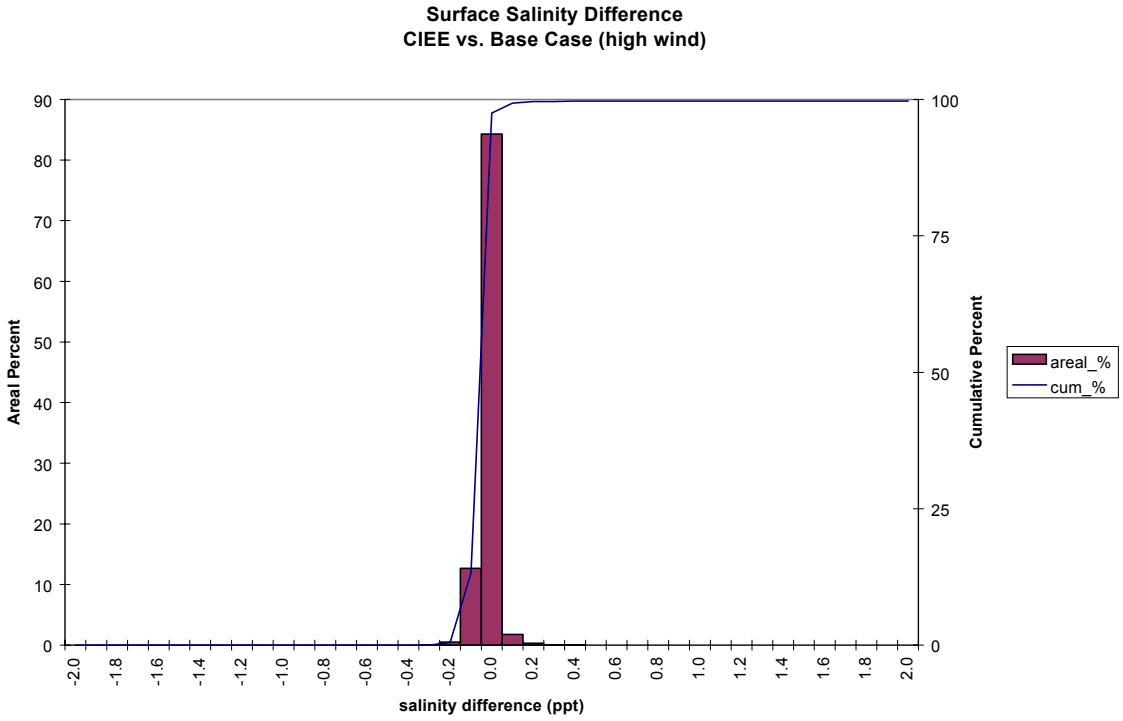

Figure 18. Frequency distribution of surface salinity average difference for the Eastward Expansion versus the Base Case during the high wind event of historical simulation.

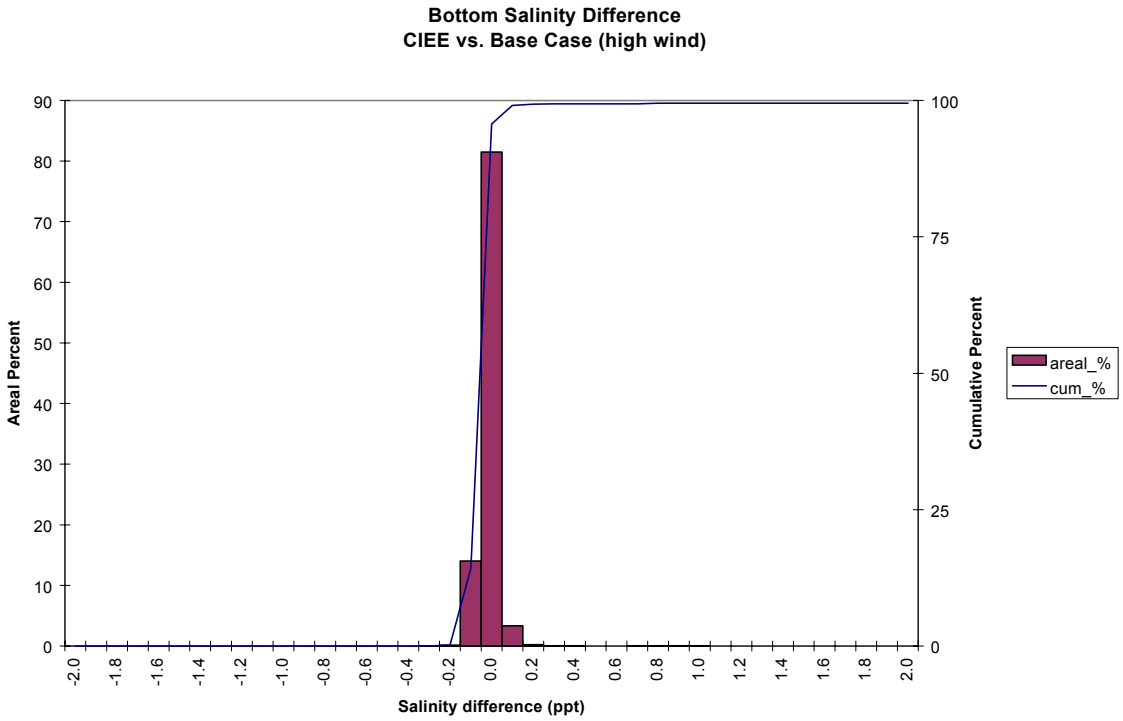

Figure 19. Frequency distribution of bottom salinity average difference for the Eastward Expansion versus the Base Case during the high wind event of historical simulation.

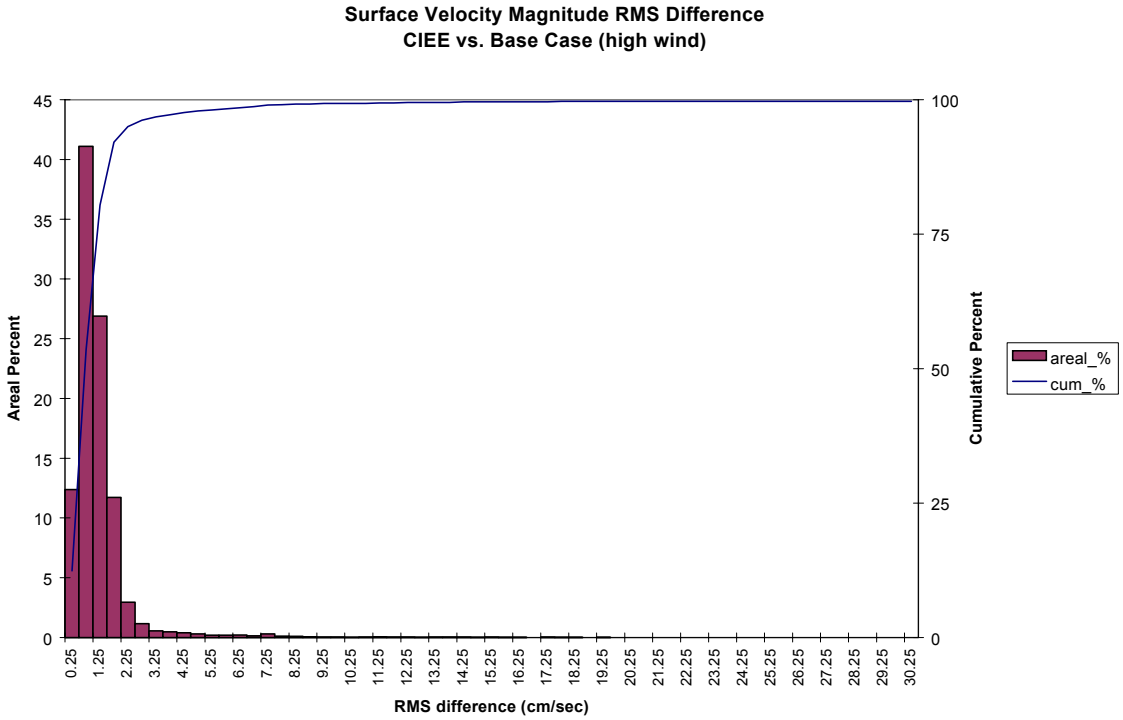

Figure 20. Frequency distribution of surface velocity RMS difference for the Eastward Expansion versus the Base Case during the high wind event of historical simulation.

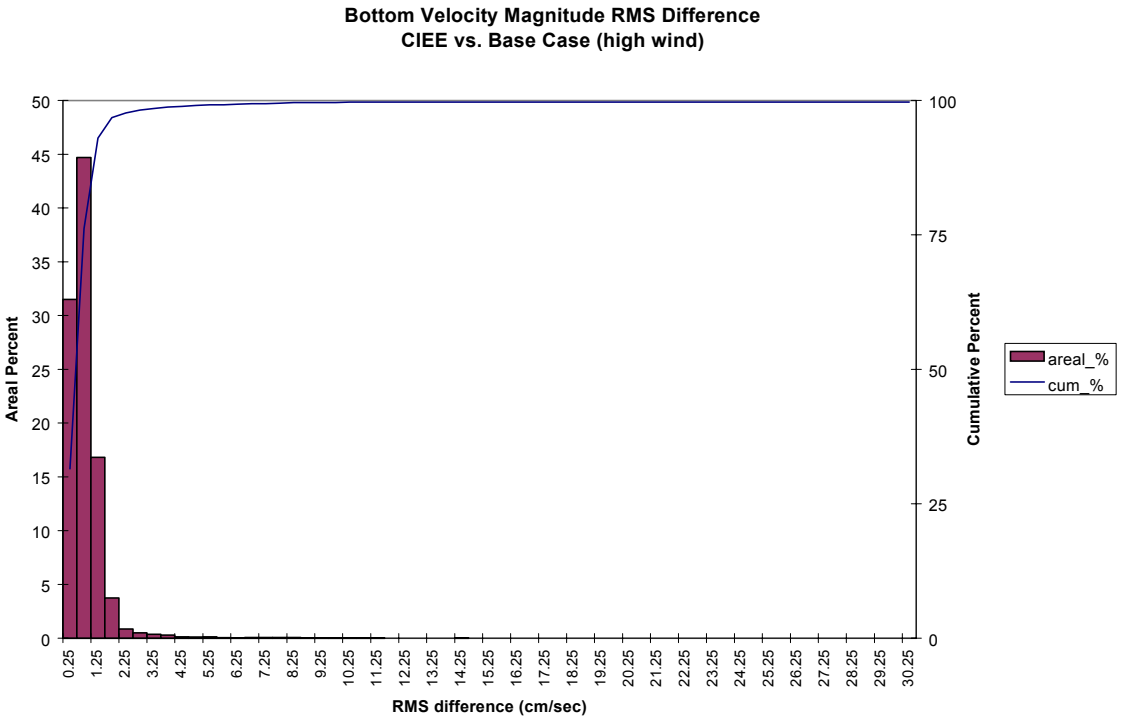

Figure 21. Frequency distribution of bottom velocity RMS difference for the Eastward Expansion versus the Base Case during the high wind event of historical simulation.

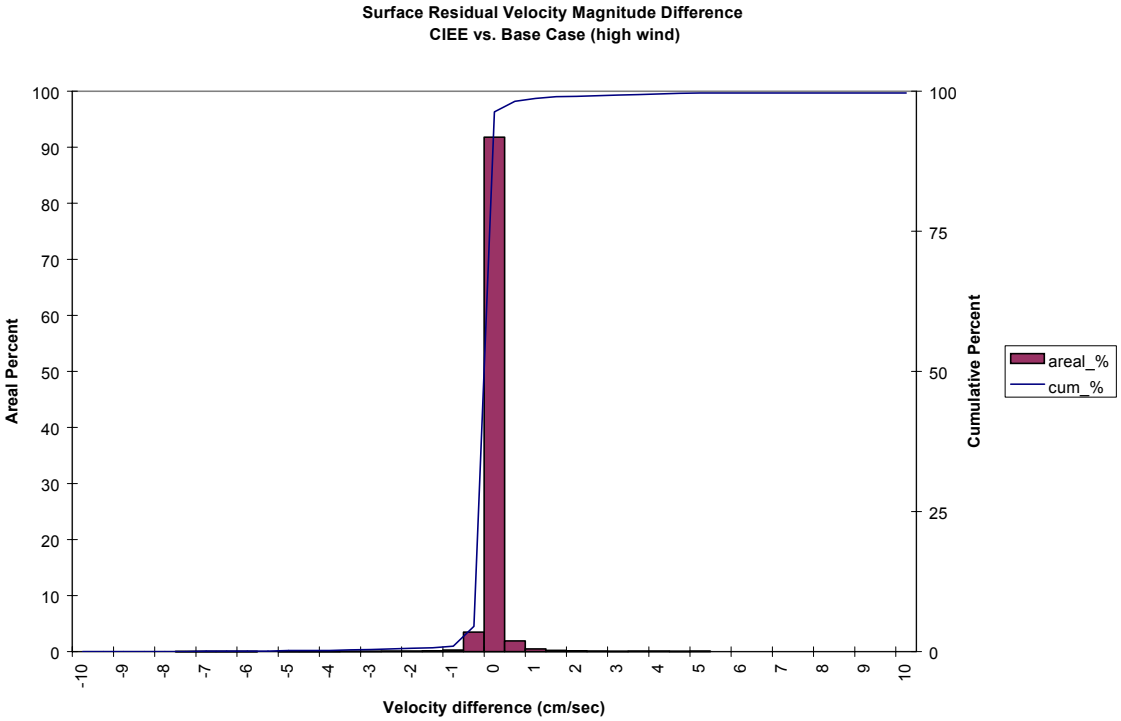

Figure 22. Frequency distribution of surface residual velocity magnitude average difference for the Eastward Expansion versus the Base Case during the high wind event of historical simulation.

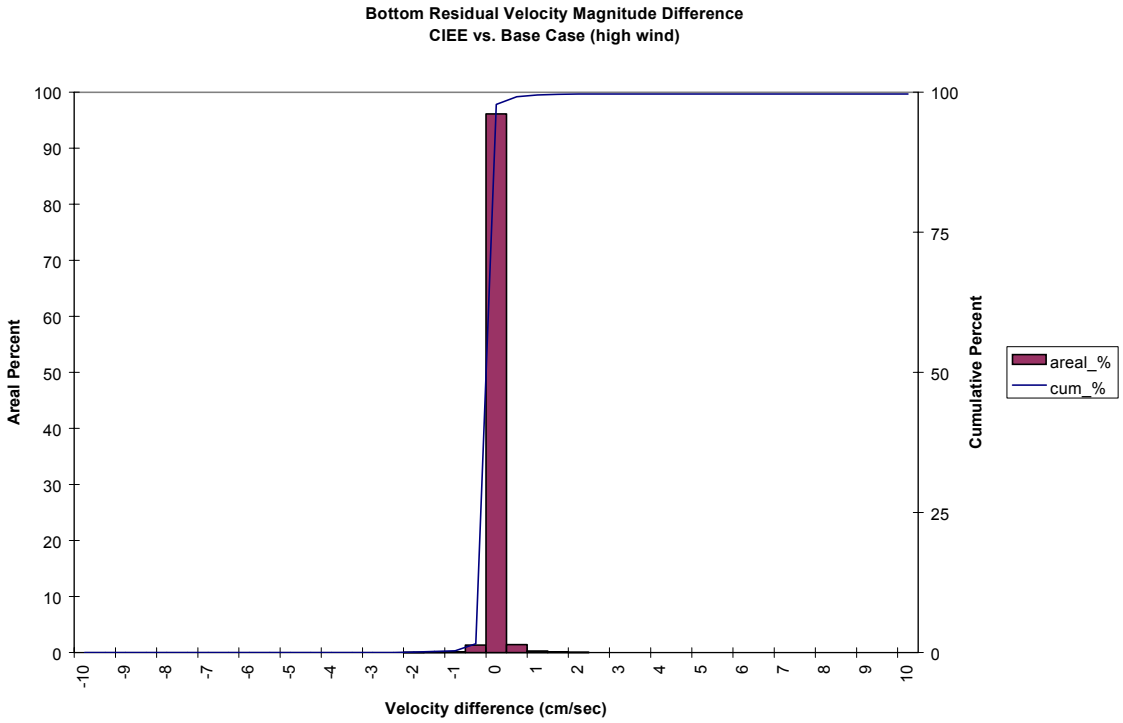

Figure 23. Frequency distribution of bottom residual velocity magnitude average difference for the Eastward Expansion versus the Base Case during the high wind event of historical simulation.

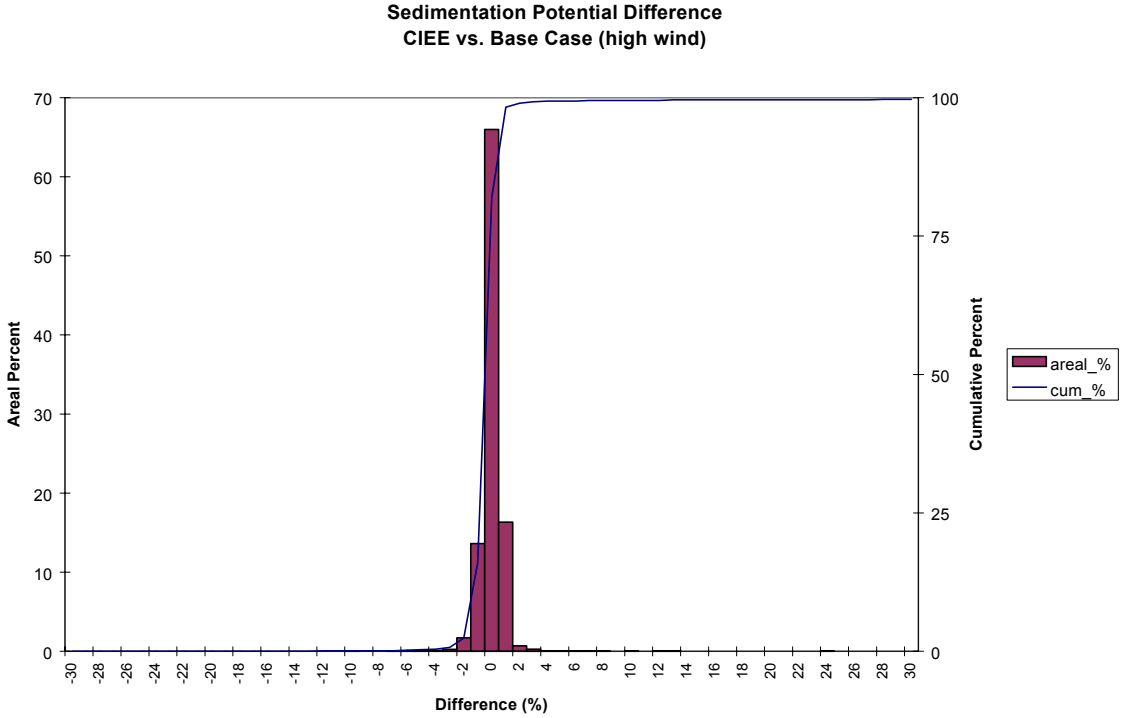

Figure 24. Frequency distribution of sedimentation potential difference for the Eastward Expansion versus the Base Case during the high wind event of historical simulation.

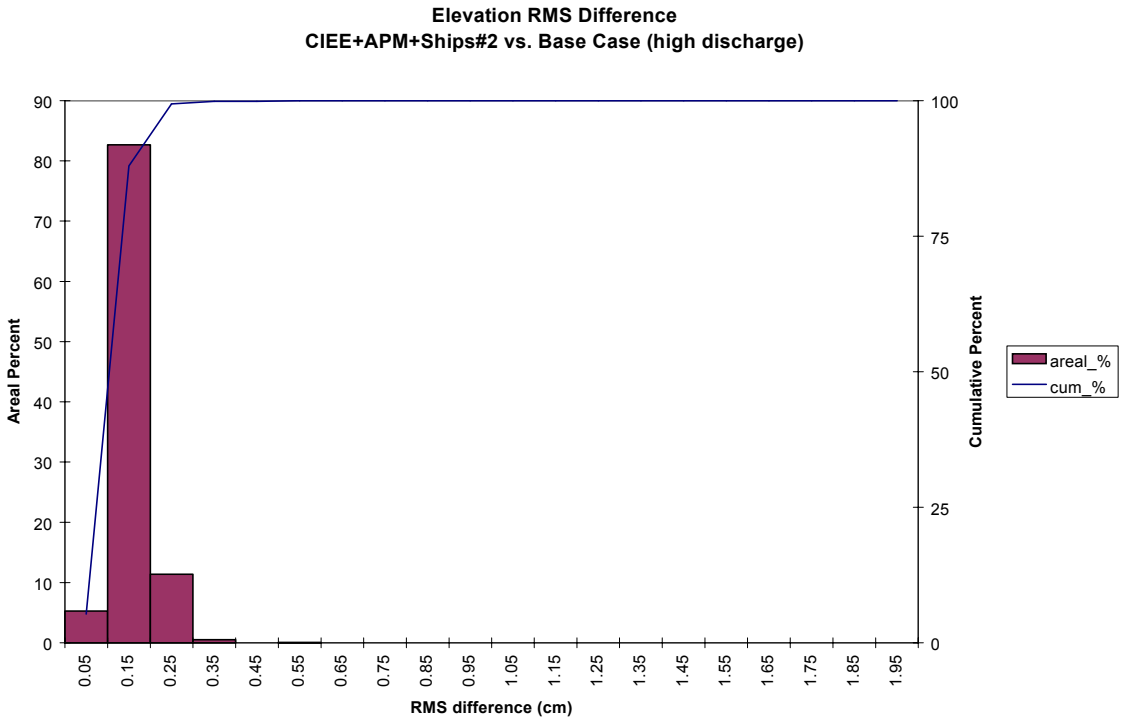

Figure 25. Frequency distribution of elevation RMS difference for the Eastward Expansion plus APM Terminal Dredging plus Ships (Case 2b) versus the Base Case during the high discharge event of historical simulation.

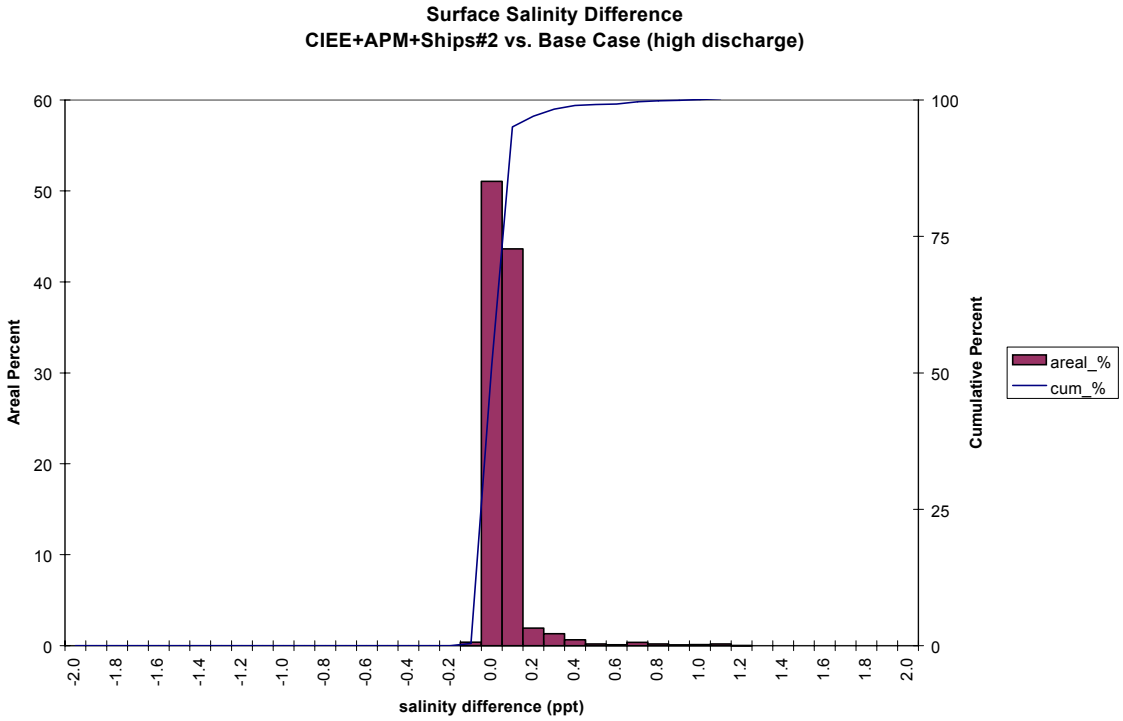

Figure 26. Frequency distribution of surface salinity average difference for the Eastward Expansion plus APM Terminal Dredging plus Ships (Case 2b) versus the Base Case during the high discharge event of historical simulation.

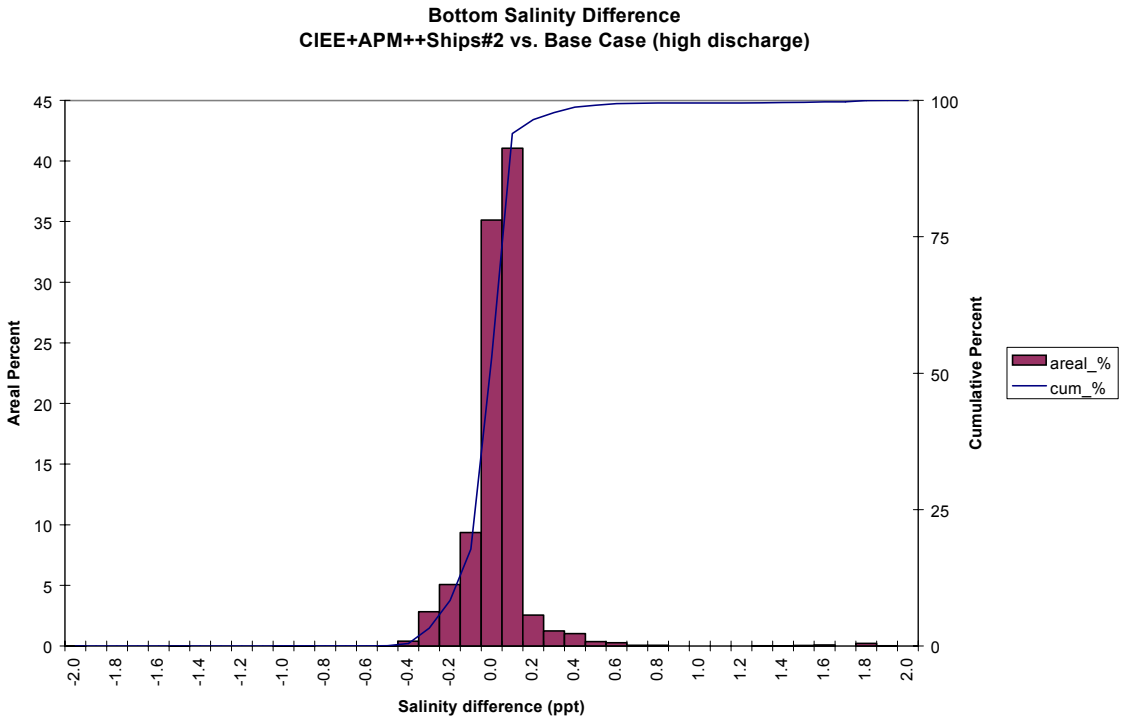

Figure 27. Frequency distribution of bottom salinity average difference for the Eastward Expansion plus APM Terminal Dredging plus Ships (Case 2b) versus the Base Case during the high discharge event of historical simulation.

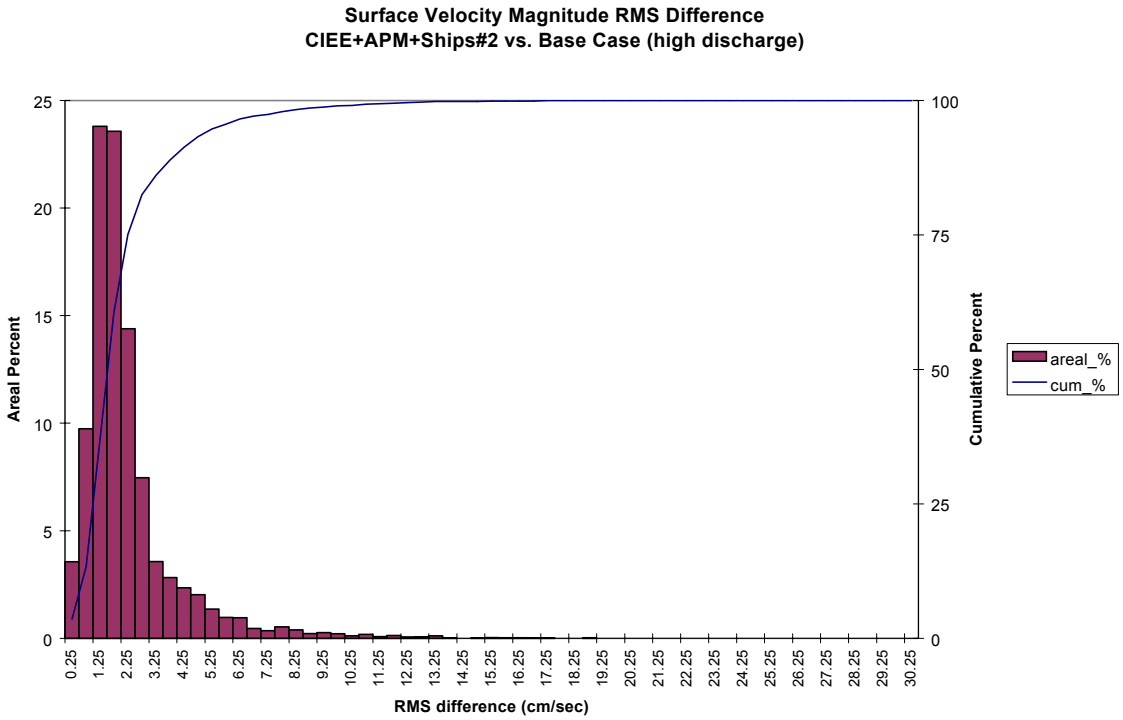

Figure 28. Frequency distribution of surface velocity RMS difference for the Eastward Expansion plus APM Terminal Dredging plus Ships (Case 2b) versus the Base Case during the high discharge event of historical simulation.

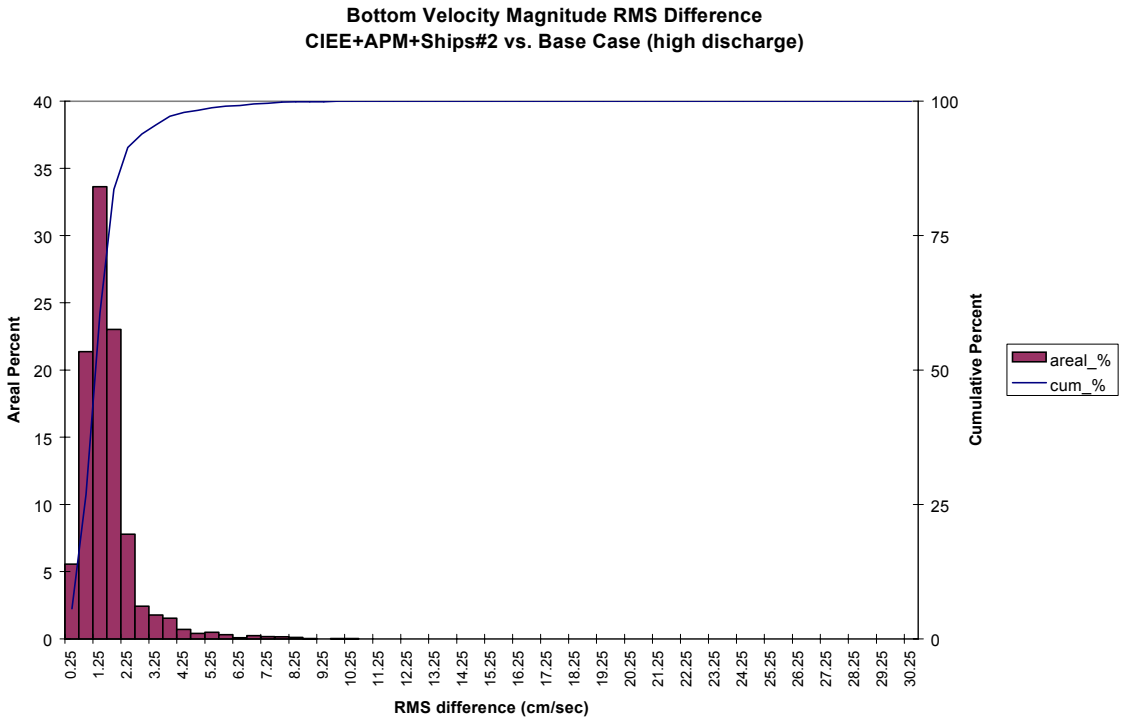

Figure 29. Frequency distribution of bottom velocity RMS difference for the Eastward Expansion plus APM Terminal Dredging plus Ships (Case 2b) versus the Base Case during the high discharge event of historical simulation.

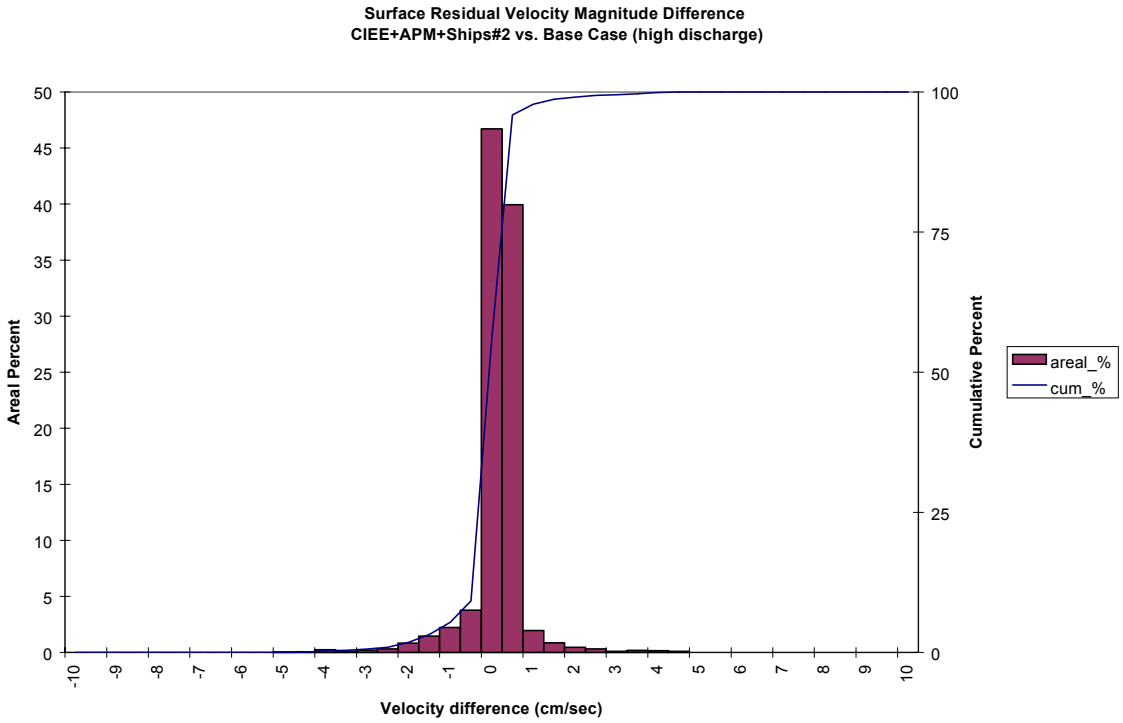

Figure 30. Frequency distribution of surface residual velocity magnitude average difference for the Eastward Expansion plus APM Terminal Dredging plus Ships (Case 2b) versus the Base Case during the high discharge event of historical simulation.

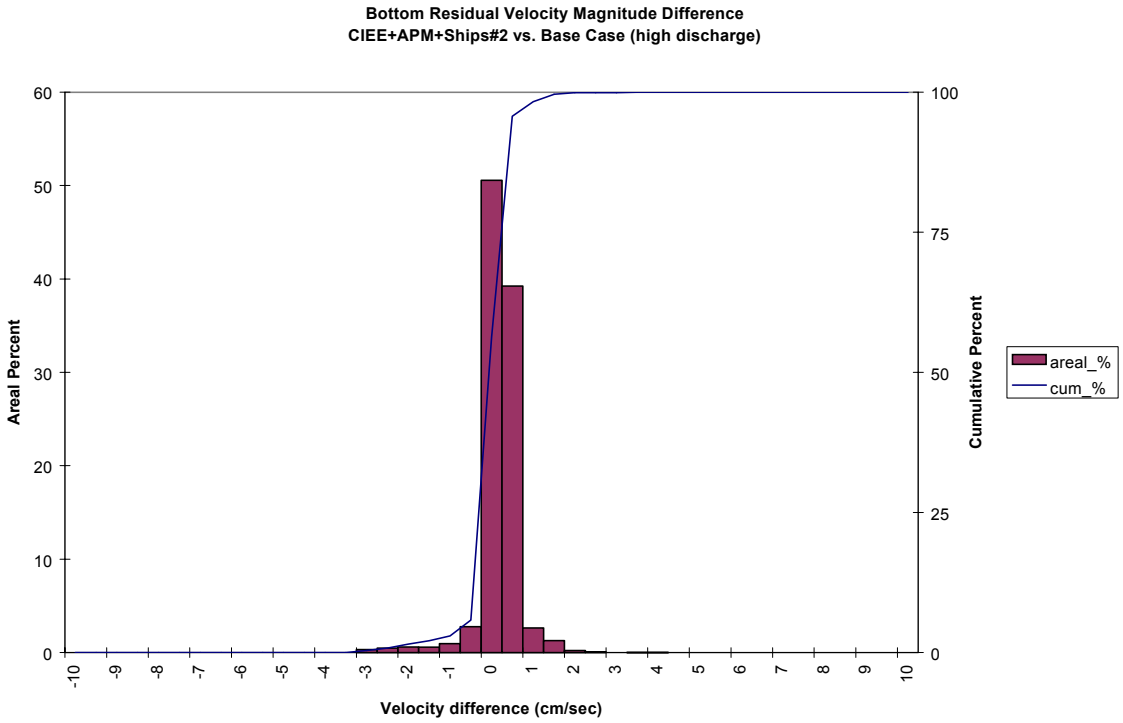

Figure 31. Frequency distribution of bottom residual velocity magnitude average difference for the Eastward Expansion plus APM Terminal Dredging plus Ships (Case 2b) versus the Base Case during the high discharge event of historical simulation.

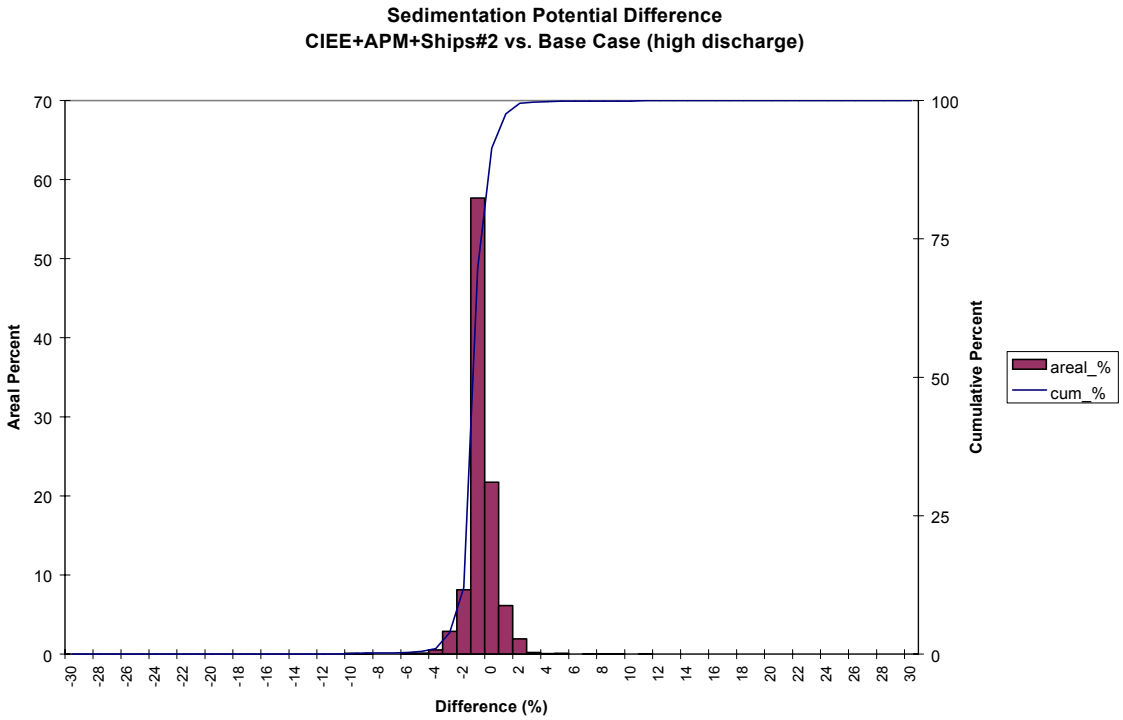

Figure 32. Frequency distribution of sedimentation potential difference for the Eastward Expansion plus APM Terminal Dredging plus Ships (Case 2b) versus the Base Case during the high discharge event of historical simulation.

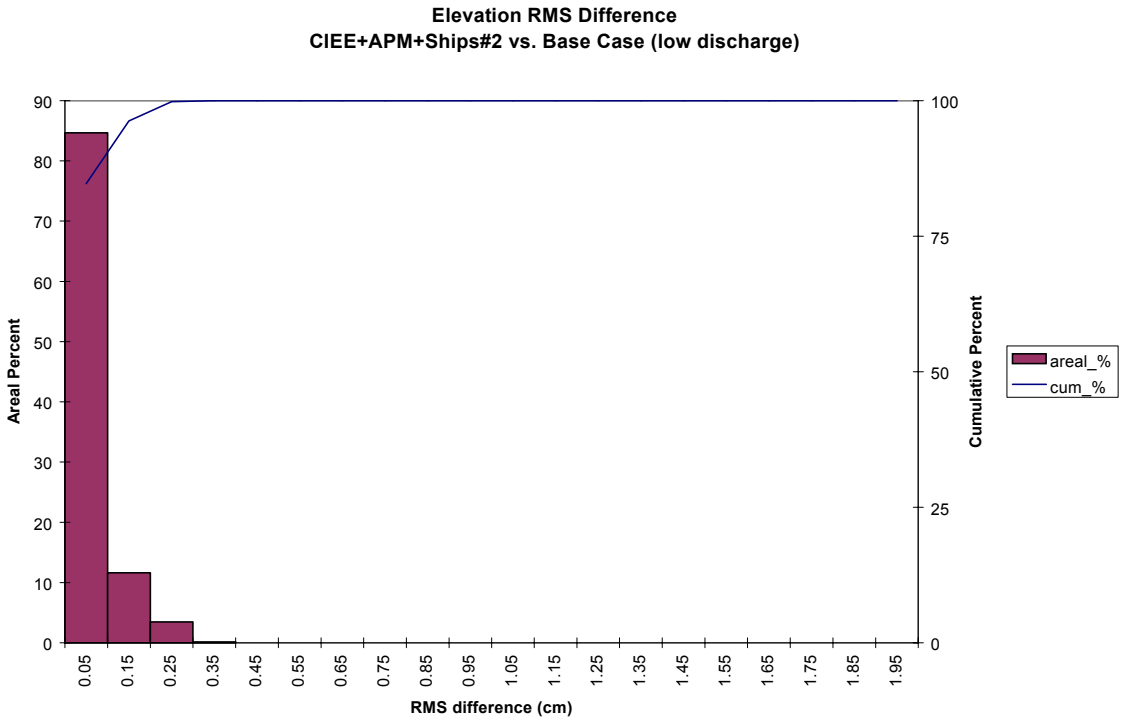

Figure 33. Frequency distribution of elevation RMS difference for the Eastward Expansion plus APM Terminal Dredging plus Ships (Case 2b) versus the Base Case during the low discharge event of historical simulation.

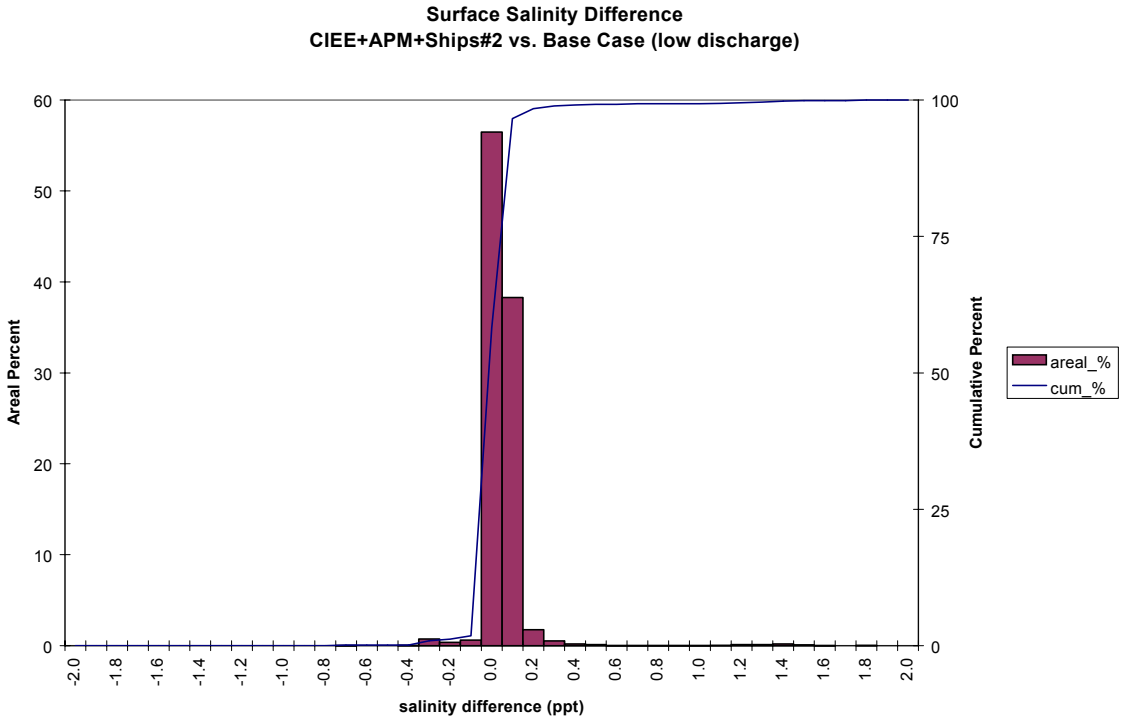

Figure 34. Frequency distribution of surface salinity average difference for the Eastward Expansion plus APM Terminal Dredging plus Ships (Case 2b) versus the Base Case during the low discharge event of historical simulation.

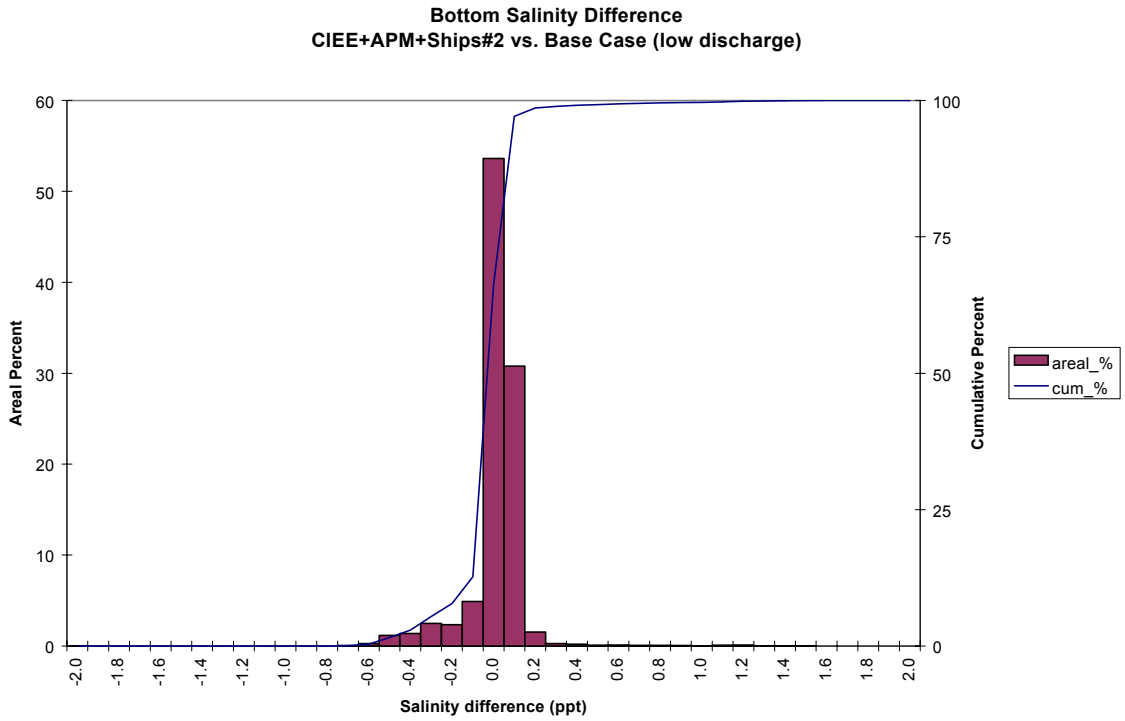

Figure 35. Frequency distribution of bottom salinity average difference for the Eastward Expansion plus APM Terminal Dredging plus Ships (Case 2b) versus the Base Case during the low discharge event of historical simulation.

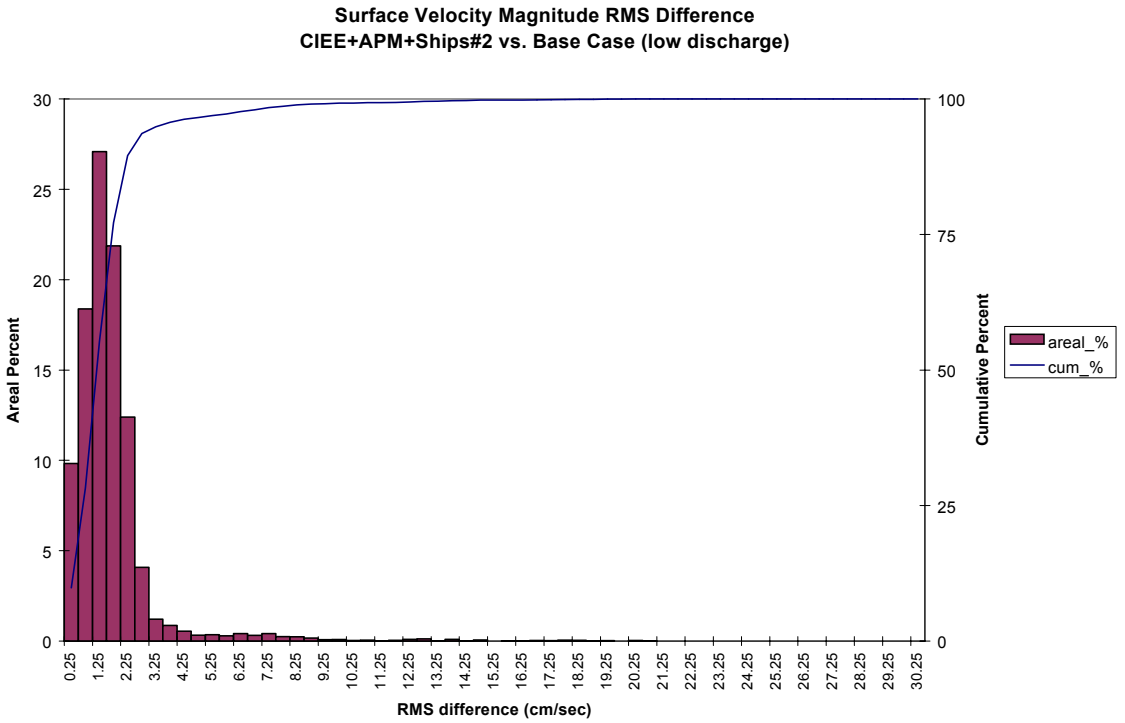

Figure 36. Frequency distribution of surface velocity RMS difference for the Eastward Expansion plus APM Terminal Dredging plus Ships (Case 2b) versus the Base Case during the low discharge event of historical simulation.

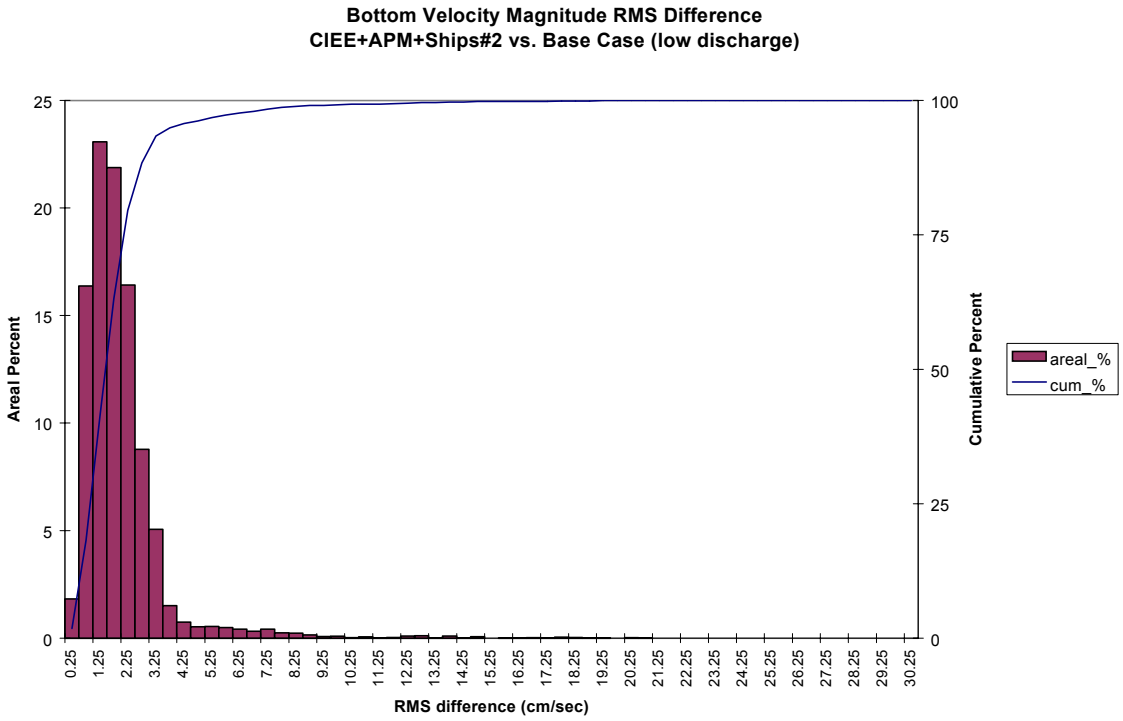

Figure 37. Frequency distribution of bottom velocity RMS difference for the Eastward Expansion plus APM Terminal Dredging plus Ships (Case 2b) versus the Base Case during the low discharge event of historical simulation.

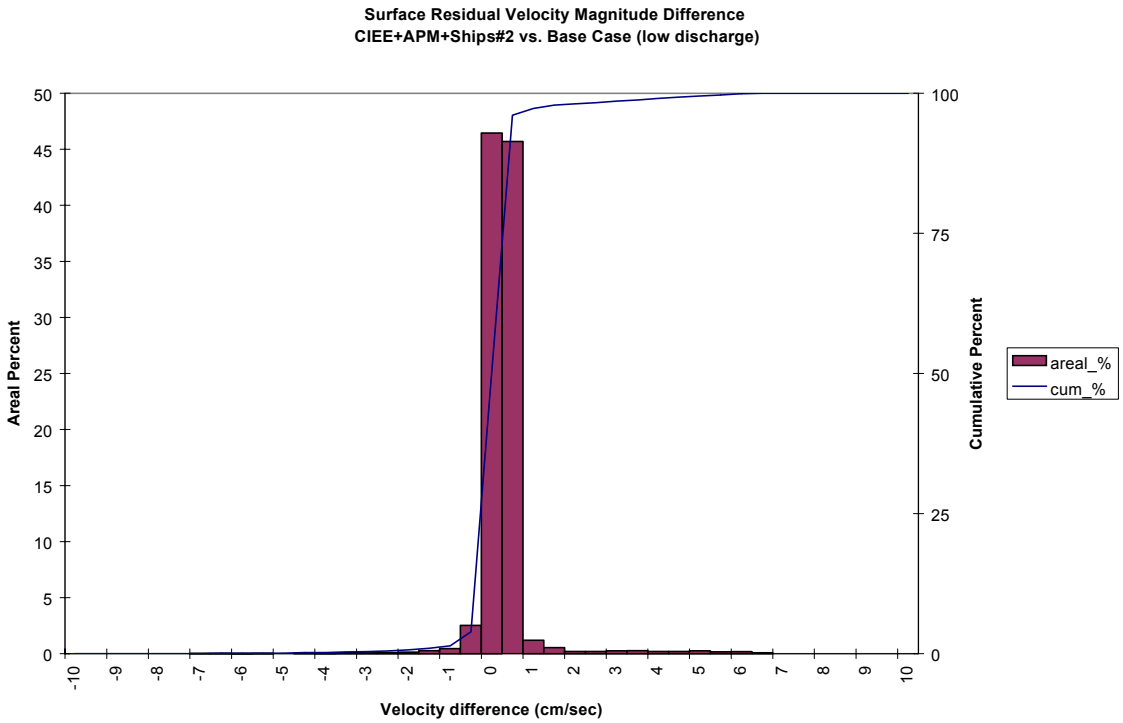

Figure 38. Frequency distribution of surface residual velocity magnitude average difference for the Eastward Expansion plus APM Terminal Dredging plus Ships (Case 2b) versus the Base Case during the low discharge event of historical simulation.

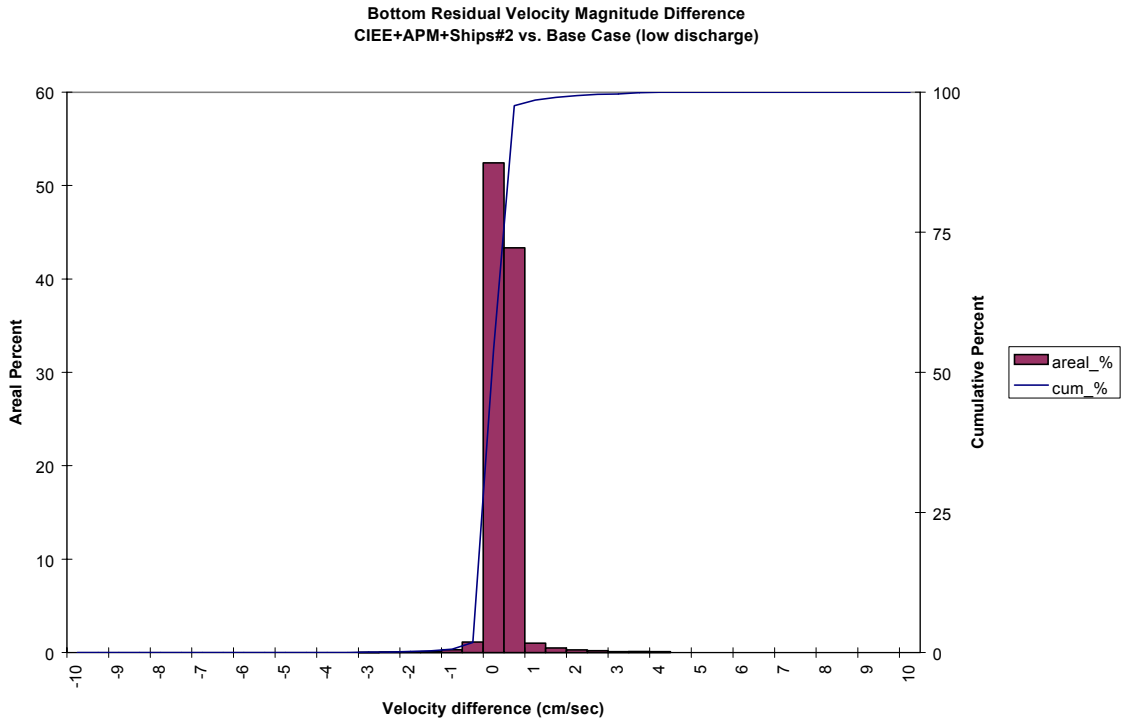

Figure 39. Frequency distribution of bottom residual velocity magnitude average difference for the Eastward Expansion plus APM Terminal Dredging plus Ships (Case 2b) versus the Base Case during the low discharge event of historical simulation.

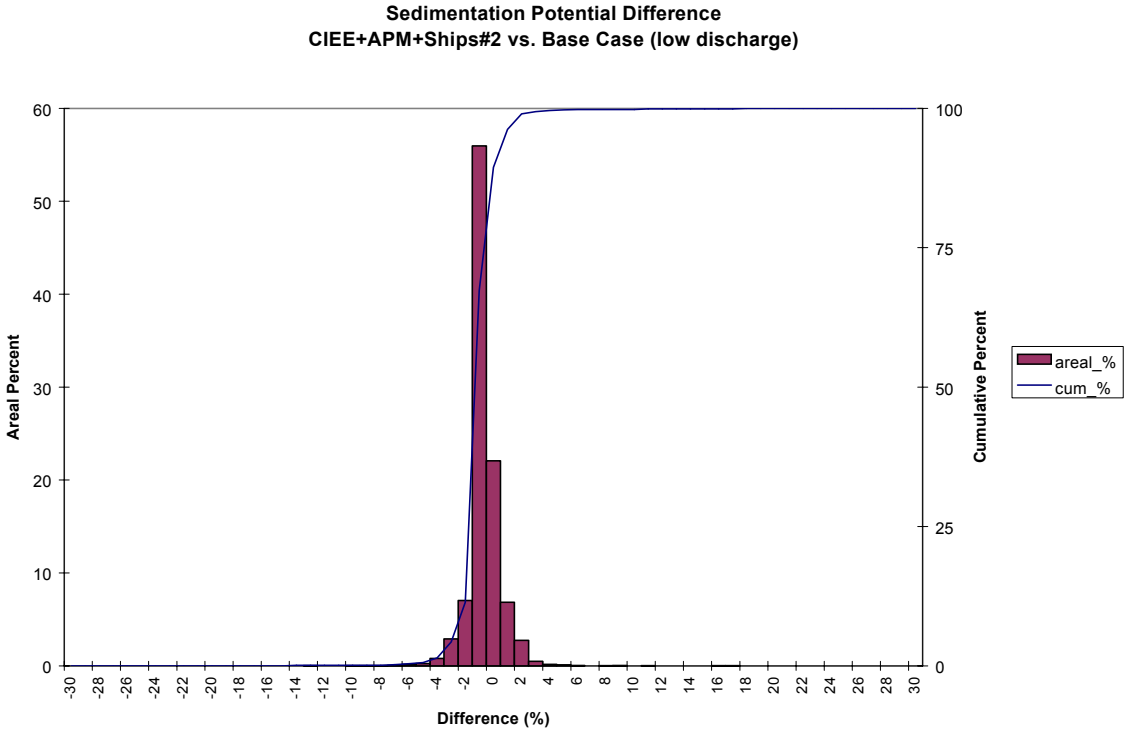

Figure 40. Frequency distribution of sedimentation potential difference for the Eastward Expansion plus APM Terminal Dredging plus Ships (Case 2b) versus the Base Case during the low discharge event of historical simulation.

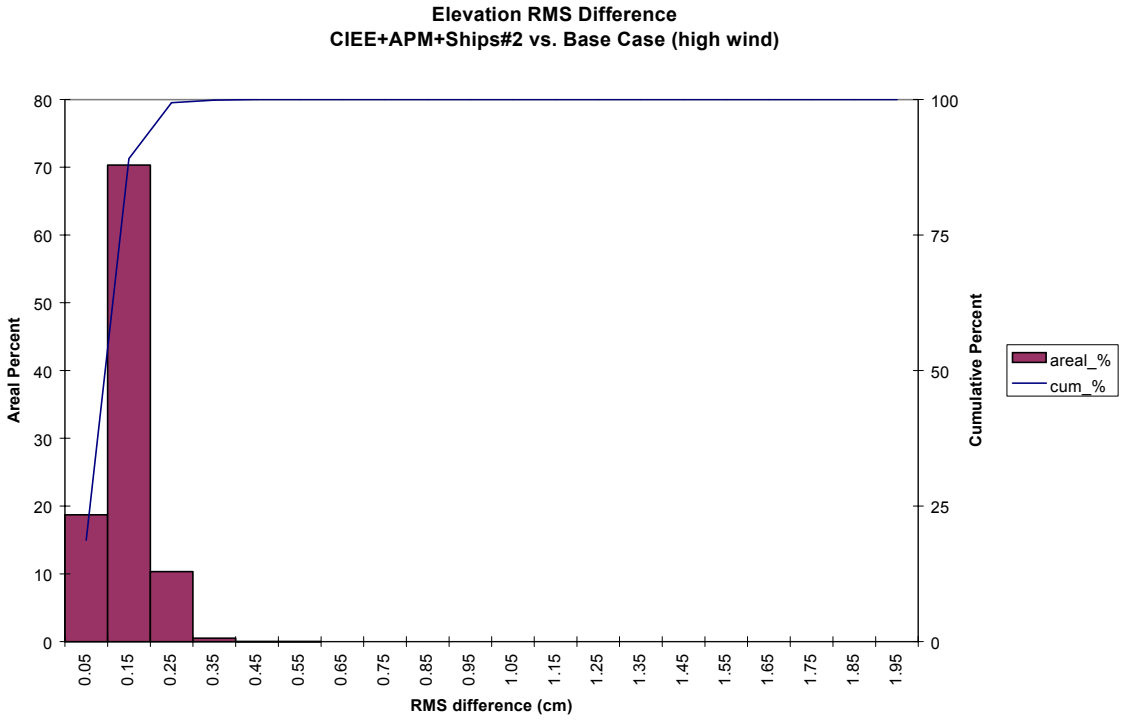

Figure 41. Frequency distribution of elevation RMS difference for the Eastward Expansion plus APM Terminal Dredging plus Ships (Case 2b) versus the Base Case during the high wind event of historical simulation.

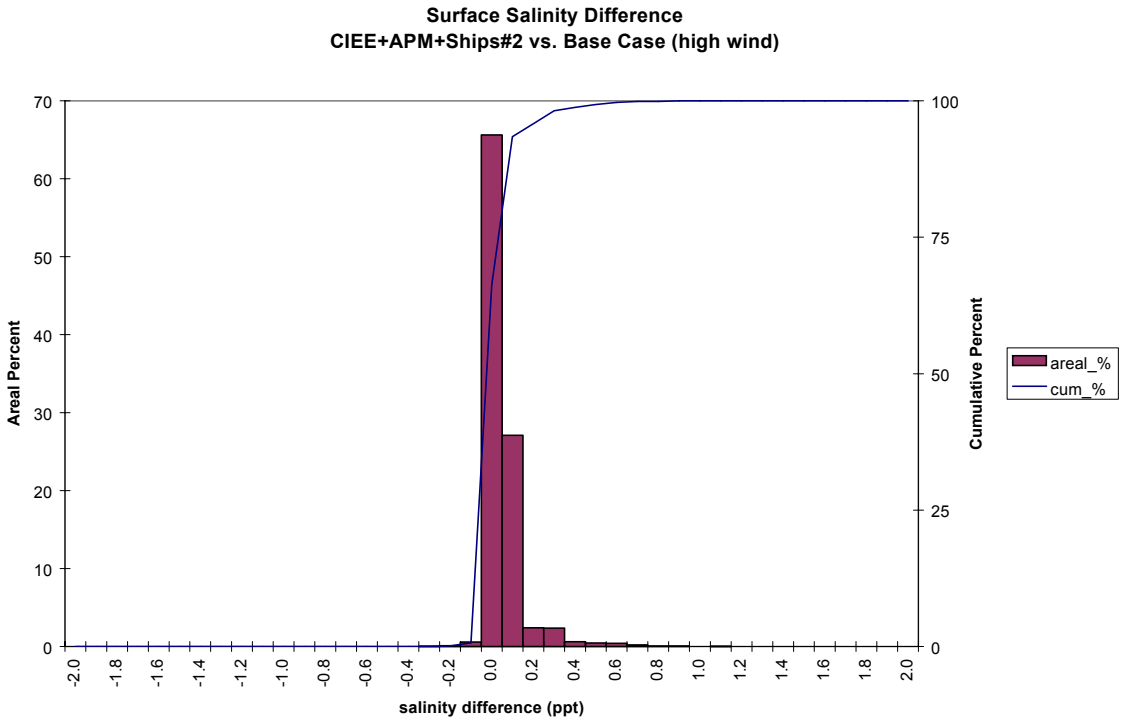

Figure 42. Frequency distribution of surface salinity average difference for the Eastward Expansion plus APM Terminal Dredging plus Ships (Case 2b) versus the Base Case during the high wind event of historical simulation.

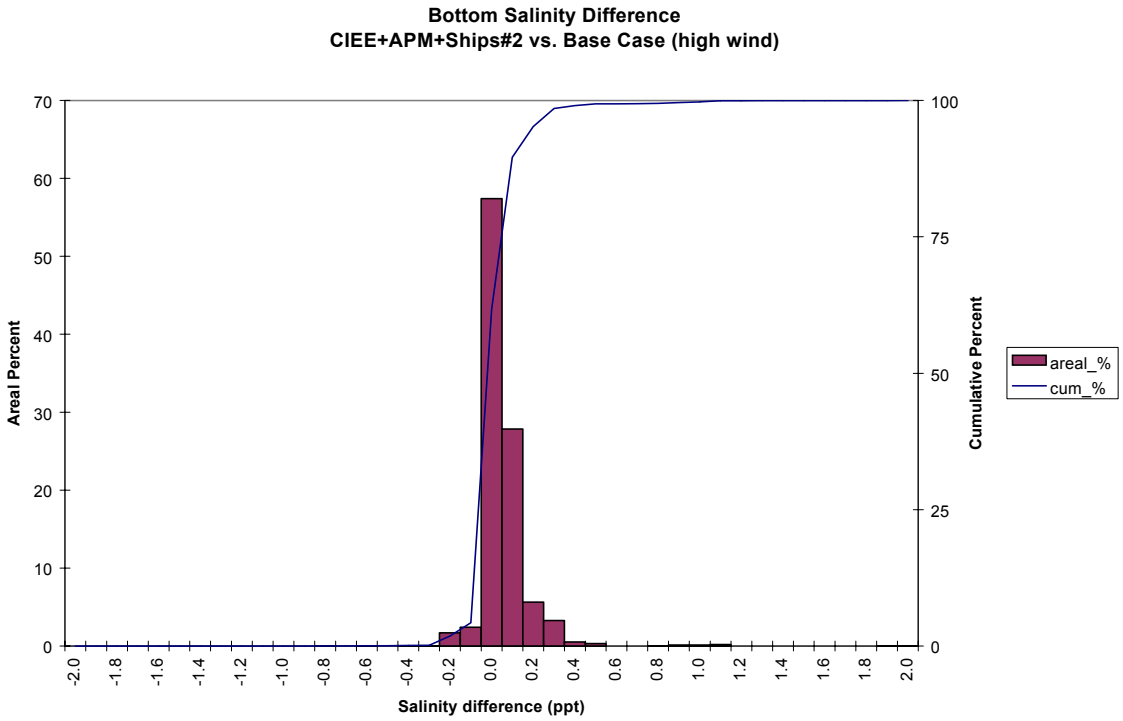

Figure 43. Frequency distribution of bottom salinity average difference for the Eastward Expansion plus APM Terminal Dredging plus Ships (Case 2b) versus the Base Case during the high wind event of historical simulation.

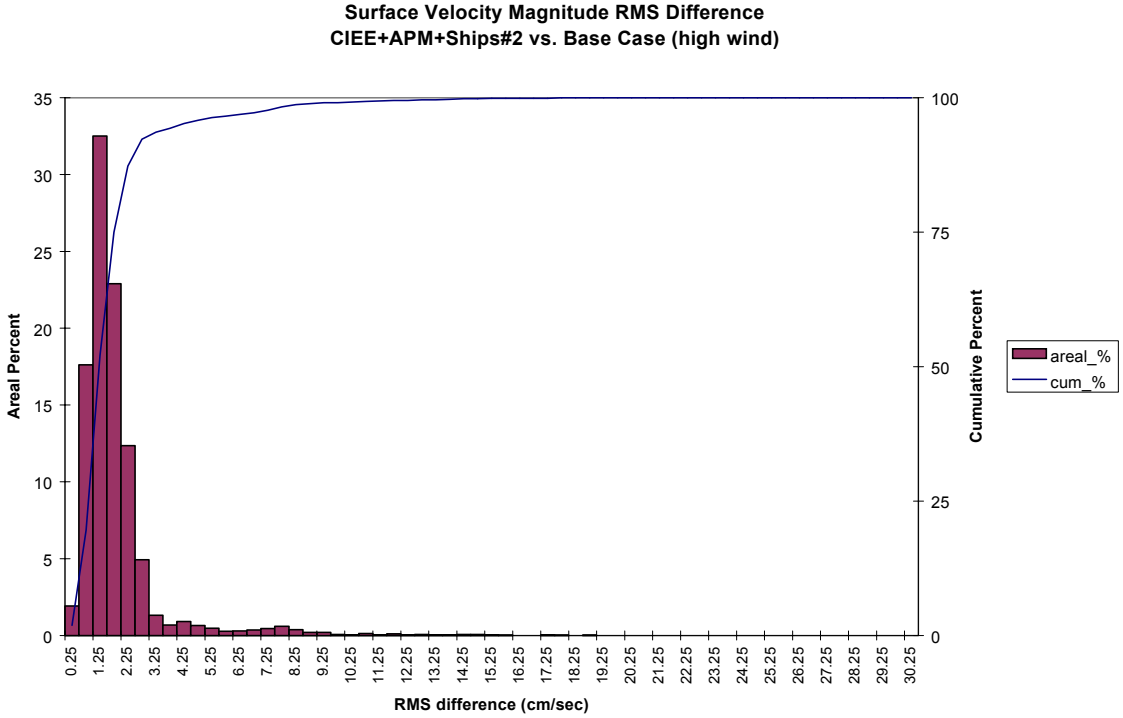

Figure 44. Frequency distribution of surface velocity RMS difference for the Eastward Expansion plus APM Terminal Dredging plus Ships (Case 2b) versus the Base Case during the high wind event of historical simulation.

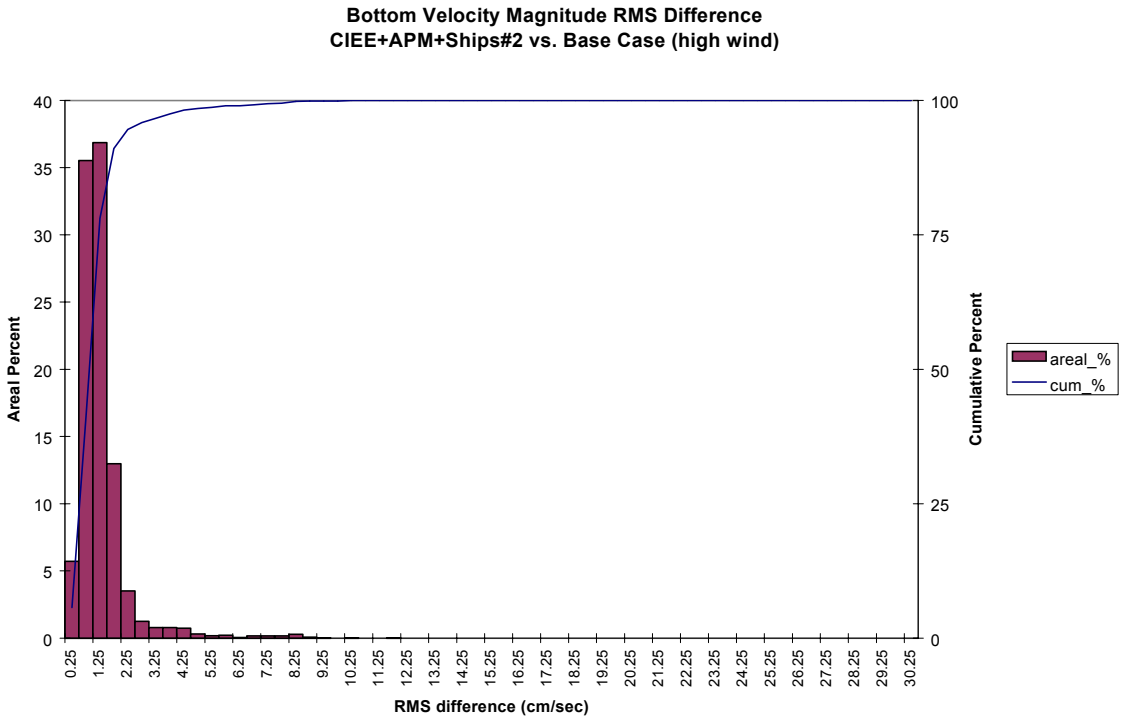

Figure 45. Frequency distribution of bottom velocity RMS difference for the Eastward Expansion plus APM Terminal Dredging plus Ships (Case 2b) versus the Base Case during the high wind event of historical simulation.

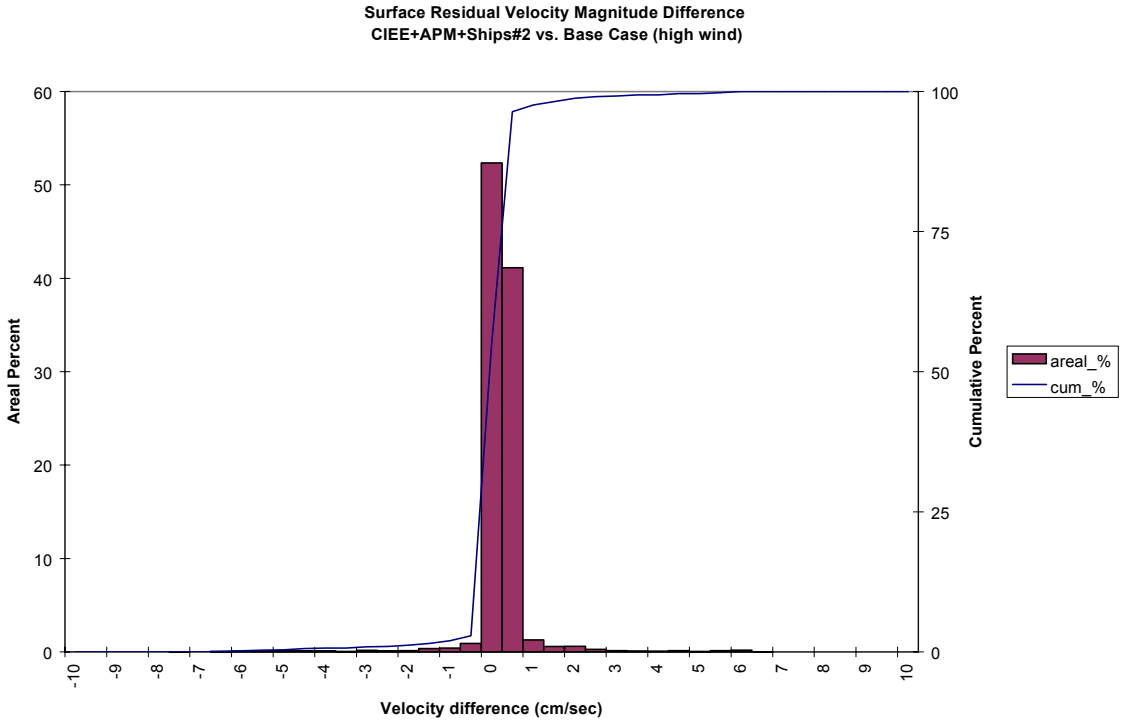

Figure 46. Frequency distribution of surface velocity residual magnitude average difference for the Eastward Expansion plus APM Terminal Dredging plus Ships (Case 2b) versus the Base Case during the high wind event of historical simulation.

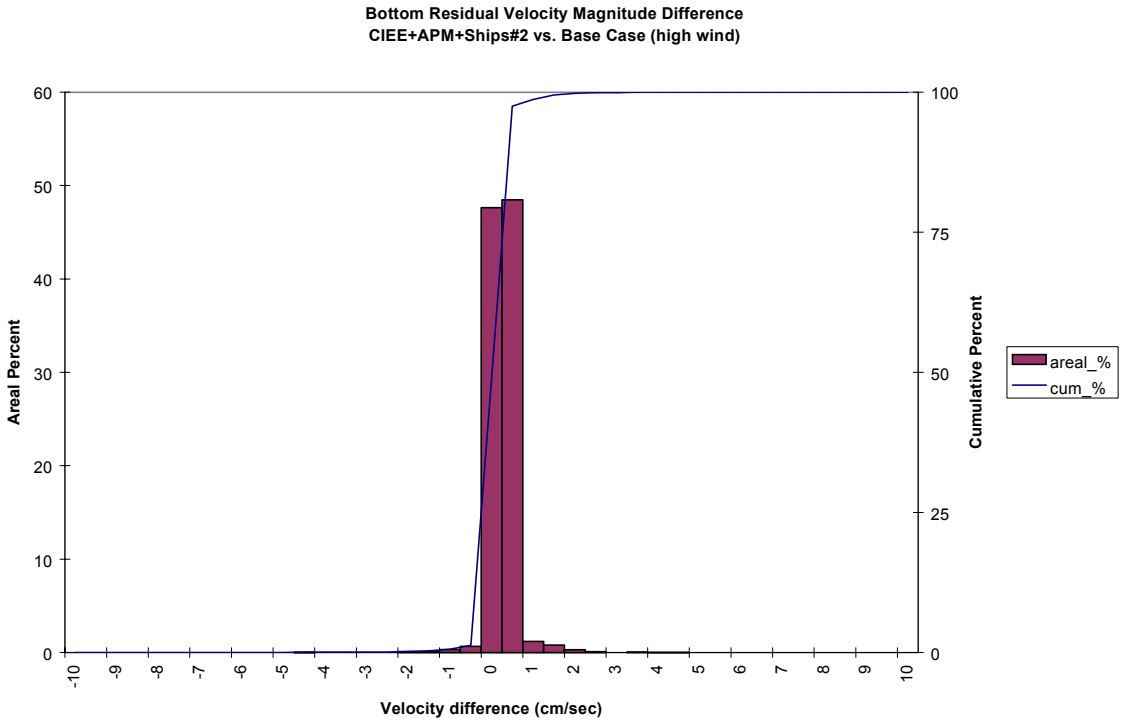

Figure 47. Frequency distribution of bottom velocity residual magnitude average difference for the Eastward Expansion plus APM Terminal Dredging plus Ships (Case 2b) versus the Base Case during the high wind event of historical simulation.

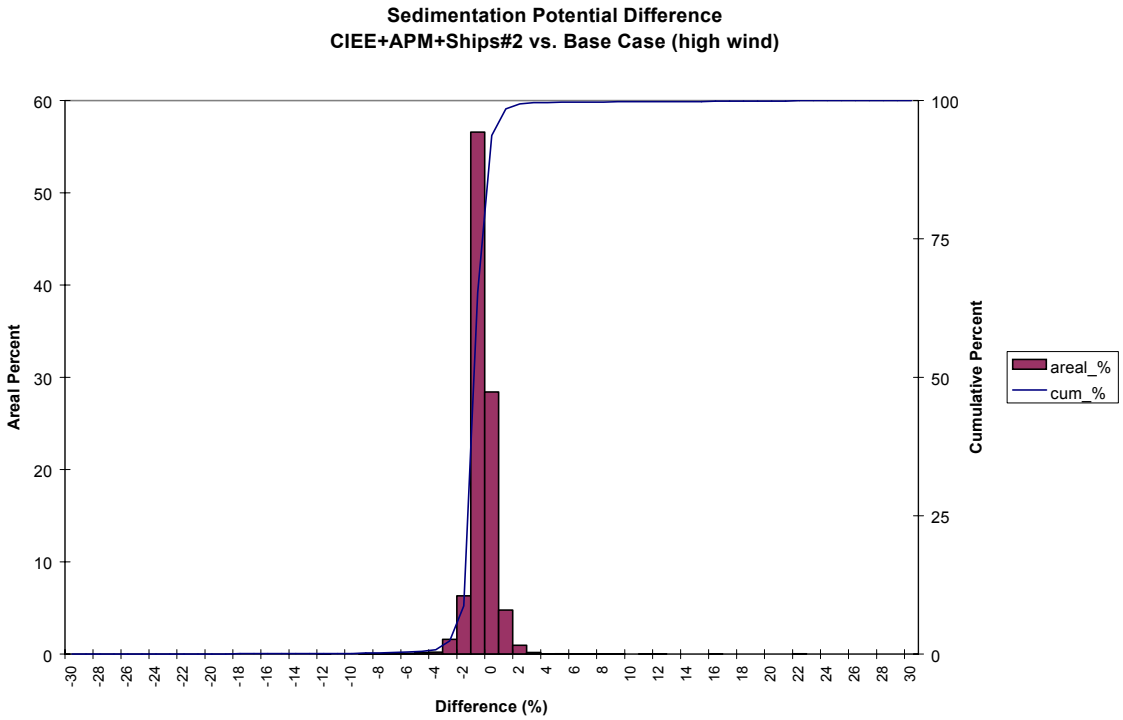

Figure 48. Frequency distribution of sedimentation potential difference for the Eastward Expansion plus APM Terminal Dredging plus Ships (Case 2b) versus the Base Case during the high wind event of historical simulation.